

2014

# Improving predictions of instantaneous camber for prestressed concrete bridge girders

James Nervig  
*Iowa State University*

Follow this and additional works at: <https://lib.dr.iastate.edu/etd>



Part of the [Civil Engineering Commons](#)

---

## Recommended Citation

Nervig, James, "Improving predictions of instantaneous camber for prestressed concrete bridge girders" (2014). *Graduate Theses and Dissertations*. 13817.

<https://lib.dr.iastate.edu/etd/13817>

This Thesis is brought to you for free and open access by the Iowa State University Capstones, Theses and Dissertations at Iowa State University Digital Repository. It has been accepted for inclusion in Graduate Theses and Dissertations by an authorized administrator of Iowa State University Digital Repository. For more information, please contact [digirep@iastate.edu](mailto:digirep@iastate.edu).

**Improving predictions of instantaneous camber for prestressed concrete bridge girders**

by

**James Nervig**

A thesis submitted to the graduate faculty

In partial fulfillment of the requirements for the degree of

**MASTER OF SCIENCE**

Major: Civil Engineering (Structural Engineering)

Program of Study Committee:  
Sri Sritharan, Major Professor  
Jon Matt Rouse, Major Professor  
Kejin Wang

Iowa State University

Ames, Iowa

2014

**Copyright © James Nervig, 2014. All rights reserved.**

## TABLE OF CONTENTS

LIST OF TABLES .....	v
LIST OF FIGURES .....	vi
ACKNOWLEDGMENTS .....	x
ABSTRACT.....	xi
CHAPTER 1. INTRODUCTION .....	1
1.1 Prestressed Concrete Beams .....	1
1.2 Production of PPCBs .....	2
1.3 Camber.....	4
1.4 Challenges Resulting from Inaccurate Prediction of Camber.....	6
1.5 Camber Measurement and Prediction .....	10
1.5.1 Fabrication Procedure of Precasters and Camber Measurement Technique .....	10
1.5.2 Designers Prediction Method and Variables Used .....	11
1.6 Scope of Research.....	13
1.6.1 Researchers Objectives to Improve Instantaneous Camber Predictions .....	13
1.7 Thesis Layout.....	14
CHAPTER 2. LITERATURE review .....	15
2.1 Introduction.....	15
2.2 Factors Influencing Instantaneous Camber.....	16
2.2.1 Prestress Losses .....	16
2.2.2 Elastic Shortening .....	17
2.2.3 Seating.....	20
2.2.4 Relaxation .....	21
2.2.5 Modulus of Elasticity .....	21
2.3 Camber Measurement Technique .....	23
2.3.1 Stretched Wire Method .....	24
2.3.2 Survey Equipment.....	28
2.3.3 Tape Measure .....	31
2.3.4 Photogrammetry.....	32
2.4 Methods of Predicting Instantaneous Camber .....	34
2.4.1 Moment Area Method.....	34
2.4.2 Elastic Shortening .....	37
2.4.3 Seating Loss .....	41
2.4.4 Relaxation .....	42
2.4.5 Modulus of Elasticity-AASHTO LRFD (2010) .....	43
CHAPTER 3. DATA COLLECTION METHODS.....	45
3.1 Introduction.....	45
3.2 Industry Practice Camber Data .....	45
3.2.1 Iowa Department of Transportation Camber Measurement Procedure .....	45

3.3 Errors with Current Camber Measurement Practice .....	54
3.3.1 Bed Deflections.....	54
3.3.2 Inconsistencies with PPCBs.....	55
3.3.3 Friction between Beam Ends and Precasting Bed .....	57
3.4 Tape Measure.....	58
3.5 Rotary Laser Level.....	59
3.5.1 Measuring Camber with a Rotary Laser Level .....	60
3.6 Support Conditions .....	63
3.6.1 Procedure for Measuring Camber when placed on Temporary Supports .....	65
3.7 String Potentiometers.....	67
 CHAPTER 4.    PREDICTING INSTANTANEOUS CAMBER .....	 70
4.1 Simplified Method for Calculating Instantaneous Camber .....	70
4.2 Prestress Force .....	70
4.2.1 Tensioning Procedure .....	71
4.3 Prestress Losses .....	72
4.3.1 Prestress Loss due to Relaxation.....	73
4.3.2 Prestress Loss due to Seating.....	73
4.3.3 Elastic Shortening .....	75
4.4 Effective Prestress Force.....	77
4.5 Moment Area Method to Calculate Camber .....	78
4.6 Modulus of Elasticity.....	82
4.7 Moment of Inertia .....	82
4.8 Deflection Due to Self-Weight of the Beam.....	83
4.9 Final Camber.....	83
 CHAPTER 5.    RESULTS AND DISCUSSION.....	 84
5.1 Factors Affecting Instantaneous Camber Measurements .....	84
5.1.1 String Potentiometer Measurements during Release of a PPCB .....	84
5.1.2 Bed Deflections.....	88
5.1.3 Inconsistent Beam Depth .....	92
5.1.4 Friction between the Beam Ends and Precasting Bed .....	97
5.1.5 Agreement of Adjusted Camber Values .....	106
5.2 Material Properties Affecting Instantaneous Camber Prediction .....	111
5.2.1 Variability of Compressive Strength .....	111
5.2.2 Modulus of Elasticity .....	115
5.3 Discrepancies with Concrete.....	123
5.3.1 Maturity of Concrete.....	123
5.3.2 Uniformity of Concrete.....	125
5.4 Discrepancies with Beams Cast on the Same Day.....	127
5.5 Analytical Prediction Variables for PPCBs .....	128
5.5.1 Moment of Inertia .....	128
5.5.4 Prestress Force .....	131
5.5.5 Prestress Losses .....	132
5.5.3 Sacrificial Prestressing Reinforcement .....	133
5.5.2 Transfer Length.....	136



5.6 Impact of Assumptions during Design of Instantaneous Camber .....	140
CHAPTER 6. CONCLUSIONS AND RECOMMENDATIONS .....	141
6.1 Conclusions .....	141
6.2 Industry Practice Camber .....	141
6.3 Camber Measurement Technique .....	142
6.4 Analytical Camber Prediction .....	143
6.5 Recommendations .....	145
6.5.1 Measuring Instantaneous and Long-Term Camber .....	146
6.5.2 Additional Recommendations to Precasters .....	149
6.5.3 Recommendations to Designers .....	149
WORKS CITED .....	151
APPENDIX A: DATA .....	154
APPENDIX B. STRING POTENTIOMETER DATA .....	291
APPENDIX C: ANALYTICAL DATA .....	327

## LIST OF TABLES

TABLE 2-1: MEASURED VERSUS ESTIMATED PRESTRESS LOSSES (TADROS, 2003) .....	18
TABLE 2-2: COMPARISON OF PRESTRESS LOSSES AND CONCRETE BOTTOM FIBER STRESS (NCHRP 496 2003) .....	19
TABLE 2-3: MEASURED LOSSES AND PREDICTED DESIGN LOSSES .....	20
TABLE 2-4: MULTIPLIERS FOR COMPRESSIVE STRENGTHS .....	22
TABLE 2-5: IMPACT OF HIGH STRENGTH CONCRETE RELEASE STRENGTHS ON CAMBER AS PER O'NEILL ET AL. 2012.....	23
TABLE 2-6: EXPERIMENTS AND RESULTS FROM NONCONTACT PHOTOGRAMMETRIC MEASUREMENT OF VERTICAL BRIDGE DEFLECTIONS (JAUREGUI ET AL. 2003).....	33
TABLE 5-1: SUMMARY OF BED DEFLECTIONS.....	91
TABLE 5-2: PERCENT DIFFERENCE BETWEEN MEASUREMENT METHODS.....	107
TABLE 5-3: AVERAGE AND STANDARD DEVIATIONS ASSOCIATED WITH CAMBER MEASUREMENTS AT TRANSFER USING A ROTARY LASER LEVEL .....	111
TABLE 5-4: MEASURED AND DESIGNED STRENGTHS AT THE TIME OF RELEASE FOR PPCBS FROM THREE PRECAST PLANTS .....	113
TABLE 5-5: BEAMS MEASURED INSTANTANEOUS CAMBER AND DATES OF CASTING AND RELEASE.....	127
TABLE 5-6: CAMBER OF 5 PPCBS WITH DIFFERENT MOMENT OF INERTIA VALUES .....	131
TABLE 5-7: SUMMARY OF DESIGNED VS. TENSIONED PRESTRESS FROM 41 PPCBS.....	132
TABLE 5-8: COMPARISON OF PRESTRESS AND CAMBER WITH AND WITHOUT PRESTRESS LOSSES .....	133
TABLE 5-9: THE PERCENT DIFFERENCE AND CONTRIBUTION TO CAMBER WITH AND WITHOUT SACRIFICIAL PRESTRESSING STRANDS .....	135
TABLE 5-10: COMPARISON OF AASHTO LRFD AND ACI TRANSFER LENGTH .....	137
TABLE 5-11: COMPARISON OF CAMBER WITH AND WITHOUT TRANSFER LENGTH .....	138
TABLE 5-12: PERCENT DIFFERENCE ASSOCIATED WITH INSTANTANEOUS CAMBER PREDICTION .....	140

## LIST OF FIGURES

FIGURE 1-1: ELEVATION VIEW OF A PPCB WITH PRESTRESSING APPLIED WITH AN ECCENTRICITY .....	1
FIGURE 1-2: A PPCB DEPICTING CAMBER .....	1
FIGURE 1-3: STRESSES FROM PRESTRESSING STRANDS SHOWN ALONG THE LENGTH OF A PPCB ...	2
FIGURE 1-4: HOYER LONG LINE METHOD OF PRODUCING PPCBS .....	3
FIGURE 1-5: CAMBER RESULTING FROM THE NET DEFLECTION BETWEEN THE UPWARD DEFLECTION CAUSED BY PRESTRESSING AND DOWNWARD DEFLECTION CAUSED BY THE BEAM SELF-WEIGHT .....	5
FIGURE 1-6: SCHEMATIC VIEW OF A PPCB SHOWING THE FORMATION OF THE HAUNCH.....	7
FIGURE 1-7: CROSS SECTION OF A PPCB, HAUNCH AND SLAB (IOWA BRIDGE DESIGN MANUAL, 2011) .....	8
FIGURE 1-8: UNDERPREDICTED, DESIGNED, AND OVERPREDICTED CAMBER .....	8
FIGURE 2-1: GIRDER LENGTH AFTER THE TRANSFER OF PRESTRESS.....	18
FIGURE 2-2: GIRDER WITH REBAR AND STRING IN PLACE FOR CAMBER MEASUREMENTS (RIZKALLA ET AL., 2011) .....	24
FIGURE 2-3: ANCHORED END WITH A PULLEY OF WIRE USED FOR THE STRETCHED-WIRE SYSTEM (O'NEILL ET AL. 2012) .....	26
FIGURE 2-4: RULER AND MIRROR LOCATED AT MIDSPAN (O'NEILL ET AL. 2012) .....	27
FIGURE 2-5: FREE END OF STRETCH-WIRE SYSTEM WITH WEIGHT AND PULLEY (O'NEILL ET AL. 2012) .....	27
FIGURE 2-6: STRETCHED WIRE SYSTEM WITH A WEIGHTED TROLLEY AT MIDSPAN (BARR ET AL. 2000) .....	28
FIGURE 2-7: CAMBER MEASURING TEMPLATE (ROSA ET AL. 2007) .....	29
FIGURE 2-8: TAKING READINGS WITH LASER LEVEL SURVEYING SYSTEM (HINKLE ET AL. 2006) ..	30
FIGURE 2-9: CAMBER MEASUREMENT MARKER (JOHNSON ET AL. 2012).....	30
FIGURE 2-10: CAMBER MEASUREMENT WITH A TAPE MEASURE AT MIDSPAN OF A PPCB (IOWA DOT PRESTRESS INSPECTION, 2013).....	32
FIGURE 2-11: PPCB WITH SACRIFICIAL, HARPED, AND BOTTOM PRESTRESSING STRANDS .....	35
FIGURE 2-12: MOMENT DIAGRAM DUE TO SACRIFICIAL, HARPED, AND BOTTOM PRESTRESSING STRANDS .....	36
FIGURE 3-1: PPCB WITH TWO CYLINDRICAL HOLES FOR INTERIOR DIAPHRAGM .....	47
FIGURE 3-2: PRECASTING BED WITH METAL CHAMFER.....	48
FIGURE 3-3: PRECASTING BED WITH A REMOVABLE RUBBER CHAMFER .....	48

FIGURE 3-4: DIFFERENCE IN MEASURED AND PREDICTED INDUSTRY PRACTICE CAMBER DATA VS. LENGTH OF PPCB.....	52
FIGURE 3-5: DIFFERENCE IN CAMBER/LENGTH OF INDUSTRY PRACTICE DATA ARRANGED IN INCREASING BEAM LENGTH.....	53
FIGURE 3-6: PPCB BEFORE THE TRANSFER OF PRESTRESS GENERATING A UNIFORM LOAD ON THE BED .....	54
FIGURE 3-7: PPCB AFTER THE TRANSFER OF PRESTRESS WITH THE BEAM SELF-WEIGHT ACTING ONLY AT TWO POINTS ON THE BED.....	55
FIGURE 3-8: INCONSISTENT TOP FLANGE SURFACE OF A PPCB DUE TO LOCAL INCONSISTENCIES	56
FIGURE 3-9: PPCB WITH TROWELED SURFACE ALONG THE LENGTH OF THE BEAM.....	57
FIGURE 3-10: TYPICAL TAPE MEASURE READING AT THE MIDSPAN OF A PPCB TAKEN AT A PRECAST PLANT .....	59
FIGURE 3-11: ROTARY LASER LEVEL .....	60
FIGURE 3-12: PPCB BEFORE THE TRANSFER OF PRESTRESS .....	61
FIGURE 3-13: PPCB AFTER THE TRANSFER OF PRESTRESS, BEFORE THE BEAM WAS LIFTED.....	61
FIGURE 3-14: PPCB AFTER THE TRANSFER OF PRESTRESS AND AFTER THE BEAM WAS LIFTED AND PLACED BACK ON THE BED .....	61
FIGURE 3-15: END OF A PPCB ON A TEMPORARY WOODEN SUPPORT .....	63
FIGURE 3-16: PPCB WITH INCREASED MIDSPAN DEFLECTION CAUSED BY THE MOMENT FROM THE OVERHANG .....	64
FIGURE 3-17: PPCB WITH INCREASED MIDSPAN DEFLECTION DUE TO SELF-WEIGHT CAUSED BY THE REDUCED CLEAR SPAN.....	64
FIGURE 3-18: INCREASED DEFLECTION OF A PPCB RELATIVE TO THE SUPPORT CAUSED BY THE OVERHANG .....	65
FIGURE 3-19: STRING POTENTIOMETER ATTACHED TO THE TOP FLANGE OF A PPCB .....	68
FIGURE 3-20: STRING POTENTIOMETER ATTACHED TO THE MIDSPAN OF A PPCB .....	68
FIGURE 3-21: STRING POTENTIOMETER ATTACHED TO THE PRECASTING BED AT THE END OF A PPCB.....	69
FIGURE 4-1: INITIAL AND FINAL POSITIONS OF HARPED PRESTRESSING STRANDS WHEN TENSIONING .....	72
FIGURE 4-2: PRESTRESSED BEAM WITH SHORTENING ACROSS THE CROSS SECTION .....	75
FIGURE 4-3: PRESTRESSED BEAM WITH ADDITIONAL SHORTENING NEAR THE CENTER OF GRAVITY OF STEEL.....	76
FIGURE 4-4: PRESTRESSED BEAM WITH ELASTIC GAINS DUE TO SELF-WEIGHT.....	76
FIGURE 4-5: MOMENT DIAGRAM DUE TO STRAIGHT SACRIFICIAL STRANDS .....	79
FIGURE 4-6: MOMENT DIAGRAM DUE TO HARPED PRESTRESSING STRANDS.....	79

FIGURE 4-7: MOMENT DIAGRAM DUE TO BOTTOM PRESTRESSING STRANDS .....	79
FIGURE 4-8: MOMENT DIAGRAM OF A PRESTRESSED CONCRETE BEAM WITHOUT TRANSFER LENGTH.....	80
FIGURE 4-9: MOMENT DIAGRAM DIVIDED INTO SECTIONS TOGETHER WITH THEIR CENTROID LOCATION .....	82
FIGURE 5-1: TIME VS. VERTICAL DISPLACEMENT OF AT BTB 100 PPCB .....	86
FIGURE 5-2: TIME VS. VERTICAL DISPLACEMENT OF AT BTE 110 PPCB .....	87
FIGURE 5-3: BED DEFLECTION VS. LENGTH OF MULTIPLE PPCBS .....	89
FIGURE 5-4: TWO PPCB ENDS IN RELATION TO THE SUPPORTS ON A PRECASTING BED.....	90
FIGURE 5-5: TWO PPCBS AND PLACEMENT THAT RESULTS IN POSITIVE BED DEFLECTION.....	92
FIGURE 5-6: INCONSISTENT TOP FLANGE SURFACES ON PPCBS.....	93
FIGURE 5-7: INCONSISTENT TROWELED SURFACE ALONG THE LENGTH OF THE BEAM .....	95
FIGURE 5-8: TEMPORARY SUPPORT USED FOR SUPPORTING A PPCB FORM .....	96
FIGURE 5-9: FORMS ON A PPCB.....	97
FIGURE 5-10: FORCE OF FRICTION VS. DEFLECTION DUE TO FRICTION FOR MULTIPLE PPCBS.....	99
FIGURE 5-11: EFFECT OF FRICTION ON CAMBER MEASUREMENTS FOR DIFFERENT TYPES AND LENGTHS OF BEAMS.....	100
FIGURE 5-12: TIME VS. DISPLACEMENT AFTER THE TRANSFER OF PRESTRESS ON A BTB 100 .....	102
FIGURE 5-13: INCREASE IN CAMBER DUE TO FRICTION FOR THREE PPCBS.....	103
FIGURE 5-14: ROLLER SUPPORT UNDER A D90 PPCB .....	104
FIGURE 5-15: ROLLER SUPPORT UNDER A PPCB .....	105
FIGURE 5-16: COMPARISON OF THE MEASUREMENT TECHNIQUE BETWEEN PRECASTERS, CONTRACTORS, AND RESEARCHERS.....	108
FIGURE 5-17: DIFFERENCES BETWEEN MEASUREMENT TECHNIQUES AFTER ADJUSTING DATA TO ACCOUNT FOR BED DEFLECTIONS, FRICTION, AND INCONSISTENT TOP FLANGE SURFACES .....	110
FIGURE 5-18: MEASURED RELEASE STRENGTH VS. TARGET RELEASE STRENGTH OBTAINED FOR 106 PRETENSIONED GIRDERS .....	114
FIGURE 5-19: IMPACT OF CONCRETE RELEASE STRENGTHS ON CAMBER .....	115
FIGURE 5-20: MEASURED CAMBER VS. ANALYTICAL CAMBER USING $E_{CI}$ OBTAINED FROM CREEP FRAMES.....	118
FIGURE 5-21: MEASURED VS. ANALYTICAL CAMBER FOR BEAMS USING AASHTO $E_{CI}$ AND SPECIFIC $F'_{CI}$ STRENGTHS THAT CORRESPOND TO MEASURED BEAMS.....	119
FIGURE 5-22: MEASURED VS. ANALYTICAL CAMBER FOR BEAMS USING AASHTO $E_{CI}$ AND RELEASE STRENGTHS OBTAINED FROM SAMPLES .....	120

FIGURE 5-23: MEASURED CAMBER VS. ANALYTICAL CAMBER USING $E_{CI}$ OBTAINED FROM CREEP FRAMES FOR SELECT BEAMS.....	121
FIGURE 5-24: MEASURED CAMBER VS. ANALYTICAL CAMBER ADJUSTING CAMBER VALUES BASED ON AVERAGES USING AASHTO $E_{CI}$ FROM SPECIFIC BEAM RELEASE STRENGTHS .....	122
FIGURE 5-25: PLASTIC MOLDED AND SURE CURE CYLINDERS.....	126
FIGURE 5-26: COMPARISON OF CAMBER USING DIFFERENT MOMENT OF INERTIA VALUES.....	130
FIGURE 6-1: PPCB WITH LOCATIONS OF 2X4'S .....	146
FIGURE 6-2: CLOSE UP OF 2X4 ON A PPCB .....	147
FIGURE 6-3: LOCATION OF CAMBER MEASUREMENTS AFTER THE TRANSFER OF PRESTRESS.....	148

## ACKNOWLEDGMENTS

The author would like to thank the following members of the Technical Advisory Committee for their support of the project and their guidance and advice: Ahmad Abu-Hawash, Dean Bierwagen, Ken Dunker, Kyle Frame, Michael Nop, and Wayne Sunday.

The author would like to thank Dr. Sritharan and Dr. Rouse for the opportunity to work on this project and gain experience in the field and with the review of design standards. It is with their guidance that the project was able to be completed with the quality of results that were obtained. In addition, the author would like to thank the following people who helped contribute to this project: Dr. Kejin Wang for serving as a committee member, Wenjun He and Ebado Hornarvar for their addition to this project with their studies of creep, shrinkage and long-term camber, and numerous students who assisted with the collection of data. The author would like to say a special thank you to Andrews Prestressed, Coreslab Structures, and Iowa Precast Company for their guidance with industry standards and allowing the author to visit their precast plants and gather data. The author would like to recognize the following individuals from the precast industry for their guidance and assistance with obtaining specific data from the precast plants:

Jeff Butler  
Dustin Davis,  
Dennis Drews  
Jim Goodknight  
Teresa Nelson  
Brian Peterson  
Mark Rasmussen  
Scott Willenborg  
John Wolf

Finally, the author would like to thank his family, especially his wife Audrey Nervig and his parents Dave and Janice Nervig for their support during the project duration.

## ABSTRACT

Inaccurate prediction of long-term camber in precast prestressed concrete beams (PPCB) creates discrepancies in bridge construction which results in increased costs and construction challenges. Although emphasis is placed on erection and long-term camber, these challenges have been found to originate from the difference between the estimated design and measured camber at the transfer of prestress and will continue to increase with time. The estimate of the instantaneous camber is influenced by factors such as the method used for determining the camber as well as the assumed modulus of elasticity and initial prestress, while the measured camber can be affected by the measurement technique, quality of formwork and construction, and uniformity of concrete. To systematically study and eliminate the construction challenges associated with camber of precast girders, a research project was undertaken to examine the differences between the measured and designed camber of Iowa girders from fabrication through erection.

This thesis focuses on the causes of error found with instantaneous camber by examining the designer's prediction method and variables used for design, the construction practices used for producing a PPCB, and the precasters camber measurement method adopted by the precast industry. While the discrepancy between the measured and designed camber was found to be dependent on the girder type, the designed camber was underestimated due to inaccurate variables used for material properties and the design prestress force. In depth analysis was conducted to investigate different methods of camber prediction and to determine the effects that material properties have on camber. Evaluation of the historical camber measurements that were previously recorded using the current measurement technique revealed that camber is over predicted the majority of the time. Further examination of historical data exposed insufficient data that did not accurately capture the instantaneous camber. For this reason, precasters fabrication procedures were observed and instantaneous camber was measured by the project team from over 100 girders. Observations and independent camber



measurements taken by the research team led to the identification of discrepancies between predicted and measured instantaneous camber.

Results found that friction, bed deflections, inconsistent top flange surfaces due to the finish that is applied, and inconsistent top flange surfaces due to the beam depth not being uniform along the length of the beam currently produce an average error of 17.6%, 2.8%, 5.2%, and 6.8% respectively. When predicting camber using the AASHTO LRFD (2010) modulus of elasticity, the agreement with the predicted and measured camber produced the best results at  $98.2\% \pm 14.9\%$  agreement. Accurately measuring camber to account for bed deflections, friction, and inconsistent top flange surfaces and predicting the material and fabricated properties of the girders, such as the modulus of elasticity, prestress force, etc., will improve the accuracy of instantaneous camber predictions.

## CHAPTER 1. INTRODUCTION

### 1.1 Prestressed Concrete Beams

Prestressing has been defined as the “intentional creation of permanent stresses in a structure or assembly, for the purpose of improving its behavior under various service conditions.” (Lin, 1981). Prestressing is used in multiple structural members, including precast, prestressed concrete beams (PPCBs). PPCBs use prestressing reinforcement in an active state to allow high compression stresses in the tension zone, thereby increasing the flexural tension resistance. Benefits associated with PPCBs include the ability to meet deflection and cracking serviceability requirements efficiently with a large span to depth ratio.

Stresses induced in PPCBs can reduce problems associated with deflection requirements at the service limit state. When an eccentric prestress force is applied, an end moment can cause an upward displacement at midspan called camber. The camber produced allows the PPCB to stay within the deflection limitations that may be present due to live and dead loads including self-weight.

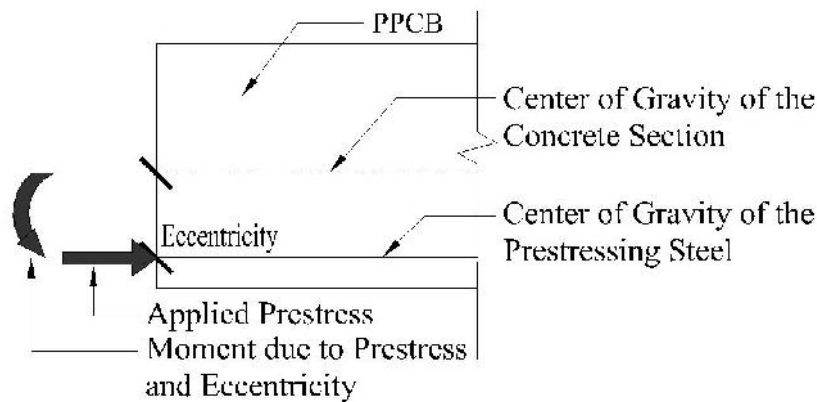


**Figure 1-1: Elevation View of a PPCB with Prestressing Applied with an Eccentricity**

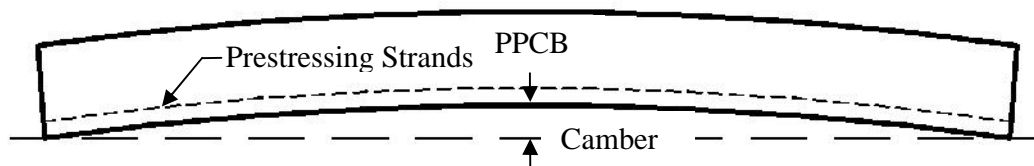


**Figure 1-2: A PPCB Depicting Camber**

An additional benefit of prestressed concrete is reducing the ability for the cross section to crack. Prestressed reinforcement will exert an axial force on a PPCB which will provide compressive stresses throughout the length of the member. The compressive stresses resulting from the prestressed reinforcement will allow the section to remain uncracked. Reducing or eliminating the cracks due to prestressing will increase the service life of a structure by eliminating spaces for contaminants to penetrate the surface and corrode reinforcement.

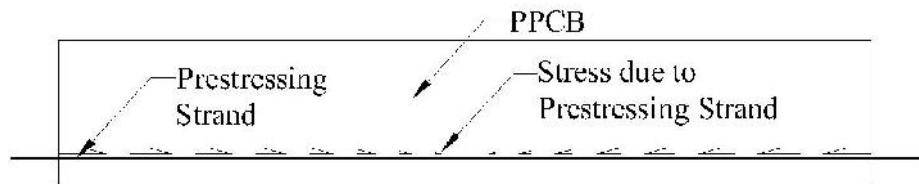


**Figure 1-3: Stresses from Prestressing Strands shown along the Length of a PPCB**

Prestressing also has the advantage of making a member more efficient with respect to size compared to reinforced concrete. Deflection limitations have the ability to restrict the design of reinforced concrete members. Prestress concrete allows members to span the same distances with smaller cross sections which will reduce the materials used and potentially reduce the cost of the member.

When constructing bridge beams from precast concrete, prestressing is typically utilized. The benefits of prestressing a precast concrete beam relate to deflection, reduction in cracking, and improved span to depth ratio. Producing PPCBs has given the concrete industry viable options for producing economical and durable girders to construct bridges.

## **1.2 Production of PPCBs**

The procedure for producing, storing, and erecting a PPCB has a significant impact on the camber and is outlined in the following paragraphs. This procedure is based on the production processes of three precast plants that fabricate and construct beams for the Iowa Department of Transportation. The processes of other precast plants may vary depending on regulations and best practices. The identities of the plants will remain anonymous and will be referred to as Plant A, Plant B, and Plant C.

These precast plants use the Hoyer, Long Line method to produce beams. In this method, two to five duplicate beams are produced simultaneously in one line. The advantages of the Hoyer Method are the cross section of the beams, formwork, location of prestressing strands, and theoretical prestressing force remains the same for all the beams produced at one time. Using the same design and producing multiple PPCBs at one time allows precasters to save time and money.

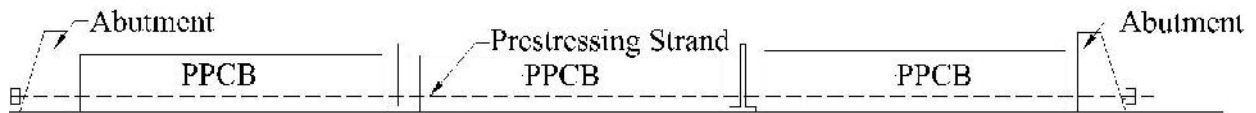


**Figure 1-4: Hoyer Long Line Method of Producing PPCBs**

The process of producing a PPCB first involves cleaning the precasting bed to ensure that it is free of all concrete debris from the previous batch of beams that were produced. The prestressed reinforcement is then laid out along the length of the bed and tensioned to an initial value of 3-5 kips. This is done so that all the prestressing strands have a uniform starting stress. The prestressing steel is then tensioned to its initial designed value. After the prestressed reinforcement is tensioned, additional shear and longitudinal reinforcement is added depending on the design specifications of the beams. Formwork is oiled and added along the length of the beam on both sides. Once this is complete, concrete is mixed and placed in the form. Workers typically roughen the top flange surface of the beam to ensure composite bonding when the bridge deck is placed at the bridge site. The concrete is covered and cured for a period of 1-3 days. Duration of curing depends on the desired strength of the concrete that needs to be achieved before removing the formwork from the beam and releasing the prestressing strands. Once the proper concrete strength is achieved, the prestressing strands are cut, which transfers the prestress force to the PPCBs. Thorough details about the transfer of prestress are listed in Chapter 3.

Beams produced at precast facilities have a designed instantaneous camber that is expected immediately after the transfer of prestress. After beams are released, they are stored in precaster's property until they are able to be shipped to the bridge site. The availability for the beams to be shipped is dependent on the contractor's schedule, who is erecting the beams.

After the beams have been shipped to the jobsite and placed on the abutments and piers, camber is checked on each girder to determine the height of the formwork throughout the length of the bridge. When this is determined, workers construct the formwork to the proper elevations and place the deck reinforcement, followed by casting of the bridge deck. Final stages of construction include placing additional features such as guardrails, signs, and additional products.

### 1.3 Camber

Camber is the net deflection caused by the upward deflection due to the applied prestress force and downward deflection due to the self-weight of a PPCB (Equation 1-1), which typically occurs from the time the prestress is transferred to PPCBs.

$$\Delta_{Camber} = \left| \Delta_{Prestress \text{ (Upward Deflection)}} \right| - \left| \Delta_{Self \text{ Weight (Downward Deflection)}} \right| \quad (1-1)$$

Eccentric prestressing steel about the center of gravity of the section produces a bending moment that can cause a girder to deflect upward (Figure 1-1). The upward deflection is dependent on the reinforcing strand placement and the amount of initial prestressing force that is applied. The self-weight deflection will cause a downward deflection in the girder. The self-weight deflection is dependent on the length of the member along with the geometry and material properties. Subtracting the self-weight deflection of the member from the upward deflection results in camber if the final value is positive.

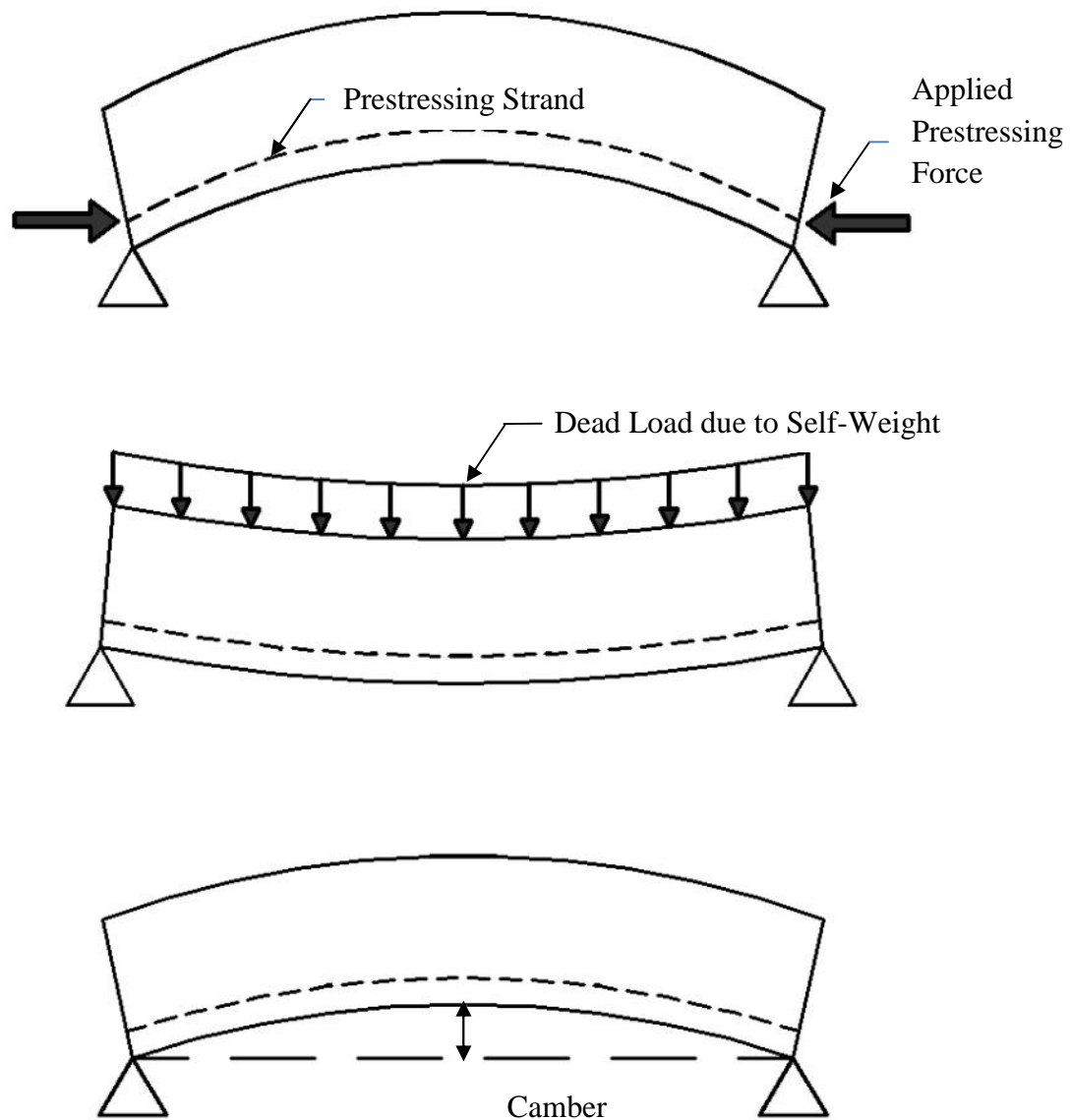


**Figure 1-5: Camber Resulting from the Net Deflection between the Upward Deflection caused by Prestressing and Downward Deflection caused by the Beam Self-Weight**

Camber can be referenced based on the time period when it is measured. The most common camber values are the instantaneous value which occurs immediately after the transfer of prestress and the long-term value at the time of erecting the beam.

Instantaneous camber is measured immediately after the transfer of prestress. The instantaneous camber is often used as a prediction basis for long-term camber and can indicate the accuracy of camber at erection and other stages of its life.

Camber changes with respect to time and is affected by many variables. These variables include creep and shrinkage of concrete and relaxation of the prestressing strands. While the beams are stored in the precaster's property prior to shipment, the camber continues to grow due to the effect of creep and shrinkage of concrete. Creep of concrete is a plastic deformation under constant pressure. The creep and shrinkage of concrete will affect the prestress force that is present in the PPCB which affects the magnitude of the relaxation losses of the prestressing strands. As the girder ages, the loss of prestress will change with time as well, which affects the rate of camber growth. The rate of creep and shrinkage of concrete is further influenced by the location of the temporary supports during storage and thermal effects. The duration of PPCB storage can have a significant effect on the camber. Due to the constantly changing prestress force and concrete properties, predicting long-term camber is a challenge.

Long-term camber can occur at different time periods in the girders life after the transfer of prestress. As mentioned earlier, the focus is typically placed on the camber at erection of girders. At erection of the girders, the elevations of the forms for constructing the concrete deck are determined. This typically occurs at a time period of one month to one and a half years. Another important time period to determine camber in a PPCBs life is at the end of the designed service life. At this time, it is imperative to find if the deflection behavior of the PPCB will still be at an allowable tolerance.

#### **1.4 Challenges Resulting from Inaccurate Prediction of Camber**

Predicting camber in pretensioned precast concrete beams (PPCBs) has been a problem that precasters, contractors, and Departments of Transportation across the country have faced for many years. Overpredicting or underpredicting camber typically causes difficulty with field assembly, delays in construction schedule and serviceability problems with structures which can increase the construction costs. The intensity of this challenge appears to have exacerbated in recent years due to the use of more advanced, high strength concrete mix designs. For this reason, it has been found that there is a significant discrepancy that exists between the designed and actual values of the instantaneous and long-term cambers. While construction challenges tend to have drawn more attention to the long-term camber, it should be realized that an error associated with the instantaneous camber will significantly affect the long-term camber.

The majority of the problems associated with inaccurate camber relates to placing the bridge deck at the jobsite. A minimum deck thickness requirement needs to be fulfilled throughout the entire length of the bridge. Different elevations that are inconsistent along the length of the girder are typically present due to camber in the girders. For example, the elevation of a prestressed girder at the midspan is typically higher than the elevation at the ends of the girders (i.e. Figure 1-6). Due to the effect of different elevations along the length of the girders, haunches are required to be built. A haunch is defined by the Subcommittee on Transportation Communications (2005) as the space between the bottom of the slab and the top of the top flanges of the beams (i.e. Figure 1-6). The purpose of a haunch is to maintain a uniform deck thickness along the length of the girders and to meet the desired bridge profile. It should be recognized that haunches vary over the length of the girder in order to account for the change in elevation over the length of the beam. Adding and adjusting haunches has been proven to be labor intensive, can add construction delays, and will increase the dead load without the addition of strength. The effects of adding and adjusting haunches can increase the cost through added labor that is unaccounted for, the possibility of liquidated damages if the project runs over the allotted time that was budgeted, and can result in serviceability issues due to the larger dead load from additional concrete that was originally unaccounted.

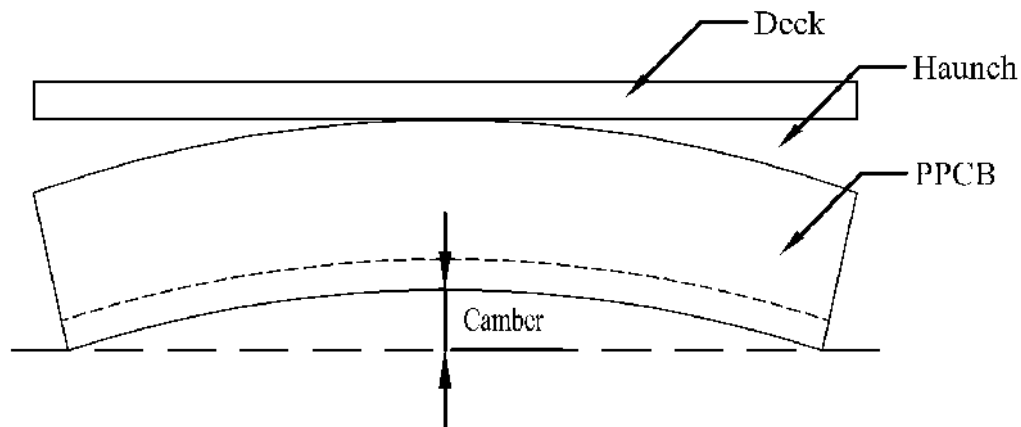


**Figure 1-6: Schematic View of a PPCB Showing the Formation of the Haunch**



Camber that is underpredicted will result in an excessive upward deflection greater than the designed camber. Conversely, camber that is overpredicted will result in an upward deflection that is less than the designed camber. The area of concern with the over and under prediction of camber is typically at midspan. Erecting girders at a bridge site typically requires haunches/embedments, grade adjustments, or a combination of both to be utilized to account for either the over or under prediction of camber.

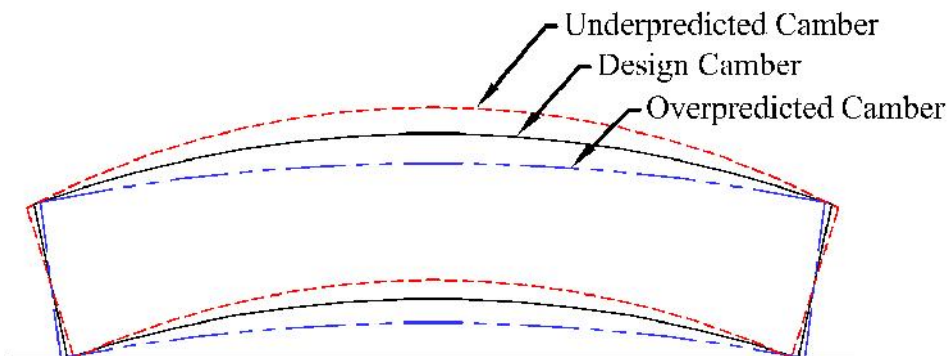


### Figure 1-8: Underpredicted, Designed, and Overpredicted Camber

Camber that is greater than the designed camber (i.e. under prediction of camber) will require haunches to be built. In the extreme cases where the maximum haunch exceeds four inches from the top flange of the girder, a grade adjustment will be considered (Iowa Bridge Design Manual 2011). Lowering the grade of the top slab may decrease the height of the haunch below the four inch maximum value. If this option is unavailable, the rebar may be bent so that clearances can be met at midspan of the girder. Additional bending of these bars will increase the labor and cost.

Camber that is underpredicted is susceptible to flexural cracking in the top flange due to tensile stresses from the prestressing that is present. While storing girders before the deck is cast, the top flange is exposed. If cracking is present, contaminants can reach the reinforcement. After the deck is placed, additional dead load is added to the girders, causing less tensile stresses to be present in the top flange and reducing the crack widths. The reduction of tensile stresses will reduce the risk that contaminants will penetrate into the girder unless camber significantly increases further due to creep. In the case where large creep is present, the deck will be susceptible to cracking and present possible serviceability problems.

Overpredicted camber will result in a value that is smaller than designed. The first option for mitigating the problem with overpredicted camber will be to build haunches along the entire length of the girder. If the haunches exceed the specified, upper limit of four inches, lowering the grade of the slab is considered. When this option is unavailable, additional nonprestressed reinforcement may be required to be added to the haunches exceeding four inches. An example of additional reinforcement that is required to be added is shown in Figure 1-7. There will be additional effort with bending and placing the extra nonprestressed reinforcement in the bridge deck to accommodate for large haunches which will increase the labor and ultimately affect the cost. Additionally, the extra concrete will add a larger dead load without increasing the strength of the bridge.

Having differential cambers on adjacent girders has been observed to cause problems at erection of the superstructure and during construction of the haunches. To solve the problem of differential cambers, designers use the appropriate size of haunches or embedment's along the length of the girders to allow for the proper elevation for the construction of the top surface of the deck. If the haunches exceed the maximum or minimum specified tolerances, grade adjustments or adding additional reinforcement is considered. Some cases require a combination

of these solutions to solve the problem as well. Problems resulting with differential cambers of adjacent girders are due to the increase in time for adjusting haunches or grades along with adding non-prestressed reinforcement and concrete materials. In extreme cases, PPCBs may be rejected or the beam seats may be adjusted.

Over and under prediction of camber causes problems with assembling the girders at the bridge site. The problems come from determining haunch heights, adjusting grade elevations of the slab, adding or bending additional non-prestressed reinforcement, and having differential cambers on adjacent girders. Although inaccurate camber prediction problems are often overlooked, they are significant if they lead to serviceability issues, increased cost due to extra materials, and liquidated damages on the project.

### **1.5 Camber Measurement and Prediction**

The causes of error found with instantaneous camber are affected by the designers and precasters. Errors that exist from designers are influenced by the variables used to represent the PPCB along with the accuracy of the prediction method. The errors that are present from the precasters are influenced by the fabrication procedures along with the camber measurement method that fails to accurately capture the camber that is present. Specifically, errors with camber measurement are due to not accurately accounting for the contribution of camber by failing to account for bed deflections, inconsistent top flange surfaces, and friction between the precasting bed and PPCB.

#### **1.5.1 Fabrication Procedure of Precasters and Camber Measurement Technique**

Three precasting plants that produce PPCBs for Iowa were observed by researchers from Iowa State University. Results found that although each plant is within the specifications for measuring camber required by Iowa Department of Transportation (IDOT), there are inconsistencies which can slightly affect camber measurements. The current camber measurement technique used in practice is given by IDOT Materials IM 570 (2013) which requires the following:

- Camber due to prestress shall be measured while the beam is on the bed by checking the beam profile immediately (within three hours) after detensioning and separation of the beam.

- Camber shall be measured from the pallet to the bottom of the beam at mid-point utilizing a conventional tape measure. Camber shall be measured and recorded to the nearest 1/8 inch. Beam shall be resting free on the pallet at the time of the camber measurement. Camber acceptance shall be achieved prior to shipping.
- Noncompliant camber of any beam shall be verified at a later date. Beams cannot be accepted without a compliant camber and specific approval of the engineer.

Over 60 observations from the research team identified the errors that are present with the current camber measurement procedure between the three precasting plants. Although every measurement was not observed at the precast plant from members of the research team from Iowa State, a concept of how precaster's take measurements and variations between the precaster's measuring techniques were noticed. Variations include the time, location, and the surface from which camber measurements are taken from along with the personnel that takes and records the camber. Although the current camber measurement method is efficient for precasters, errors that result from the variations in measurement are due to inconsistent beam depths, bed deflections, and potentially friction if the beam is not lifted.

Fabrication procedures were also monitored at three precast plants. It was observed that prestress force, consistency of concrete mixes, and curing conditions may differ for identical beams cast on separate days and also from the design specifications. Fabricating a PPCB to be identical to the design specifications is difficult due to the accuracy of the instruments, concrete mix designs, and thermal conditions.

### **1.5.2 Designers Prediction Method and Variables Used**

While precaster's camber measurement technique and accuracy of fabrication to specifications accounts for errors with accurate representation of camber, designer's prediction method and variables used for design also contribute to the problem of inaccurate instantaneous camber. Assumptions made pertaining to the prediction technique and variables used have been observed, in accordance with material properties studied by He (2013), to be inaccurate from the actual behavior of a PPCB at transfer.

The prediction technique used by designers for determining camber at the transfer of prestress assumes that the beam is elastic, prestress force is constant throughout the length of the beam, and the beam has a uniform, uncracked cross section. While these assumptions are

typically true for most PPCBs, there may be cases where this is inaccurate. During the transfer of prestress, creep of concrete begins. As mentioned in Section 1.3, creep of concrete is a plastic deformation that is present. Although the behavior of the PPCB is assumed to be elastic, there is some plastic deformation that is present, which makes the prestress force inconsistent along the length of the beam. The location where prestressing strands are tensioned on the beam line, referred to as the dead end, may have slightly less prestress force present. The cross section remaining uniform and uncracked is a variable that is not always achieved. Humps or sags in the top flange surface have been measured and quantified. Additionally, small cracks before the transfer of prestress have also been observed. The assumptions that designers use to predict the instantaneous camber of a PPCB is close to the behavior that is experienced by PPCBs at the transfer of prestress, but may have some discrepancies.

Designers use the Iowa Beam Standard that specifies various material properties used for the design of a PPCB. Specified information includes the strength of the concrete, modulus of elasticity, moment of inertia, prestress force, locations of prestressing strands, and dimensions of the beam. The specified variables are not as accurate due to the fabrication precision by the precasters to within  $\pm 10$  percent and up to 35 percent for the concrete release strengths. This should be accounted for by designers. Typically, precasters produce concrete mix designs that exceed the designed concrete strength to ensure minimum requirements are met within the desired schedule of the precasters. Increase in release strength will increase the designed modulus of elasticity, which in turn will reduce the camber. The moment of inertia is also specified by designers using the gross section properties of the concrete cross section. Failure to account for the rigidity of the prestressed and non-prestressed reinforcement will cause inaccuracies in the predicted moment of inertia value. The prestress force is a specified value that can be difficult to replicate. The precasters have a  $\pm 5$  percent tolerance to obtain the specified prestress force. Agreement of the specified and actual prestress force to which the prestressing strands are tensioned is dependent on the accuracy and precision of the equipment used and the laborers that operate it. Additionally, prestress losses such as elastic shortening and seating loss may be present. The accuracy of predicting the prestress losses will affect the agreement with designed and actual prestress force. Although many variables are influenced by the fabrication of the PPCB, knowledge and correct tolerances of material variables and fabrication procedures will improve the accuracy of the designed instantaneous camber.

## **1.6 Scope of Research**

The scope of this research project is to improve camber predictions at the transfer of prestress; while complimenting work that is being done on improving time dependent, long-term predictions of camber (He 2013). The overprediction and underprediction of instantaneous camber originates from inaccurate design variables, camber prediction technique used in design, accuracy of fabrication from specified values, and inaccurate camber measurement in the plant. Systematically addressing the designers' prediction methods and variables used and the precasters' fabrication and camber measurement procedures will improve the prediction of the instantaneous camber which will significantly improve the desired camber value for long-term camber.

### **1.6.1 Researchers Objectives to Improve Instantaneous Camber Predictions**

In order to successfully complete the scope of this project, a plan was established that involves conducting analysis on bridge girders to validate the accuracy of camber prediction techniques and variables used, organizing and evaluating past camber measurements, and taking camber measurements independent of the precasting plants. Evaluating all three parts of the project has presented valuable insight into camber prediction that has been used to help mitigate the problem of inaccurate camber prediction. In addition, recommendations on variables to use for design, fabrication procedures, and a plan to measure instantaneous camber in agreement with measurements taken by contractors at the jobsite was discussed.

Analytical camber predictions on specific beams were made to determine the accuracy with which camber can be predicted. This process helped find the most suitable variables used for camber prediction, including the modulus of elasticity, prestress force that is initially applied, and prestress losses. Determining the magnitude of how much variables will influence camber gave designers insight into which variables to adjust to represent current conditions to accurately predict camber. Through these analytical evaluations and their comparisons with experimental results, a suitable simplified approach for determining camber during the design process was established.

Quantifying the prediction accuracy and comparing predicted values to measured camber from multiple beams portrayed where the current practice is most effective and also exposed why

camber is sometimes overpredicted whereas sometimes it is underpredicted. Improvements in calculating the predicted camber along with procedural improvements relating to fabrication and measuring camber should be made in order to determine a simplified approach to improve camber predictions.

### **1.7 Thesis Layout**

The report is composed of six chapters that describe the background methods and results of accurately predicting and measuring instantaneous camber. A summary of each chapter is listed below:

- Chapter 1-Introduction: An introduction of prestressed concrete, the current challenges with predicting instantaneous camber, the scope of research, and the research methods were discussed.
- Chapter 2-Literature Review: A summary of published camber studies that includes the topics of camber measurement, material properties, prediction methods, and fieldwork were discussed.
- Chapter 3-Methods: Description of the methods that were used to measure camber at the transfer of prestress by precast plant personnel and by the research team.
- Chapter 4-Analytical Camber Prediction: In this chapter, methods that were used to predict instantaneous camber by researchers were evaluated and discussed.
- Chapter 5-Results and Discussion: Data that was gathered from field observations and measurements along with analytical camber predictions were analyzed and discussed.
- Chapter 6-Conclusions: A summary of the results of from field evaluation, analytical predictions, conclusions found from this study, and recommendations for future practices.

## CHAPTER 2. LITERATURE REVIEW

### 2.1 Introduction

This chapter introduces the background of factors that affect camber such as material properties, camber measurement techniques and methods of estimating instantaneous camber; and how they have been accounted for in the past. The challenges of predicting instantaneous camber are shared by the designers and precasters. Current challenges that exist for designers are the accuracy of variables used for design and the prediction techniques, while precasters face difficulties with the current measurement method and fabrication procedures adopted for PPCBs. These challenges result in camber that may vary by as much as 50 percent (Tadros et al. 2011). To improve and understand instantaneous camber prediction on PPCBs, an investigation of past studies was undertaken and discussed in this chapter.

Factors that affect camber, such as variables used in design, can complicate the ability for designers to accurately predict camber. Variables that are used to calculate the instantaneous camber that affect the prediction accuracy include the modulus of elasticity of the concrete, the prestress force, and the estimated prestress losses. Predicting the modulus of elasticity of concrete has presented problems due to the variability associated with concrete properties. Each concrete mix is composed of disproportions of materials and different curing conditions that can complicate the prediction of this variable. Additionally, the prestress force applied to the PPCB can lack accuracy in the tensioning procedure and with predicting prestress losses. For long-term camber, further challenges arise as concrete and prestressing properties continuously change with time. The rearrangement and reduction in concrete materials as a result of the creep of concrete and shrinkage along with relaxation of the prestressing strands will result in a reduction of prestress force. The creep of concrete, shrinkage, and loss of prestress force will affect the long-term camber and present further challenges with camber prediction.

Difficulties with measuring camber are present at the transfer of prestress and throughout the life of the girders. Many measurement techniques have been recommended and some are more frequently being used than others for measuring camber. Methods employed differ among precasters and regions, and are certainly different from those used by other researchers for accurately measuring camber. A common goal of finding a method to measure camber accurately without extensive amounts of time is desired. The different methods of taking camber



measurements will be outlined and discussed in Section 2.3 along with the potential errors that each method can present.

Camber prediction methods have been investigated in past research as well. This topic includes simplified methods as well as methods such as those based on advanced finite element models. The accuracy of simplified hand calculations and finite element models are dependent on the accuracy of the material properties of concrete and steel, and the assumptions used for each method. Reviewing previous research in Sections 2.2-2.4 helped determine assumptions used in both simplified and advanced models that cause discrepancies between analytical and measured camber.

## **2.2 Factors Influencing Instantaneous Camber**

In addition to errors associated with the measurement technique and camber prediction technique, variables such as the prestress force, prestress losses, and modulus of elasticity affect the accuracy of instantaneous camber prediction. A review of past research of the factors that influence camber predictions is presented in this section.

### **2.2.1 Prestress Losses**

Prestress losses are the loss of tension in the prestressing steel. Prestress losses are subtracted from the tensioning prestress force to determine the effective prestress force that is present in a PPCB. Underestimation of prestress losses will result in reduction of camber while overestimation of prestress losses can result in excessive camber.

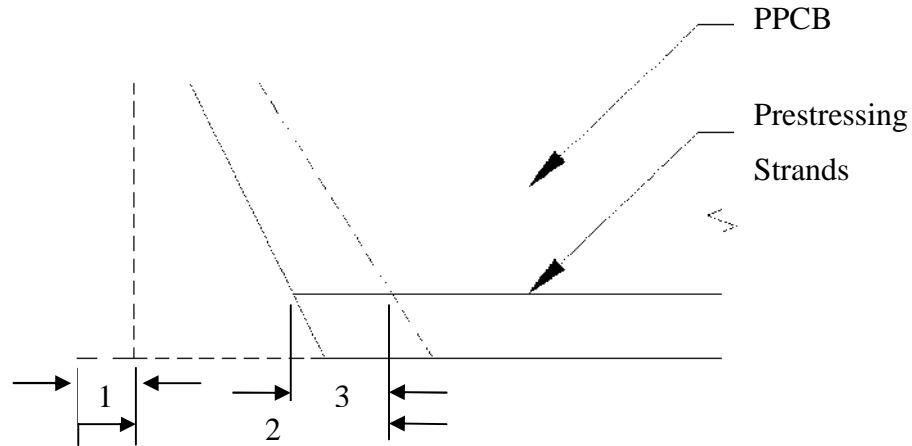
Prestress losses can be divided into the time periods of instantaneous and long-term losses. Instantaneous prestress losses primarily include elastic shortening, seating, and relaxation after the initial tensioning to the time of bonding to the concrete. Both seating and relaxation are sometimes ignored when calculating instantaneous prestress losses because they are typically small in magnitude. Long-term losses include the instantaneous losses as well as losses due to creep and shrinkage of concrete. The primary focus of this study is to determine the instantaneous camber, and thus instantaneous losses will be discussed in detail.

Various models used to predict prestress losses differ from each other by their ability to apply material properties, time increments, and prestress losses. According to Gilbertson et al. (2004), the parameters that have the greatest impact on prestress losses are the initial strand

stress, initial concrete strength at release, relative humidity, and strand eccentricity. Methods of predicting prestress losses have different levels of computational involvement, time, and accuracy. Three common methods listed in order of assumed accuracy according to Jayaseelan et al. (2007) are the time-step method, refined method, and the lump sum method. The time step method requires dividing the time into intervals as the concrete ages (Jayaseelan et al. 2007). Iterating the stress in the strands for each time step allows for the calculation of the prestress values at a specific time. It is the most involved method as multiple iterations are usually required. Refined methods use prestress losses from elastic shortening and time dependent losses that are calculated separately. The total loss is the sum of the individual losses that are calculated. The lump sum loss method has utilized parametric studies for beams based on average conditions. Trends obtained from parametric studies have resulted in the lump sum method (Jayaseelan et al. 2007). Naaman (2004) states that although the three procedures vary in the method used to determine the long-term prestress losses, they all use primarily the same method of calculating instantaneous losses. The following in Sections 2.2.2-2.2.5 focus on the agreement with designed and measured instantaneous losses.

### **2.2.2 Elastic Shortening**

When prestress is transferred to a PPCB, the prestressing strands exert a prestress force that acts along the length of the beam. This force will cause the beam to shorten from its original length by a small amount. Due to the bonding between the prestressing strands and the concrete, the prestressing strands shorten as well. As a result, there is a reduction of the amount of initial prestress strain in each strand and thus the overall prestress force of the beam is reduced. Conversely, if a beam cambers upward, the self-weight of the beam causes an increase in the strain of the prestressing strands that are located below the neutral axis. The sum of the three components is referred to as elastic shortening and is further discussed in Chapter 4.3.3.



- where
- 1 = Girder shortening due to applied prestress force.
  - 2 = Girder shortening due to the application of prestress at the centroid of the prestressing strands.
  - 3 = Increase in girder length due to self-weight.

**Figure 2-1: Girder Length After the Transfer of Prestress**

Throughout different code changes, calculating the elastic shortening by determining the average compressive stress in the concrete at the center of gravity of the tendons has remained constant. Differences have occurred with how the average compressive stress in the concrete at the center of gravity of the tendons is calculated.

Comparing different methods of calculating elastic shortening with measured elastic shortening values allowed researchers to see which method agrees best. Tadros et al. (2003) found that the proposed detailed method of calculating prestress losses agreed with the measured value. This method warrants neglecting the calculation of elastic shortening losses when using transformed section properties. Results of Table 2-1 shows seven PPCBs from different locations and the agreement with the measured vs. estimated elastic shortening values.

**Table 2-1: Measured versus Estimated Prestress Losses (Tadros, 2003)**

Girder	Elastic Shortening		
	Measured (kips)	Estimated (kips)	Percent Error
Nebraska G1	17.02	19.67	15.6
Nebraska G2	16.50	19.67	19.2
New Hampshire G3	25.17	17.94	28.7

**Table 2-1 continued**

New Hampshire G4	24.42	17.94	26.5
Texas G7	12.88	14.71	14.2
Washington G18	27.62	20.87	24.4
Washington G 19	25.49	20.87	18.1

Five prestress loss methods, including the proposed detailed method that was used in Table 2-1, were compared in Tadros et al. (2003). The five different methods, which can be seen in Table 2-2, included an AASHTO LRFD Lump-Sum method, AASHTO LRFD Refined method, proposed approximate method using gross section properties, proposed approximate method using transformed section properties, and the proposed detailed method. Results from Table 2-2 show that there are slight differences with calculated elastic shortening losses. For the purpose of comparison between the methods when using transformed section properties, elastic losses were neglected and the total elastic shortening losses due to a combination of prestress transfer and girder self-weight were estimated.

**Table 2-2: Comparison of Prestress Losses and Concrete Bottom Fiber Stress (NCHRP 496 2003)**

Loading stage	Loading	Prestress loss method* (ksi)					Concrete bottom fiber stress (ksi)				
		1	2	3	4	5	1	2	3	4	5
Prestress transfer	$P_i$	26.13	29.50	29.50	26.13	29.50	4.16	4.69	4.69	4.16	4.69
Girder self-weight	$M_g$	-6.01	-6.80	-6.80	-6.01	-6.80	-1.08	-1.20	-1.20	-1.08	-1.20
	Elastic loss		-2.95	-2.95		-2.95		-0.47	-0.47		-0.47
Subtotal		20.12	19.75	19.75	20.12	19.75	3.08	3.02	3.02	3.08	3.02

\* Method 1: Proposed approximate method with transformed section properties.

Method 2: Proposed approximate method with gross section properties.

Method 3: AASHTO LRFD Lump-Sum method with gross section properties.

Method 4: Proposed detailed method with transformed section properties.

Method 5: AASHTO-LRFD Refined method with gross section properties.

Ahlborn et al. (2000) instrumented two PPCBs and compared measured prestress losses to predicted values using the following methods: Time Step Methods, PCI Committee (1975), PCI

Handbook (1992) and AASHTO LRFD (1996). Results in Table 2-3 are in terms of the percentage of strand stress at the time of initial tensioning. Evaluating the percent loss with respect to the initial tensioning value includes relaxation losses however, this value is affected by the ambient temperature for Girder I and Girder II.

**Table 2-3: Measured Losses and Predicted Design Losses**

	Measured <sup>1</sup>		Time Step	Time	PCI	PCI	AASHTO
	Girder I*	Girder II*	Nominal Design Case <sup>2</sup>	Step HSC Nominal Case <sup>3</sup>	Committee (1975)	Handbook (1992)	(1996)
Initial	15.5 %	18.6%	11.2%	13.8%	10.6%	9.9%	10.2%

<sup>1</sup> Lower bound measured losses from vibrating wire gages embedded in each girder.

<sup>2</sup> Predictions using nominal design values with normal strength concrete relationships.

<sup>3</sup> Predictions using nominal design values with high strength concrete relationships.

\* Concrete stress before transfer is assumed to be zero.

Results in Table 2-3 indicate that the Time Step HSC (High Strength Concrete) Nominal Case has greater initial prestress losses than the Time Step Nominal Design Case. The elastic modulus that correlates with the measured HSC model is lower than the normal strength model, which results in a higher elastic shortening loss seen in Table 2-3 (Alhborn et al. 2000). Additionally, methods such as the PCI Committee (1975), PCI Handbook (1992), and AASHTO (1996) use normal strength concrete properties to obtain prestress losses as well. The method that agreed best with the measured prestress losses from the two girders that were instrumented is the Time Step HSC Nominal Case. This is because high strength concrete was used in Girders I and II and was also used in the prediction method.

### 2.2.3 Seating

Seating is the movement of prestressing steel when it is allowed to rest in the anchorage. After the prestress is applied, anchoring devices (chucks) are placed around the prestressing strands to hold the prestress force while workers fabricate the beam and place the concrete in the forms. The chucks are known to slip a small distance when the strands are initially tensioned. The slip or seating will result in a loss of prestress force. Seating losses are typically small and if a long prestressing bed is used, are ignored (Zia 1979). However, the Committee on Prestress

Losses (PCI 1975) suggests that seating losses should be taken into account, regardless of the length of the prestressing bed, when determining the effective prestress force.

#### **2.2.4 Relaxation**

Relaxation occurs due to the loss in tension in a prestressing strand with respect to time when it is held at a constant length. The effect of losing tension in a stressed prestressing strand reduces the prestressing force. Relaxation occurs from the time the prestressing strands are tensioned to the end of the service life of the member. Methods used to predict relaxation typically neglect relaxation from the time of tensioning to the time of transfer of prestress. However, ACI Committee 343R-95 suggests including the relaxation loss during the time before the transfer of prestress.

#### **2.2.5 Modulus of Elasticity**

The modulus of elasticity is an important variable in prestressed concrete. Concrete is a non-homogeneous material composed of aggregates, cement paste, water, and additional chemicals. Predicting the behavior of a composite material has posed difficulty for designers, researchers, and precasters. Tadros et al. (2003) states in NCHRP 496 that factors that affect the modulus of elasticity are the moisture content, loading rate, specimen shape and size, stiffness of cement paste, porosity and composition of the boundary zone between paste and aggregates, stiffness and porosity of the aggregates, and proportion of the concrete constituents. Additionally, the behavior of the modulus of elasticity of concrete is further complicated when estimating this value at a specific time. The AASHTO LRFD (2010) method of computing the modulus of elasticity accounts for time dependent effects by using the compressive strengths. The factors that influence the compressive strength gain over time are the fineness of cement (Type I versus Type III), the curing procedure, (moist, heat or steam cured), and the reduction of water-to-cementitious materials ratio for high strength concretes (Ahlborn et al. 2000). If the beam is steam cured, the strength of the test cylinders loosely reflect the maturity of the concrete by the strength that is achieved. Therefore, time dependent effects on the modulus of elasticity can be accounted for by using the release strength following the AASHTO LRFD (2010) recommendation for finding  $E_c$ .

As stated in Section 1.5.2, the specified modulus of elasticity is dependent on the release compressive strengths when using AASHTO LRFD (2010). The measured release strengths are required to be greater than the designed strength in order to transfer the prestress to the PPCB. Increase in compressive strength will give a larger modulus of elasticity, which will decrease the camber. Adjusting the compressive strength so that it is representative of the strength of the beam is important for accurately predicting camber. O’neill et al. (2012) suggests that release strength data that was collected from 2006-2010 on average is 15.5% higher than the  $f'_{ci \text{ design}}$  with some cases reaching as high as 35%. Rizkalla et al. (2011) found that release strengths were underpredicted by 24% on average with the maximum ratio of measured to designed release strength of 110 percent. The 24% underprediction of release strength affected the modulus of elasticity by 15%. To solve this problem, Rizkalla et al. (2011) suggests a multiplier of 1.25 to be used to account for the underpredicted release strengths. Table 2-4 shows past studies where release strengths were obtained and measured. Based off of the average ratio of measured to designed release strengths, multipliers were developed by both O’neill et al. (2012), Rizkalla et al. (2011), and Rosa et al. (2007) to accurately predict the modulus of elasticity as seen in Equation 2-1.

$$f_{ci}^* = f'_{ci} * \text{multiplier} \quad (2-1)$$

where:  $f'_{ci}$  = the specified concrete strength

**Table 2-4: Multipliers for Compressive Strengths**

Reference	Multiplier for Instantaneous Release Strength	Multiplier for Long-Term Release Strength
O’neill et al. (2012)	1.15	-
Rizkalla et al. (2011)	1.25	1.45
Rosa et al. (2007)	1.10	1.25

Determining the effect that release strength has on the modulus of elasticity and ultimately camber was conducted by O’neill et al. (2012). Due to the modulus of elasticity being a function of the square root of the concrete strength, the increase in compressive strength does not correlate to the same decrease in camber. In this study, the modulus of elasticity was determined by using the ACI 363R-10. The results revealed that the AASHTO LRFD 2010 equation for the modulus of elasticity should replace the ACI 363 equation that was currently used by MnDOT in

camber calculations due to the ability to account for stiffer concrete that was being produced at the precast plant (O'Neill et al. 2012). Therefore, the decrease in the design release camber by increasing the concrete strength was replicated in Chapter 5 using the AASHTO LRFD (2010) method of determining the modulus of elasticity.

**Table 2-5: Impact of High Strength Concrete Release Strengths on Camber as per O'Neill et al. 2012**

Percent Increase in Concrete Strength	Percent of Reduction in Release Camber (ACI 363)
5%	1.6%
10%	3%
15%	4.5%
20%	7.6%
25%	7.1%
30%	8.3%
35%	9.4%

### 2.3 Camber Measurement Technique

Over the past several decades, research efforts attempted to resolve camber measurement problems at the transfer of prestress. Many methods have been recommended and some are currently being used for measuring camber in precast plants. Methods include measuring camber with the stretched-wire system, survey equipment from the top or bottom flange, tape measure from the bottom flange, and photogrammetry.

Inaccurate camber measurement techniques can fail to represent the correct camber that is actually present in a PPCB. Unexpected camber growth will ensue when they are based on inaccurately measured camber. When evaluating if analytical prediction methods are accurate based off the agreement with measured camber, the accuracy of the measurement technique is equally important. Eliminating potential errors due to the measurement technique will allow researchers to determine the magnitude of errors relating to the analytical camber. The errors associated with measuring camber can be related to the accuracy of the instrument that is used,



the location from which measurements are taken, the time when camber is measured, and additional measurement factors such as friction between the precasting bed and beam, bed deflections, and the roughness of the surface where camber is measured from. Evaluating the measurement technique based off these factors can provide a guide to accurate measurement techniques. The following section investigates the methods used to measure camber from past research.

### 2.3.1 Stretched Wire Method

A system that has been used by precasters and multiple researchers is the stretched-wire method. This method uses a wire that is stretched along the length of the girder. The distance between the string and the top flange at midspan is measured to obtain the camber measurement.

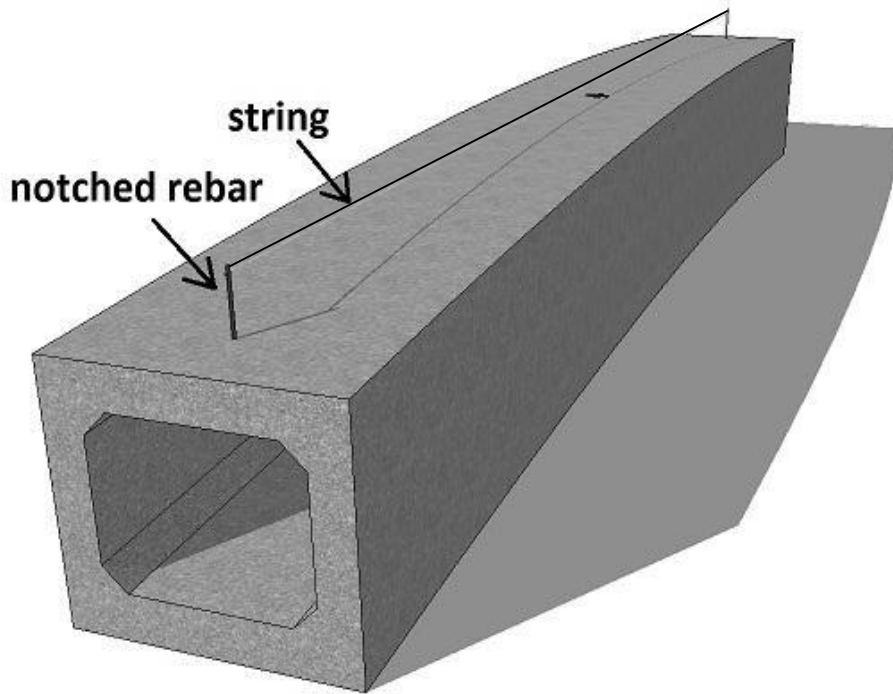


**Figure 2-2: Girder with Rebar and String in Place for Camber Measurements (Rizkalla et al., 2011)**

The method used for measuring camber with the stretched-wire method involves attaching the string at each end of the beam at the same elevation. The string is pulled tight or calibrated to a certain tension. A measurement of the distance between the string and the top of the girder at midspan is taken. Since the midspan measurement is taken with respect to the elevation of the

ends of the girder, the distance between the string and the top flange at midspan is a representation of camber. Precasters and past research that have used the stretched-wire system have variations regarding the anchorage of the string to the ends of the beam, the materials used, the location from where the measurement was taken, and the procedure for measuring camber. All of the variations influence the accuracy of instantaneous camber.

Anchoring the string at each end of the girder was done multiple ways. The most common way to attach the string to the girder end is by an anchor bolt that is attached to the beam. Anchor bolts can be embedded or drilled into the concrete surface. Figure 2-3 shows the string being connected to the end of a beam using an anchor bolt. In Figure 2-3, the pulley that is shown was also used to position the string at the correct height at the anchored end. Another alternative to using anchor bolts to connect the string to the ends of the beam is embedding pieces of rebar. Rizkalla et al. (2011) attached the string to the end of the beam by embedding a piece of rebar on each end with a notched surface (Figure 2-1). The notched surface was a specified distance above the end of the top flange to ensure that end elevations will be equal. If unequal end elevations were present, the measured camber would not represent the camber accurately.



**Figure 2-3: Anchored End with a Pulley of Wire Used for the Stretched-Wire System  
(O’neill et al. 2012)**

A sag in the string due to the self-weight may be present when using the stretched-wire system. The accuracy may depend on the type of wire, the tension put on the wire, and the ambient temperature. Variations from piano wire used by Kelly et al. (1987) to 80 pound fishing wire used by O’neill et al. (2012) have been used in the past. Additionally, calibrating the wire before camber measurements are taken so that the discrepancy caused by temperature and relaxation in the wire is reduced is important to the accuracy of the stretched wire system. Various methods of calibration have been used in the past. One method to calibrate the tension in the wire includes attaching a mirror and ruler at midspan (Figure 2-4). In this method, the mirror is used to eliminate the effects of parallax while the ruler reading is recorded and serves as a reference point to the initial position of the string at midspan. Subsequent measurements are then compared to the baseline reading. Calibration can occur by increasing tension with mechanical means or by hanging a weight at the end of the string as seen in Figure 2-5. Another method that is used is hanging a 35 pound trolley from the midspan (Figure 2-6). Hanging the trolley minimizes the vibration in the wire at midspan which can misrepresent camber. The method involving a trolley at midspan would also require adjustment to the tension in the wire due to relaxation and thermal effects.



**Figure 2-4: Ruler and Mirror Located at Midspan (O'Neill et al. 2012)**



**Figure 2-5: Free End of Stretch-Wire System with Weight and Pulley (O'Neill et al. 2012)**

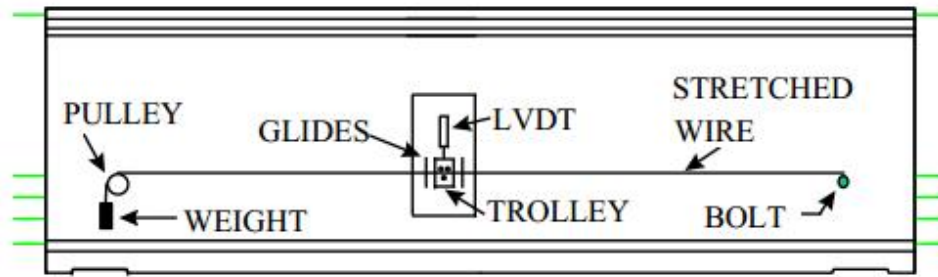


**Figure 2-6: Stretched Wire System with a Weighted Trolley at Midspan (Barr et al. 2000)**

The location of camber measurement using the stretched-wire system has been observed to be different from study to study. Kelly et al. (1987) measured camber using the stretched wire system from the bottom flange. Complications with measurements from the bottom flange are present due to inconsistent beam depths. Using the stretched-wire method, Rizkalla et al. (2011) takes camber measurements from the top flange using rebar that extends above the top flange surface. This is beneficial because the same reference point from the top flange will be used by contractors at the bridge site to set the haunch heights (see section 1.5).

Results from using the stretched-wire method may differ depending on the time the camber measurements are taken. A camber measurement was taken before the transfer of prestress by O'Neill et al. (2012) to establish a datum. Additional measurements were taken immediately after the transfer of prestress and periodically throughout the life span of the girder. Taking the original datum ensured that the camber measurements could be compared by a similar reference point and that any inconsistencies in the beam depth would be accounted for.

Multiple errors can be eliminated with the stretched wire system method by eliminating the influence of bed deflections, friction between the beam ends and the precasting bed if the measurement occurs after the beam has been lifted, and inconsistent top flange surfaces. Variations regarding the anchorage of the string to the ends of the beam, the materials used to take measurements, the measurement location, and the procedure for measuring camber can influence the accuracy in the camber too.

### 2.3.2 Survey Equipment

Survey equipment such as a transit, total station, and laser level have been used to measure camber. The survey equipment is used to take elevation readings of the PPCB to determine the

relative displacement of the midspan with respect to the ends. Subtracting the average elevation readings of both ends from the midspan elevation reading will give the camber at the midspan. Variations of this method depend on the location of the measurements, the time the measurement was taken, and the equipment used.

The location of the camber measurement when taken with survey equipment has been observed to differ with past studies. Rosa et al. (2007) took camber measurements from the web of the beam using a wooden template to reduce errors. A template was made and fitted to the web with a ruler attached (Figure 2-7). Survey readings of the ruler were able to be taken at the ends and at the midspan of the girder to determine camber. The discrepancy between the web and the bottom flange of the girder due to inconsistencies in the beam depth were observed to be within the range of  $\pm 0.25$  inches which resulted in a 7.1 percent difference. Measuring camber from the bottom flange using a laser level was conducted by Hinkle (2006). A template was made that fit on the top of the bottom flange (Figure 2-8). This ensured that the measurement consistently occurred from the same location on the bottom flange. Similarly, Woolf et al. (1998) measured camber using a grade rod that was fabricated to have a 90 degree angle that extended below the bottom flange to obtain the camber.

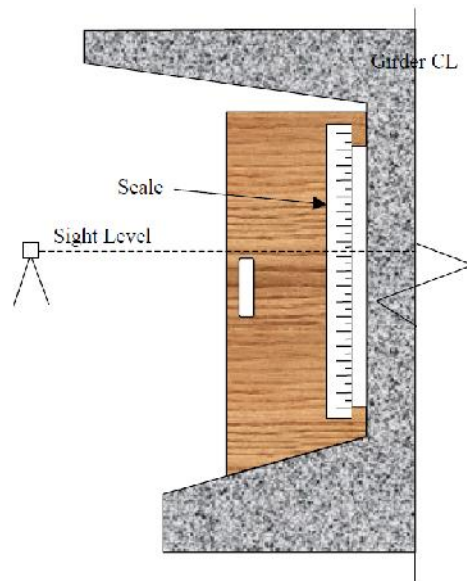


**Figure 2-7: Camber Measuring Template (Rosa et al. 2007)**





**Figure 2-8: Taking Readings with Laser Level Surveying System (Hinkle et al. 2006)**

Measurements from the top flange were also taken by Johnson et al. (2012). In this study, bolts were embedded into the surface so that elevation measurements were taken from the same location at various times throughout the girders life (Figure 2-9).



**Figure 2-9: Camber Measurement Marker (Johnson et al. 2012)**

The time the camber measurement is taken affects the accuracy. During the transfer of prestress, Woolf et al. (1998) noticed friction between the precasting bed and beam inhibited the

camber from reaching its full potential. Due to the girder shortening after the transfer of prestress, the ends will attempt to overcome friction and slide toward each other. When the girder ends overcome the friction of the precasting bed, the camber increases at midspan. The procedure for quantifying the increase in camber due to friction was determined by taking the average of camber measurements before and after the girder was lifted and placed down on the precasting bed after the transfer of prestress. Taking the average of the camber readings before and after the beam was lifted was believed by O'Neill et al. (2012) to be a close approximation of reverse friction, or the midspan elevation decreasing due to reverse of the friction forces. In a similar study, Rosa et al. (2007) found the influence of friction to be 0.15 inches. The study conducted by Woolf et al. (1998) and O'Neill et al. (2012) signify the importance of taking camber measurements before and after lifting the PPCB to determine the magnitude of friction. In addition to friction, creep of concrete will begin immediately after the transfer of prestress. The constant prestress force that is applied to a PPCB will allow creep to occur, thus increasing camber with respect to time. Failure to take camber measurements where friction and creep of concrete is misrepresented will inhibit the accuracy of camber. The topics of friction and creep are discussed in Chapter 5 in more detail.

### **2.3.3 Tape Measure**

Using a tape measure to determine camber is one of the simplest ways to measure camber. Precasters typically measure the camber of the girders while they rest on the precasting bed or while they are suspended by a travel crane. In this method, instantaneous camber measurements are taken by reading the midspan elevation relative to the precasting bed with a tape measure (Figure 2-10).





**Figure 2-10: Camber Measurement with a Tape Measure at Midspan of a PPCB (Iowa DOT Prestress Inspection, 2013)**

This measurement method has inaccuracies due to not accounting for bed deflections, friction between the precasting bed and beam if the beam is not lifted, and inconsistent beam depths along the length of the girder. In a study conducted by Rosa et al. (2007), it was observed that precasters took camber measurements from the bottom flange while the beam was suspended by travel cranes. Camber is calculated from this method by subtracting the midspan measurement from the average of the two end measurements. Difficulties from this technique that will result in inaccurate measurements include the travel cranes not being able to hold the beam at a consistent elevation, the effect of wind acting on the beam, and an increase in camber due to the location of lifting the beam.

#### **2.3.4 Photogrammetry**

In addition to the methods listed above, camber measurements have been recorded by using photogrammetry. Photogrammetry involves taking two dimensional photographs and relating them to three dimensional measurements of an object. The process involves taking pictures of an

object with targets on it and control points around it before and after an event. The difference between the two pictures allows researchers to determine the change in deflection of a beam. Typically, this measurement technique is not used by precaster's due to the high cost, time commitments, and limited use.

The specific experiment conducted by Jauregui et al. (2003) investigated noncontact photogrammetric measurements on two bridges and one laboratory test on a girder. The test compared the method of photogrammetry to dial gauge readings, a total station, survey level and rod, and also a finite element model. Results in Table 2-6 show that close agreement with the different methods and photogrammetry are possible. Errors introduced between methods could be resulting due to uneven surface conditions along with inaccuracies of the equipment that is being compared to the photogrammetry.

**Table 2-6: Experiments and Results from Noncontact Photogrammetric Measurement of Vertical Bridge Deflections (Jauregui et al. 2003).**

<b>Test and Specimen</b>	<b>Experiment</b>	<b>Methods Compared with Noncontact Photogrammetry</b>	<b>Results</b>
<b>Laboratory Experiment-W21X62 Steel Beam</b>	1. Loaded with steel plates to compare deflection.	Dial Gauge Readings	0.02-0.05 in. difference in measurements which represent 2-10% accuracy.
<b>Field Test 1- Prestressed Concrete Bridge Girder</b>	1. Initial girder camber compared with level and rod.	Level and Rod	Agreement of 1-10% of the maximum measured camber.
	2. Girder deflection caused by concrete deck and traffic barriers.	Total Station	Agreement of 0.13 inch with total station before and after concrete deck and traffic barriers were cast.
<b>Field Test 2- Noncomposite Steel Girder</b>	1. Live load girder deflections with two dump trucks (56 kips each)	Level Rod and Finite Element Models	0.02-0.06 agreement between level rod readings, and conjugate beam method.

Of the measurement methods used in the past by researchers and precasters, errors can be introduced by bed deflections, friction between the precasting bed and beam, inconsistent top flange surfaces that affect camber, or even operator error. Some methods, although convenient,

are not practical from a researcher's standpoint as they can lack accuracy. Contrarily, labor intensive methods of taking camber measurements are inefficient for the tight schedule precasters are often faced with.

## **2.4 Methods of Predicting Instantaneous Camber**

When predicting camber, several methods have been used by designers. Designers generally use computer programs to predict instantaneous and long-term camber on prestressed concrete beams. Examples of some of these programs include PG Super (Bridgesight 2008-2010), Conspan (CONTECH Construction Products Inc., 2002-2010), CSI Bridge (Computers and Structures, Inc., 1978-2011), and Pbeam (Suttikan, 1978). Along with predicting camber using computer models, designers can also use simplified, hand calculation methods to verify results. Verifying the moment area method, Ahlborn et al. (2000) found that camber prediction results were nearly identical for the nominal design case when compared to the finite element model in Pbeam (Suttikan, 1978). Additionally, variables such as prestress losses and modulus of elasticity also affect the accuracy of predicting instantaneous camber. An investigation into the methods used to predict instantaneous camber along with variables important to the camber calculations is discussed.

### **2.4.1 Moment Area Method**

The moment area method uses linear elastic analysis to predict the upward deflection of prestressed concrete beams. Assumptions when using the moment area method for a prestressed concrete beam include that the prestress force is constant along the beam length, the member is not undergoing plastic deformation, and the cross section is uniform and uncracked. When these assumptions are used, the moment area method captures the behavior of a PPCB at release and can be considered adequate for predicting instantaneous camber. Using simple elastic beam formulas, the downward deflection due to self-weight of the beam can also be determined. Adding the upward and downward components gives the total instantaneous camber.

The moment area method uses the moment created by the prestressing strands to relate to the beams elastic deflection curve (Hinkle 2006). The first step in using the moment area method is determining the moment diagram due to the prestress force. Multiplying the effective prestress force by the eccentricity of the prestressing strands from the centroid of the cross section will

provide the moment diagram at a specific location of the beam (Figure 1-1). Since the profile of prestressing strands is usually composed of straight bottom strands, sacrificial top strands, and harped layouts, the moment for each set of strands is determined independently. Taking the sum of the moments caused by the straight bottom strands, sacrificial top strands, and harped strands will give the total moment due to prestressing at certain locations of the beam.

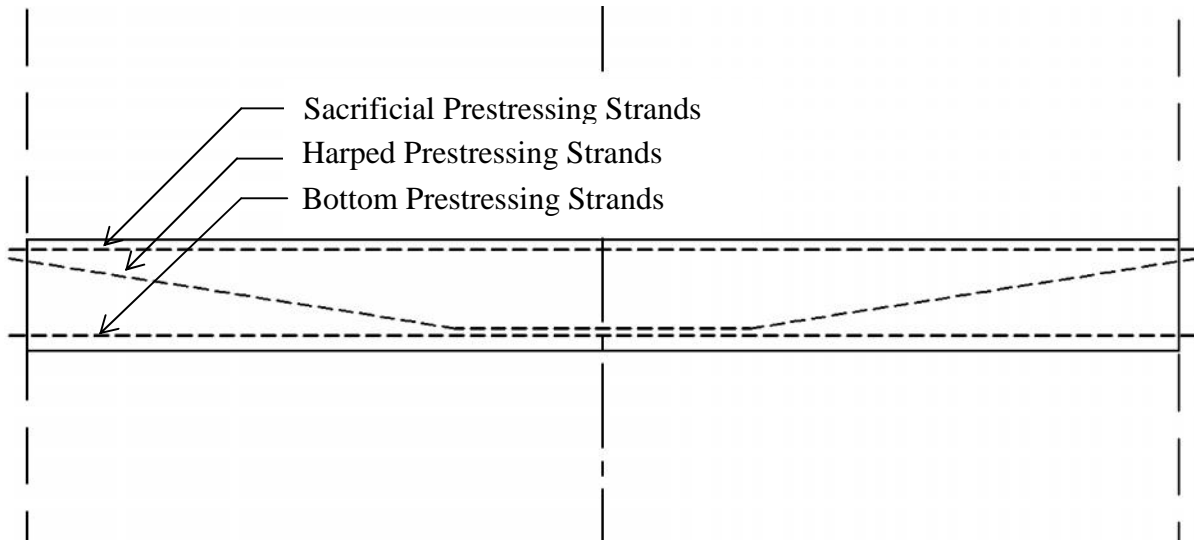


**Figure 2-11: PPCB with Sacrificial, Harped, and Bottom Prestressing Strands**

Once the moment diagram is established, it is integrated. This integrated area is multiplied by the distance from the end of the beam to the centroid of the section of interest. In order to simplify calculations, various sections of the moment diagram can be broken into different areas as seen in Figure 2-12. Taking the product of the area and distance to the centroid of the section on the moment diagram will give the moment ( $M$ ) of the beam. Dividing the moment ( $M$ ) by the product of the modulus of elasticity ( $E$ ) and the moment of inertia ( $I$ ) will give the upward deflection due to the prestressing.

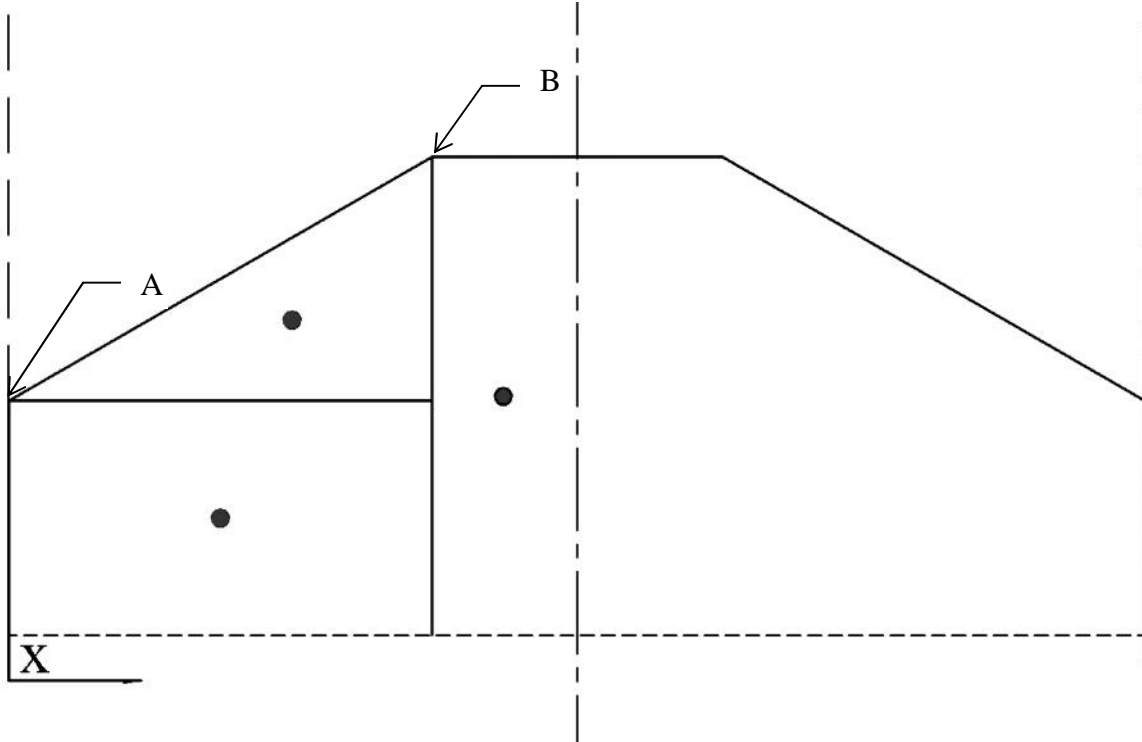


**Figure 2-12: Moment Diagram due to Sacrificial, Harped, and Bottom Prestressing Strands**

Determining the downward deflection due to the self-weight of the beam is determined using an elastic beam formula. Precast, prestressed concrete beams are simply supported until composite action is achieved when the piers and girders are bonded together through a

diaphragm. The elastic equation for a simply supported beam at midspan is  $\Delta_{sw} = \frac{5wl^4}{384EI}$ . The moment of inertia can vary along the length of the beam depending on the profile of the prestressing strands and the value  $I$  is based on transformed section properties. Adjusting the moment of inertia so that it is representative of the behavior that the beam is experiencing is important for accurate results. The final camber can be determined by adding the deflection from the upward deflection due to prestressing and the downward deflection due to self-weight (Equation 1-1).

Naaman (2004) presents pre-derived formulas for prestressing and deflection based on multiple prestressing and loading cases. The pre-derived formulas shown are obtained by the moment area method but can be verified by other linear elastic methods. The moment area

method was used for this study however; Naaman's method of using the pre-derived formulas was not used for calculating instantaneous camber due to the inability to account for the transfer length and material properties that vary.

### 2.4.2 Elastic Shortening

Elastic shortening occurs when there is a reduction in strain in the prestressing strands at the transfer of prestress due to the concrete member shortening. The three components, listed in Section 2.2.4, contribute to the total elastic shortening loss. Representing the change in stress of the prestressing strands due to elastic shortening is completed in different ways, which is further discussed in subsequent sections.

#### 2.4.2.1 AASHTO LRFD (2010)

The AASHTO LRFD method for predicting elastic shortening is listed in Equation 2-2. This method involves calculating the concrete stress at the center of gravity of the prestressing strands and multiplying it by the ratio of the modulus of elasticity of steel to concrete.

$$\Delta f_{pES} = \frac{E_p}{E_{ci}} f_{cgp} \quad (2-2)$$

where:  $E_p$  = modulus of elasticity of prestressing steel (ksi)  
 $E_{ci}$  = modulus of elasticity of concrete at transfer or time of load application (ksi)  
 $f_{cgp}$  = the concrete stress at the center of gravity of the prestressing tendons due to the prestressing force immediately after transfer and the self-weight of the member at the section of maximum moment (ksi)

Determining the concrete stress at the center of gravity of the prestressing tendons has been done multiple ways. Typically, iterations are required to determine the stress in the strands after elastic shortening losses occur. Variables that are required to determine the concrete stress at the center of gravity include the initial jacking force of the prestressing tendons, the moment of inertia, area of the section, the eccentricity between the center of gravity of the section and the prestressing strands, and the moment caused by the girder self-weight. Differences with the

variables used to calculate elastic shortening losses occur with cross section properties and the initial jacking force that is used.

When determining the initial jacking force prior to the transfer of prestress ( $P_o$ ), calculations by the Department of Transportations have been observed to be different. The Iowa Beam Standard (2011) suggests that the initial jacking force be taken as 72.6% of the nominal prestressing force while AASHTO LRFD (2010) and ACI 318-08 was taken as 75% of the nominal strength multiplied by the area of the strand. Using a reduced percentage of the nominal prestressing force, such as 72.6%, is done to eliminate the inaccuracies with tensioning prestressing strands due to losses associated with cold weather stressing. When reducing the prestress force from 75% to 72.6% of the nominal prestressing force, additional strands may need to be added to account for the reduction in prestress. However, the standard remains constant at 75% for most applications unless specified differently.

It is stated in AASHTO LRFD (2010) that if gross section properties are used, the prestress force may be assumed to be 90 percent of the initial prestress force before transfer. Through iteration of  $f_{cgp}$ , the prestress loss due to elastic shortening will converge. The concrete stress at the center of gravity can be calculated using Equation 2-3 when gross section properties are used.

$$f_{cgp} = \left( \frac{P_i}{A_g} + \frac{P_i e^2}{I_g} \right) - \frac{M_g e}{I_g} \quad (2-3)$$

where:  $P_i$  = total prestressing force immediately after transfer (initially assumed to be 90 percent of jacking force)

$e$  = eccentricity of the centroid of the prestressing strands at midspan with respect to the centroid of the girder

$A_g$  = area of the gross cross section of the girder

$I_g$  = moment of inertia of the gross cross-section of the girder

$M_g$  = moment at midspan due to girder self-weight, assuming simply supported conditions

$$= \frac{w_g L^2}{8}$$

$w_g$  = uniformly distributed load due to girder self-weight

$L$  = girder length

If transformed section properties are used to calculate the stress at the center of gravity, it is assumed that the PPCB behaves as a composite section where the steel and concrete are equally strained. AASHTO 2010 states that if transformed section properties are used, the effect of losses and gains due to elastic shortening deformations are implicitly accounted for and  $f_{pES}$  should not be included in the prestressing force applied to the transformed section at transfer. In other words, instead of using the 90 percent of the initial prestressing force, use of the initial or jacking prestressing force is sufficient.

$$f_{cgp} = \frac{P_o}{A_{tr}} + \frac{P_o e_{tr}^2}{I_{tr}} - \frac{M_g e_{tr}}{I_{tr}} \quad (2-4)$$

where:  $P_o$  = initial prestressing force prior to transfer

There has been discussion on whether it is appropriate to use the gross or transformed section properties when calculating elastic shortening. Namman (2004) states that transformed section properties will result in greater accuracy but gross section properties can be used as a first approximation. Tadros et al. (2003) shows in NCHRP 496 Report that when using transformed section properties, elastic shortening can be represented by Equation 2-4. Comparing different methods of calculating elastic shortening with the use of transformed and gross section properties led to the following results presented in Table 2-3. It also suggests that elastic shortening loss of prestress are automatically accounted for if transformed properties are used in the analysis. In the AASHTO LRFD Bridge Design Specifications, Swartz et al. (2012) confirms that NCHRP 496 by saying that using transformed section properties will provide a direct solution by applying the prestressing force before transfer (not calculating any elastic shortening losses explicitly) to the transformed section properties.

Additionally, the loss due to elastic shortening in pretensioned members may be determined by Equation 2-5.

$$\Delta f_{pES} = \frac{A_{ps} f_{pbt} (I_g + e_m^2 A_g) - e_m M_g A_g}{A_{ps} (I_g + e_m^2 A_g) + \frac{A_g I_g E_{ci}}{E_p}} \quad (2-5)$$



where:

- $A_{ps}$  = area of prestressing steel (in.<sup>2</sup>)
- $A_g$  = gross area of section (in.<sup>2</sup>)
- $E_{ci}$  = modulus of elasticity of concrete at transfer (ksi)
- $E_p$  = modulus of elasticity of prestressing tendons (ksi)
- $e_m$  = average prestressing steel eccentricity at midspan (in.)
- $f_{pbt}$  = stress in prestressing steel immediately prior to transfer (ksi)
- $I_g$  = moment of inertia of the gross concrete section (in.<sup>4</sup>)
- $M_g$  = midspan moment due to member self-weight (kip-in.)

Equation 2-5 is a general equation used to summarize the elastic shortening of an entire beam. When more detailed elastic shortening analysis is desired, calculating the elastic shortening from Equation 2-2 should be used. Equation 2-2 has the ability for variables to be adjusted for the different properties of the beam at specific locations.

Rosa et al. (2007) used AASHTO 2006 guidelines to calculate the prestress losses due to elastic shortening. When using this method, complications arose due to calculation of losses of permanent and temporary prestressing strands. Temporary prestressing strands are external reinforcement used to minimize damage to the beam during storage and shipping. Both groups of strands were accounted for by calculating different levels of stress separately. Using equilibrium and strain compatibility conditions, Rosa et al. (2007) was able to determine the prestress force after the transfer of prestress.

$$P_i = \frac{P_j + M_{sw} e_p A_p n}{1 + np \left( 1 + e_p^2 \frac{A_c}{I_g} \right)} \quad (2-6)$$

where:  $n$  = modular ratio

$$= \frac{E_p}{E_c}$$

= reinforcement ratio

$$= \frac{A_{ps}}{A_c}$$

#### 2.4.2.2 PCI Method (2010)

The PCI Method of calculating prestress losses follows the AASHTO LRFD (2010) method found in Equation 2-2 through 2-4. The jacking force is multiplied by 90 percent, which is assumed to be the reduction in prestress due to elastic shortening; however, the procedure is not iterated. The initial jacking force is taken as 75% of the nominal strength multiplied by the strand area.

#### **2.4.3 Seating Loss**

As stated in Section 2.2.3, the seating loss is caused by the movement of the prestressing strand before the chucks can anchor and hold the prestressing force. According to AASHTO LRFD 2010, the seating loss causes most of the difference between jacking stress and stress at transfer. Ultimately, the seating settlement of the prestressing strands depends on the tensioning system and anchors that are used. Power seating is recommended (AASHTO LRFD, 2010) for short tendons since the prestress loss tends to be significant. However, the power seating is not necessary for long tendons since the loss of prestress is minimal. For wedge type strand anchors, the seating may vary between 0.125 and 0.375 inches but 0.25 inches is the value that is recommended (in AASHTO LRFD, specifications (2010)).

Although AASHTO does not give the equation for seating losses, using Hooke's law in Equation 2-8 will relate the stress and strain to give an accurate seating value. Rearranging values will result in Equation 2-9, which is used to calculate the loss in prestress due to seating.

$$\Delta_s = \frac{\Delta P_{ps} L}{AE} \quad (2-8)$$

$$\Delta P_{ps} = \frac{\Delta_s AE}{L} \quad (2-9)$$

where:  $\Delta P_{ps}$  = prestress loss due to seating (kips)

$\Delta_s$  = seating distance (in.)

$L$  = length of the prestressing strand (in.)

$A$  = cross sectional area of the prestressing strand (in<sup>2</sup>)

$E$  = modulus of elasticity of the prestressing strand (ksi) and is taken as 28,500 ksi

An example of a PPCB is explained to clarify the impact seating can have on the prestress force and ultimately the camber. A BTE 145 PPCB (Bulb T Section E with length 145 feet long) has 42 straight bottom prestressing strands and 10 harped strands. If the prestressing strand length is 440 feet and the seating distance is assumed to be 0.25 inches, there will be a 0.29 kip reduction in prestress per strand. Although this seems insignificant, multiplying the loss per strand by the total number of strands results in a 15.22 kip or 0.7% reduction in prestress.

#### 2.4.4 Relaxation

Relaxation, as stated in section 2.2.4, is the loss in tension in a prestressing strand with respect to time when it is held at a constant length. Relaxation is dependent on the properties of steel, the applied tension, and the temperature that the prestressing strands are subjected to. In design, relaxation is accounted for after the transfer of prestress. ACI Committee 343R-95 accounted for the loss in prestress due to relaxation at the time between tensioning to transfer. Rizkalla et al. (2011) agreed with ACI Committee 343R-95 and used Equation 2-7 for calculating relaxation where time is divided into two periods, before and after the transfer of prestress.

$$\Delta f_{pR1} = \frac{\log(24t)}{40} \left[ \frac{f_{pJ2}}{f_{py}} - 0.55 \right] f_{pJ2} \quad (2-7)$$

where:  $t$  = time estimated in days from stressing to transfer (days)  
 $f_{pJ2}$  = initial stress in the tendon at the end of stressing or jacking (ksi)  
 $f_{py}$  = specified yield strength of the prestressing steel (ksi)

An example of how relaxation losses affect the prestress force is described below. A BTE 145 PPCB that is tensioned on a Friday and concrete is placed on a Monday morning will have 2 full days of relaxation losses before concrete is bonded to the prestressing tendons. Assuming the initial jacking force ( $f_{pJ2}$ ) is 196 ksi after seating losses with a yield strength of the prestressing steel is 243 ksi, the loss in prestress when using Equation 2-7 is 2.11 ksi or 0.46 kips

per prestressing strand. Multiplying the loss per strand by the total number of strands results in a 23.85 kip or 1.08% reduction in prestress.

#### 2.4.5 Modulus of Elasticity-AASHTO LRFD (2010)

AASHTO LRFD states that Equation 2-10 is suitable for concrete with the unit density between 90 and 155 pcf. Additionally, compressive strengths can be at 15.0 ksi or less.

$$E_c = 33K_1w_c^{1.5}\sqrt{f'_c} \quad (2-10)$$

where:  $E_c$  = elastic modulus of elasticity of concrete (psi)  
 $K_1$  = correction factor for source of aggregate to be taken as 1.0 unless determined by physical test, and as approved by the authority of jurisdiction  
 $w_c$  = unit density of concrete (lb/ft<sup>3</sup>)  
 $f'_c$  = specified compressive strength of concrete (psi)

Tadros et al. (2003) investigated the modulus of elasticity and the correlation to specific material properties. Since AASHTO LRFD previously did not account for material properties, it was suggested a  $K_1$  and  $K_2$  factor be adopted to account for the stiffness of the aggregate and the upper and lower bound that the data should fall within. In 2007, AASHTO LRFD adopted the modulus of elasticity equation seen in Equation 2-10, where aggregate stiffness ( $K_1$ ) is considered.

A review of past literature shows that multiple studies have been conducted over the topic of predicting camber in PPCBs. Of these studies, the primary focus has been on long-term camber prediction and long-term prestress losses. While long-term camber is important, instantaneous camber can be an indicator of the magnitude of long-term camber. For this reason, focus was placed on instantaneous camber in the following chapters. From research that has been conducted on instantaneous camber, topics such as prestress losses, material properties, measurement techniques, and prediction methods have been investigated.

When predicting camber, Naaman (2004) states that although the procedures vary in the method used to determine the long-term prestress losses, they all use primarily the same method

of calculating instantaneous losses. Differences that exist with calculation of instantaneous losses occur due to different variable properties used for concrete and prestressing steel. Tadros et al. (2003) and Ahlborn et al. (2000) found that AASHTO LRFD instantaneous prestress losses agree closely with the behavior of PPCBs. However, AASHTO LRFD (2010) neglects the losses due to relaxation from the time the tendon is tensioned to the time it is released. Accounting for the relaxation prestress losses along with the proper estimation of elastic shortening and seating losses will improve the prediction of the amount of prestress that will be applied to a PPCB, thus improving camber. Additional factors that are found to contribute to the accuracy of the camber prediction are the modulus of elasticity and concrete release strength. It was found that concrete release strengths are higher than designed, which cause an increase in the modulus of elasticity and decrease in camber. Using concrete material properties that model the behavior of concrete is suggested and was done in the following chapters.

When evaluating the past measurement techniques, methods such as the stretched-wire method and survey equipment is the most common. Inaccuracies occur with each method depending on the equipment that is used or procedures that are followed. Due to the misrepresentation of the measured camber, a new method of camber measurement was used to gather data and a simplified method was proposed for future measurements in Chapter 3.

The camber prediction method for instantaneous camber can be conducted by advanced finite element modeling or by simplified, hand calculations. Of the different hand calculation methods, similarities were found due to the initial assumptions that linear elastic behavior was present in the PPCB. Due to similarities in instantaneous camber prediction methods, the moment area method was chosen because of its simplicity and ability to account for transfer length and varying material properties.

## **CHAPTER 3. DATA COLLECTION METHODS**

### **3.1 Introduction**

Problems with predicting camber are typically evident at the bridge site after girders have been set on the piers. Although camber prediction problems are present at the bridge site, they have originated from inaccurate predictions with the design of the girder, in the precast plant during fabrication, or with the transfer of prestress. Investigating inaccurate instantaneous camber measurements was accomplished by examining past camber measurements as well as measuring camber at three precast plants and five bridge sites. A combination of the measurement techniques used by precasters and researchers along with new methods were explored to determine a consistent, accurate way to measure the instantaneous camber. While some previous measuring methods neglect measurement errors caused by bed deflections, inconsistent beam depths, friction between the beam and bed, the measurement method used to gather data on over 100 PPCB in Chapter 3.5 accounts for each of these sources of error.

### **3.2 Industry Practice Camber Data**

A database of over 1300 instantaneous cambers was available, which consisted of measured and recorded data by precast plant foremen and DOT inspectors at three precast plants that produce bridge girders for the Iowa Department of Transportation. The method that was used to measure camber was dictated by the Iowa DOT and is listed below.

#### **3.2.1 Iowa Department of Transportation Camber Measurement Procedure**

The Iowa DOT camber measurement procedure according to IDOT “Precast & Prestressed Concrete Bridge Units” (2013) is as follows:

- Camber due to prestress shall be measured while the beam is on the bed by checking the beam profile immediately (within three hours) after detensioning and separation of the beam.
- Camber shall be measured from the pallet to the bottom of the beam at mid-point utilizing a conventional tape measure. Camber shall be measured and recorded to the nearest 1/8 inch.

- Beam shall be resting free on the pallet at the time of the camber measurement. Camber acceptance shall be achieved prior to shipping.
- Noncompliant camber of any beam shall be verified at a later date. Beams cannot be accepted without a compliant camber and specific approval of the engineer.

The Iowa Department of Transportation standard for measuring camber is applicable for instantaneous and long-term camber and is followed throughout all the precast plants that make bridge girders for the state of Iowa. However, small changes in technique have been observed to differ between the three plants that produce PPCBs. The common discrepancies between precast plants are:

- Location along the beam where the camber measurement is taken;
- Accuracy of the value that is read from the tape measure; and
- Time the camber measurement is taken.

Detailed discussion about each of these issues is given in section 3.2.1.1 through 3.2.1.3.

#### 3.2.1.1 Location of Camber Measurement

It has been observed that a foreman, quality control manager, or construction engineer is the person who measures camber from the bottom flange at the midspan of the girder at the transfer of prestress. The person measuring camber after the transfer of prestress typically found the center of the beam by a centerline mark made on the precasting bed or by estimating where midspan will be relative to the cylindrical holes used for the interior diaphragms of the beam. The cylindrical holes used to attach the interior diaphragms were located in the web of the beam and the placement was determined by the designer (see Figure 3-1). The project team observed that diaphragm placement was typically anywhere from 1-1/2 ft. to 20 ft. from the centerline of the beam. Approximating where the midspan is located on a girder based on the diaphragm holes can allow precast personnel to measure camber at an incorrect location on the PPCB.

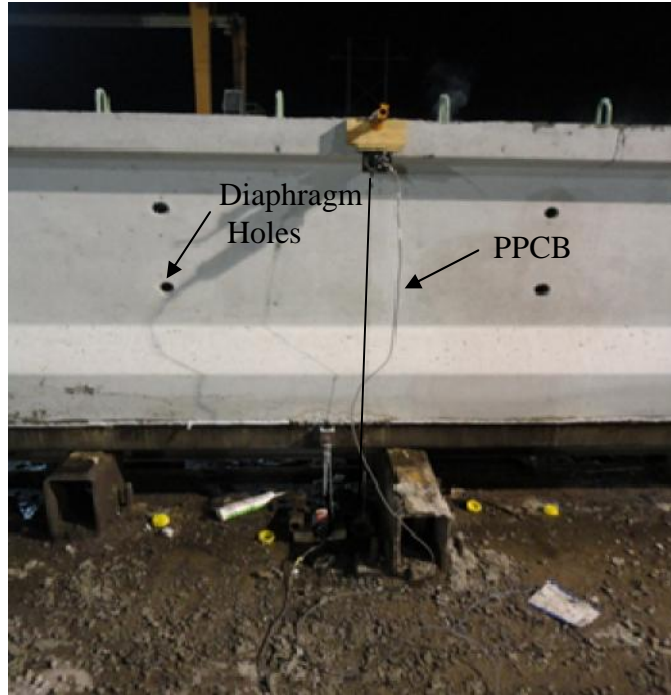


**Figure 3-1: PPCB with Two Cylindrical Holes for Interior Diaphragm**

### 3.2.1.2 Accuracy of Camber Measurement

Camber measurements are taken by a tape measure while the girder is resting on the precasting bed, before the girder is lifted. Although most workers read the tape measure to the nearest  $\frac{1}{16}$  inch, the camber is recorded to the nearest  $\frac{1}{8}$  inch or  $\frac{1}{4}$  inch. The camber tape measure reading is taken from the top of the precasting bed to the bottom flange of the girder. Problems with accuracy were evident at two precast plants due to a permanent metal chamfer that is attached to the precasting bed (Figure 3-2). In this case, a tape measure reading was taken from the top of the metal chamfer to the top of where the chamfer was when the beam was cast. This produces uncertainty due to the consistency of concrete on the edge where the chamfer was resting when the beam was cast. One plant uses a removable rubber strip to create the chamfer at the bottom flange of the beam (Figure 3-3). The rubber chamfer can be removed and a tape measure reading can be taken from the precasting bed to the smooth bottom surface of the beam (Figure 3-10) which results in higher accuracy when camber is measured from the bottom flange. However, the camber is measured from the top flange when the PPCBs are erected which may result in a discrepancy from the instantaneous camber that is measured from the bottom flange.





**Figure 3-2: Precasting Bed with Metal Chamfer**



**Figure 3-3: Precasting Bed with a Removable Rubber Chamfer**

#### 3.2.1.3 Time of Camber Measurement

The time when measurements were taken depends on the precast plant's release process and the availability of the foreman, quality control manager, or construction engineer. The process of releasing a PPCB is different from the three different plants based off the equipment and

methods used. It should be known that due to friction between the precasting bed and beam along with creep, the camber at midspan continually grows after the transfer of prestress. Due to the increase in camber after the transfer of prestress, the time camber measurements are taken can impact the recorded camber. Below is a summary of the precasting plants and when camber has been observed to be measured.

- Top sacrificial prestressing strands and harped strands, if present, were released by using an acetylene torch. If there were any harped, hold down points, they were released next by using a wrench. Depending on the precasting plant, an acetylene torch or hydraulic jack was used to detension the bottom prestressing strands. If bottom prestressing strands were released by the hydraulic jack, workers then cut the strands that are present in between adjacent beams. After the last reinforcement strands were released but before the beam was lifted from the precasting bed, a tape measure reading was recorded. The recorded tape measure reading most frequently occurred immediately after the last prestressing strand had been released. However, there were times when camber was recorded before the prestressing strands were completely free or other times 1-1/2 hours after release.

Organizing and evaluating past data obtained from precasters and DOT inspectors from three separate precast plants has provided valuable insight into understanding the quality of data and the problem that the DOTs, precast plants and contractors face on a regular basis. An examination of the data from three different precast plants produced similar trends, which may be due to comparable procedures adopted for camber measurements, concrete properties due to close geographic location, and methods for fabricating and constructing the girders.

Figure 3-4 shows the absolute difference in measured and predicted camber of bulb-tee PPCBs arranged in order of increasing girder length. Due to the large scatter that was present, data was regrouped in Figure 3-5. Figure 3-5 shows trends that were found by organizing the difference between the designed and the measured camber and dividing by the length of the beam (Equation 3-1). Data were then arranged in increasing girder length.

$$\text{Error of Camber With Respect to Length} = (\text{Measured Camber} - \text{Designed Camber}) / \text{Length} \quad (3-1)$$

Dividing the difference between the measured and designed camber by length normalizes error and eliminates the variable of length. Arranging the girders in increasing length, starting with the shortest, provides the following trends:

- For each girder type, the error between the measured and predicted camber is not consistent.
- On average, as the girder length increases, the error between predicted and measured camber also increases.

Arranging the industry practice camber data revealed that PPCBs have errors resulting in measured camber that are in disagreement with the predicted camber. The trends discovered from Figure 3-5 show that camber is overpredicted 75% of the time. However, for certain girder types, the agreement between the measured and predicted camber is underpredicted. This indicates that the differences in camber are most likely due to unique conditions in fabrication, measurement, and materials. Additionally, the trend that as the girder length increases, the error between the predicted and measured camber increases is also shown in Figure 3-5. This is caused by inaccuracies with the industry practice camber measurement technique that fail to account for bed deflections, inconsistent top flange surfaces along the length of the PPCB and across the top flange and friction between the precasting bed and the beam. As the beams increase in length, the weight of the beam typically increases. The increase in weight causes more bed deflection and more friction to be present. Failing to account for these factors results in inaccurate instantaneous camber measurements compared to the camber that is actually present. Inaccurate instantaneous camber measurements hinder the accuracy of the camber prediction technique and estimation of the long-term camber.

Due to previously inaccurate camber measurements, an investigation on the method that is used to measure camber at the transfer of prestress was undertaken. As part of the research reported herein, a combination of the measurement techniques used by precasters and past research studies along with new methods were explored to determine a consistent, accurate way

to measure the instantaneous camber. While some previous measuring methods neglect bed deflections, inconsistent beam depths and surfaces, friction between the beam and bed, the method used accounts for each of these issues as accurately as possible and quantifies their impact on instantaneous camber measurement.

Focus was placed on measuring camber on over 100 girders from three different precast plants. Three different methods were used to measure camber that included a tape measure from the bottom flange at midspan, a rotary laser level, and string potentiometers. The current errors with camber measurement along with the procedure of measuring camber with three different methods are listed in the following sections.

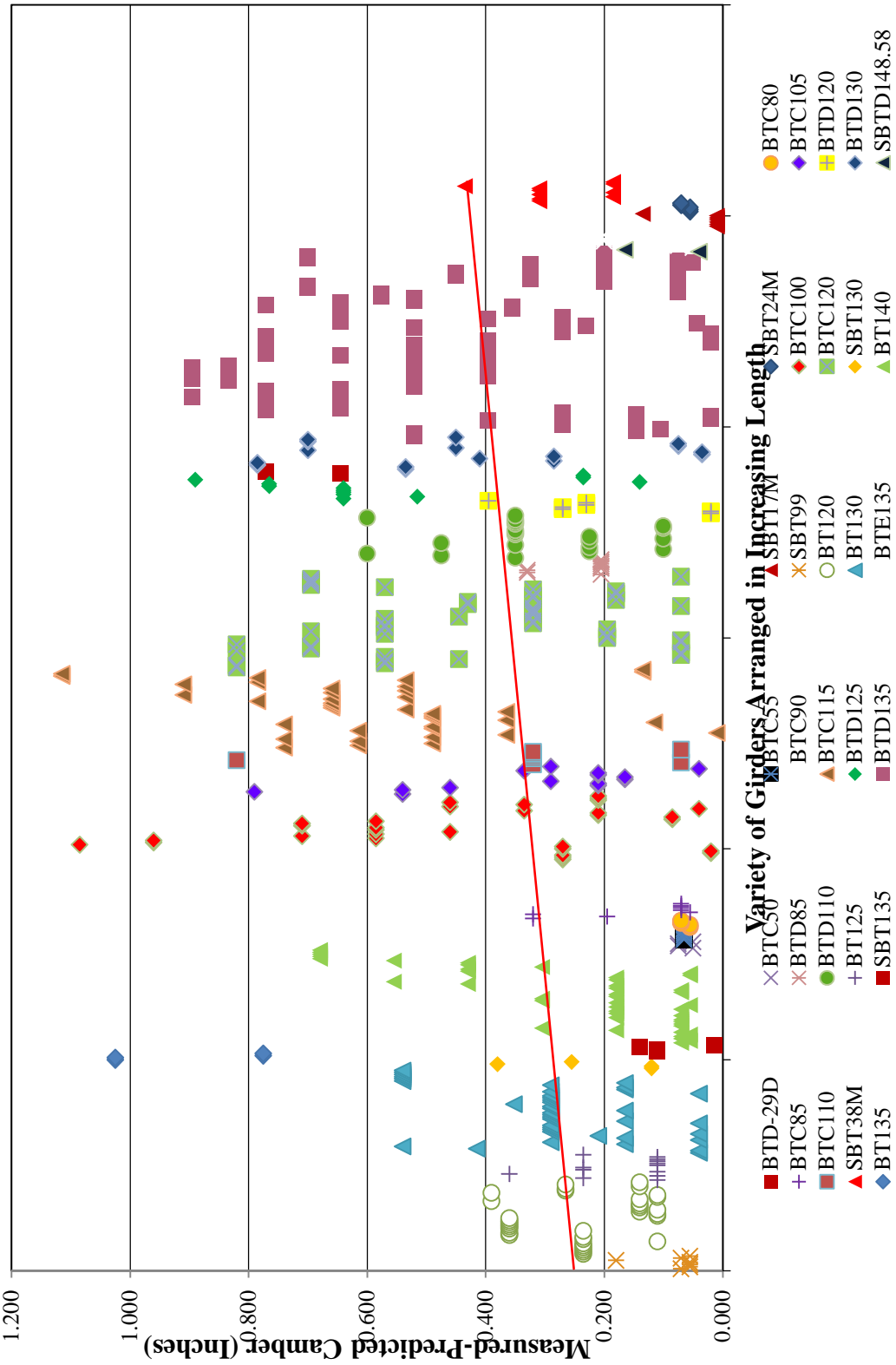


Figure 3-4: Difference in Measured and Predicted Industry Practice Camber Data vs. Length of PPCB

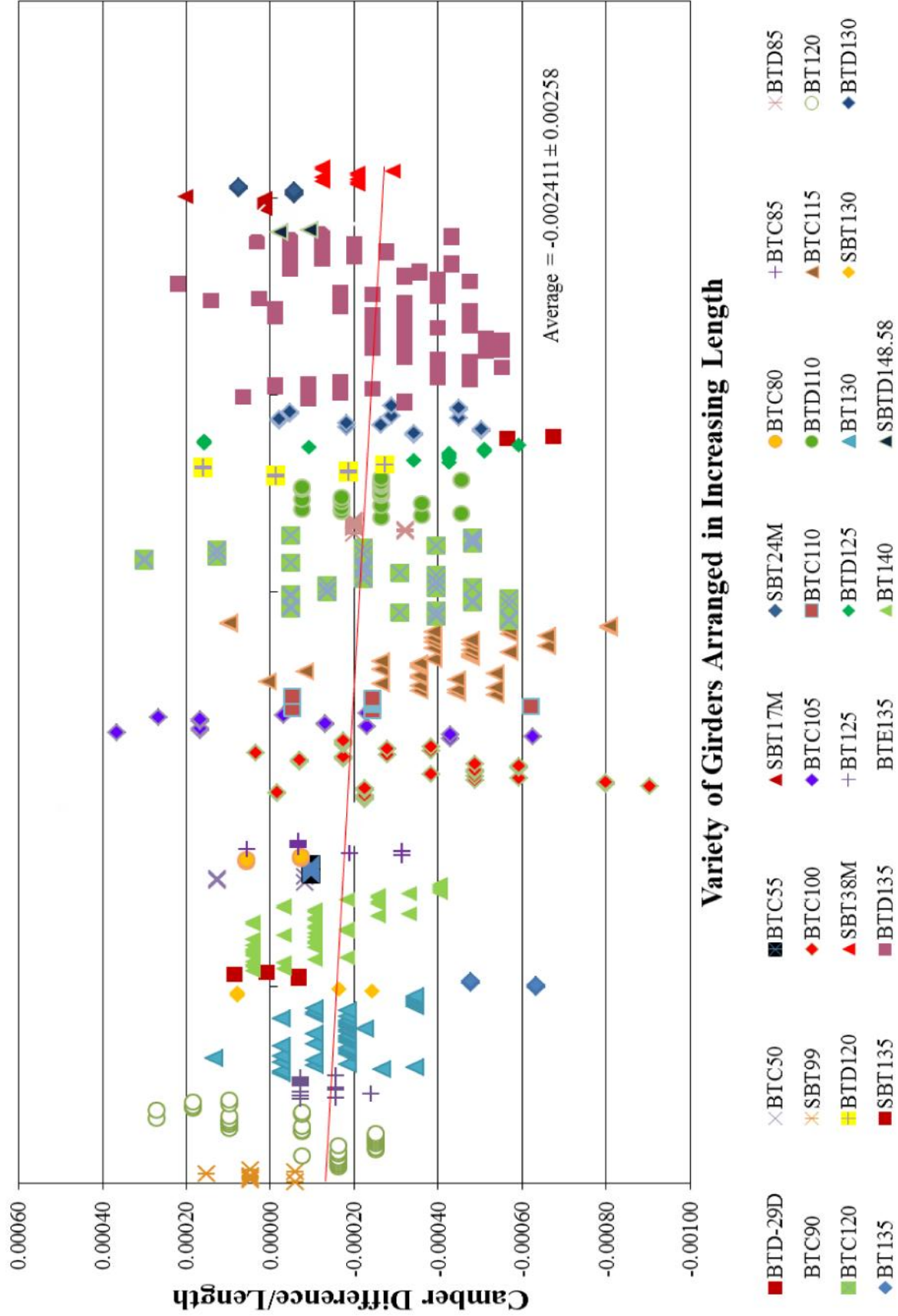


Figure 3-5: Difference in Camber/Length of Industry Practice Data Arranged in Increasing Beam Length

### 3.3 Errors with Current Camber Measurement Practice

Evaluating the industry measurement practices in Chapter 3.2 and conducting independent measurements on girders confirmed errors with the current industry practice measurement technique were present. This section presents detailed sources of errors that have been observed to contribute to instantaneous camber measurement. They include bed deflections, friction between the precasting bed and end of the beam, inconsistent top flange surface along the length of the beam and inconsistent top flange surface due to local effects. All of these issues are discussed in detail.

#### 3.3.1 Bed Deflections

A prestressed concrete beam that has not been released exerts a uniformly distributed load along the length of the bed due to its self-weight (Figure 3-6). When the prestressing strands are released, prestress force that is applied to the beam may cause the beam to camber. When camber is present, the weight of the beam shifts from being uniformly distributed load along the length of the bed to two point loads at the girder ends (Figure 3-7). Shifting of the beam's weight to the ends produces downward bed deflections at the ends of the beam and upward rebounding of the bed at midspan, which will cause a discrepancy between the measured and actual camber. The magnitude of the bed deflection will depend on where the girder ends are situated in relation to the precasting bed supports.

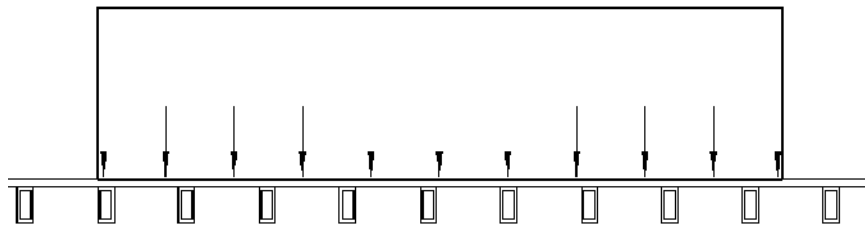


**Figure 3-6: PCB before the Transfer of Prestress Generating a Uniform Load on the Bed**

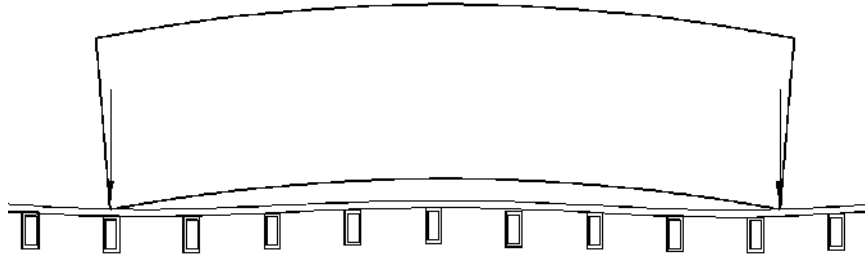


**Figure 3-7: PPCB after the Transfer of Prestress with the Beam Self-Weight Acting only at Two Points on the Bed**

### **3.3.2 Inconsistencies with PPCBs**

PPCBs typically have a rough top flange surface, which is required to ensure sufficient bonding to the deck concrete when it is cast (Figure 3-8). The consistency of the top flange surface results in two types of errors. When camber is measured from the top flange, errors include inconsistent beam depth along the length of the beam and local inconsistencies across the top flange surface. Although the instantaneous camber is typically measured by the precasters with respect to the bottom surface, all field camber measurements are taken from the top surface, ultimately causing discrepancies between the measured and expected camber and casting a doubt on the initial camber produced for the beam.

#### **3.3.2.1 Inconsistent Beam Depth along the Length of the Beam**

Beam depth is assumed to be constant along the length of PPCBs. Quality control by plant personnel and representatives hired by owners hold precasters to strict limits with beam height tolerances. However, the depth of PPCBs has been found to be inconsistent depending on how the forms are set as well as the consistency of finish chosen for the top flange. Having an increase or decrease in the beam at midspan before the transfer of prestress may cause the camber to be over or underpredicted after the transfer of prestress occurs.

#### **3.3.2.2 Local Inconsistencies of the Top Flange Surface**

The top flange surface has been observed to have local inconsistencies. The local inconsistencies are caused by the roughened surface finish that is applied by workers at the precasting plant. The rough finish that is applied is due to partially exposed aggregate that protrudes from the surface and the inconsistent elevation of the concrete. The magnitude of the



local inconsistencies is dependent on the workers applied finish and has been observed to be consistent despite different beam lengths. The rises and falls in the surface of the beam and pose a problem when taking camber measurements from the top flange. A smooth surface is applied along the edge of the top flange surface in an attempt to remove local inconsistencies (Figure 3-9). Although this surface is applied to nearly every beam, it is often failed to be utilized as a measurement location by contractors in the field.



**Figure 3-8: Inconsistent Top Flange Surface of a PPCB Due to Local Inconsistencies**



**Figure 3-9: PPCB with Troweled Surface along the Length of the Beam**

### **3.3.3 Friction between Beam Ends and Precasting Bed**

After the transfer of prestress while the PPCB is resting on the precasting bed, friction is present between the beam ends that are in contact with the bed. The friction introduced at the girder ends, inhibits the girder from achieving its full instantaneous camber. The ability for the girder to overcome friction by having the ends slide towards each other on the precasting bed will increase the measured camber at the midspan. After all the prestressing strands are released, there was a gradual increase in camber that was observed. This was suspected to be due to the beam ends overcoming the friction induced between the beam and bed. The amount of vertical displacement at the midspan that will be gained by accounting for friction may be determined by lifting the girder from the precasting bed, setting it down, and re-measuring the camber. The difference between the camber that is recorded before and after the girder was lifted can be attributed to friction.

Although errors relating to bed deflections, top flange inconsistencies, and friction between the precasting bed and beam vary in magnitude, they have been observed to be consistently present at three different precast plants. The magnitude of the errors is dependent on a

combination of fabrication procedures and the method used for the transfer of prestress along with the precasting bed and concrete material properties. While the behavior of the PPCB is dependent on the precasters procedures and material properties of the PPCB, the resulting camber can be accurately captured by using the correct measurement technique. The following sections in Chapter 3 will display the methods used to measure camber in this research project. Although it is noted in Chapter 3.2 that the current industry practice fails to account for these errors, it should be recognized that researchers are able to capture and quantify bed deflections, inconsistent top flange surfaces along the length and locally and friction.

### **3.4 Tape Measure**

A tape measure reading at the midspan of PPCBs at the transfer of prestress is one method that is used to determine camber. This is done by first taking a tape measure reading across the entire length of the beam and determining where midspan of the beam is located. After all prestressing strands are detensioned, a tape measure was used to measure the distance from the bottom flange of the beam to the surface of the bed (Figure 3-10). The tape measure readings were recorded at a maximum of 30 minutes after the last prestressing strand was released. Although measuring camber with a tape measure is efficient for precasters with respect to time and schedule, it fails to account for inconsistent beam depths, bed deflections, and potentially friction if the beam is not lifted.

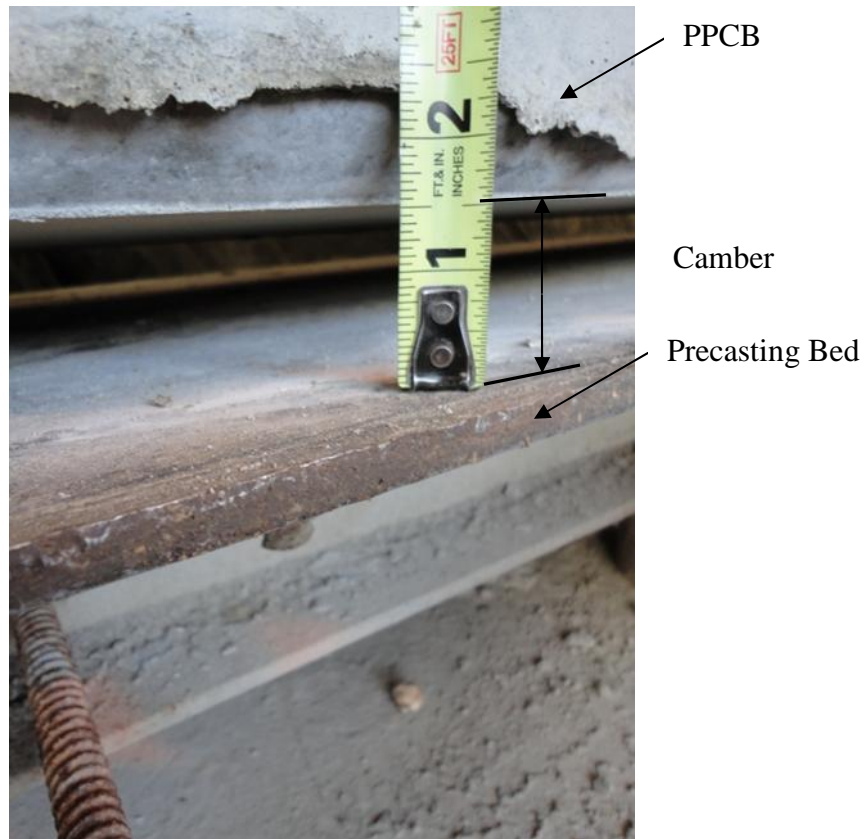


**Figure 3-10: Typical Tape Measure Reading at the Midspan of a PPCB Taken at a Precast Plant**

### **3.5 Rotary Laser Level**

A rotary laser level was also used to take camber measurements on PPCBs. The rotary laser level operates by projecting a horizontal laser beam that can be detected by a receiver. The receiver mounts on a grade rod which can be read to determine elevations with respect to the laser level. Since the laser level is stationary during the whole process, any differences in measurements can be related to deflections of the beams or precasting bed. The manufacturer's reported precision for the rotary laser level device used in the study was  $\pm 1/16$  inch at 100 feet.



**Figure 3-11: Rotary Laser Level**

### **3.5.1 Measuring Camber with a Rotary Laser Level**

Measuring camber with a rotary laser level included a number of measurements and procedures to account for bed deflections, inconsistent beam depths and friction between the beam and the precasting bed. To limit the error associated with the inconsistent top flange surface, a marker was used to trace the cross section of the grade rod when it was placed for the first measurement. The remaining measurements throughout the transfer of prestress were taken by placing the grade rod in the location of the marker outline where the first measurement was taken. This would ensure that the error associated with the inconsistent top flange surface was eliminated. When using the receiver and grade rod for taking camber measurements, a level that is built in to the receiver was used to ensure that the grade rod was held perpendicular to the top flange surface.

Before the transfer of prestress, measurements were taken on the precasting bed at the ends of the beam and on the top flange at midspan as seen in Figure 3-12. After the transfer of prestress but while the beam is resting on the precasting bed, measurements were taken on the precasting bed at the beam ends and along the top flange at the ends and at midspan. The measurement locations can be seen in Figure 3-13. Once the beam is lifted, the friction forces are dissipated and another reading is taken along the top flange at the ends and at midspan. Figure 3-14 represents the PPCB after the beam has been lifted.

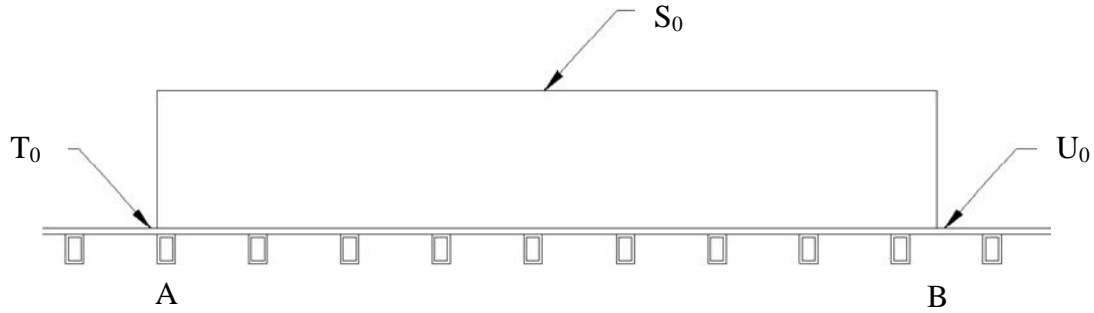


**Figure 3-12: PPCB before the Transfer of Prestress**

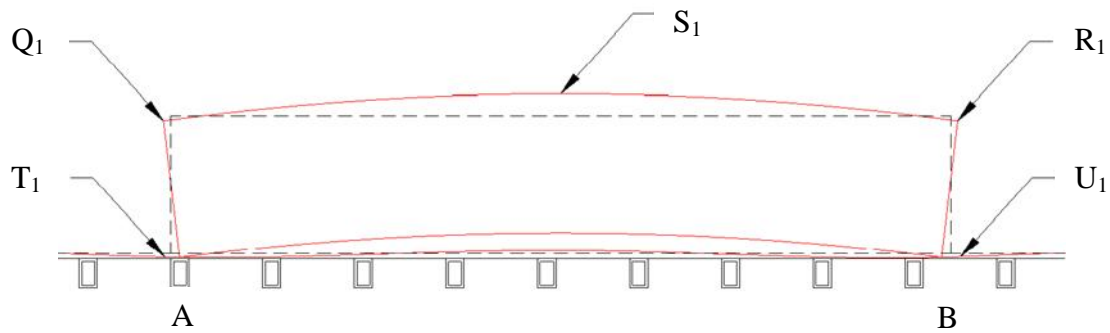


**Figure 3-13: PPCB after the Transfer of Prestress, before the Beam was Lifted**

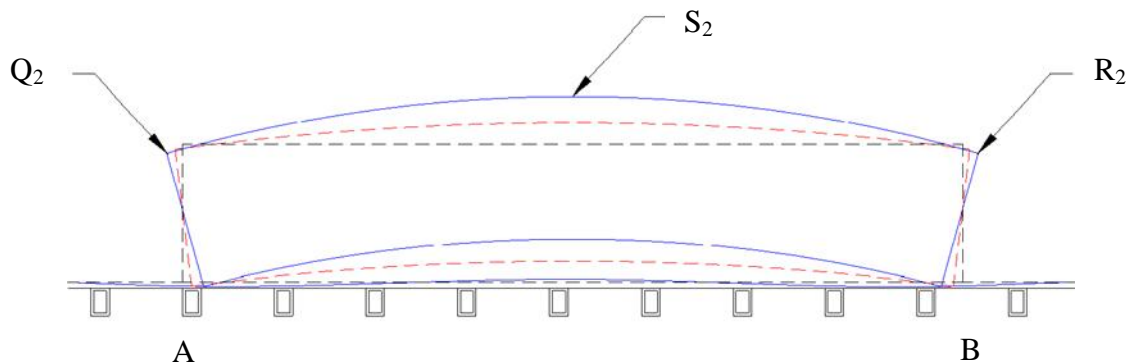


**Figure 3-14: PPCB after the Transfer of Prestress and after the Beam was Lifted and Placed Back on the Bed**

The following is the procedure used for calculating the camber using the measurements that were taken. This method accounts for inconsistencies in the top flange surface, bed deflections, and friction between the bed and beam.

Bed deflections are accounted for by taking laser level measurements of the bed elevation before and after the transfer of prestress. By determining the differential bed elevations at the



end of the beam from before to after the transfer of prestress, the magnitude of the bed deflection can be obtained.

$$\text{Bed deflections at points A and B} = T_0 - T_1 \text{ and, respectively } U_0 - U_1 \quad (3-2)$$

Equation 3-2 gives a bed deflection at each end of the beam. To determine the total effect of bed deflections on camber, the average elevation of the bed at each end is computed to get the bed deflection with respect to the beam.

$$\text{Bed deflection with respect to the beam at midspan} = \frac{(T_0 - T_1) + (U_0 - U_1)}{2} \quad (3-3)$$

Inconsistent beam depths were found to cause a misrepresentation of camber if the midspan of the beam does not have an identical cross section compared to the ends. Equation 3-4 is used to determine the differential change in deflection at midspan. By taking an elevation measurement at the same location before and after the transfer of prestress, the inconsistent top flange surface is accounted for.

$$\text{Change in deflection at midspan, accounting for inconsistent top flange surface} = S_0 - S_1 \quad (3-4)$$

The issue of friction is present in determining camber at the transfer of prestress. Friction develops at the transfer of prestress as a result of the beam and bed being in contact with each other. The friction can inhibit the full deflection from being detected. Lifting the beam and placing it down on the precasting bed dissipated the friction between the beam and bed. However, the process of lifting and setting the beam may cause it to be displaced from its original position. To solve this problem, top flange measurements were taken at the midspan and at the ends of the beam before and after the beam was lifted. Subtracting the upward deflection before the beam was lifted from the upward deflection after the beam was lifted gives the increase in camber due to dissipation of friction (Equation 3-5).

$$\text{Deflection due to dissipation of friction} = \left( \frac{(Q_2 + R_2)}{2} - S_2 \right) - \left( \frac{(Q_1 + R_1)}{2} - S_1 \right) \quad (3-5)$$

In the absence of beam overhangs after the lift/set of PPCBs, it is possible to determine the total camber from Equations 3-2 through 3-5.

$$\text{Camber} = \left( \frac{(T_0 - T_1) + (U_0 - U_1)}{2} \right) + S_0 - S_1 + \left( \frac{(Q_2 + R_2)}{2} - S_2 \right) - \left( \frac{(Q_1 + R_1)}{2} - S_1 \right) \quad (3-6)$$

### 3.6 Support Conditions

Problems are introduced if precasters are not able to lift and set the beams on the precasting bed to dissipate the force of friction in PPCBs. It has been observed that precasters tend not to lift and set down the PPCBs on the precast bed to eliminate friction. This is due to the risk of damaging the newly cast beam and the precasting bed along with the schedule and economic issues related to lifting a precast beam multiple times. Instead, precasters prefer to lift the beams from the precasting bed and place them on temporary supports in a storage yard until they can be shipped to the jobsite. The supports are placed anywhere from the edge of the PPCB to several feet in from the end of the beams. When PPCBs have the supports placed in from the ends, measured camber will be greater due to an elastic deformation.

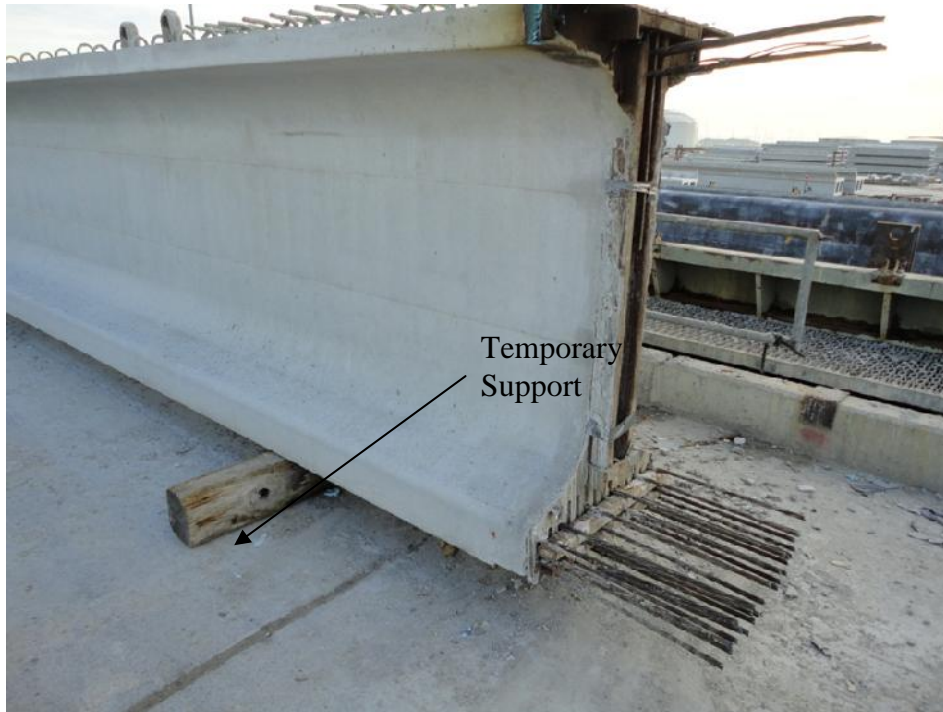


**Figure 3-15: End of a PPCB on a Temporary Wooden Support**



The increase in camber due to shifting of supports can be quantified by three components. One component is the added moment at the support from the overhanging end of the beam (Figure 3-16). This moment acts to increase the camber at the midspan. The second component is the reduced clear span length (Figure 3-17). While the beam is resting on the precasting bed, the clear span length is assumed to be the length of the beam. When supports are placed in from the ends, the clear span is reduced. A smaller clear span length will result in smaller self-weight deflections at midspan. In simple, elastic beam formulas, the clear span length is typically multiplied to the fourth power, which changes the final deflection. The third component is from the deflection at the end relative to the support caused by the cantilever section (Figure 3-18). Although this deflection is typically small, it should be recognized for research purposes.

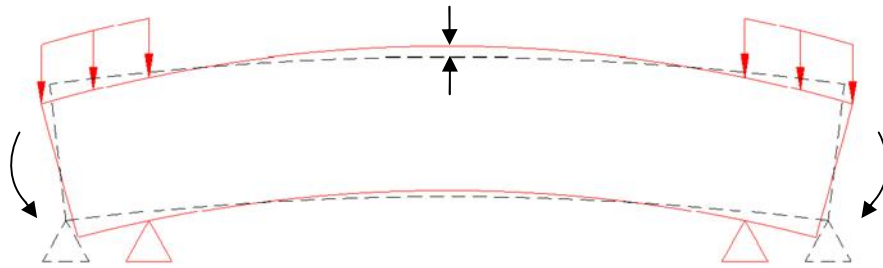


**Figure 3-16: PPCB with Increased Midspan Deflection Caused by the Moment from the Overhang**

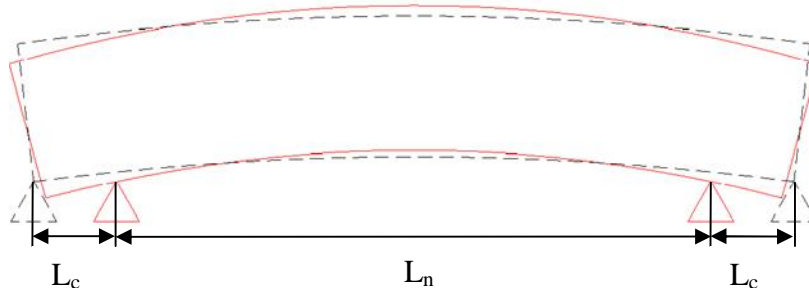


**Figure 3-17: PPCB with Increased Midspan Deflection due to Self-Weight caused by the Reduced Clear Span**

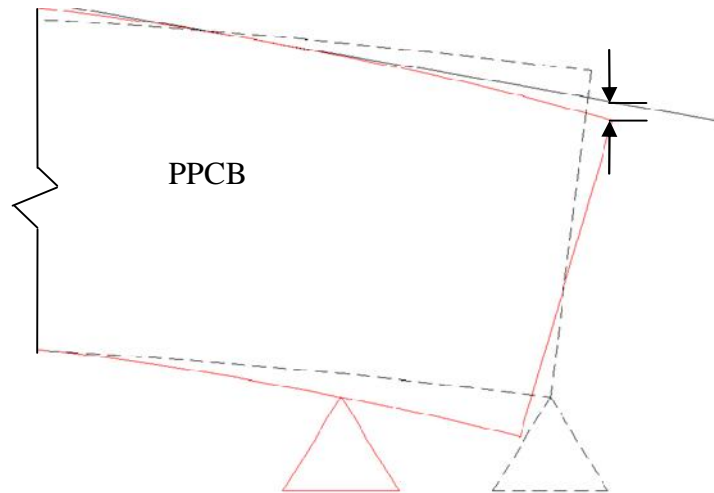


**Figure 3-18: Increased Deflection of a PPCB Relative to the Support Caused by the Overhang**

### 3.6.1 Procedure for Measuring Camber when placed on Temporary Supports

An elevation survey that determines the haunch thicknesses are taken at the time of erection of the PPCB. The supports at erection are typically 6-10 inches in from the end of the beam. Since this is the most critical time for the prediction of camber and the supports are near the end of the beam, all other camber measurements should be compared to a beam with zero overhang to maintain accuracy.

The elastic deformation that is present when shifting the supports closer to the center of the beam will misrepresent the contribution of friction and thus, the amount of camber that is present if it is not revised. In order to determine the contribution of the elastic deformation, the camber must be measured at the ends of the PPCB when resting on temporary supports and the distance from the ends of the beam to the supports must also be measured.

Equation 3-7 is used to calculate the deflection due to the self-weight of a PPCB when the supports are placed at the end of the beam. This represents the support conditions that the girder is exposed to while resting on the precast bed immediately after the transfer of prestress.

$$\Delta_{DL} = \frac{5w_{sw}l^4}{384EI} \quad (3-7)$$

After the beam is lifted and placed on the supports in the precast yard, additional measurements taken at the ends and midspan of the beam are adjusted to compare the beam to the zero overhang condition. Through observation and confirmation from the precast plants, overhangs are typically equal on each end of the beam. Equation 3-8, which was used by Rosa et al. (2007), can determine the contribution of camber due to the supports for beams with equal overhangs.

$$\Delta_{SW} = \Delta_{OVERHANG} + \Delta_{MIDSPAN} \quad (3-8)$$

where  $\Delta_{OVERHANG}$  = the deflection of the overhang relative to the support

$$= \frac{w_{sw} L_c^2}{24 E_c I} [3 L_c^2 (L_c + 2 L_n) - L_n^3] \quad (3-9)$$

where  $\Delta_{MIDSPAN}$  = the deflection at midspan relative to the support

$$= \frac{w_{sw} L_n^2}{384 E_c I} [5 L_n^2 - 24 L_c^2] \quad (3-10)$$

where  $L_n$  = distance between supports

$L_c$  = length of overhang

$E_c$  = modulus of elasticity of the concrete when the load is applied

$I$  = moment of inertia

Subtracting the result of Equation 3-8 from Equation 3-7 gives the additional deflection caused by temporary supports relative to the datum point established at the beginning of the measurements (Equation 3-11).

Difference in Deflection due to Self-Weight from the Movement of Supports =

$$\Delta_{OVERHANG} + \Delta_{MIDSPAN} - \frac{5 w_{sw} l^4}{384 E I} \quad (3-11)$$

In cases where the girder is lifted and placed on temporary supports, the contributions in camber due to friction can be determined by subtracting the value of friction that was obtained from Equation 3-5 from the difference in deflection due to the self-weight from the movement of the supports (Equation 3-11). The result of the contribution of camber due to friction when accounting for the elastic deformation due to temporary supports is shown in Equation 3-12.

$$\text{Adjusted deflection due to dissipation of friction} = \frac{\text{DEFLECTION DUE TO DISSIPATION OF FRICTION} - \text{Difference in Deflection due to Self-Weight from the Movement of Supports}}{(3-12)}$$

The final camber, when adjusting for the temporary supports, is defined by Equation 3-13.

$$\begin{aligned} \text{Camber} = & \left( \frac{(T_0 - T_1) + (U_0 - U_1)}{2} \right) + S_0 - S_1 + \left( \frac{(Q_2 + R_2)}{2} - S_2 \right) - \left( \frac{(Q_1 + R_1)}{2} - S_1 \right) \\ & - \frac{5w_{sw}l^4}{384EI} - \frac{w_{sw}L_c}{24E_cI} [3L_c^2(L_c + 2L_n) - L_n^3] + \frac{w_{sw}L_n^2}{384E_cI} [5L_n^2 - 24L_c^2] \end{aligned} \quad (3-13)$$

### 3.7 String Potentiometers

String Potentiometers have been used to instrument the beam at several different locations to verify camber measurements and also vertical movement of the precasting bed during release. String potentiometers are composed of a string that is wrapped around a spring loaded coil. One end of the coil is connected to an external hook that can be pulled from the string potentiometer to record a displacement. When an object moves that has a string potentiometer attached, the string will be unraveled from the internal portion of the string potentiometer. The string potentiometers are connected to a data recording device which was set to measure the displacement of each string potentiometer once every second. This allows a displacement vs. time graph to be obtained for multiple string potentiometers at different locations along the beam and precasting bed. Recording significant events during the transfer of prestress and relating them to the time vs. displacement graphs, gives clear evidence on the behavior of the beam and precasting bed during release.

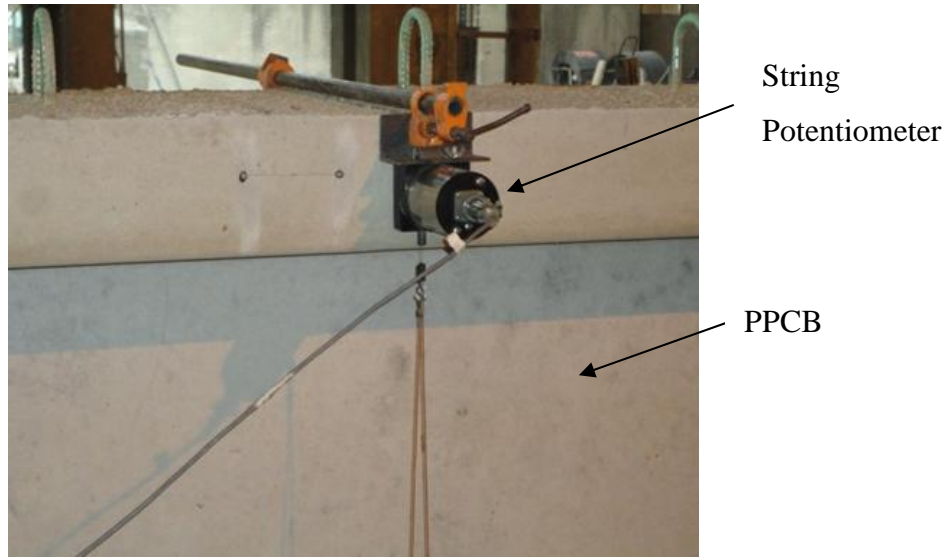


**Figure 3-19: String Potentiometer Attached to the Top Flange of a PPCB**

String potentiometers were attached to the beams by clamping the instrument at the top flange of the girder at midspan. A string was connected from the string potentiometer to a weight that rests on the ground beside the precasting bed (Figure 3-20). The weight is placed on the ground and does not move during the process of the release. Connecting the instruments to the beam before the transfer of prestress took place and monitoring them during the release gave valuable information about displacements at critical points.

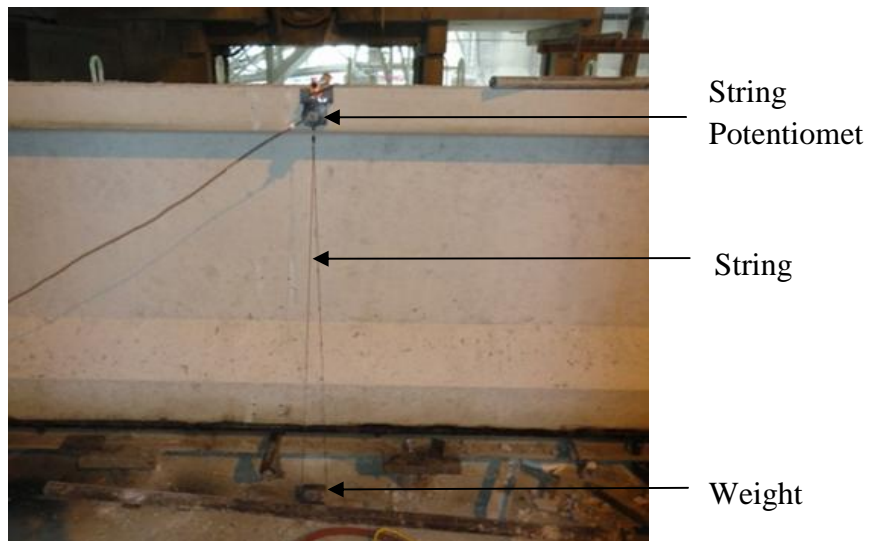


**Figure 3-20: String Potentiometer Attached to the Midspan of a PPCB**

When monitoring the precasting bed for deflections, a different method was used to attach and instrument the string potentiometers. String potentiometers were attached to a wood block that was anchored to the ground by weights. A magnet was attached to the precasting bed with a rod that extended out (Figure 3-21). Connecting a small chain from the rod to the string potentiometer resting on the ground gave valuable information about the upward and downward precasting bed displacements that were present at the midspan and ends of the girder respectively during the transfer of prestress.



**Figure 3-21: String Potentiometer Attached to the Precasting Bed at the End of a PPCB**

## **CHAPTER 4. PREDICTING INSTANTANEOUS CAMBER**

Challenges faced with predicting instantaneous camber during design are related to the designer's ability to accurately estimate material properties and to model the applied forces exerted to the beam after accounting for the effect of prestress losses. Correctly representing both the material properties and the prestressing force when an active combination of prestressing steel and concrete is present is important to accurately determining the camber of a PPCB. This chapter focuses on the equations and methods that can be used to predict instantaneous camber accurately.

### **4.1 Simplified Method for Calculating Instantaneous Camber**

Calculating camber using simplified methods is a straightforward procedure that involves calculating the upward deflection due to prestress and the downward deflection due to the self-weight of the beam. The net deflection between the two components will give the instantaneous camber (See Figure 1-7). Due to the ability to represent the material properties and behavior of the PPCB accurately, the moment area method was chosen to calculate the instantaneous camber and is discussed in the subsequent sections.

The first step in calculating camber using the moment area method is gathering accurate variables for the beam of interest. The types of beams that are produced have specified variables in the IDOT Bridge Design Specifications (2011). The specifications give the design properties of materials used and fabrication variables that are required to produce a PPCB. Included in the specifications are the non-prestressed and prestressed reinforcement layout, material properties of the reinforcing steel, cross section dimensions, area, moment of inertia, target release strength, target instantaneous camber, and other geometric variables that may be necessary in producing a PPCB. To closely replicate the behavior of the PPCB, variables obtained from design documents along with variables that are in agreement with the material properties of the specimen are used. Using a combination of specified variables and variables that are in agreement with the properties for each beam results in accuracy with predicted and measured camber values.

### **4.2 Prestress Force**

The prestress force in PPCBs is an important variable that is sensitive to the amount of camber that will be present. In PPCBs produced by precasters for the Iowa Department of

Transportation, there are sacrificial top prestressing strands, straight bottom strands, and if specified, harped prestressing strands. Iowa DOT gives prestress values that are desired for each beam immediately before the transfer of prestress. It is the precasters responsibility to tension the strands to within  $\pm 5\%$  so that the prestress force is in agreement with the target prestress value. Losses, such as seating and relaxation of the prestressing strands from the time of initial tensioning to immediately before the transfer of prestress, can be accounted for by precasters by exceeding the target prestress value by 1-5%. Other precasters neglect this value due to the small percentage of prestress loss that is associated with each loss.

When calculating camber, the prestress force for the harped strands, straight bottom strands and sacrificial strands were calculated separately in this study. Due to the different tensioning forces applied to all three groups and the harped strand profile crossing above and below the neutral axis, it was necessary to keep the prestressing forces separate for each group. The prestress force value was determined from the tensioning sheets that were obtained from precasters. Calculating the prestress force from the precaster's as-built tensioning sheets allowed researchers to closely model the prestress force that was applied to specific PPCBs. Below is a summary of the tensioning procedure and how the prestress forces were calculated in this study.

#### **4.2.1 Tensioning Procedure**

In the tensioning process, top sacrificial prestressing strands were completed first. The number of top sacrificial prestressing strands were determined by the beam specifications but can range from 2-6 strands that were tensioned with a single jack to the pressure of 3 to 5 kips in each strand. Once the top sacrificial strands are tensioned, the harped strands, if any, are laid out along the length of the bed. Initially, the harped strands are positioned to the elevation of the final height near the end of the beam line. An example of this can be seen in Figure 4-1. While in this position, the strands are tensioned to an initial value which is less than the final prestress force ( $P_1$  in Figure 4-1). Mechanical means of raising the interior harped strands at the end of every beam were then completed.



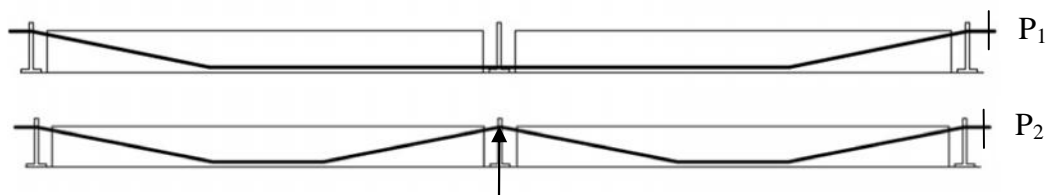


**Figure 4-1: Initial and Final Positions of Harped Prestressing Strands when Tensioning**

As a result of raising the interior harped supports to the final location where the prestressing strand is positioned in Figure 4-1, additional prestress force is added. The total amount of prestress force present in harped strands was determined by adding the prestress force before the interior supports are raised with the additional prestress force caused by the elongation from raising the harped supports to their final location.

The method of tensioning the straight bottom strands is unique to each precaster. It has been observed that some precasters use a multi-pull jack that has the ability to tension multiple prestressing strands to the desired tension. Other precasters use a single prestressing jack to tension all of the bottom strands. Iowa DOT requires strands to be pulled to an elongation and then checked with the gauge reading to verify the correct prestress force. It has been observed that precasters pull the prestressing strands to a minimal force of approximately 3 kips as a reference point for the start of the elongation. After the initial pull to 3 kips, precasters are able to mark the initial distance and tension the prestressing strands until the designed elongation is reached.

### 4.3 Prestress Losses

Instantaneous prestress losses result from elastic shortening and seating. At the time of instantaneous losses, there is some relaxation that has occurred from the time in between the initial stressing of the prestressing strands to the transfer of prestress. A combination of the instantaneous losses along with the relaxation that is present can be calculated and subtracted from the initial prestress force obtained from the tensioning sheets to determine the effective prestress force. When calculating instantaneous camber for beams in this study, prestress losses caused by creep and shrinkage of concrete were not considered. During the time when the girder is fabricated until the time when it is released, there is no load applied. After the transfer of prestress, the girder is axially loaded through prestressing stands and is subjected to self-weight and prestress moments. Instantaneous camber measurements occur immediately after the

transfer of prestress which allows researchers to neglect the effects of creep of concrete during this time period. The curing duration for a PPCB is typically 18-24 hours. During this time, the concrete is usually steam cured in a moist environment. Due to the curing conditions, it is assumed that minimal shrinkage of concrete occurs and can be ignored in calculating camber at the transfer of prestress.

#### 4.3.1 Prestress Loss due to Relaxation

The effect of losing tension in a stressed tendon due to relaxation reduces the prestressing force. Relaxation occurs from the time the prestressing strands are tensioned to the end of the service life of the member. For the purpose accurately predicting instantaneous camber in this research study, the prestress loss due to relaxation from the time the prestressing strand was tensioned to the time it was released was approximately estimated. Equation (4-1) lists the prestress loss due to relaxation, as recommended in AASHTO LRFD Bridge Design Specifications 5.9.5.4.2c-1.

Low relaxation strand:

$$\Delta f_{pR1} = \frac{\log(24t)}{40} \left[ \frac{f_{pJ2}}{f_{py}} - 0.55 \right] f_{pJ2} \quad (4-1)$$

$$\Delta P_{pR1} = A_p \Delta f_{pS} \quad (4-2)$$

- where:
- $t$  = time estimated in days from stressing to transfer (days)
  - $f_{pJ2}$  = initial stress in the tendon at the end of stressing or jacking (ksi)
  - $f_{py}$  = specified yield strength of the prestressing steel (ksi)
  - $f_{pR1}$  = prestress loss due to relaxation (ksi)
  - $P_{pR1}$  = prestress loss due to relaxation (kips)
  - $A_p$  = area of each prestressing strand (in<sup>2</sup>)

#### 4.3.2 Prestress Loss due to Seating

Seating losses occur due to a slip experienced within anchorage chucks that occurs when the prestress in each strand is transferred from the jack to the anchorage. As noted in Section 4.2, prestressing strands can be tensioned by a single prestressing jack or by a multi-pull jack system.

In both cases, the jack is used to pull the prestressing strand to a certain distance to create prestress force in each strand. At the time when the strand is pulled to the correct elongation that gives the target prestress force, an anchor will be placed on the strand. The purpose of the anchor is to hold the strand to a specific distance so that the proper prestress force is maintained until the concrete can bond to the prestressing strand. The prestressing strand will slip past the anchor a small distance before properly gripping on to the strand. The distance that is lost due to the anchor seating will reduce the amount of prestress per strand. The loss in prestress as a result of seating is calculated in Equation 4-3 which was derived from Hookes Law.

$$\Delta P_{ps} = \frac{\Delta_s AE}{L} \quad (4-3)$$

where:  $\Delta P_{ps}$  = prestress loss due to seating (kips)  
 $L$  = length of the prestressing strand (in.)  
 $A$  = cross sectional area of the prestressing strand (in<sup>2</sup>)  
 $E$  = modulus of elasticity of the prestressing strand (ksi)  
 $\Delta_s$  = seating distance (in.)

Knowing the properties of the prestressing strands along with the length of the strands allows researchers to calculate the prestress loss due to seating. The magnitude of prestress loss due to seating (  $\Delta P_{ps}$ ) is dependent on four variables including: the area of the prestressing strands, the modulus of elasticity of the prestressing strand, the distance the prestressing strand moves due to seating, and the length of the strands when seating occurs.  $A$  and  $E$  are dependent on the type of prestressing strand that is used. The distance of seating (  $\Delta_s$  ) is typically between the values of 0.125 in. and 0.375 in depending on the type of anchorage was used. For the purpose of this study, a value of 0.23 was used as this corresponded to the distance of seating for the wedge commonly used by precasters. The length of the prestressing strand is a variable that differed between 250 feet to 440 feet between the different plants and the appropriate value was used in each case.

The prestress loss due to seating (  $\Delta P_{ps}$ ) found in Equation 4-3 is applicable for each prestressing strand. To determine the total loss due to seating, the prestress loss per strand (  $\Delta P_{ps}$ ) needs to be multiplied by the number of prestressing strands that were tensioned.

Although this number is small, it should be accounted for because the effect of prestress on camber is sensitive and could produce discrepancies with actual camber behavior.

### 4.3.3 Elastic Shortening

As stated in Chapter 2.2.2, when a PPCB is loaded at the transfer of prestress, a large force is applied along the length of the beam by the prestressing strands, causing the beam to shorten from its original length by a small amount. The reduction of prestress due to shortening of the beam and prestressing strands is referred to as elastic shortening (E.S.).

There are three components of elastic shortening that contribute to the change of prestress. Assuming a constant prestress force acting at the centroid over the full length of the beam, a shortening of the entire cross section occurs (Figure 4-2). The placement of the prestressing strands will affect if any eccentricity is present in the PPCB which essentially causes camber. The placement of the prestressing strands will cause greater shortening at the center of gravity of prestressed steel compared to locations further from it (Figure 4-3). When the moment caused by the eccentrically placed prestressing strands and prestress force is greater than the moment caused by the girder self-weight, camber will be present. When camber is present, the girder's self-weight will cause elastic gains in the prestressing steel (Figure 4-4). An iterative process to find the prestress loss due to elastic shortening from these three components is presented in Equations 4-5 through 4-10.

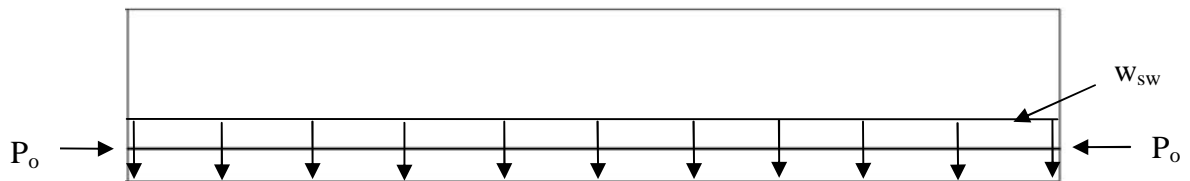


**Figure 4-2: Prestressed Beam with Shortening across the Cross Section**

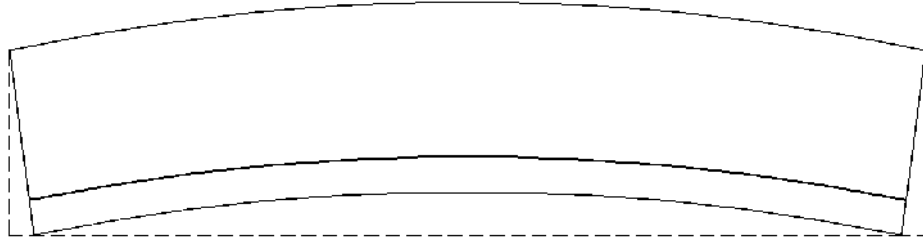


**Figure 4-3: Prestressed Beam with Additional Shortening near the Center of Gravity of Steel**

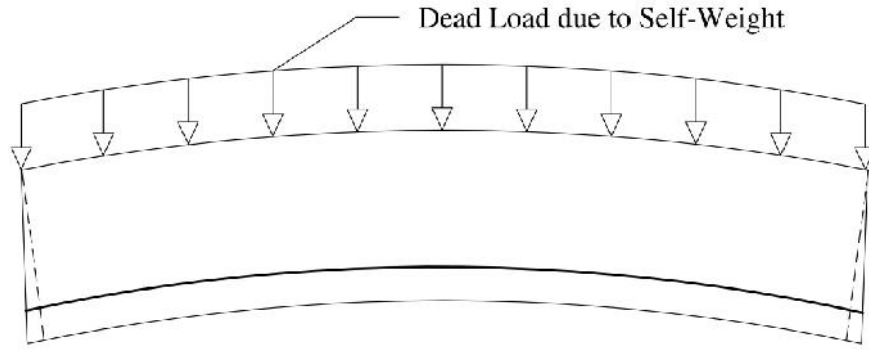


**Figure 4-4: Prestressed Beam with Elastic Gains due to Self-Weight**

$$M_{sw} = \frac{w_{sw} L^2}{8} \quad (4-4)$$

$$P_{at} = A_{ps} * f_{pat} \quad (4-5)$$

$$f_{cgp} = -\frac{A_{ps} f_{pat}}{A} - \frac{A_{ps} f_{pat} (e)^2}{I} + \frac{M_g e}{I} \quad (4-6)$$

$$\Delta f_{pES} = abs(f_{cgp}) \frac{E_p}{E_{ci}} \quad (4-7)$$

$$f_{pat} = f_{bpt} - \Delta f_{pES} \quad (4-8)$$

$$f_{pat} = f_i - \Delta f_{pS} - \Delta f_{pR1} \quad (4-9)$$

where:  $f_i$  = strand stress before relaxation and seating (ksi)  
 $M_{sw}$  = girder dead load moment at midspan  
 $P_{at}$  = final prestress force after transfer (kips)  
 $A_{ps}$  = total strand area (in<sup>2</sup>)  
 $f_{pat}$  = strand stress immediately after transfer (ksi)  
 $f_{pbt}$  = strand stress immediately before transfer (ksi)  
 $f_{cgp}$  = concrete stress at the level of the strands due to the weight of the girder and the prestress force after transfer (ksi)  
 $f_{pES}$  = prestress loss due to elastic shortening (ksi)  
 $P_{pES}$  = prestress loss due to elastic shortening (kips)

The process of calculating the loss due to elastic shortening is typically iterative and begins with an initial assumed prestress force of  $f_{pat}$ . The loss due to elastic shortening occurs after seating and relaxation losses. The initial prestress strand stress ( $f_{pat}$ ) should be computed by subtracting the losses due to relaxation and seating as shown in Equation 4-9.

Using the assumed initial strand stress immediately after transfer ( $f_{pat}$ ) with Equations 4-5 through 4-9, the solution will produce a revised strand stress after transfer. Reiterating Equations 4-5 through 4-8 will allow the strand stress after transfer to converge. Taking the stress before the transfer of prestress and subtracting the change in stress due to elastic shortening (Equation 4-8) produces the stress in the prestressing steel after the transfer of prestress including the effects of elastic shortening.

#### 4.4 Effective Prestress Force

The effective prestress force is the force that is present in the prestressing steel immediately after the transfer of prestress. The stress obtained from Equation 4-9 can be converted to the effective prestress force by Equation 4-10. The prestress losses due to seating and relaxation are included by being subtracted from the initial iteration in the elastic shortening equation. After the elastic shortening equation converges, the effective prestress is obtained and it was possible to use the moment area method to calculate the instantaneous camber. The effective prestress force for the sacrificial, harped, and straight bottom strands were calculated separately. This

made calculating the eccentricities of the groups and the prestress force associated with each group easier and more accurate.

$$P_{at} = f_{pat} A_{ps} \quad (4-10)$$

#### 4.5 Moment Area Method to Calculate Camber

The moment area method was used as a simplified method to calculate camber. The first step in calculating the camber with the moment area is to determine the prestress force and eccentricity of the group of prestressing strands with respect to the centroid of the section (see Equation 4-10). Multiplying the eccentricity by the respective prestress force for the top, bottom, and harped prestressing strands at certain locations of the beam will result in the moment diagram due to the prestress force.

$$e = cg - cgs \quad (4-11)$$

where:  $e$  = eccentricity of the group of prestressing strands of interest  
 $cgs$  = center of gravity of the prestressing strands of interest  
 $cg$  = center of gravity of the section

The center of gravity of the section ( $cg$ ) was given in the Iowa DOT beam specification and slightly modified for the transformed section properties. Naaman (2004) notes that transformed section properties or gross properties can be used for the calculation of camber. The use of gross section properties result in accurate findings however, transformed section properties agree well.

The moment diagrams for the harped strands, bottom straight strands, and top sacrificial strands are shown in Figures 4-5 through 4-7. The magnitude of the moment diagram for each of these groups is dependent on the prestress force and the eccentricity that is present.

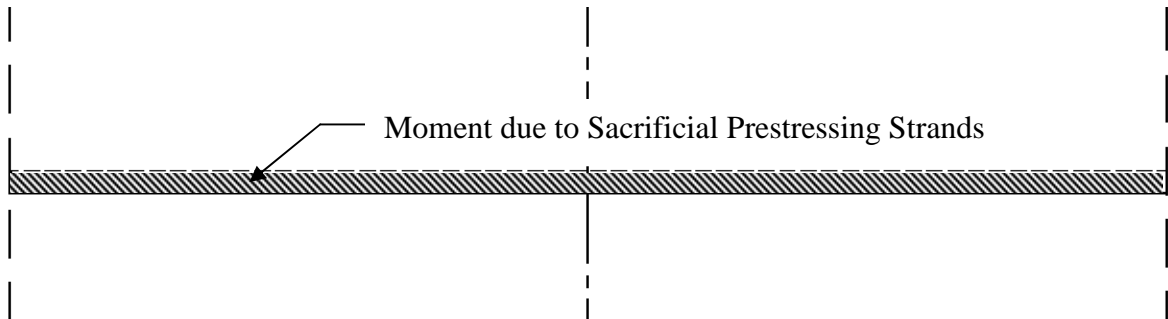


**Figure 4-5: Moment Diagram due to Straight Sacrificial Strands**

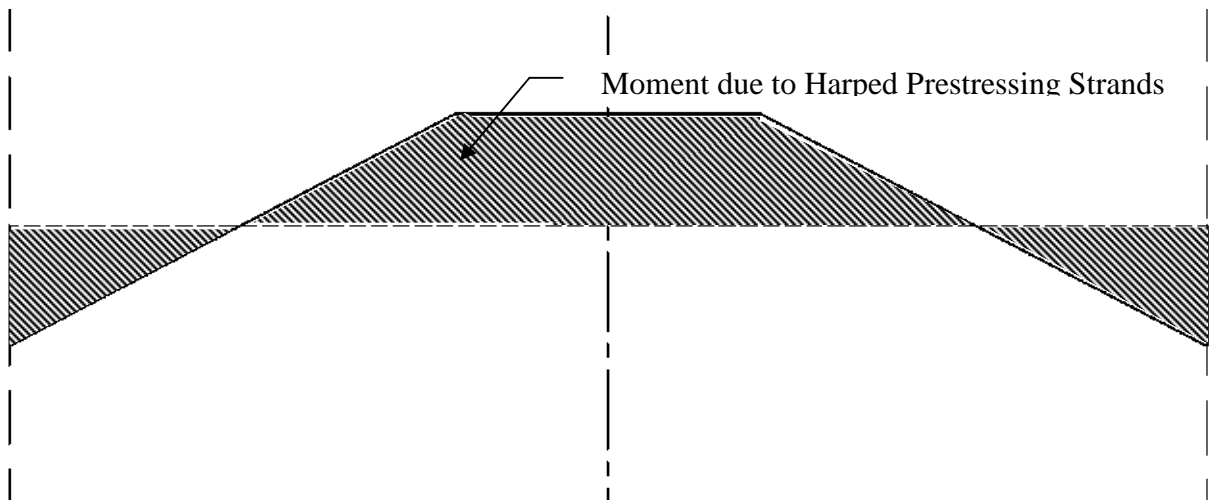


**Figure 4-6: Moment Diagram due to Harped Prestressing Strands**

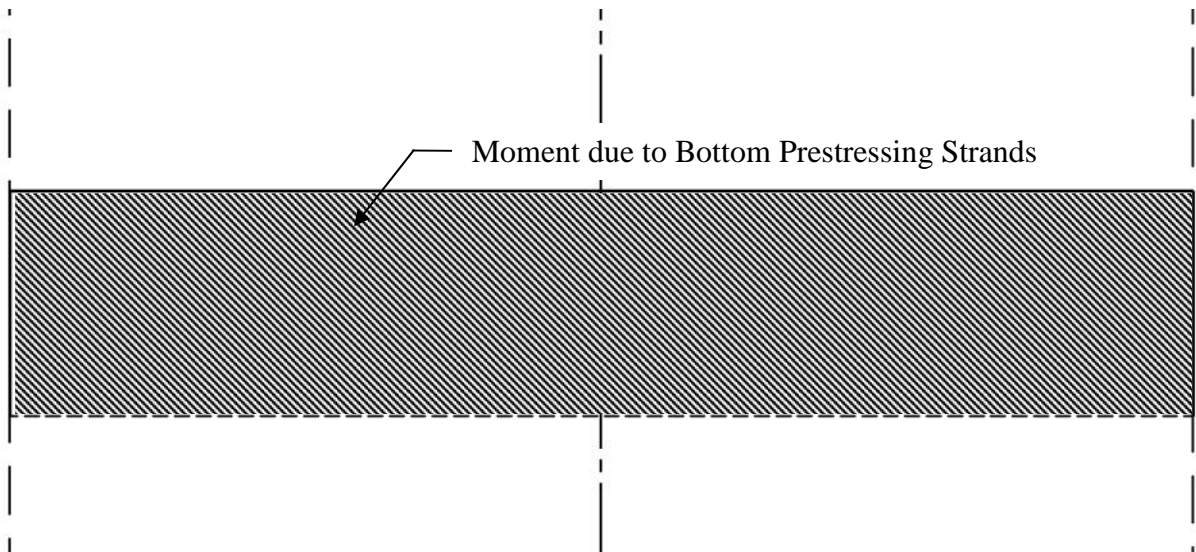


**Figure 4-7: Moment Diagram due to Bottom Prestressing Strands**



Combining the moment produced by the harped, straight, and sacrificial stands will produce a graph similar to Figure 4-8. After the moment diagram due to prestressing is produced, points A and B in Figure 4-8 are determined. Finding the magnitude of point A and B is necessary for determining the area and centroid of the moment diagram.

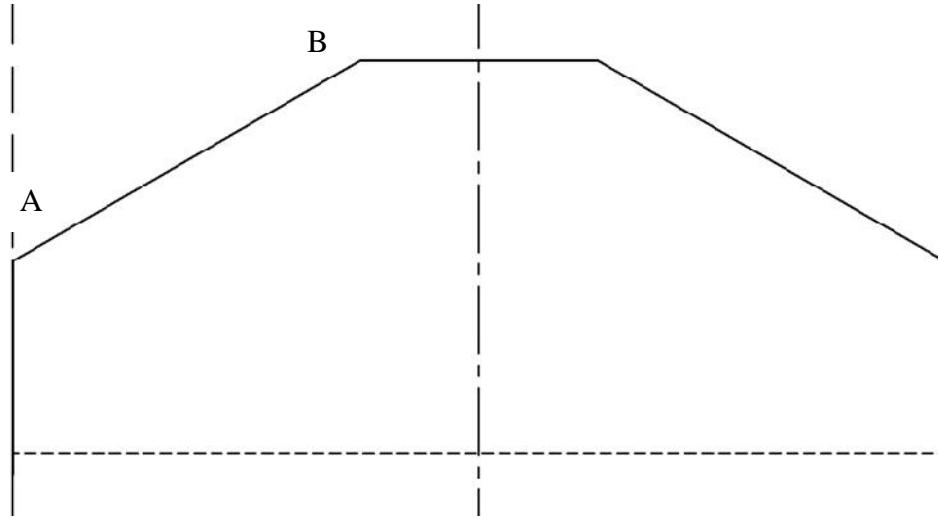


**Figure 4-8: Moment Diagram of a Prestressed Concrete Beam without Transfer Length**

To closely capture the moment diagram due to prestressing on a PPCB, transfer length is accounted for. The transfer length occurs at the beam ends as a result of the prestress going from zero stress at the end of the beam and reaching the effective prestress force a short distance in from the end of the beam. Point A in Figure 4-9 is the location where the effective prestress force is fully reached at the end of the transfer length. The transfer length is found by using Equation 4-12 and is in accordance with AASHTO LRFD Bridge Design Specifications 5.11.4.1.

$$\text{Transfer length} = d_b * 60 \quad (4-12)$$

where:  $d_b$  = diameter of the strand

Points A and B correspond to the sum of the moments from the straight bottom strands, sacrificial strands, and the harped strands at the transfer length and at the hold down point of the harped strands, respectively (Equation 4-13). Once the value of the moments at points A and B are determined, the area under the moment diagram can be calculated. Due to simplicity, the moment diagram can be broken into different shapes that are easy to calculate the area and the

centroid of the section (Figure 4-9). The area and the respective centroid of the section can be multiplied together to obtain the deviation of the tangent at the midspan with respect to the tangent at the beam end (Equation 4-14). Taking the sum of the components of the different sections together for half of the beam and dividing by the modulus of elasticity and the moment of inertia will result in the upward deflection due to prestressing as detailed below:

$$M_{AorB} = P_{atS}e_s + P_{atH}e_h + P_{atB}e_b \quad (4-13)$$

where:  $M_A$  = moment due to prestressing force at point A  
 $M_B$  = moment due to prestressing force at point B  
 $P_{atS}$  = effective prestress force of sacrificial strands  
 $P_{atH}$  = effective prestress force of harped strands  
 $P_{atB}$  = effective prestress force of bottom strands  
 $e_s$  = eccentricity of sacrificial strands  
 $e_h$  = eccentricity of harped strands  
 $e_b$  = eccentricity of bottom strands

$$T_{total} = (A * x) \quad (4-14)$$

where:  $A$  = area of the section of interest  
 $x$  = distance from the end of the beam to the centroid of the section of interest  
 $T_{total}$  = deviation of the tangent from the end of the beam to the centerline.

$$\Delta_{PRESTRESS} = \frac{T_{total}}{EI} \quad (4-15)$$

where:  $\Delta_{PRESTRESS}$  = upward deflection due to prestress

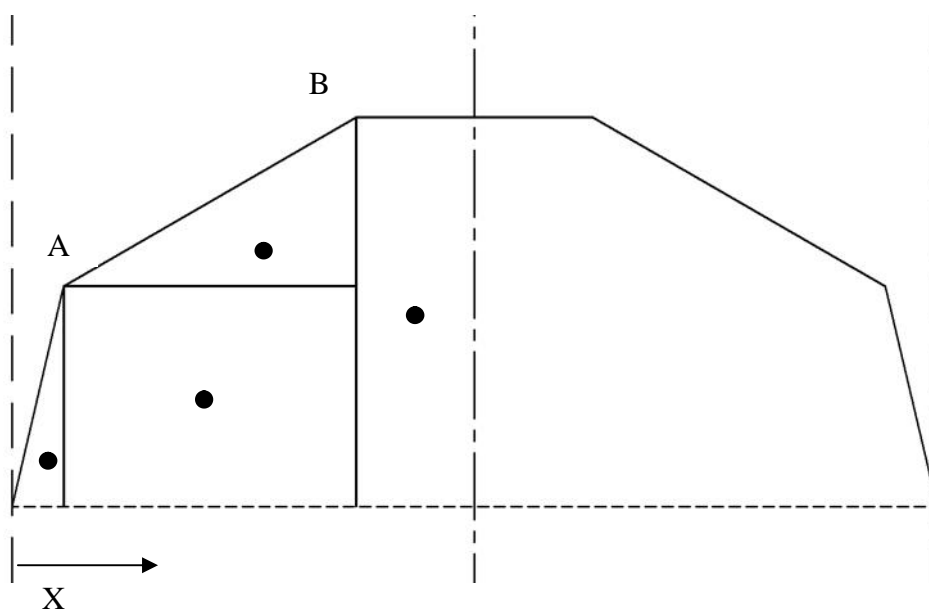


**Figure 4-9: Moment Diagram Divided into Sections together with their Centroid Location**

#### 4.6 Modulus of Elasticity

The modulus of elasticity is a variable that influences both instantaneous and long-term camber. For the purpose of convenience for designers and the close agreement with measured and predicted camber, the method of calculating camber based off AASHTO LRFD (2010) was used. In this method, the unit weight of concrete and the compressive strength are needed. The equation is shown in Equation 4-16.

$$E_{ci} = 33K_1 w_{sw}^{1.5} \sqrt{f'_{ci}} \quad (4-16)$$

where:  $w_{sw}$  = unit weight of the concrete (lb/ft<sup>3</sup>)  
 $f'_{ci}$  = release strength of concrete (psi)  
 $K_1$  = correction factor for source of aggregate to be taken as 1.0 unless determined by physical test, and as approved by the authority and jurisdiction

#### 4.7 Moment of Inertia

The moment of inertia is also an important variable to accurately represent camber. As mentioned in Section 4.5, the use of transformed moment of inertia can be used in camber

calculations since there will not be a significant change when compared to the gross moment of inertia. Due to the similar results that are achieved with both moment of inertia values, transformed section properties were used for the purpose of this study. Difficulty was caused when harped strands were present because to the ability for the transformed moment of inertia to change along the length of the beam. In this case, the transformed moment of inertia was calculated at points along the length of the beam. The final transformed moment of inertia was then determined by taking a weighted average along the length of the PPCB.

#### 4.8 Deflection Due to Self-Weight of the Beam

After the transfer of prestress, a PPCB is assumed to be simply supported with only the ends of the beam are in contact with the precasting bed. The self-weight of the beam will resist the camber by causing a downward deflection. The deflection due to the self-weight of the beam at midspan can be represented in Equation 4-17.

$$\Delta_{SELF-WEIGHT} = \frac{5w_{sw}l^4}{384EI} \quad (4-17)$$

where:  $l$  = length of the beam assuming only the ends of the beam are in contact with the precasting bed

$\Delta_{SELF-WEIGHT}$  = downward deflection due to the self-weight of the beam

#### 4.9 Final Camber

The final camber value is obtained from adding the upward deflection due to prestressing to the downward deflection due to the self-weight of the beam. These equations assume an elastic relationship from the concrete and prestressing steel materials. The final camber can be calculated from Equation 4-18.

$$TOTAL = PRESTRESS + SELF-WEIGHT \quad (4-18)$$

## **CHAPTER 5. RESULTS AND DISCUSSION**

Using the methods described in Chapter 3 and 4, it was possible to quantify the errors associated with both camber measurement and variables used to predict camber. The following is a description of the results of errors that are present in camber measurements and prediction.

### **5.1 Factors Affecting Instantaneous Camber Measurements**

It was noted that over 105 independent instantaneous camber measurements were taken at three precast plants (see Section 3.3). In this effort, tape measure, rotary laser level, and string potentiometers were used to measure camber at the transfer of prestress, and quantify various errors. Additionally, variables that influence the predicted camber were investigated. This section discusses the potential errors and quantities that influence the instantaneous camber measurements and predictions.

#### **5.1.1 String Potentiometer Measurements during Release of a PPCB**

String potentiometers were instrumented on the precasting bed and multiple PPCBs before, during, and after the transfer of prestress. Recording the displacement with respect to time made it possible to continuously monitor progressive change in camber of the PPCBs and the corresponding impact to the precasting bed. The results from two PPCBs that were each instrumented with 3 string potentiometers are shown in Figures 5-1 and 5-2. Both beams, which were cast for Iowa Department of Transportation bridge projects, were similar in length (100 ft vs. 110 ft). However, they were cast and released at separate precasting plants, had different cross sections, amounts of prestress, concrete mixes, and went through different prestressing releasing procedures. Despite the differences that were present between the two beams, similarities with the behavior of the string potentiometer's vertical displacements are present.

The string potentiometers in Figures 5-1 and 5-2 were instrumented at midspan on the PPCB and on the precast bed at the end of the beam and at midspan. At time 0, data collection was started. As time progresses, workers cut the top sacrificial prestressing strands. Low prestress force caused small changes of vertical displacement which is noted in Figures 5-1 and 5-2. The next event in the recorded data is the release of the harped prestressing strands (HSRC) which also caused a small vertical uplift. The magnitude of the vertical displacement is controlled by the amount of harped reinforcement present and the eccentricity. The string potentiometer at the

end of the beam on the precasting bed in Figure 5-1 was observed to undergo a downward vertical displacement after the prestressing strands were released. This is because the beam weight shifted from being applied along the length of the beam to the location where the string potentiometer was located. Figure 5-2 shows a small positive displacement after the harped reinforcement was released for the string potentiometer located at the beam end. The small positive displacement was due to the positive moment produced by the harped prestressing strands that outweighed the girder self-weight. During the release of the bottom strands, the negative moment applied by the transfer of prestress shifted the weight of the girder towards the ends of the beam. The result is downward deflections for the string potentiometers at the ends of the beam and an upward deflection for the string potentiometers at the midspan of the precasting bed. Additionally, the prestress force caused the beam to start to camber upward. The points where the bottom strands were completely free represent the time when the full prestress was applied to the beam while resting on the precasting bed.

There was still a small increase in camber as a function of time due to the beam overcoming friction between the precasting bed and the beam. Figure 5-2 shows small discontinuities in the increase in vertical displacement after the bottom strands were released. This can be attributed to the precaster's lifting adjacent PPCBs off the precasting bed. In Figure 5-1, precasters were able to lift the PPCB and place it down on the precasting bed after the last prestressing strands were released. At the time the beam was lifted (LB), there is a large vertical increase shown in Figure 5-1. The lift released the remaining friction that is present and allowed the beam to reach its full instantaneous camber. After the beam was set down, there was a slight decrease in camber. This could be due to the beam readjusting on the precasting bed or could be due to the effects of reverse friction. Precasters from Figure 5-2 were unable to lift/set the beam because of manufacturing time constraints and the potential for damaging the newly cast beam. There is believed to be an additional upward displacement that would take place at the ending time due to the release of friction; however, recording data was terminated before the precaster transported the beam to the storage yard. Continuing to instrument PPCBs with string potentiometers and also take laser level readings made it possible to verify the behavior of beams and quantify the magnitude of bed deflections, inconsistent top flange surfaces along the length and due to local effects, and friction.

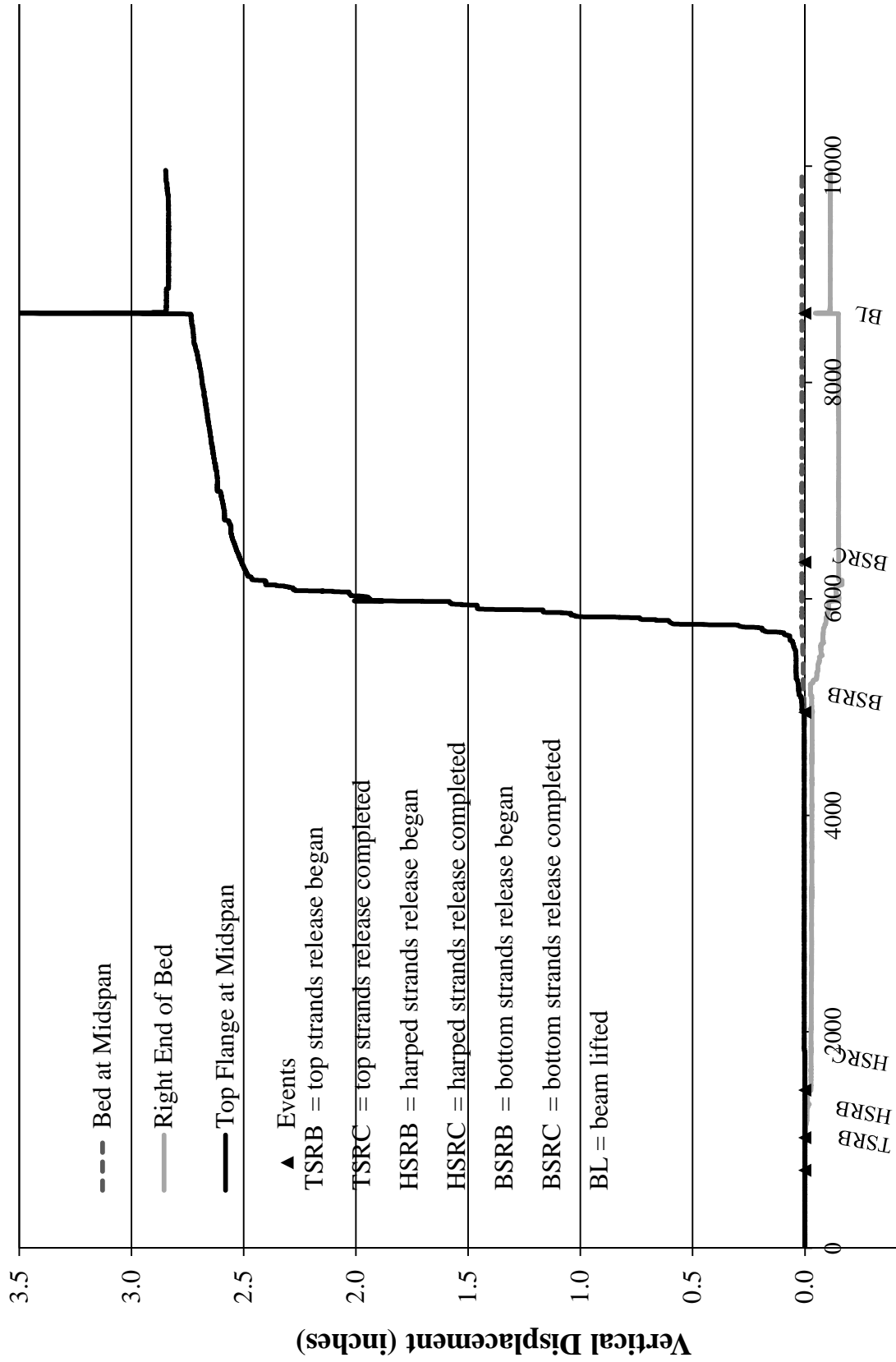


**Figure 5-1: Time vs. Vertical Displacement of at BTB 100 PPCB**

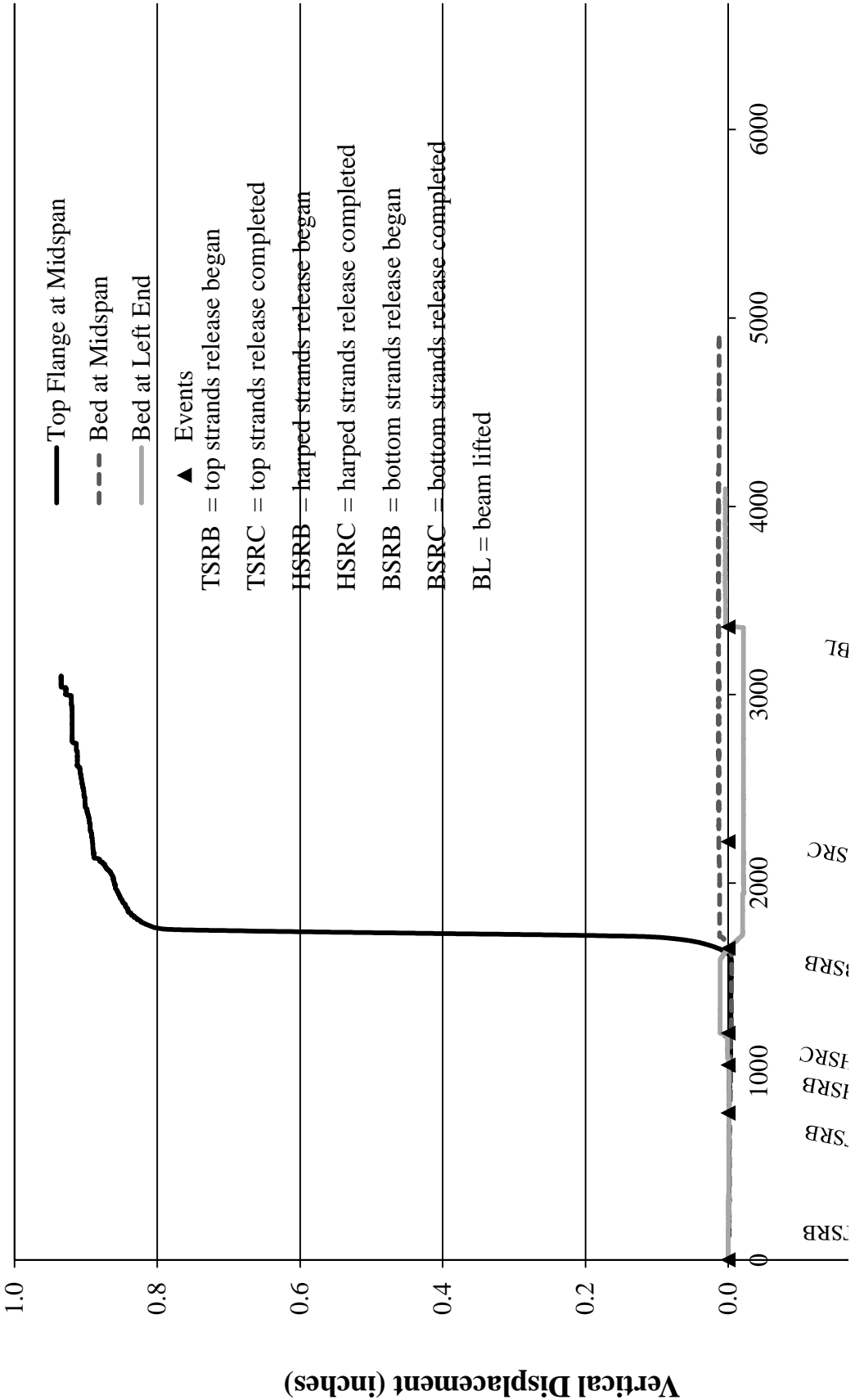


**Figure 5-2: Time vs. Vertical Displacement of at BTE 110 PPCB**



### 5.1.2 Bed Deflections

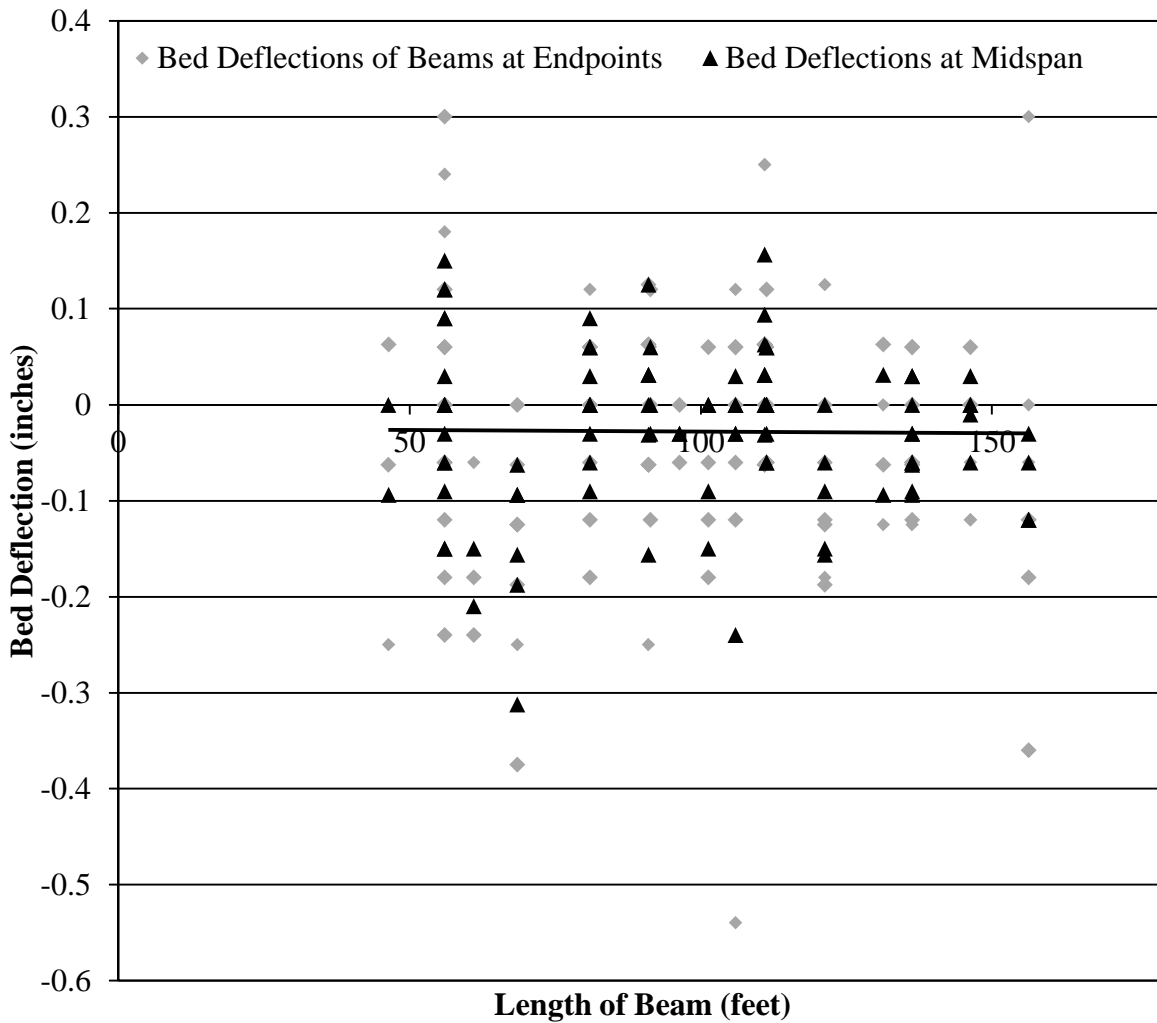
As mentioned in Chapter 3.1.1, bed deflections are present due to a shift in weight during the transfer of prestress. There are a number of factors that influence the magnitude of bed deflections which include; the materials properties of the precasting bed, the design of the precasting bed members, the foundation of the precasting bed, and the distance between the precasting bed supports.

Figure 5-3 displays the bed deflections taken by a rotary laser level. The graph is composed of the difference of individual points on the precasting bed before and after the transfer of prestress and the average of bed deflections from the individual bed elevation readings. The average of the bed elevation readings is the most accurate value because it is taken with respect to the midspan rather than the deflection locally at the end of the beam. The bed deflections are represented in Figure 5-3 by triangles and are arranged on the x axis in order of increasing length. Trends from Figure 5-3 show:

- The average of the final camber with respect to the ends is below the zero line, which suggests that there is a negative bed deflection with the average of all of the measured beams. This is in agreement with the theory that as the weight of the beam shifts to the ends, the bed elevation will produce a downward displacement.
- As the beams increase in length, the bed deflections increase as well. The weight of the beam is affected by the size of the cross section, unit weight of concrete, and the length of the beam. PPCBs produce beams that have similar cross sections and unit weights of concrete. As the length of the beam increases, the weight of the beam will also increase thus, causing an increase in bed deflection at the end of the beam.

Figure 5-3 has a large scatter due to different precasting beds between the three precasting plants and the sensitivity to measurement locations. Bed deflection measurements were taken from three precasting beds that had similar designs. However, the location of the PPCBs relative to the precasting bed supports influenced the magnitude of the bed deflections. Figure 5-4 shows the ends of two PPCBs as they rested on the precasting bed. When the ends of the PPCBs are placed directly over the bed's supports, the net bed deflection was reduced compared to the alternative of having the beam ends be placed in between the precasting bed supports. In

addition, measurements taken after the transfer of prestress are prone to the beam shifting along the length of the prestressing bed due to the uneven release of prestress. Shifting of the beam inhibited the ability to measure the bed elevation after release from the exact position where the bed elevation was measured before the transfer of prestress.



**Figure 5-3: Bed Deflection vs. Length of Multiple PPCBs**



**Figure 5-4: Two PPCB Ends in Relation to the Supports on a Precasting Bed**

Results from over 100 beams measured by researchers indicate that neglecting bed deflections will reduce camber by 2.80% ( $\pm 8.21\%$ ). The average bed deflection was -0.0297

inches with the maximum value being 0.3125 inches. Additionally, results from bed deflection with respect to the midspan are listed in Table 5-1.

**Table 5-1: Summary of Bed Deflections**

Average (inches)	-0.0297
Standard Deviation (inches)	0.0615
Maximum (inches)	0.1563
Minimum (inches)	-0.3125

#### 5.1.2.1 Positive Bed Deflection

When recording bed measurements with the rotary laser level, there were cases that suggest upward bed deflections occur at the ends of the beam. This is contrary to the expectation that after the transfer of prestress, the weight shifts to the ends of the beam causing a downward deflection. Due to adjacent beams and the placement of supports, it is possible for a positive bed deflection to occur. A scenario when a beam end can have a positive bed deflection is outlined in the following steps.

1. Two separate beams are placed adjacent to each other at a close distance.
2. One beam end is placed in between two precast bed supports while the adjacent beam end falls closer to the support.
3. The cantilever action of the first beam forces the adjacent beam to have an upward bed displacement.
4. Since the beam may slide during the release process, the original measurement location was used in order to eliminate the effects of inconsistencies on the precasting bed surfaces. The resulting measurement distance that is away from the girder can result in positive deflection after the transfer of prestress (Figure 5-5).

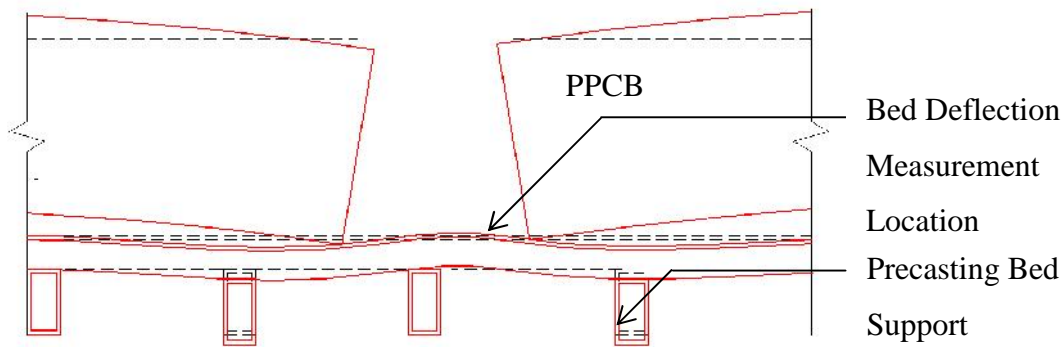


**Figure 5-5: Two PPCBs and Placement that Results in Positive Bed Deflection**

### 5.1.3 Inconsistent Beam Depth

The elevation of the top flange has been observed to vary across the length and width of the PPCB. This results in inconsistent elevations before the transfer of prestress, which can give the illusion of more or less camber than is present. The inconsistent elevation has been observed to vary along both the length and width of the beam. The causes of the inconsistent top flange on PPCBs were found to be due to how the forms are set as well as the type and consistency of finish that is used. Although the instantaneous camber is not typically measured with respect to the top surface, all field camber measurements are taken from the top surface, ultimately causing discrepancies between the measured and expected camber and casting a doubt on the initial camber produced for the beam.

#### 5.1.3.1 Inconsistent Surface Finish due to Local Inconsistencies

Workers finishing the top flange of the beams intentionally roughen the surface which leads to problems with measuring camber from the top flange. Conducting several measurements across the top flange were conducted to determine what local deficiencies were present. Results found that the average difference across the top flange length is 0.113 inches while a maximum value has been observed to be 0.90 inches. Failure to account for the inconsistent top flange due to local imperfections misrepresents camber by -4.37% ( $\pm 12.82\%$ ).

Results from measuring the local inconsistencies reveal that the roughness of the top flange surface is not dependent on the beam length. The roughness of the beam is intended to be similar for all beams so that the surface of the deck will bond easily to the top flange. However,

there is an observable trend with the relationship between the level of roughness and the precasting plant. The roughness of the top flange surface is uniform between different beams produced at the same plant due to the same finishing practices but differ from each plant. Results from the roughness of the top flange surface are displayed in Appendix C.



**Figure 5-6: Inconsistent Top Flange Surfaces on PPCBs**





**Figure 5-6: continued**

#### 5.1.3.2 Inconsistent Finished Surface along the Length of the Beam

The finish that is applied by workers can contribute to the inconsistent depth of the beam along the length. After the concrete is placed in the form, workers tend to evenly distribute the concrete so that the top flange surface maintains a constant thickness. The ability for workers to uniformly finish the beam is often impeded by the stirrups that protrude from the top flange. Finishing the concrete around the stirrups along the length of the beam can cause rises and falls in the surface. Consistently keeping a uniform thickness along the length is directly related to finishing practices.



**Figure 5-7: Inconsistent Troweled Surface Along the Length of the Beam**

Measuring the elevation of the top flange of the beam before the transfer of prestress made it possible to see if the midspan of a beam is higher or lower than the average of the two ends. From these results, it is possible to determine if the beam has an upward or downward elevation at the midspan before applying prestress. Results found that the greatest difference along the top flange length was 0.7875 inches while an average value was 0.0990 inches. Failure to account for the inconsistent top flange along the length of the beam misrepresents camber on average by 5.16% ( $\pm 24.55\%$ ). Trends with the top flange inconsistencies along the length reveal that as the beam length increases, the magnitude of out of planeness increases. This is due to the increase in the adjustment with the multiple forms that are needed to meet the required length requirements of the beam. Additionally, it has been observed that on average, Plant A had the largest difference in inconsistencies in camber along the length of the girder. Plant B and C had similar average values for inconsistent beam length of 0.145 inches and 0.155 inches, respectively. Reasons for why Plant A had larger values for the inconsistent top flange along the length was the quality of uniform depth of formwork or the survey of the forms before casting. Additional results are shown pertaining to the inconsistent top flange along the length in Appendix C.



### 5.1.3.3 Method of Setting Forms

Precasters' methods of setting forms will affect the uniformity of the elevation of the beam before the transfer of prestress in PPCBs. The ability for a precaster to produce a uniform beam relies heavily on the trueness of the forms and the way they are assembled around the precasting bed. The forms that are used from three precast plants are free standing forms. Free standing forms rest on supports that are connected to the precasting bed. The process for setting forms is described for each of the plants below.

In one plant, free standing forms are put into place by a crane. The forms are placed on movable metal supports that lie every 10-20 feet. A string is strung along the length of the top flange of the beam. Bends from adjacent forms are adjusted based on the distance from the form to the string. After the bends are taken out of the forms, workers take measurements from the top of the precasting bed to the top of the form. This is typically done every 10-20 feet. If adjustments need to be made to the height of the form, workers can shim the forms up or down to meet the correct elevations. Workers will then place intermediate supports along the length of the beam similar to Figure 5-8 and secure the forms.



**Figure 5-8: Temporary Support used for Supporting a PPCB Form**

In another plant, free standing forms on rollers are utilized. This consists of having a form that is typically moved six inches to and from the precasting bed. The other side of the form can be rolled from the precasting bed. When placing the forms, the back form is rolled into place

before the prestressed reinforcement is tensioned. When the remaining reinforcement is placed and tied, the other form is rolled into place. It is assumed that the forms are in correct tolerance along the length of the beam. The forms are secured together a specified distance from each other along the top and bottom flange.

The third plant uses free standing forms that are placed by a travel lift crane on the bed supports. The longitudinal length of the precasting bed requires multiple sets of forms to be placed along the length of the bed. The multiple sets of forms can have slight bends along the length of the precasting bed. Similar to the first plant, a string is tightly strung between the lift up hooks on the beam. This string lies in the center of the top flange of the beam. Workers can measure the distance between the string and the top of the form to make sure the distances are uniform along the length of the beam. If distances from the top of the form and string are different along length of the beam, workers use a small hand jack to raise the bottom of the form on the opposing side so that the top of the form rotates into place. Once the forms are slightly adjusted, they can be secured into place by tightening the clamps at the bottom of the form.



**Figure 5-9: Forms on a PPCB**

#### **5.1.4 Friction between the Beam Ends and Precasting Bed**

After the transfer of prestress, friction between the beam ends and the precasting bed is present. This friction has been observed to inhibit the beam from reaching its full instantaneous

camber immediately after release. The force of friction that limits the increase in camber is found in Equation 5-2 and is dependent on the normal force and the coefficient of friction. The normal force is the force acting perpendicular to the plane of contact and is from the weight of the beam. Since friction is acting when the beam has cambered, only half of the beam's weight is at the point of contact. Select beams were cast with metal sole plates in the ends. The purpose of a sole plate is to prevent damage to the bottom flange of the beam. Due to the smooth precast surface and the similar trends in Figure 5-10 for beams with and without sole plates, the coefficient of friction was assumed to be 0.35 based on AISC coefficient of friction for surfaces that are unpainted, clean mill steel.

$$F_f = F_n * \mu \quad (5-2)$$

where:     $F_f$        = force of friction  
               $F_n$        = normal force  
               $\mu$          = coefficient of friction

Figure 5-10 displays the force of friction obtained from Equation 5-2 vs. the measured deflection due to friction. Results show scatter throughout all values of the force of friction, which is due to the wide variety of beams produced at three different plants. While plants have similar bed dimensions and procedures, it should be noted that small discrepancies may be present due to coefficient of friction and precasting bed geometry specific to each plant.

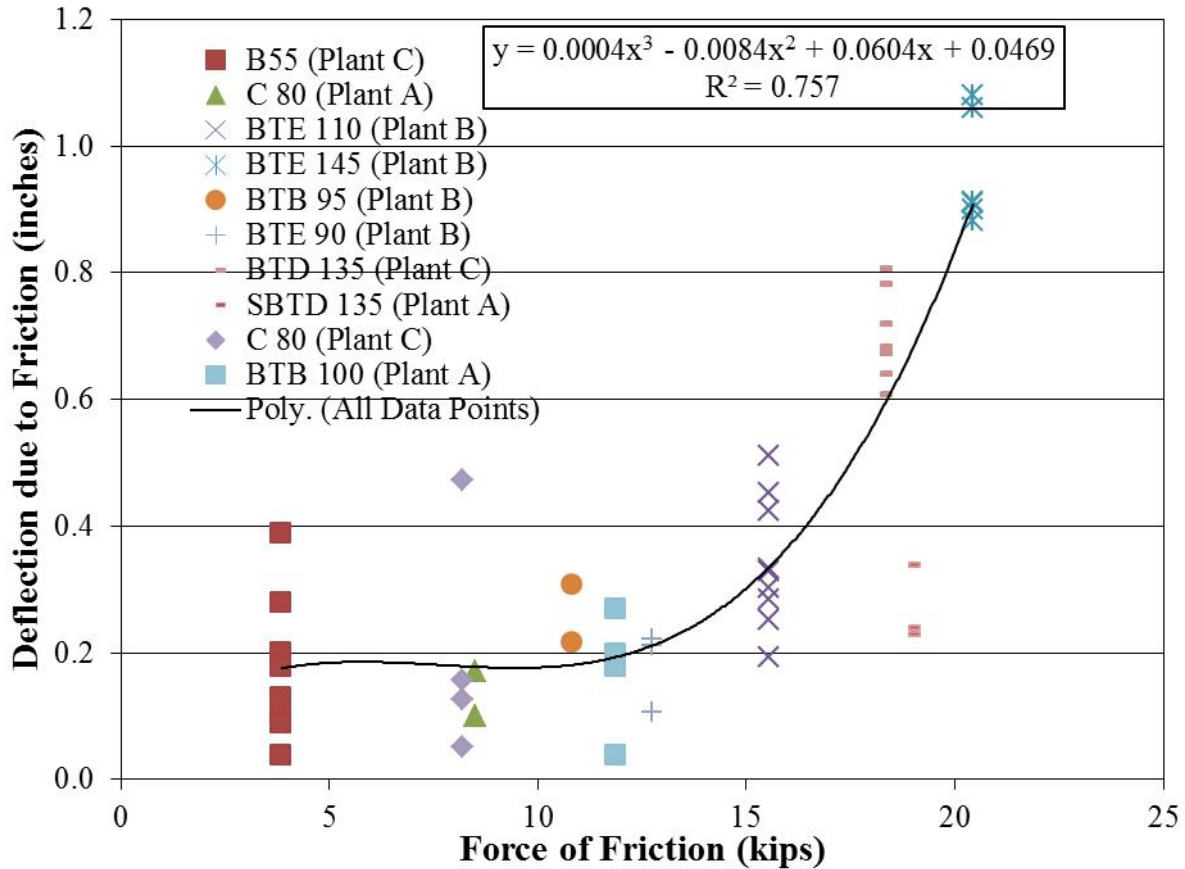


**Figure 5-10: Force of Friction vs. Deflection due to Friction for Multiple PPCBs**

Taking rotary laser level measurements before and after the beam was lifted made it possible to quantify the contribution of friction on PPCBs (Figure 5-11). The lengths of the beams that friction was measured vary from 56 feet to 146.33 feet and consisted of beam types A-D and Bulb-Tee beams. As Figure 5-11 shows, lifting the beam immediately after detensioning can produce up to 1.08 in. increase in measured camber. Out of 50 PPCBs that were studied for friction, there was an average of 17% difference between camber measured before lifting the girders and after lifting the girders.

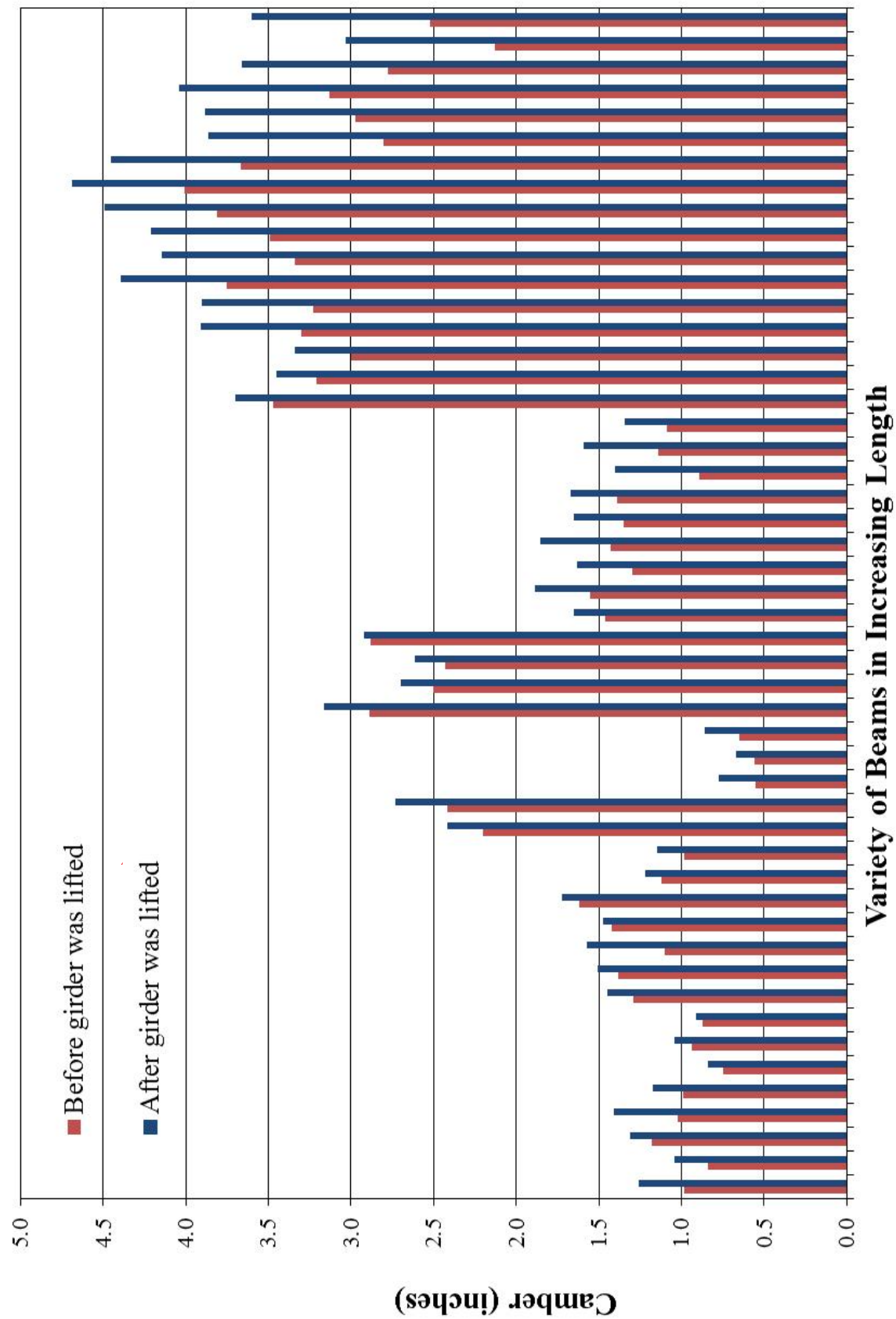
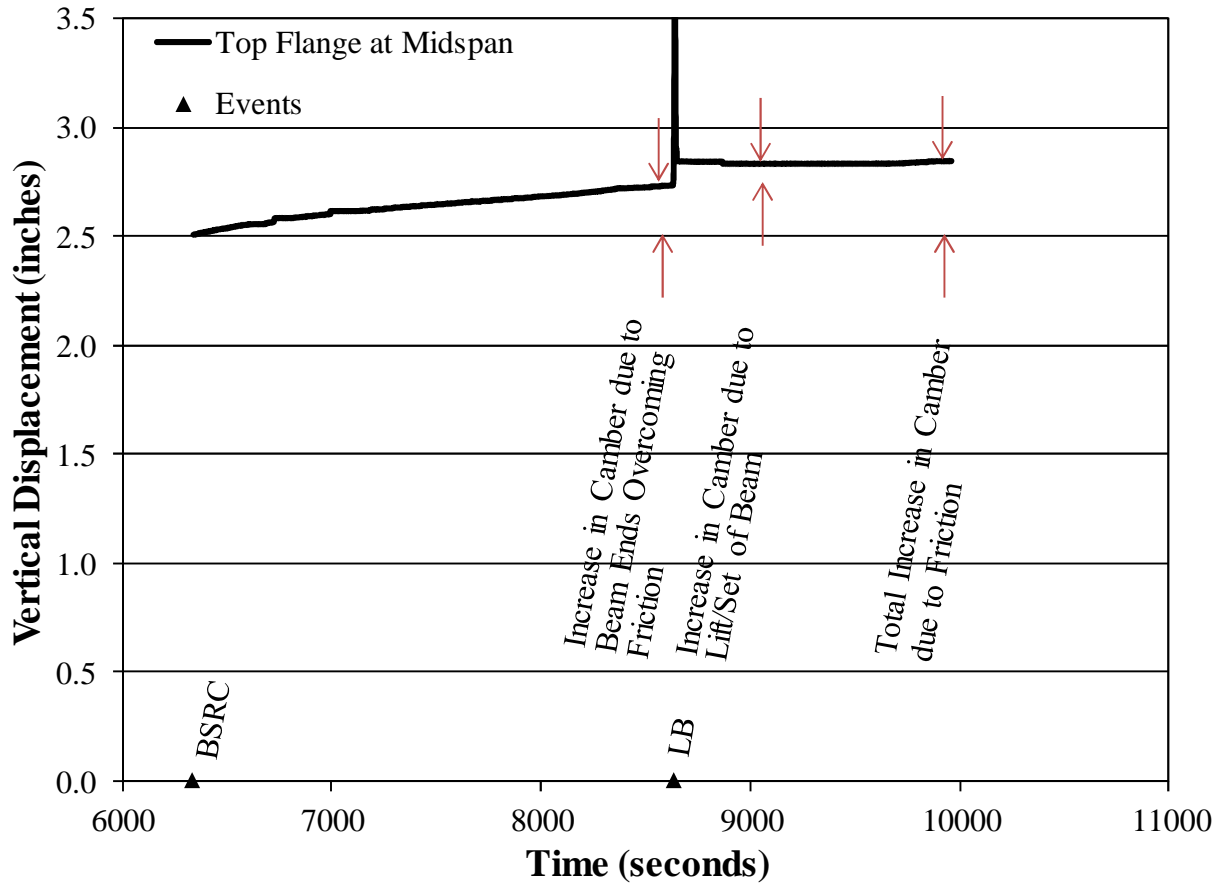


Figure 5-11: Effect of Friction on Camber Measurements for Different Types and Lengths of Beams

#### 5.1.4.1 Evaluating Friction with String Potentiometers

Instrumenting girders at midspan with string potentiometers made it possible to focus on the contribution of friction on camber with respect to time. After the last prestressing strand was cut during the transfer of prestress, there were no outside forces acting on the girder. The increase in vertical displacement that is observed beyond this is a result of the beam ends overcoming friction and sliding towards each other.

The contribution of friction is shown in Figure 5-12 and can be divided into two components. The first component is the gradual increase in camber after the last prestressing strand was detensioned. The second part is the additional camber that was gained when the PPCB was lifted from the precasting bed and placed back down. Once the girder had been lifted and was no longer in contact with the bed, the friction forces were released and there was an increase in camber. It should be noticed that if the gradual increase in camber due to overcoming the force of friction was extrapolated over an extended time, the final camber value appears to reach the same value that was obtained from lifting the beam. However, an error that could be introduced if beams were allowed to sit for an extended period of time would be the gain in vertical displacement due to creep of the concrete.



**Figure 5-12: Time vs. Displacement after the Transfer of Prestress on a BTB 100**

#### 5.1.4.2 Effect of Friction with different Beam End Constraints

An additional exercise was conducted to investigate the effects of camber when eliminating friction on beams. In this experiment, three beams were instrumented with string potentiometers at midspan. The process of releasing the prestressing strands was conducted under normal conditions. After the last prestressing strands were released, the time vs. displacement for three different end restraints on three different beams was observed (Figure 5-13). The string potentiometers were left on each beam after the transfer of prestress for an extended period of time to compare the effects of friction. The graph starts after the last prestressing strand was cut and all beams were resting on the precasting bed freely.

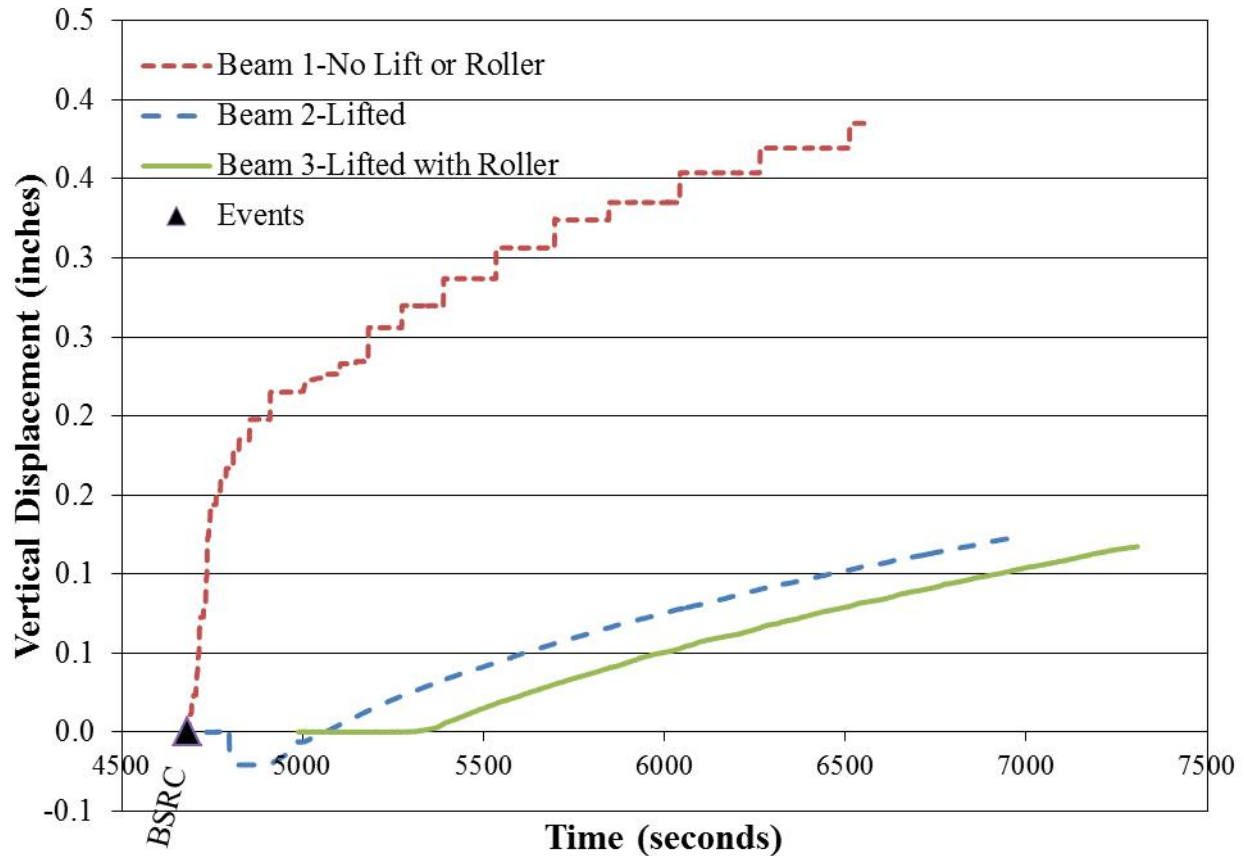


**Figure 5-13: Increase in Camber due to Friction for Three PPCBs**

Beam 1 was not lifted and has friction and creep contributing to the growth of camber. Since beam 1 was undisturbed, a portion of friction would still be present at the last recorded time. Lifting the beam and setting it back down would increase the amount of camber due to releasing the remaining friction. The large amount of growth in beam 1 in the early stages after release can be explained by the beam initially overcoming friction. As time increases, the rate of growth due to friction decreases.

Beam 2 released the friction forces by lifting the beam and setting it immediately back down on the precasting bed. Since the friction was immediately released, camber growth smaller than beam 1 was expected and observed. Immediately after the beam was lifted and placed back down, there was a small decrease in vertical displacement. Over time step 4767 through 4988 when the downward displacement is noticed, beam 3 was lifted from the precasting bed. Beams 2 and 3 were placed adjacent to each other so the shift in weight from beam 3 influenced the camber in beam 2. After this downward deflection, there was a slight growth in camber. The



camber growth of 0.12 inches at time 7300 can be attributed to creep since there were no other forces acting on the beam at that time.

In beam 3, friction is eliminated by lifting the beam immediately after the transfer of prestress and placing it down on a roller support resting on the precasting bed (Fig. 5-14 and Fig. 5-15). Since one end of the beam is resting on a frictionless roller support, the beam had the ability to camber to its full potential. Like beam 2, there was a slight increase in camber after the beam had been placed on the roller support. The resulting increase in camber can be attributed to creep since the beam had the ability to move longitudinally in and out from the midspan with relatively little effort to overcome the friction of a roller support.



**Figure 5-14: Roller Support Under a D90 PPCB**



**Figure 5-15: Roller Support Under a PCB**

#### 5.1.4.3 Reverse Friction

Reverse friction occurs when the girder end is set on the bed and friction acts in the opposite direction to resist the weight of the girder pushing the girder end back outward (French et al., 2012). This effect is believed to be present in prestressed beams after lifting and setting beams down after the transfer of prestress. Ahlborn et al. (2000) suggests that reverse friction should be accounted for in the recorded camber by taking the average of the camber measurements before and after the lift/set of the beam. The reason for taking the average of the two measurements is researchers believe that before lifting the beam, friction is inhibiting the upward growth. After the beam is lifted and placed back down on the precasting bed, friction is inhibiting the downward sagging of camber. A correct representation of camber according French et al. (2012) would be the average of two measurements. This is incorrect as per Figure 5-13, which shows that after beam 3 had been lifted and placed back down; there was no downward decrease in camber. If reverse friction was present, a downward displacement would be shown in beam 3.

Results seen from the three instrumented beams have definitive trends that are summarized below.

- Beam 1 had significantly greater increase in camber than beam 3. This can be attributed to the friction that was still present.
- The increase due to friction was eliminated after being lifted and sat down on the precasting bed. Since beam 3 had a roller present, it was allowed to move in and out

freely without the effect of friction. The similar rate of growth in beam 2 and beam 3 proves that friction was no longer present in beam 2.

- The additional increase in camber after the friction was no longer present for the beams 2 and 3 can be attributed to creep, which was 4.5% of the total camber.
- The downward deflection in beam 2 occurred when beam 3 was lifted from the precasting bed.
- Reverse friction, if present, was small in magnitude and can be ignored.

### **5.1.5 Agreement of Adjusted Camber Values**

The process and procedures of taking camber measurements from three precast plants for girders made for six bridge sites provided insight into possible discrepancies in the instantaneous camber due to the method of taking measurements at the precast plant. When evaluating data obtained from girders at transfer of prestress, it is possible to determine a range that bed deflections, friction, and inconsistent top flange surfaces contribute to camber. While each of these factors individually may play a minor role in camber discrepancies, the combined effect can introduce a significant error in the measured camber. Additionally, comparing the standard practice of measurements from precasters, contractors, and the method outlined in Chapter 3.5.1 has shown discrepancies between the equipment used for measurements, time dependent effects, and the chosen location to measure the camber by each group.

To compare the measurement discrepancies between the methods used by contractors and precasters, data taken at the time of transfer of prestress was evaluated. The benefit of comparing measurement techniques at the transfer of prestress is that the long-term effects of creep and shrinkage are not introduced yet and cannot further complicate the instantaneous camber measurement and prediction. Using a tape measure from midspan, camber was measured at the transfer of prestress. This was replicated after the current method precasters use to measure the instantaneous camber. The method that represents the contractors camber measurement procedure if the beams were released and set on the bridge abutments or piers immediately was also calculated. Additionally, the method that accounts for bed deflections, friction, and inconsistent surface finishes (Chapter 3.5.1) was also compared to the precasters' and contractors' methods of taking camber measurements. Table 5-2 summarizes the results of the differences between measurement methods on 50 PPCBs that were cast at three different precast plants. Figure 5-16 also illustrates the difference between measurement methods on the same 50 beams that were summarized in Table 5-2 in a graphical form. Results show that

contractors' measured camber would be 7.56 percent greater than the accepted researchers' method. Precasters' measured camber has a 26.17 percent difference between the contractors' method. When comparing the researcher to the precasters' method of measurement, there is an 18.75 percent difference. Results from Figure 5-16 conclude that there are discrepancies with the accuracy of the precasters' and contractors' measurement methods being used. The precasters method fails to account for friction between the precasting bed and beam, bed deflections, and surface conditions on the top flange. The contractor's method fails to account for the inconsistent top flange surface along the length of the beam and local inconsistencies on the top flange. There is an error associated with both methods due to not accurately accounting for all of the factors that influence camber. Using the proposed measurement method in Chapter 6.5.1 will eliminate the magnitude of discrepancies between the precasters and contractors.

**Table 5-2: Percent Difference between Measurement Methods**

	Percent Difference between		
	Researcher and Precaster	Contractor and Precaster	Researcher and Contractor
<b>Average</b>	18.75	26.17	-7.56
<b>Standard Deviation</b>	16.6	18.32	8.11
<b>Maximum</b>	88.91	95.31	-43.11

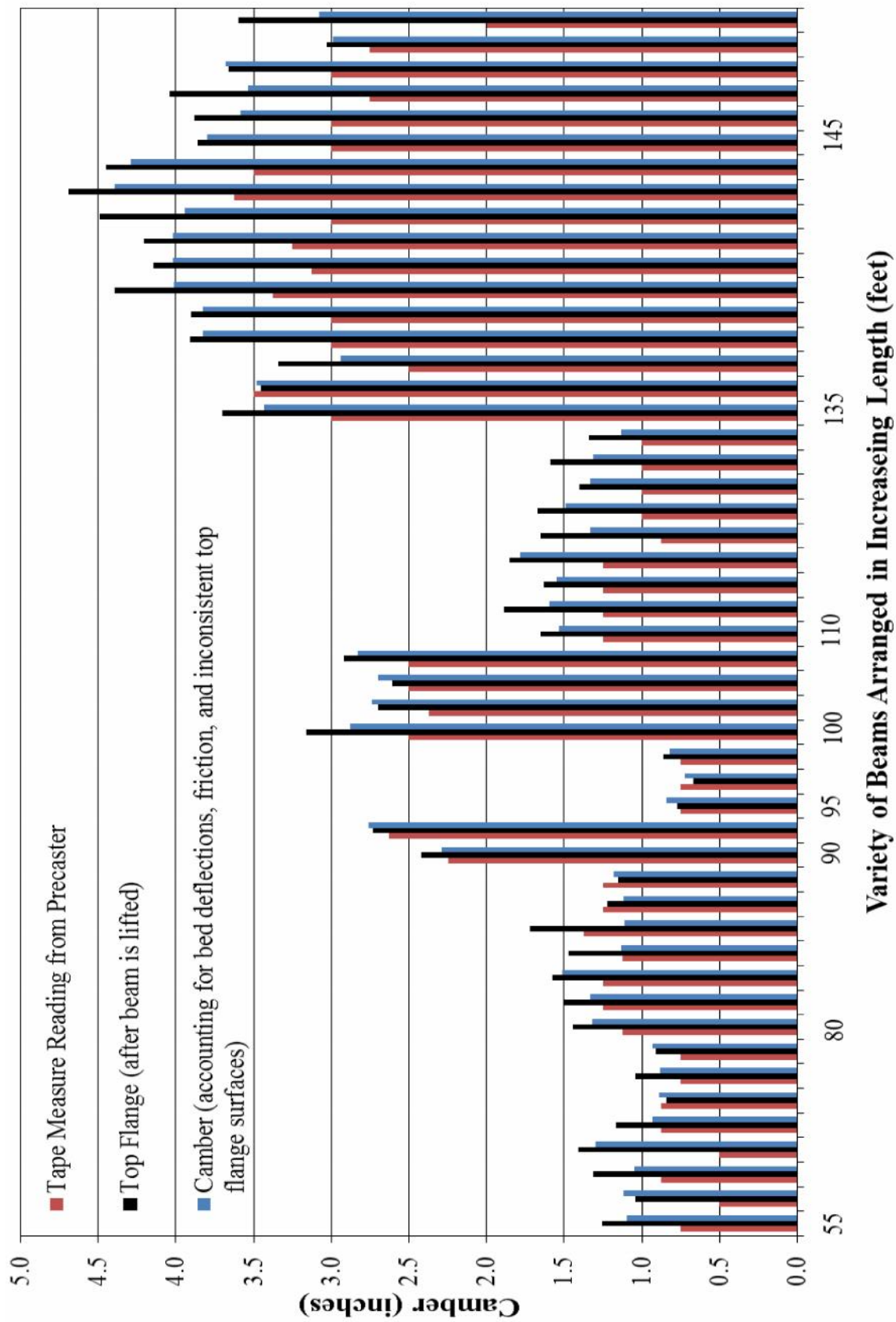


Figure 5-16: Comparison of the Measurement Technique between Precasters, Contractors, and Researchers

Figure 5-17 shows the comparison of three different measurement techniques that were adjusted to account for bed deflections and friction that is present in the PPCBs. Results show close agreement with the rotary laser level camber measurement, which accounts for the measurement errors when following the procedure outlined in Chapter 3.5.1. Discrepancies between the measurement techniques can be attributed to the time measurements were taken and the precision of the tape measure readings. Laser level readings and string potentiometer readings were recorded immediately after transfer of prestress. Tape measure readings were typically taken immediately after transfer but fluctuated by two hours depending on precasters' schedule. Camber readings that were taken with a tape measure rounding to the nearest 1/8 inch lacked precision in comparison to the readings obtained with a laser level or string potentiometer. Due to the agreement when comparing the three methods of camber measurement in Figure 5-17, it is appropriate to state that regardless of the method used, adjusting for the possible errors will result in accurate camber measurements.

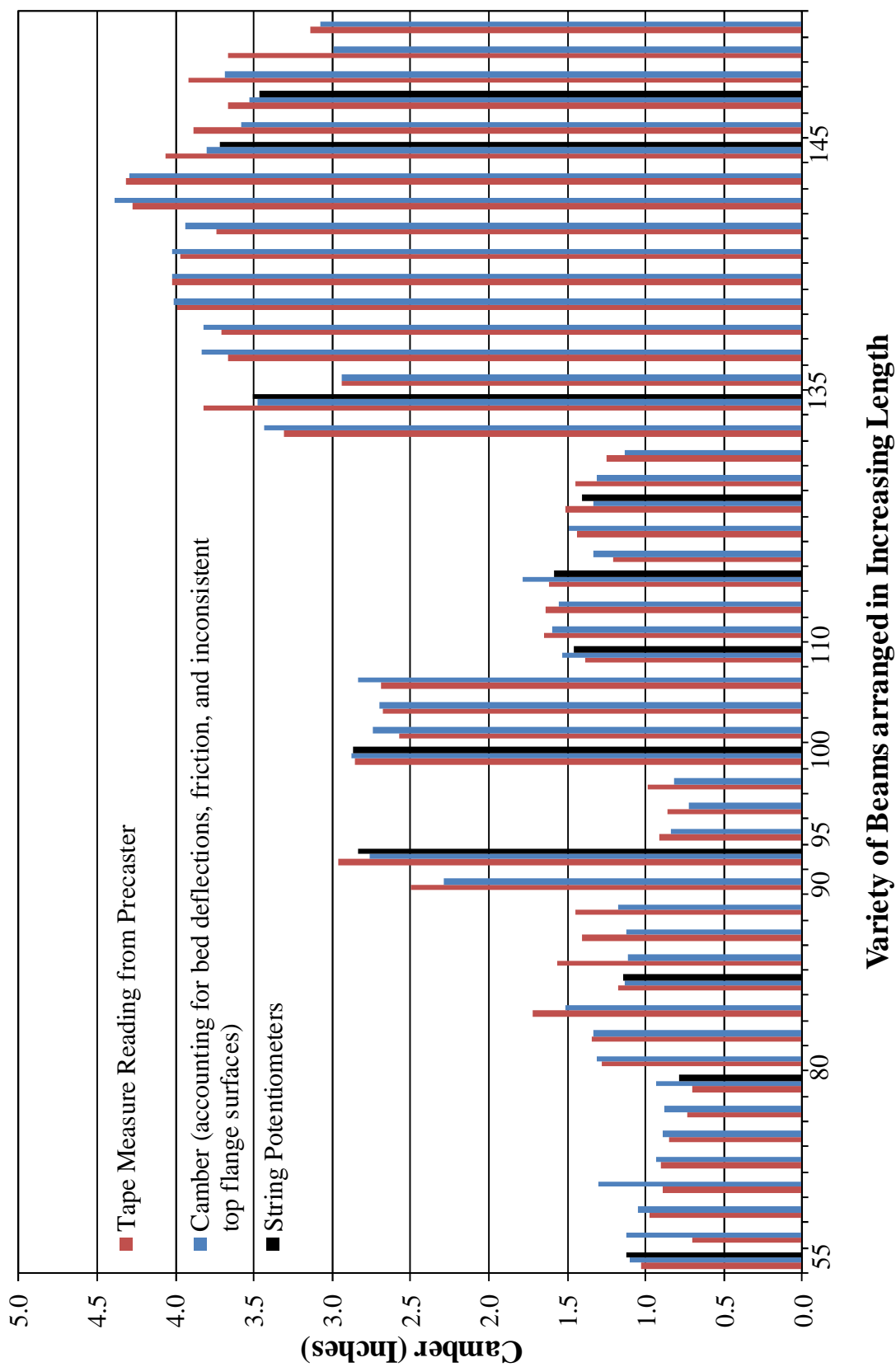


Figure 5-17: Differences between Measurement Techniques after Adjusting Data to Account for Bed Deflections, Friction, and Inconsistent Top Flange Surfaces

**Table 5-3: Average and Standard Deviations Associated with Camber Measurements at Transfer using a Rotary Laser Level**

Possible Errors	Maximum Value	Minimum Value	Average Value	Standard Deviation
<b>Bed Deflections</b>	-0.313 in.	0.000 in.	-0.030 in.	0.062 in.
<b>Friction</b>	1.080 in.	0.040 in.	0.392 in.	0.294 in.
<b>Inconsistent top flange depth along the length of the beam</b>	0.788 in.	0.000 in.	0.099 in.	0.142 in.
<b>Inconsistent Top Flange due to Local Inconsistencies</b>	0.900 in.	0.000 in.	0.113 in.	0.119 in.

## 5.2 Material Properties Affecting Instantaneous Camber Prediction

Accurately predicting material properties of concrete and prestressing steel pose difficulty when determining the correct variables to be used in the design camber of PPCBs. The uncertainty associated with properties of concrete such as the modulus of elasticity, compressive strength, creep, and shrinkage can lead to a large scatter in variables. Additionally, other variables such as the curing conditions affect the maturity of concrete which further impede the ability to accurately predict the behavior of concrete.

### 5.2.1 Variability of Compressive Strength

In the Iowa Beam Standard that is used for design of Iowa precast, prestressed concrete beams, minimum  $f'_{ci}$  values are specified for each type of beam (Equation 2-10). The purpose of the minimum  $f'_{ci}$  values is to ensure the concrete will safely handle the stress applied to the concrete from the tensioned prestressing strands. Testing to make sure that the proper compressive strengths are met is ensured by the precast plant by taking the average strength from three cylinders. The average of the three compressive strength values has to be higher than the designed release strength in order for precasters to transfer the prestress to the beam. Since schedule is a crucial part of the productivity of the precast industry, urgency for a beam to reach the release strength, and the workers to release and move the beam off the prestressing bed is encouraged. The urgency of obtaining the release compressive strengths quicker resulted in concrete compressive strengths being greater than the designed value. Higher compressive



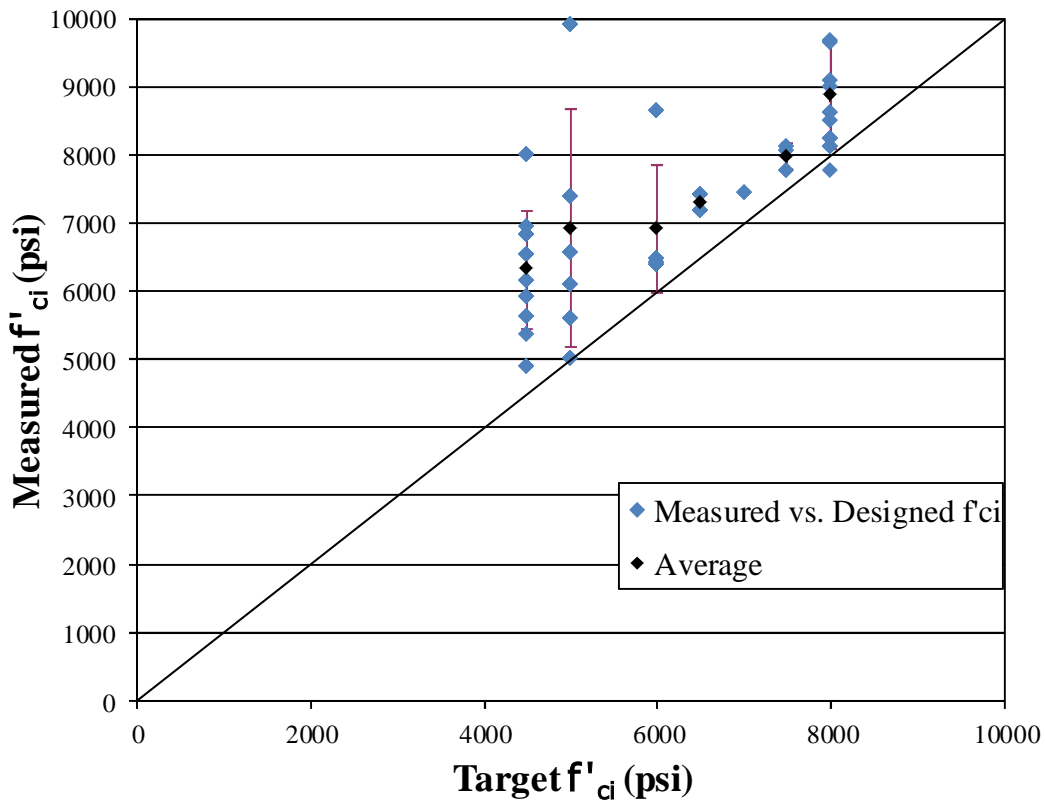
strengths will result in a higher modulus of elasticity when using the AASHTO LRFD (2010) method (Equation 4-16), causing lower measured cambers compared to the design camber.

Figure 5-18 shows a comparison of measured release strength vs. designed release strength of 104 PPCBs that were included in this camber study. The line that extends from the vertex at a 45 degree angle signifies the point where the design strength meets the measured strength. It is expected that the measured release strength is higher than the design strength in order to safely transfer the prestress to the PPCB. The further the points are away from this line, the higher the measured compressive strength.

One trend with the measured vs. design strength reveals that as the release strength increases, the agreement with the 45 degree line improves. For beams with designed release strengths of 4500-5500 psi, the measured  $f'_{ci}$  was 39.5% higher than the designed value. For designed release strengths of 6000-8000psi, the measured  $f'_{ci}$  was 11.5% higher than the measured value. High release strength concrete mixes are often used for normal design strength values to ensure that specified strengths are met within one day and prefabrication schedules remain on time. As the release strengths increase, the capacity of the release strengths remains constant. This causes the higher design strengths to fall closer to the measured release strengths.

**Table 5-4: Measured and Designed Strengths at the Time of Release for PPCBs from Three Precast Plants**

	Design Release Strength							
	4500	5000	5500	6000	6500	7000	7500	8000
<b>Plant A</b>								
Average	6936.7	7373.3			7292.2	7450		8915.9
Standard Dev.	-	-			129.9	-		951.5
Percent Increase	54.2	47.5			12.2	6.4		11.5
Quantity	2	3			8	2		14
<b>Plant B</b>								
Average		5812.8					7978.7	9298.4
Standard Dev.		596.6					179.1	873.0
Percent Increase		16.3					6.4	16.3
Quantity		12					6	8
<b>Plant C</b>								
Average	6269.5	9885.0		6905.8				8750.7
Standard Dev.	874.2	-		942.3				675.0
Percent Increase	39.3	97.7		15.1				9.4
Quantity	27	4		14				8
<b>Total</b>								
Average	6315.5	6916.5		6905.8	7292.2	7450.0	7978.7	8875.0
Standard Dev.	859.8	1738.6		942.3	129.9	-	179.1	804.6
Percent Increase	40.3	38.3		15.1	12.2	6.4	6.4	9.4
Quantity	29	19		14	8	2	6	30



**Figure 5-18: Measured Release Strength vs. Target Release Strength Obtained for 106 Pretensioned Girders**

As discussed in Chapter 2.2.5, the impact of high strength concrete release strengths will affect camber. The decrease in the release camber by increasing the concrete strength was replicated by using the AASHTO LRFD (2010) method of determining the modulus of elasticity. Additionally, determining the modulus of elasticity using ACI 363 was also plotted in Figure 5-19. Results show that as the concrete strength increased, the modulus of elasticity increased as well which reduced the camber. The reduction of camber was greater when using the AASHTO LRFD (2010) modulus of elasticity compared to ACI 363. Results from Figure 5-19 show that failing to account for the increase in concrete strengths by up to 40 percent will misrepresent the initial camber by decreasing the predicted value by 14%.

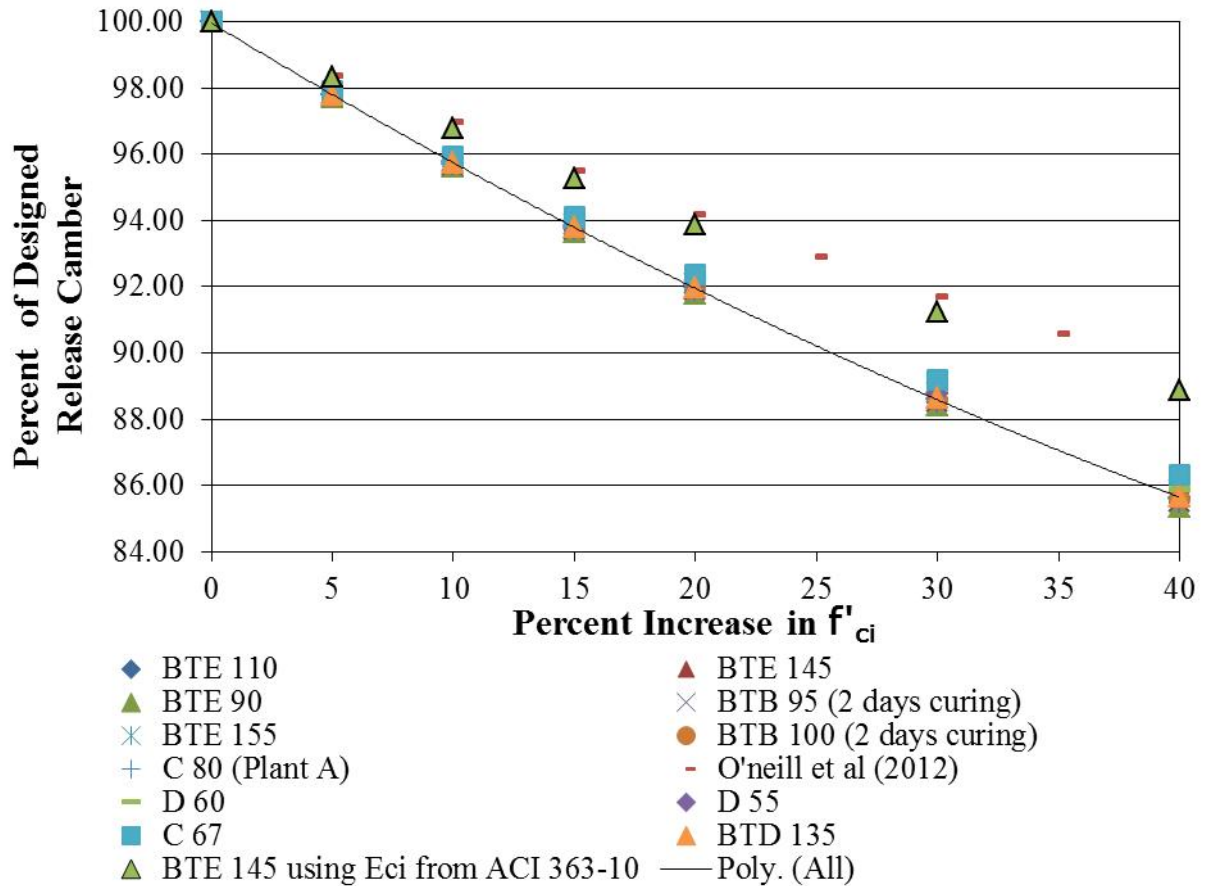


**Figure 5-19: Impact of Concrete Release Strengths on Camber**

### 5.2.2 Modulus of Elasticity

The modulus of elasticity plays a significant role in the camber at transfer of prestress. A study focusing on the modulus of elasticity was conducted by He (2013), which gathered material samples from the same three precast plants that were used to collect instantaneous camber measurements. Another common method used by the Iowa Department of Transportation to determine the designed modulus of elasticity is by the 2010 AASHTO LRFD equation (Eq. 4-16). Variations with results of this method may exist as it is dependent on the unit weight of concrete and the release strength. Comparing calculated camber values to measured camber values using different modulus of elasticity resulted in overprediction or underprediction of camber and made it possible to determine which modulus of elasticity method produced the best agreement.

Figure 5-20 through Figure 5-24 shows the measured vs. predicted camber using different values for the modulus of elasticity. In these figures, there are multiple lines that project outward from the vertex. The line that extends at a 45 degree angle from the vertex shows where the measured and predicted cambers should be if predicted and measured values match exactly with each other. In the 2003 National Cooperative Highway Research Program Report 496 (NCHRP 496), it was reported that material properties can cause the AASHTO LRFD modulus of elasticity to vary by approximately  $\pm 20$  percent. The two lines that bound the data are a representation of the range of the AASHTO LRFD (2010) modulus of elasticity if adjusted by  $\pm 20$  percent.

The different modulus of elasticity methods that were evaluated include: the modulus of elasticity obtained from creep frames using material samples from the three precast plants (Figure 5-20), AASHTO LRFD method with release strengths that correspond to specific beams that were measured (Figure 5-21), and AASHTO LRFD using release strengths obtained from the Iowa State compressive tests for specific mix designs obtained from the precasting plants (Figure 5-22). Results between the measured and calculated instantaneous camber using the modulus of elasticity obtained from creep frames that correspond to specific mix designs used at the observed three precast plants gave an agreement of  $91.18 \pm 19.48$  percent (Figure 5-20). Results between the measured and calculated camber from the AASHTO LRFD (2010) method with release strengths specific to the beams measured produced an agreement of  $98.24 \pm 14.91$  percent (Figure 5-21). AASHTO LRFD (2010) modulus of elasticity using the release strengths obtained from researchers after a sample of 3 cylinders were broken gave agreement between the measured and calculated camber of  $95.56 \pm 14.13$  percent (Figure 5-22).

Out of the three methods that were compared, the AASHTO LRFD (2010) method using the release strengths that correspond to the measured beams gave the best results. Calculating the  $E_{ci}$  value that was obtained from creep frames of concrete mixes obtained from three precast plant produced the least accurate results relative to the other two methods used. Applying the material properties obtained from creep frames for specific mixes to a large range of beams that use a wide variety of mixes may contribute to the discrepancy between designed and measured camber. When eliminating beams that were not composed of the specific mix design that was used to obtain the modulus of elasticity using the creep frames, the agreement is  $87.81 \pm 10.73$  percent (Figure 5-23). Although the agreement is lower, the standard deviation is also lower.

This suggests that if plant personnel were to use a multiplier to adjust for the modulus, the scatter in data could be significantly reduced. Conclusions from the results obtained are that using material properties from specific samples that correspond to the measured values will result in close results between the measured and predicted cambers.

Adjusting the average of the data so that it agrees with the 45 degree line made it possible to evaluate the scatter in the data. By taking the most accurate method for determining the modulus of elasticity to predict camber, it possible to adjust the average value of each precast plant by a single multiplier. Results of adjusting the average value by multipliers can be seen in Figure 5-24. When doing this, agreement with the predicted and measured camber went from 98.24 percent to 100 percent. The standard deviation decreased from 14.91 percent to 10.37 percent. When adjusting each plant's data by a single multiplier, it is possible to reduce scatter and obtain closer agreement with predicted and measured camber.

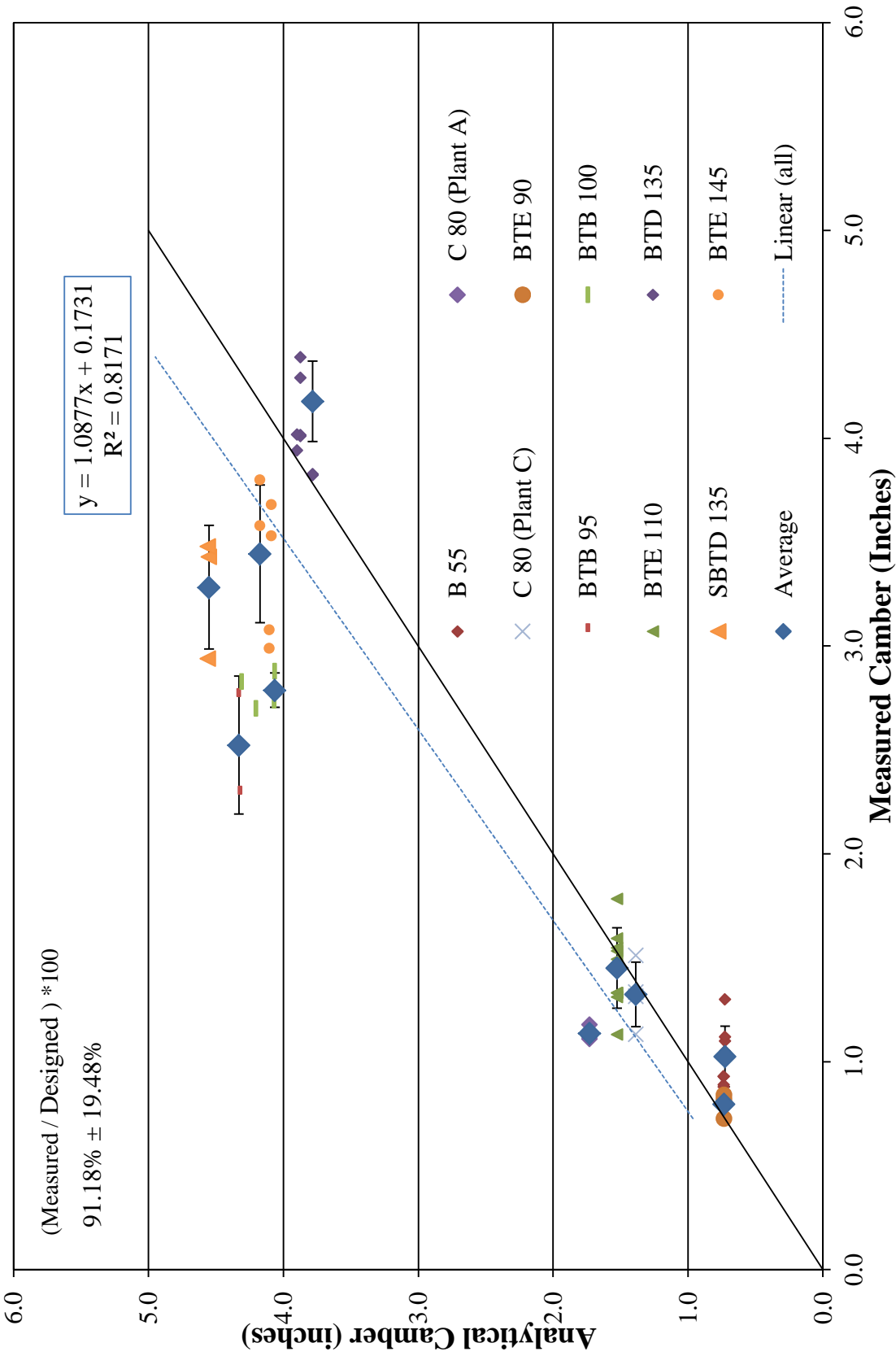
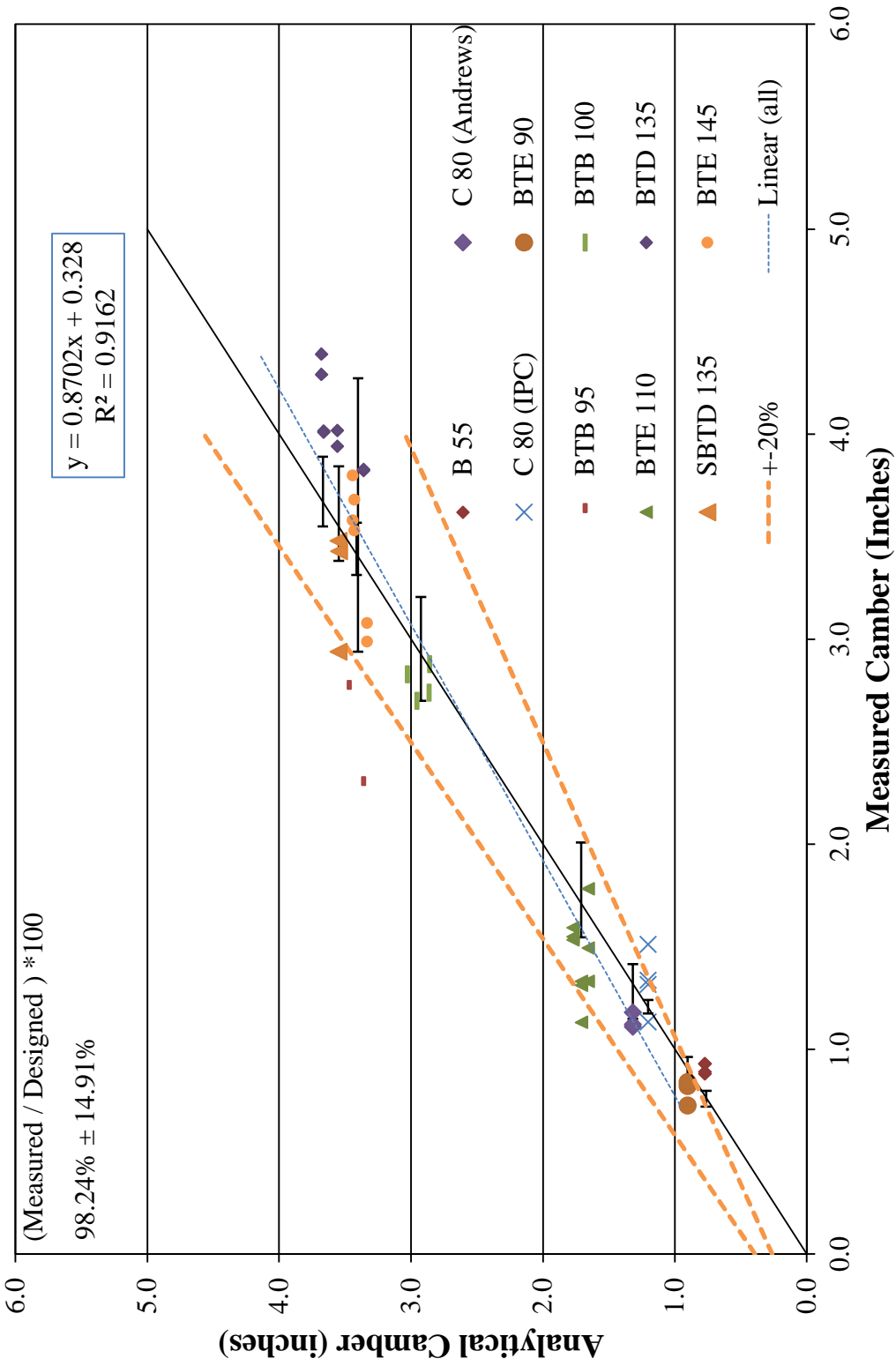


Figure 5-20: Measured Camber vs. Analytical Camber using  $E_{ci}$  obtained from Creep Frames





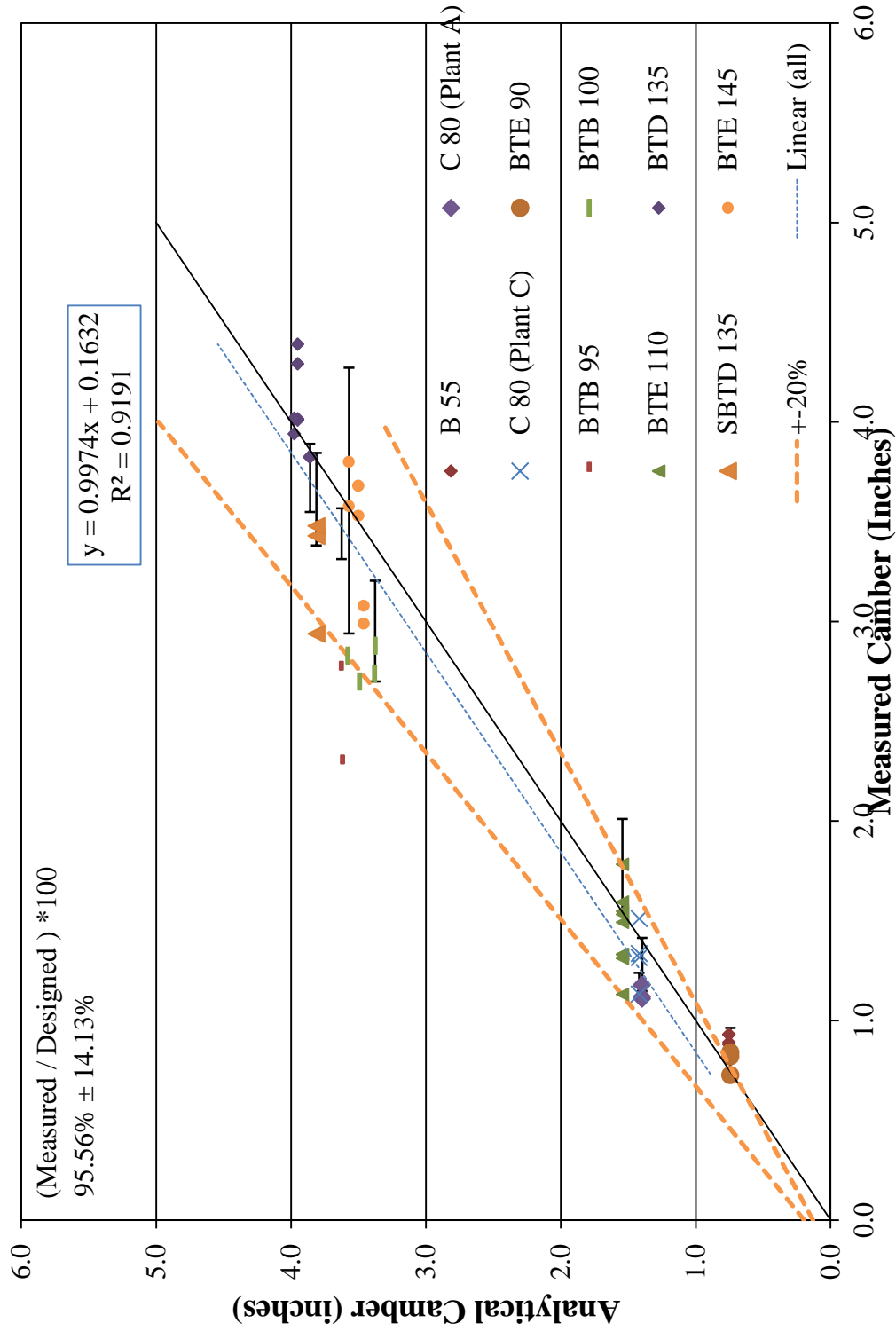


Figure 5-22: Measured vs. Analytical Camber for Beams using AASHTO  $E_{ci}$  and Release Strengths Obtained from Samples

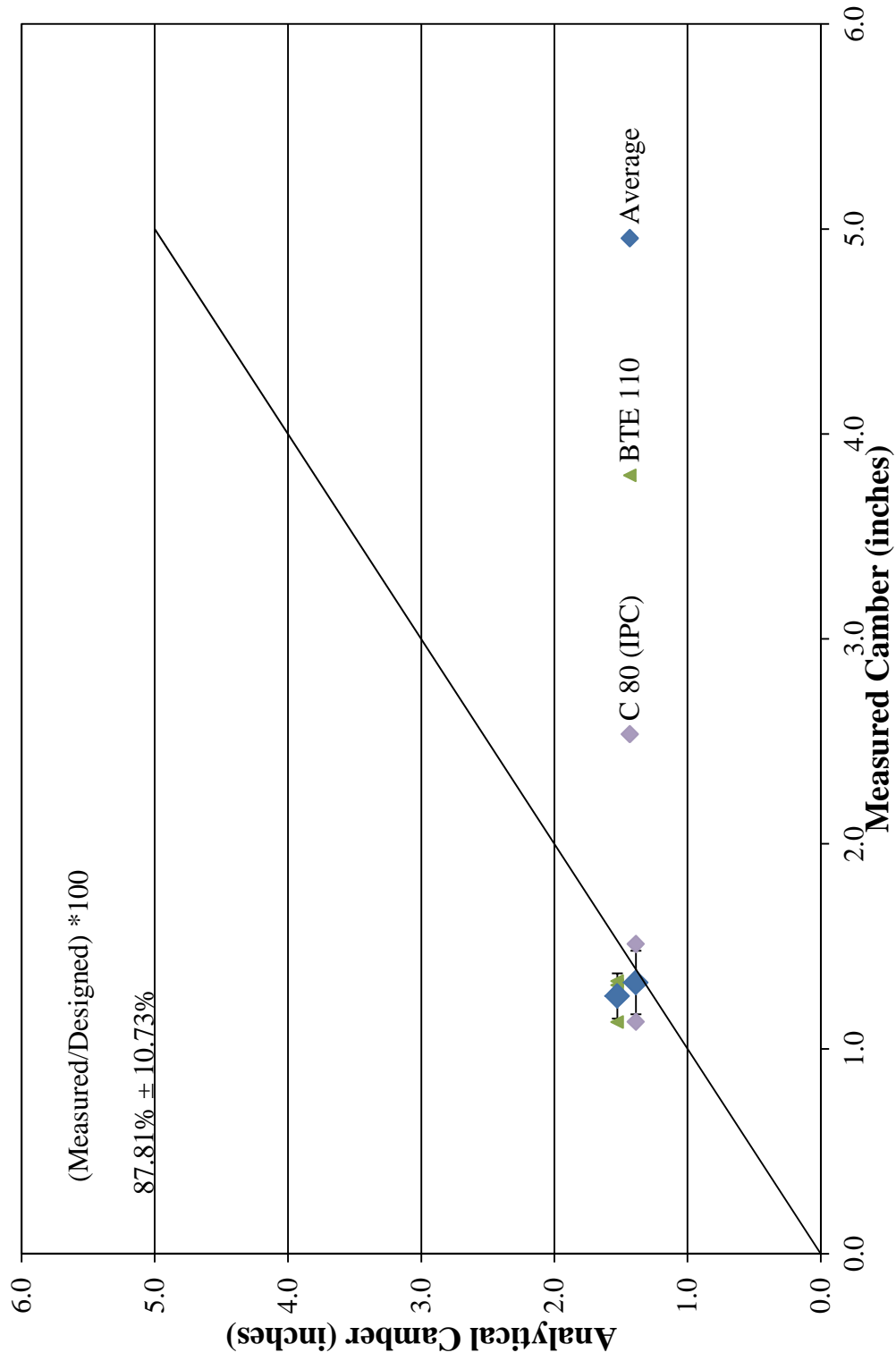
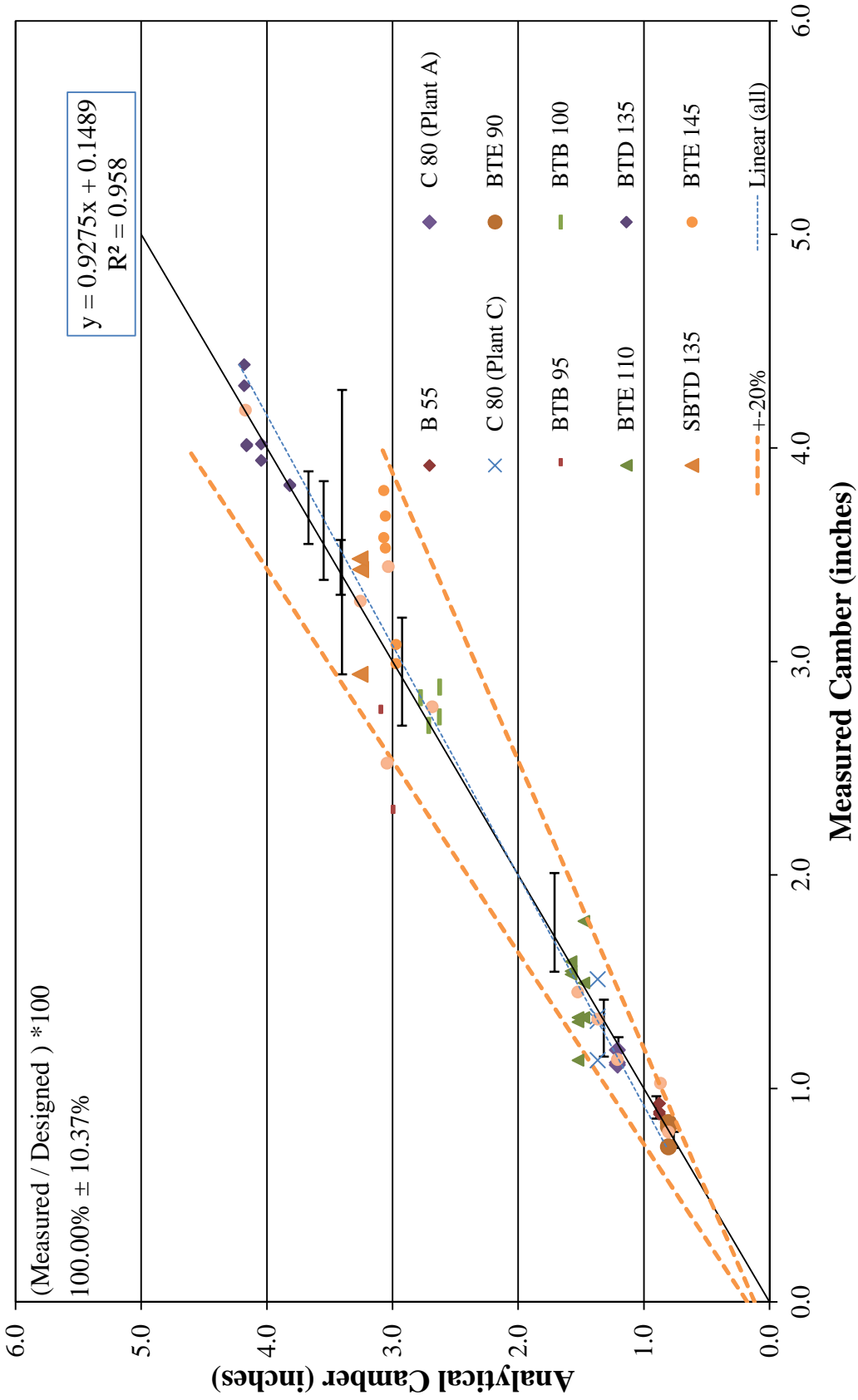


Figure 5-23: Measured Camber vs. Analytical Camber using  $E_{ci}$  obtained from Creep Frames for Select Beams



**Figure 5-24: Measured Camber vs. Analytical Camber adjusting Camber Values based on Averages using AASHTO  $E_{ci}$  from Specific Beam Release Strengths**

### **5.3 Discrepancies with Concrete**

Factors that affect the behavior of concrete are consistency and the maturity. Maturity is dependent on the time and temperature of the specimen during curing. The consistency and maturity are also affected by the precaster's method of producing beams and the uniformity of the materials used. These variables are difficult to predict due to the inconsistencies of concrete. Additionally, the curing conditions between PPCBs and also between the cylinders during curing and storage can produce discrepancies between the predicted and the actual concrete properties.

#### **5.3.1 Maturity of Concrete**

Problems resulting with the prediction of material properties from the maturity of concrete are due to different curing methods, curing temperatures, and curing durations between test cylinders and beams that they correspond to. Using steam or natural curing is dependent on the precasters preference and the weather conditions at the time of casting. It has been observed that the majority of the time, steam curing was used. The temperature when producing PPCBs were similar for multiple beams cast on the same day on the same precasting bed. Differences in temperature occur due to the uniformity of insulating covers used and the placement of the beams. If steam curing is used, the steam is applied to the beam underneath the insulated cover. Beams that are better insulated will have a higher temperature and reach greater maturity. The placement of the beam will also affect the ability to cure under the same temperatures as other beams. Interior beams may reach greater temperatures due to heat from adjacent beams. Beams cast at the ends of the line may be subject to wind and other thermal effects if not properly insulated which will affect the maturity of the concrete.

Discrepancies between the properties of the sample cylinders and the concrete beams may also differ. The difference between the sample cylinders and concrete beams are dependent on the uniformity of concrete and the maturity of concrete. The following is the procedure for obtaining sample cylinders and is in accordance with IDOT Materials IM 570 (2013) which states:

“For each release and shipping strength a set of three (3) cylinders representing three different portions of the line cast (each end and the center) shall be cast. The average of three (3) cylinders shall be used to determine the minimum strength requirements for either release or shipping.

For either release or shipping strengths the set of cylinders tested shall meet the following requirements:

- a. The average strength of the specimens tested shall be equal to or greater than the minimum strength required.
- b. No individual cylinder of the set tested shall have a compressive strength less than 95% of the specified strength.
- c. If both conditions a. & b. are not met after the appropriate curing period, another set of specimens representing the line shall be tested.”

Further text goes on to mention the curing of concrete test cylinders which states:

“6. Concrete strength specimens shall receive the same curing as the cast units. Curing can be accomplished by either steam-cure or sure-cure systems.”

The three plants that were included in this study cure 4 inch by 8 inch cylinders with a sure-cure system. The sure-cure system uses temperature sensors that are placed in the interior of the precast beam to regulate the temperature of the cylinders. Advantages of this system are the precasters can keep track of the internal temperature of the beam and adjust the steam based on the desired temperature during curing. This allows beams to mature quicker and reach higher strengths within a shorter amount of time which allows the precasters schedule not to be hindered.

A disadvantage of the sure-curing system includes cylinders may have a higher maturity than the beams that they correspond to. One reason discrepancies occur between the maturity of the PPCB and the sample cylinder is due to the placement of the sure cure sensor in the beam. If the sensor is placed closer to the steam on the precast bed, the temperature from the sensor will be higher than the rest of the beam. The cylinder will then be heated to the same temperature of the sensor and the maturity of the concrete cylinder will be greater than the beam. Another reason the maturity between the sample cylinders and the beams may be different is due to the volume to surface ratio. A 4 inch by 8 inch cylinder has a smaller volume to surface ratio than a precast, prestressed concrete beam. When a sure cure cylinder is heated, the temperature is regulated by a mold that heats the outside of the cylinder. The smaller amount of volume of concrete will reach a greater maturity than the beam will and ultimately, misrepresent the strength of the concrete in the beam. Relying on the compressive strengths of cylinders that have a greater

maturity than the beam can produce inconsistencies in the release strength and ultimately, the modulus of elasticity.

Naturally cured cylinders are also used to determine the compressive strengths of the concrete. The accuracy of the compressive strength of a naturally cured cylinder can also be misrepresented. Naturally cured concrete cylinders are cured with the concrete beams under the tarps or insulated covers. Since quality control personnel need to determine the compressive strength before uncovering the beam and removing the molds, cylinders are typically placed in areas where they are easily accessible. Potential problems arise when cylinders are placed in areas that are not as insulated as the rest of the beam may be. Cylinders that are not heated to the same temperatures as the beam will be misrepresented by having a lower maturity of concrete than the beam.

The duration of curing between the sample cylinders and the beams may differ. Sample cylinders are broken prior to workers releasing PPCBs. The additional time that it takes workers to release beams when release strengths are met can range from zero to four hours. The additional time the beam has to cure will increase the maturity of the beam and misrepresent the sample cylinder and beams correlation.

### **5.3.2 Uniformity of Concrete**

The consistency of a mix design is dependent on the materials along with the ability for quality control personnel to regulate each batch of concrete. The materials may be unique for each batch depending on the uniformity of the properties of materials or the consistency of the quantity of materials in each batch. The properties of the materials would include the moisture content of the aggregate, the shape of the coarse and fine aggregate, and the hardness of the aggregate. The quantities of each material and the special additives can slightly differ from each batch. Both the consistency and quantity of materials can influence the strength, amount of creep and shrinkage that will be present, along with other factors that will affect the camber of a PPCB.



**Figure 5-25: Plastic molded and Sure Cure Cylinders**

Errors that are present when relating cylinder properties of concrete to the beam properties are the concrete consistency between different batches in the same and adjacent beams. When placing concrete, some beams require multiple batches to complete the beam. Although quality control personnel monitor the consistency of the batches, there is the possibility that batches may be inconsistent. Creating different consistencies in batches will affect the behavior of the beam and depending on when the sample cylinders were obtained and from what batch, may detract from the ability to predict camber.

Another area of concern is the disturbance of concrete samples relative to the beam. Concrete samples that are cured near the beams are typically handled before they are taken to the lab to be tested. Although the simple task of transporting cylinders to the quality control room seems insignificant, handling the cylinders may cause them to break earlier than expected.

Modeling the material properties of the beams based on the test cylinders is a challenging task due to the numerous variables that are present between the two. Although small changes in curing, concrete batches, and testing seem insignificant, they can influence the analytical variables used to predict camber. It is important to recognize the sources of error with sample

cylinders and realize that the behavior of cylinders as well as differential beams may be different from each other.

#### 5.4 Discrepancies with Beams Cast on the Same Day

Measured camber will often vary between identical beams. Multiple variables can contribute to the inconsistencies between measured values. It is believed that measured camber for beams cast on the same bed on the same day vary less than beams cast on different days on different precasting beds. Variables that affect the consistency of camber for beams cast on the same day include; prestress force, prestress losses, and the maturity of concrete. The following examples explain why discrepancies between precast beams cast together may have different camber values.

Six BTE 145's (Bulb Tee E of length 145 feet) were cast at one plant. All of the beams were installed on the same bridge and were designed to have the same camber. Bed dimensions allowed the precaster to produce two beams at a time. Information relating to the six beams is listed in Table 5-5.

**Table 5-5: Beams Measured Instantaneous Camber and Dates of Casting and Release**

<b>Beam</b>	<b>Date Cast</b>	<b>Date Released</b>	<b>Instantaneous Camber (inches)</b>
BTE 145	6/26/2012	6/27/2012	3.80
BTE 145	6/26/2012	6/27/2012	3.58
BTE 145	6/28/2012	6/29/2012	3.53
BTE 145	6/28/2012	6/29/2012	3.68
BTE 145	7/24/2012	7/25/2012	2.99
BTE 145	7/24/2012	7/25/2012	3.08

Results indicate that beams cast on the same day have closer camber values, but there are differences in measured values between two beams cast and released on the same date. Additionally, comparing beams cast on separate dates tend to have a larger range in camber. The differences in camber in this case can be attributed to a variation of prestress force including losses, mix consistency, and curing conditions.

The mix consistency may also be contributing to the discrepancy with beams cast on the same day. The bulb tee 145 beams require 30.4 cubic yards of concrete. The limitations of the



precasting plant require multiple trips to the batch plant to fill each concrete beam. Within the multiple batches of concrete that are used, it is possible to have slightly varying properties of materials which could affect the camber.

The curing conditions between the beams are certainly different on separate days. The sure cure system that is used helps regulate the temperature to the desired temperature to accelerate curing. Depending on the time when the beam was cast, temperature to cure the beam can be pushed to the maximum or be at normal conditions to meet the strength requirements within the next day.

A combination of all of these factors can exist in beams cast on the same day and certainly between beams cast on separate days. The discrepancies in materials and fabrication procedures will cause different measured camber at the transfer of prestress.

## **5.5 Analytical Prediction Variables for PPCBs**

### **5.5.1 Moment of Inertia**

The moment of inertia influences the ability of a beam to resist bending. For a prestressed concrete beam, determining the correct value for the moment of inertia will influence the accuracy of camber predictions. Since this study is primarily concerned with the prediction of instantaneous camber, the gross or transformed moment of inertia are appropriate to use since the cross section is not cracked. The gross moment of inertia is calculated based on assumption that the entire section is composed of concrete. This can bring in a small error since prestressed concrete beams use prestressed and nonprestressed steel. Steel has a higher modulus of elasticity and therefore, the ability to undergo greater stresses and strains than concrete does. This is accounted for in the transformed moment of inertia because the reinforcement is converted, by the modular ratio, to an equivalent unit that represents the property of bending in terms of concrete.

The transformed moment of inertia varies due to the cross section and the amount of reinforcement that is present. In the Iowa Beam Specification (Iowa DOT Index of Beam Standards, 2011), beams are grouped according to types and arranged according to lengths. With varying lengths, the amount of prestressed and non prestressed reinforcement will change. The increase in reinforcement is to account for the additional forces due to the increased span and amount of loading that a beam can withstand. As the amount of reinforcement changes, the

transformed moment of inertia will also change. Naaman (2004) states that using the transformed moment of inertia is acceptable on members with bonded tendons although the additional calculations do not result in increased accuracy.

Complications when determining the transformed moment of inertia can occur due to the use of harped prestressing strands. Harped strands are prestressing reinforcement that start at one elevation and change throughout the length of the beam. The Iowa Department of Transportation uses beams that are doubly harped, or have two bends in the reinforcement over the length of the beam. Due to the varying height of the harped reinforcement over the length of the beam, the transformed moment of inertia will change over the length of the beam. Taking a weighted average of the transformed moment of inertia along the length of the PPCB gives an accurate representation of the moment of inertia.

A parametric study investigating the effects of moment of inertia on camber was conducted. In this study, camber was determined based on the gross moment of inertia, transformed moment of inertia at the ends of the beam, transformed moment of inertia at the midspan of the beam, and the transformed moment of inertia over the whole length of the beam. While holding all other variables fixed, the effects of the moment of inertia can be seen in Figure 5-28.

The most accurate variable in Figure 5-26 is the transformed moment of inertia ( $I_{tr}$ ) along the length of the section. Comparing the  $I_g$ ,  $I_{tr}$  at the beam ends,  $I_{tr}$  at midspan, and  $I_{tr}$  along the length of the beam gives camber comparisons with five beams. It should be noted that different beams have different quantities of harped and straight reinforcement. The variation of prestressed reinforcement can change the difference that is observed between the transformed moment of inertia across the whole section and other moment of inertia values.

Results show that  $I_g$  has a 2.90 percent difference when compared to  $I_{tr}$  along the length of the beam. This is because  $I_{tr}$  is a larger value due to accounting for the rigidity of the reinforcement. Accounting for the rigidity of the reinforcement will produce less bending which will result in lower camber than  $I_g$ . Another trend is the transformed moment of inertia along the length of the beam agrees closely with the measured camber value. Taking the moment of inertia along the length of the beam compared to the gross moment of inertia is believed to accurately represent the reinforcement that is present. Additionally, the close agreement with the measured values led researchers to calculate instantaneous camber on multiple beams using the corresponding transformed moment of inertia along the length of the beam.

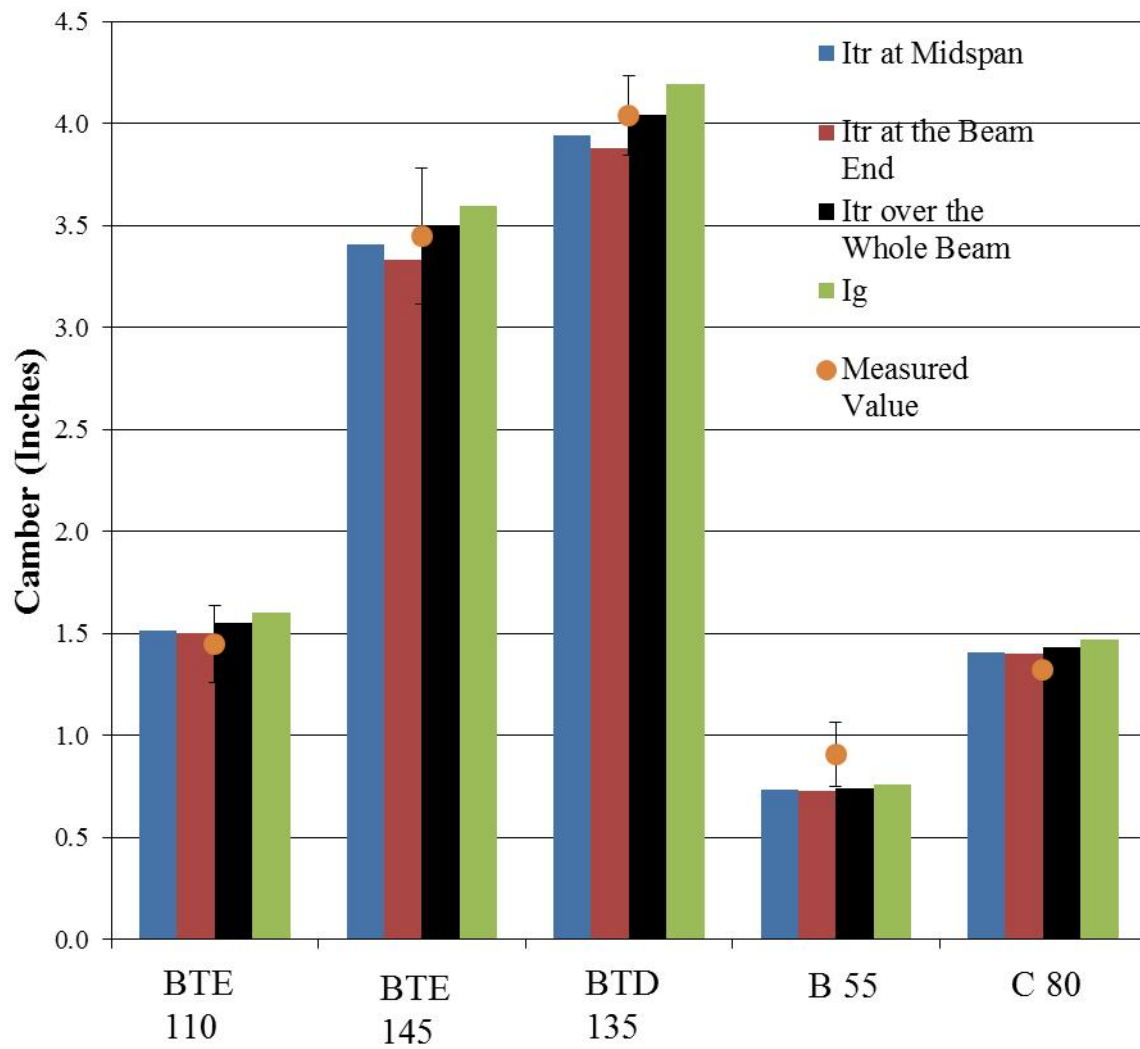


**Figure 5-26: Comparison of Camber using Different Moment of Inertia Values**

**Table 5-6: Camber of 5 PPCBs with Different Moment of Inertia Values**

<b>Camber (inches)</b>				
<b>Beam</b>	<b>I<sub>tr</sub> along the length of the beam</b>	<b>I<sub>tr</sub> at Midspan of the PPCB</b>	<b>I<sub>tr</sub> at End of the PPCB</b>	<b>I<sub>g</sub></b>
<b>B55</b>	0.7433	0.7327	0.7319	0.7599
<b>C80</b>	1.4328	1.4090	1.3989	1.4694
<b>BTE 110</b>	1.5519	1.5151	1.5033	1.6014
<b>BTB 135</b>	4.0420	3.9395	3.8786	4.1941
<b>BTE 145</b>	3.4930	3.4044	3.3335	3.5963

#### 5.5.4 Prestress Force

The force of prestress that is applied to the beam is an important variable in predicting camber. The amount of prestress force per strand, total amount of prestress force per beam, and the prestress material properties are dictated by the Iowa DOT. The specified prestressing strands are ASTM A416 grade 270, 0.6 in, low relaxation prestressing strands. Eqs. 5-1 and 5-2 show the steps in calculating the designed prestress force per strand and per beam.

$$72.6\% \times f_{pu} = \text{force/area} \quad (5-1)$$

$$72.6 \times 270 \text{ ksi} = 196.02 \text{ ksi}$$

$$\text{force/area} \times \text{area of prestressing strands} = \text{force} \quad (5-2)$$

$$196.02 \text{ ksi} \times 0.217 \text{ in}^2 = 42.53 \text{ kips/strand}$$

The prestress force that is specified on the Iowa Beam Standard represents the force of prestress before the transfer of prestress. Therefore, seating losses along with relaxation losses from the time of jacking to right after release would be included. Tolerances set by the Iowa DOT restrict precasters to fabricate PPCBs within  $\pm 5$  percent of the designed prestress force. A comparison of the designed prestress force and the as-built tensioning force recorded by precasters for specific beams was summarized in Table 5-7 and in Appendix C. Results show that the averages of 41 PPCBs that were investigated have an agreement of  $100.87\% \pm 2.50\%$

and fall within the  $\pm 5\%$  tolerance that is accepted. However, when looking at individual beams, the maximum and minimum values are  $+8.95\%$  and  $-3.79\%$ , respectively. The maximum applied ratio of applied to designed prestress force of  $8.95\%$  lies outside of the allowable tolerance for Iowa beams of  $\pm 5\%$ .

**Table 5-7: Summary of Designed vs. Tensioned Prestress from 41 PPCBs**

	<b>Difference of Designed and Tensioned Prestress (kips)</b>	<b>Ratio (Tensioned Prestress/Designed Prestress)</b>
<b>Average</b>	-11.0362	1.0087
<b>Standard Deviation</b>	33.9093	0.0250
<b>Maximum</b>	40.3700	1.0895
<b>Minimum</b>	-87.8450	0.9621
<b>Plant A</b>	-19.5668	1.0086
<b>Plant B</b>	-10.6194	1.0057
<b>Plant C</b>	-0.9753	1.0109

### 5.5.5 Prestress Losses

A parametric study was conducted to determine the effect of camber due to the prestress losses. When determining the prestress force, tensioning sheets from the precasters were used to get the initial jacking force of the prestressing strands on specific beams. Using the initial jacking force and the methods that coincide with Chapter 4, the magnitude of prestress that is lost due to elastic shortening, seating and relaxation was calculated. The prestress force before and after prestress losses was used to compare the effect of prestress losses on camber.

Results from Table 5-8 show the prestress and camber values before and after prestress losses. Additionally, the ratio of prestress and camber before and after prestress losses is shown. Results from Table 5-8 indicate that the average ratio of prestress losses is  $7.34\%$ . However, the  $7.34\%$  ratio of loss affects camber on average by  $11.94\%$ . Through evaluating 43 beams, it was found that individual beams have the capability of having a reduced camber by as much as  $14.97\%$  if failing to account for prestress losses.

**Table 5-8: Comparison of Prestress and Camber with and without Prestress Losses**

<b>Beams</b>	<b>Prestress Force Before Losses (kips)</b>	<b>Prestress Force After Losses (kips)</b>	<b>Difference in Prestress without and with losses (kips)</b>	<b>((Prestress with Losses/Prestress without Losses)-1)*100</b>	<b>Camber with Losses (inches)</b>	<b>Camber without Losses (inches)</b>	<b>((Camber with Losses/Camber without Losses)-1)*100</b>
BTE 145	2211.57	2040.32	171.25	8.39	3.4287	3.9967	-14.21
BTE 110	1292.82	1199.71	93.11	7.76	1.7705	1.9949	-11.25
BTD 135	2332.50	2154.74	177.76	8.25	3.5591	4.1624	-14.50
B 55	519.46	490.73	28.73	5.85	0.7711	0.8310	-7.20
C 80	950.58	902.42	48.16	5.34	1.3178	1.4397	-8.46
BTE 90	870.06	816.78	53.28	6.52	0.9022	0.9903	-8.90
BTB 95-3 Days Curing	1867.66	1721.75	145.91	8.47	3.3588	3.8291	-12.28
D 55	523.91	499.21	24.70	4.95	0.1851	0.2009	-7.88
D 60	620.62	585.95	34.67	5.92	0.2977	0.3276	-9.12
D 90	924.09	876.09	48.00	5.48	1.2422	1.3645	-8.96
D 105	1405.79	1307.76	98.03	7.50	2.1988	2.4832	-11.45
C 67	795.60	740.33	55.28	7.47	0.7538	0.8471	-11.02
BTD 130-2 Days Curing	2337.81	2161.67	176.14	8.15	3.7476	4.3326	-13.50
BTB 100-2 Days Curing	1881.35	1800.11	81.24	4.51	3.0259	3.4258	-11.67
D110-1 Day Curing	1477.22	1371.79	105.43	7.69	2.4413	2.7811	-12.22
BTE 135-3 Days Curing	2031.72	1875.80	155.92	8.31	2.8588	3.3227	-13.96
SBTD 135-3 Days Curing	2327.60	2158.19	169.41	7.85	3.5504	4.1326	-14.09
BTC 120-1 Day Curing	2229.30	2070.34	158.96	7.68	3.6055	4.1624	-13.38
<b>Average</b>				<b>7.00</b>			<b>-11.34</b>
<b>Maximum</b>				<b>8.47</b>			<b>-7.20</b>
<b>Minimum</b>				<b>4.51</b>			<b>-14.50</b>

### 5.5.3 Sacrificial Prestressing Reinforcement

Iowa Department of Transportation specifications require reinforcement in the top flange of PPCBs. Installing non-prestressed reinforcement along the entire length of the beam to the correct height is time consuming and requires a lap splice between two non-prestressed

reinforcing bars. Instead of using non-prestressed reinforcement, precasters often times used 2-6 strands of prestressed reinforcement tensioned from 3-5 kips along the top flange of the beam. The advantage of using prestressed reinforcement along the top flange is the ease of fabrication, the close tolerances that can be achieved, reduced reinforcement with no lap splices, and being able to hang shear stirrups, lifting hooks, and other non prestressed reinforcement along the length of the beam.

When determining the analytical camber, accounting for the sacrificial strands has been observed to contribute an additional 2.62% on average to the final camber value. On specific beams, the contribution to camber can be as high as 6.67% or as low as 0.75%. The contribution of the sacrificial prestressing strands on camber is affected by the amount of sacrificial prestressing strands that are present, the sacrificial prestressing strand force, and the eccentricity of the sacrificial prestressing strands to the center of gravity of the cross section. Table 5-9 shows 20 PPCBs with camber calculated with and without the sacrificial prestressing strands. The difference, percent difference, and ratio of the effect of the sacrificial strands are also given. There are cases where multiple beams of the same cross section and length are listed multiple times. These are instances that apply to specific PPCBs, but were cast and released on different days from each other. Notice that the prestressing force, prestress losses, and material properties may differ between beams of the same cross section and length.

**Table 5-9: The Percent Difference and Contribution to Camber with and without Sacrificial Prestressing Strands**

<b>Beam</b>	<b>Camber with Sacrificial Strands (inches)</b>	<b>Camber without Sacrificial Strands (inches)</b>	<b>Difference in Camber Between No Sacrificial Strands and Sacrificial Strands (inches)</b>	<b>Percent Difference</b>	<b>(Camber without Sacrificial Prestressing Strands/Camber with Sacrificial Strands)*100</b>
BTE 145	3.3346	3.4882	0.1536	4.50	104.61
BTE 145	3.4434	3.4693	0.0259	0.75	100.75
BTE 145	3.4287	3.5393	0.1107	3.18	103.23
BTE 110	1.7705	1.8437	0.0732	4.05	104.13
BTB 135	3.6779	3.7316	0.0537	1.45	101.46
B 55	0.7561	0.7848	0.0287	3.72	103.79
C 80	1.1922	1.2448	0.0525	4.31	104.40
C 80	1.3178	1.3480	0.0301	2.26	102.29
BTE 90	0.9022	0.9624	0.0602	6.46	106.67
BTE 155-1 Day Curing	3.9459	4.0243	0.0783	1.97	101.99
BTE 155-2 Day Curing	3.9072	3.9870	0.0798	2.02	102.04
BTE 155-3 Day Curing	3.6425	3.7226	0.0801	2.17	102.20
BTB 95	3.4682	3.5630	0.0948	2.70	102.73
D 90	1.2422	1.2689	0.0266	2.12	102.14
D 105	2.1988	2.2279	0.0292	1.32	101.33
BTB 100	3.0259	3.0890	0.0631	2.06	102.08
D110	2.3680	2.3994	0.0314	1.32	101.33
BTE 135	2.8588	2.9119	0.0531	1.84	101.86
SBTD 135	3.5445	3.6065	0.0620	1.73	101.75
BTC 120	3.6055	3.6670	0.0614	1.69	101.70
<b>Average</b>				2.58	102.62
<b>Maximum</b>				6.46	106.67
<b>Minimum</b>				0.75	100.75
<b>Plant A</b>				1.82	101.83
<b>Plant B</b>				3.09	103.15
<b>Plant C</b>				2.58	102.63



### 5.5.2 Transfer Length

The transfer length is the distance for the prestressing strand to transfer the effective prestress force to the concrete. The force on the beam end is assumed to be zero and increases rapidly until it is fully developed to the effective prestress force at the transfer length distance. Transfer length is affected by the ability of the concrete to bond to the tensioned prestressing strand. Factors that influence the ability for a prestressing strand to bond are the amount of prestress force applied to the prestressing steel, the maturity of the concrete and the mechanical bond that is created from the geometry of the prestressing strand. Whereas factors that affect camber are the effective prestressing force per strand, the method used to predict transfer length, the length of the beam, and the amount of prestressing strands.

There are multiple methods to predict the transfer length. Researchers compared the camber when using two methods to predict the transfer length on 5 PPCBs (Table 5-10). The methods that were compared were AASHTO LRFD transfer length and ACI transfer length. Holding other variables the same, it was possible to determine the difference in camber when using two different transfer length prediction methods. Results show that the percent difference between the two methods is  $0.65 \% \pm 0.05\%$ . Due to the small differences between the calculated camber using AASHTO and ACI, it was concluded to use AASHTO LRFD for the remaining transfer length calculations. In addition to the small difference between the two methods, AASHTO LRFD is currently used by the Iowa Department of Transportation for camber calculations.

**Table 5-10: Comparison of AASHTO LRFD and ACI Transfer Length**

<b>Beam</b>	<b>Method Used</b>	<b>Transfer Length (feet)</b>	<b>Camber (inches)</b>	<b>Difference (inches)</b>	<b>Percent Difference</b>
BTE 110	AASHTO LRFD	3.0	1.5821		
BTE 110	ACI	3.1186	1.5813	0.0008	0.049
BTE 145	AASHTO LRFD	3.0	3.4057		
BTE 145	ACI	3.0392	3.4051	0.0006	0.018
BTD 135	AASHTO LRFD	3.0	4.1908		
BTD 135	ACI	3.0306	4.1896	0.0011	0.027
C 80	AASHTO LRFD	3.0	1.3835		
C 80	ACI	3.1053	1.3822	0.0013	0.096
B 55	AASHTO LRFD	3.0	0.6691		
B 55	ACI	3.0306	0.6682	0.0009	0.133

Researchers were able to analytically predict camber with and without the transfer length on multiple girders. Conducting a parametric study allowed the effects of transfer length to be quantified and the percent difference to be calculated. The beams analyzed consisted of Bulb Tee and AASHTO girders. Lengths ranged from 46.33 feet to 156.33 feet. The results of analytically determining camber with and without the transfer length are shown in Table 5-11. Multiple beams of identical design were analyzed using the AASHTO equation for transfer length (Eq. 4-12). Differences between the identical beams are due to the applied prestress force, modulus of elasticity for a specific beam, and the curing duration.

**Table 5-11: Comparison of Camber with and without Transfer Length**

<b>Beams</b>	<b>Calculated Camber with Transfer Length using AASHTO LRFD Method (inches)</b>	<b>Calculated Camber without Transfer Length (inches)</b>	<b>Camber with Transfer Length using AASHTO LRFD Method/ Camber without Transfer Length)*100</b>	<b>Difference (inches)</b>	<b>Percent Difference</b>
BTE 145	3.3346	3.3744	98.82	-0.0398	-1.19
BTE 145	3.4434	3.4837	98.84	-0.0403	-1.16
BTE 145	3.4287	3.4694	98.83	-0.0407	-1.18
BTE 110	1.7705	1.7893	98.95	-0.0188	-1.05
BTB 135	3.3593	3.4086	98.55	-0.0493	-1.46
BTB 135	3.6779	3.7324	98.54	-0.0545	-1.47
BTB 135	3.6608	3.7150	98.54	-0.0542	-1.47
BTB 135	3.5591	3.6112	98.56	-0.0521	-1.45
B 55	0.7561	0.7799	96.95	-0.0238	-3.10
B 55	0.7711	0.7953	96.96	-0.0242	-3.08
C 80	1.1922	1.2212	97.63	-0.0290	-2.40
C 80	1.3178	1.3491	97.68	-0.0312	-2.34
BTE 90	0.9022	0.9121	98.92	-0.0099	-1.09
BTE 155	3.9459	3.9966	98.73	-0.0506	-1.28
BTB 95	3.4682	3.5220	98.47	-0.0538	-1.54
D 55	0.1851	0.1863	99.34	-0.0012	-0.66
D 60	0.2977	0.2993	99.45	-0.0016	-0.55
D 90	1.2422	1.2703	97.79	-0.0280	-2.23
D 90	1.2494	1.2779	97.77	-0.0285	-2.25
D 105	2.1988	2.2307	98.57	-0.0319	-1.44
D 106	2.4965	2.5335	98.54	-0.0370	-1.47
C 67	0.7538	0.7570	99.58	-0.0032	-0.42
BTC 45	0.2028	0.2043	99.22	-0.0016	-0.78
BTB 130	3.7476	3.7966	98.71	-0.0490	-1.30
BTB 100	3.0259	3.0763	98.36	-0.0503	-1.65
D110	2.4413	2.4734	98.70	-0.0321	-1.31
BTE 135	2.8588	2.8904	98.91	-0.0316	-1.10
BTC 120	3.6055	3.6587	98.55	-0.0531	-1.46

**Table 5-11 continued**

Average	2.2369	2.2697	98.52	-0.0328	-1.50
Minimum	0.1851	0.1863	96.95	-0.0545	-3.10
Maximum	3.9459	3.9966	99.58	-0.0012	-0.42
Plant A	2.4571	2.4927	98.59	-0.0356	-1.42
Plant B	2.6843	2.7189	98.78	-0.0346	-1.23
Plant C	1.7618	1.7911	98.33	-0.0293	-1.69

Evaluating the results from Table 5-11 revealed results with camber and transfer length. The results include:

- As the girder length increases, the impact on camber due to transfer length decreases.
- The contribution of camber due to the transfer length is dependent on the amount of prestress force in the PPCB.

Utilizing the full potential of prestressing strands requires designers to tension each strand to its specified capacity regardless of the beam length to maximize efficiency. Since prestressing strands in shorter beams have the same or similar stress per prestressing strand applied as long beams do, the transfer length will be comparable between short and long beams. However, the length of the beam will influence how much the final camber is affected by the transfer length. When calculating camber, ignoring the prestress force over a short length will be more significant than ignoring the same length over a long beam. For example, ignoring 3 feet of transfer length on a beam that is 56 feet long will have more impact on camber than ignoring the same transfer length over a beam that is 156 feet long.

Another result recognized that some shorter beams had a smaller impact on the camber due to transfer length than longer beams. This can be related to the amount of prestress force that is present in PPCBs. A BTE 110 has fewer prestressing strands which will result in lower compressive forces acting along the length of the beam than a BTE 145 or BTD 135. It is assumed the same distance is required to reach the effective prestressing in each of these beams. Since the total force that is reached in the BTE 110 is significantly less than the BTE 145 and BTD 135, the effect of transfer length is also less significant. These results from Table 5-11

prove that the effect transfer length has on camber can be related to the length of the beam and the effective prestressing force.

### 5.6 Impact of Assumptions during Design of Instantaneous Camber

The variables that affect instantaneous camber design include material properties along with design procedures. Material properties include the modulus of elasticity, while design procedures include prestress force, prestress losses, transfer length, sacrificial prestressing strands, and the moment of inertia. Correctly modeling the material properties and design procedures will result in agreement with the measured instantaneous camber when measured correctly. The percent difference of camber was calculated by conducting a parametric study which determined the effect of each variable and how it affects camber. Calculating camber based on of using the designed camber variables and the variables that are representative of the PPCB are summarized in Table 5-12.

**Table 5-12: Percent Difference Associated with Instantaneous Camber Prediction**

	Average Percent Difference	Maximum Percent Difference	Minimum Percent Difference
Modulus of Elasticity based off of designed $f'_{ci}$ vs. measured $f'_{ci}$	-14.74	-0.12	-28.88
Applied Prestress Force vs. Designed Prestress Force	11.48	16.19	7.22
Prestress Losses vs. No Prestress Losses	13.67	17.61	2.60
AASHTO LRFD (2010) Transfer Length vs. No Transfer Length	-1.50	-0.42	-3.40
Sacrificial Prestressing Strands vs. No Sacrificial Prestressing Strands	-2.58	-0.75	-6.46
$I_{tr}$ vs. $I_g$	2.90	3.69	2.21

## **CHAPTER 6. CONCLUSIONS AND RECOMMENDATIONS**

### **6.1 Conclusions**

Predicting camber in prestressed precast concrete beams has been a challenging problem that has led to increased cost and construction delays during bridge construction in the field. While construction challenges tend to have drawn more attention to the long-term camber, it should be realized that an error associated with the measured and expected instantaneous camber affects the long-term camber, among other factors. The overprediction and underprediction of instantaneous camber stems primarily from inaccurate estimate of the material properties of concrete which is only a few hours old, discrepancies between designed and as-built values, camber estimation technique used in design and inaccurate camber measurements in the precasting plant. Systematically addressing each of these issues will improve the prediction of the instantaneous as well as the long-term camber.

### **6.2 Industry Practice Camber**

Industry practice camber measurements recorded by precast plants on beams that were previously cast were organized to determine the following preliminary conclusions:

- Camber was overpredicted 75% of the time.
- The magnitude of overprediction in camber increased as beam length increased.
- As beams increased in length, there was greater scatter in the overprediction and underprediction.
- Specific groups of beams have a tendency to be overpredicted or underpredicted

The current camber measurement technique was investigated by researchers and revealed that the current measurement technique which was used to evaluate the industry practice camber data failed to account for various factors that misrepresent the camber that is present. Therefore the above conclusions have limited value. Complications with accurately measuring camber and the past mix designs that are no longer used to construct beams led researchers to independently measure camber on 105 PPCBs.

### 6.3 Camber Measurement Technique

As part of the research reported herein, different measurement techniques were explored to determine a consistent, accurate way to measure the instantaneous camber. The measurement techniques include what the precast industry is currently using, methods that were used in past research studies, and a measurement method that accounts for previous errors that were neglected.

While most state Department of Transportations have guidelines on how to measure camber, it was determined that there is not a consistent, industry standard that is used. Common methods of camber measurement for the precast industry include using different instruments such as a stretched wire along the length of the beam, tape measures, and occasionally survey equipment to measure camber. There is also variability on if camber is measured from the top flange, bottom flange, or web. The time after release when the camber measurement is taken has been observed to vary between before the transfer of prestress is complete to 3 hours after the transfer of prestress.

Camber research that was previously conducted involved taking independent camber measurements from precast plants. Methods employed to take independent camber measurements included the stretched wire method, survey equipment from top and bottom flange, and photogrammetry. The different methods that were used in past research studies to determine camber often fail to account for variables such as precast bed deflections, inconsistent top flange surfaces, and friction that inhibits the PPCB from reaching its full instantaneous camber.

While some previous measuring methods used by precasters and with past research neglect bed deflections, inconsistent beam depths, and friction between the beam and bed, a new method to measure camber was used that accounts for each of these issues accurately and quantifies their impact on instantaneous camber measurement. Additionally, the industry standard for instantaneous camber measurements along with instrumenting the PPCBs with string potentiometers was conducted to compare results. Using newly collected data from precast plants on 105 PPCBs, the causes of error associated with instantaneous camber was investigated, which led to the following conclusions:

- Factors such as bed deflections, friction, and inconsistent top flange surfaces misrepresent the camber that is recorded at the precast plants.
- Values obtained from field measurements show camber is affected, on average, by bed deflections by  $0.030 \pm 0.062$  in., friction by  $0.392 \pm 0.294$  in., inconsistent top flange surfaces along the beam length by  $0.099 \pm 0.142$  in. and inconsistent top flange surfaces due to local effects by  $0.113 \pm 0.119$  in.
- Through the measurement technique in this study, bed deflections were found to contribute to an error in camber up to 16.13%, friction between the beam ends and precasting bed up to 38.43%, inconsistent top flange surface along the length of the beam up to 29.14%, and inconsistent top flange surface due to local effects up to 66.02%.
- Obtaining data from girders at the transfer of prestress with the tape measure, rotary laser level, and string potentiometers shows good agreement when adjusting for the possible camber measurements errors. Despite good agreement between the tape measure and rotary level, the data based on a tape measure is easily affected by the precision of the person taking the measurement.
- Reverse friction is small in magnitude and can be ignored. This is verified by string potentiometer graph in Figure 5-12 and additional string potentiometer data in Appendix B. The contribution of vertical displacement due to friction can be obtained by lift/set of a beam and then taking a camber measurement.

Although errors associated with measuring instantaneous camber due to bed deflections, friction, and inconsistent top flange surfaces may be small individually, failing to account for each can result in an error up to 150% between measured and designed camber. Using the proposed camber measurement procedure in Chapter 6.5.1 will account for errors that are currently not being accounted for, which in turn will improve the camber prediction and reduce unforeseen construction issues relating to camber in PPCBs.

#### **6.4 Analytical Camber Prediction**

Predicting camber has also presented challenges due to the need to accurately model the concrete and prestressing steel properties. Relating the calculated camber to the measured



camber is dependent on the ability to model material properties and the actual conditions of the PPCB. Instantaneous camber was predicted based on the minimum specified variables. This includes using the minimum design release strengths to predict the modulus of elasticity, the designed prestress forces, accounting for prestress losses, AASHTO transfer length, and neglecting sacrificial prestressing strands. Instantaneous camber was also predicted for beams that were previously constructed using variables that were accurate with the material properties of the beam. Comparisons between the analytical predictions of camber using properties used in design and properties based off of previously cast PPCBs results in different instantaneous camber values. The analytical camber predictions could also be compared to camber that was measured on over 105 PPCBs. Additionally a parametric study was conducted that compared the effects of neglecting different variables. Based on the analytical camber predictions and the parametric study, the following conclusions can be made about analytical camber prediction and the accuracy of the material properties that are used.

- The modulus of elasticity using the AASHTO LRFD (2010) provides  $98.24\% \pm 14.91\%$  agreement with measured camber values when using the specific unit weight and release strengths corresponding to specific beams.
- A multiplier was used to adjust the analytical camber to the measured camber. This resulted in 100 % agreement with a standard deviation of 10.37 %. The standard deviation of 10.37 % can be attributed to the inconsistent material properties and fabrication procedures.
- The AASHTO LRFD modulus of elasticity is dependent on the designed release strength. The release strength is higher than the design strength by 39.5% and 11.5% for beams with designed release strength of 4500-5500 psi and 6000-8500 psi, respectively.

Conducting a parametric study on the variables that affect instantaneous camber revealed the following conclusions:

- The designed prestress force has an agreement with the precasters' applied prestress force value of  $100.87\% \pm 2.50\%$  when evaluating 41 PPCBs.

- 34 % of PPCBs fell outside the  $\pm 5\%$  tolerance set by the Iowa Department of Transportation for applied prestress vs. designed prestress force. The Maximum and minimum ratios of applied to designed prestress force were 108.95% and 96.21% respectively.
- The sacrificial prestressing strands are affected by the prestress force and the eccentricity from the strands to the center of gravity of the section. On average, this affects camber by 2.58 percent. Ignoring the sacrificial prestressing strands can contribute to an error of up to 6.67 percent.
- Prestress losses at the transfer of prestress include elastic shortening, seating losses, and relaxation. A combination of prestress losses contributes to a reduction in prestress by 7.00% on average which reduces camber on average by 11.34%.
- The moment of inertia can be represented by the transformed section along the length of the beam. The transformed moment of inertia along the length of the beam compared to the gross moment of inertia will produce instantaneous cambers that have +2.90 percent difference.
- The transfer length between the ACI method and AASHTO LRFD method produced an average difference of  $0.646\% \pm 0.048\%$ .
- The average percent difference of -1.50 is present when ignoring the transfer length and using the AASHTO LRFD method. Ignoring transfer length can contribute to an error of up to 3.05 percent.

Determining the potential errors and magnitude of each error allows designers to adjust design procedures to more accurately predict instantaneous camber. Improving instantaneous camber predictions will also improve erection and long-term camber predictions.

## 6.5 Recommendations

Throughout the study of improving camber predictions on PPCBs, production and design procedures have been observed to significantly affect the accuracy of predicted and measured camber. Evaluating and improving design and production procedures will result in closer

agreement of designed and measured camber. The following is a list of recommendations that are suggested for precasters, contractors and designers.

### 6.5.1 Measuring Instantaneous and Long-Term Camber

Precasters and contractors current camber measurement method has been observed to differ from the time the measurement is taken and the location on the beam where it is measured from. By observing and taking independent camber measurements, it was found that the error between the two groups on average is 26.17%. To eliminate the difference in camber due to measurement technique, a simplified procedure that both precasters and contractors can use to accurately measure camber was developed. The following are recommendations for the new camber measurement procedure.

1. Place a 2x4 on the top flange of the PPCB at the ends and at midspan (Figures 6-1 and 6-2).
2. Cast the concrete to the elevation of the 2x4 to ensure that a flat surface will be produced.

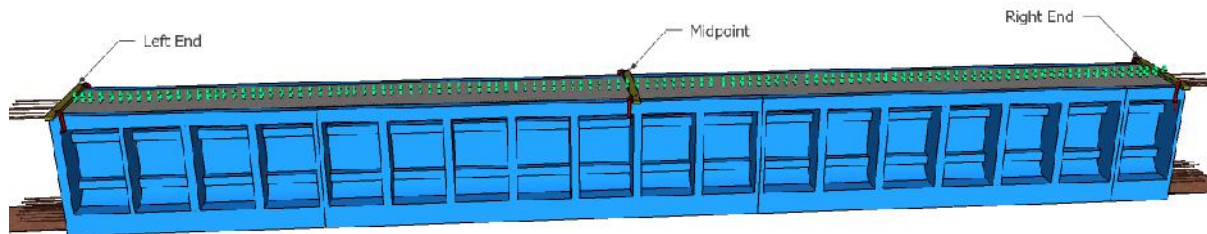


**Figure 6-1: PPCB with Locations of 2x4's**

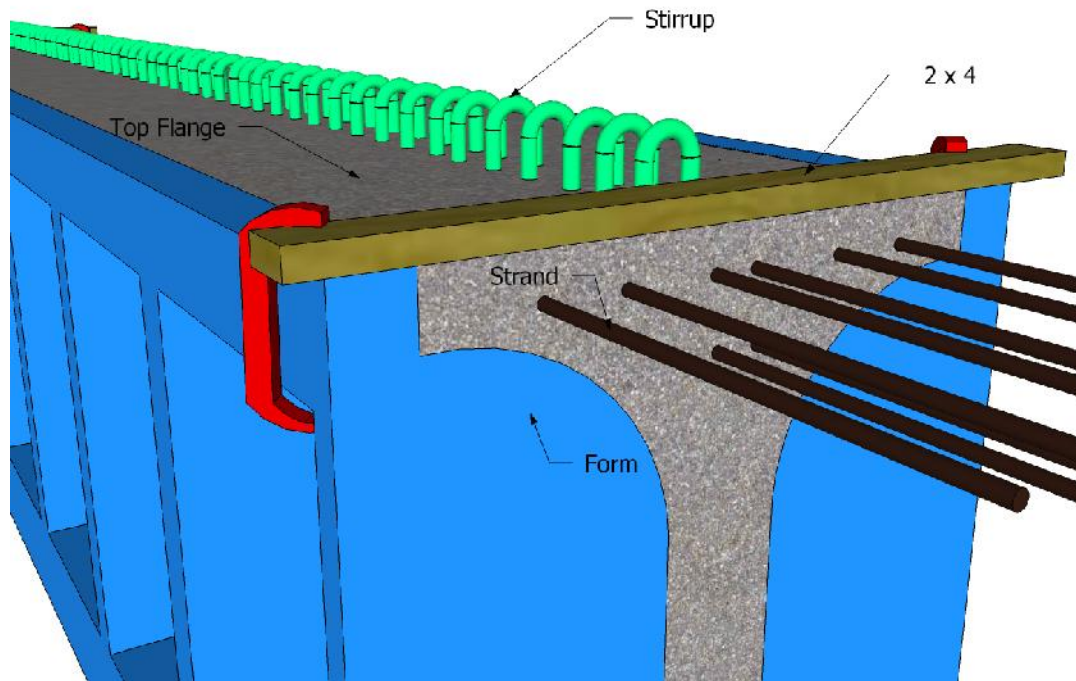


**Figure 6-2: Close up of 2x4 on a PCB**

3. Allow beam to cure under normal steam or natural curing circumstances
4. Remove the 2x4's from the top flange.
5. After the beam has been released, precaster's have one of the following options:
  - a. Lift/set the beam on the precasting bed.
  - b. Lift the beam and move it to the storage yard, placing it on temporary wooden supports.
6. Measure the elevation of the beam with a rotary laser level, total station, or other survey equipment at the midspan and the ends in the locations that correspond to the 2x4's. At each location, take measurements at each side and in the middle of the top flange.

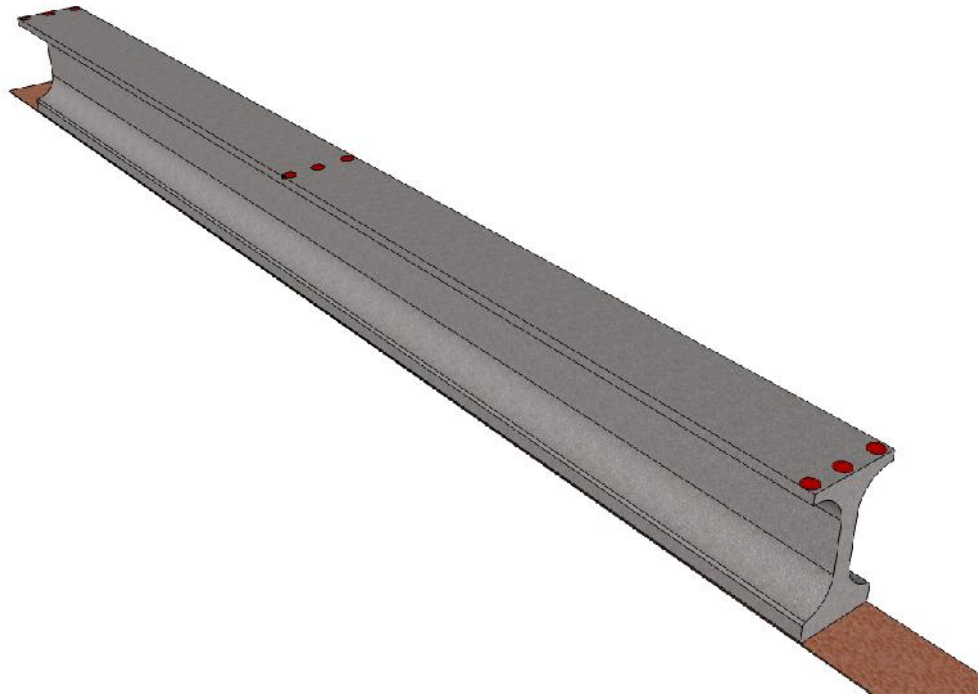


**Figure 6-3: Location of Camber Measurements after the Transfer of Prestress**

7. If option 5.b. is used, determine the contribution in camber due to the reduced clear span and overhang caused by the temporary supports.
8. Take the average of the end elevation readings and subtract from midspan camber elevation reading.
9. If option 5.b. is used, subtract the contribution in camber due to the temporary support placement from the camber value calculated in step 8.

The recommended procedure for measuring camber has benefits with accuracy and time savings for the precaster. Measuring camber with this method eliminates inaccurate representation of camber due to friction, inconsistent top flange surfaces, and bed deflection. The 2x4's cast in the top flange will ensure that the same reference point is being used for measuring camber. Although the time to measure camber will be somewhat greater than the existing method for precasters, it will produce accurate results.

### 6.5.2 Additional Recommendations to Precasters

Observing and taking independent camber measurements at three separate precast plants led researchers to recommendations on how to improve the ability to predict camber on PPCBs.

- The prestress force is highly sensitive to camber; therefore monitor and closely adhere to the designed prestress force.
- Aim for reaching the design release strength at the transfer of prestress of PPCBs.
- Ensure that materials and mixes used on beams are identical to each other.
- Insulate and cure beams similar to adjacent beams.
- Replicate the beams curing conditions to the sample cylinders used for obtaining the release strength.
- Use the proposed measurement procedure to take instantaneous camber measurements
- Store beams with the appropriate overhangs to encourage or discourage camber growth.

Performing the recommendations above will help precasters produce PPCBs that have camber in agreement with the designed camber value. Material and fabrication deficiencies may not be avoided due to the unpredictable behavior of concrete and the control of the equipment used to produce the beams.

### 6.5.3 Recommendations to Designers

Predicting instantaneous camber was studied by researchers using the moment area method. The following recommendations are made for the prediction of instantaneous camber for designers.

- The decrease in camber due to transfer length is dependent on the amount of prestressing strands and the length of the beam. Due to convenience of design and accuracy, AASHTO LRFD (2010) equation for transfer length should be used.
- The modulus of elasticity is a sensitive variable and can impact the accuracy of camber. Using the AASHTO LRFD (2010) modulus of elasticity with an accurate release strength and unit weight will improve camber predictions.

- When calculating the design release camber, designers should increase the design release strength by 40% and 10% for beams with designed release strength of 4500-5500 psi and 6000-8500 psi, respectively.
- Moment of inertia of the section changes along the length of the beam if harped sections are used. Due to convenience of design, the gross moment of inertia should be used for design equations.
- The prestress force is an important variable that is highly sensitive to the camber. Close agreement with designed and actual prestress force will give good agreement between the designed and measured camber.
- Prestress losses have been observed to reduce the initial prestress force by 7.00%. The camber will be affected on average by 11.34%. Therefore, prestress losses should be accounted for in design.
- Sacrificial prestressing strands will reduce the camber by as much as 6.46 % and should be accounted for.

It is recognized that all variables may not be accurately adjusted due to the uncertainty of the fabrication and materials used for constructing PPCBs. Using the above recommendations will reduce the current error between designed and measured camber.

## WORKS CITED

- American Association of State Highway and Transportation Officials (AASHTO) (2007). *AASHTO LRFD Bridge Design Specifications, 4<sup>th</sup> edition*.
- American Association of State Highway and Transportation Officials (AASHTO) (2010). *AASHTO LRFD Bridge Design Specifications, 5<sup>th</sup> edition*. 2010. Print
- American Concrete Institute (ACI). (2008). Building Code Requirements for Structural Concrete (ACI 318-08). ACI, Farmington Hills, Michigan.
- Ahlborn, T.M., Shield, C.K. and French, C.W. (2000) "High-Performance Concrete Prestressed Bridge Girders: Long Term and Flexural Behavior." Report 2000-32, Minnesota Department of Transportation, St. Paul, MN 91 pp.
- Barr, P., Fekete, E. Eberhard, M., Stanton, J., Khaleghi, B., Hsieh, J. (2000). "High Performance Concrete in Washington State SR 18/SR 516 Overcrossing: Interim Report on Girder Monitoring." Report Number FHWA-RD-00-070. Federal Highway Administration (FHWA). Washington, D.C.
- Branson, D.E., Meyers, B.L., and Kripanarayanan, K.M., (1970). "Loss of Prestress, Camber, and Deflection of Noncomposite and Composite Structures Using Different Weight Concretes." University of Iowa Final Report.
- "Chapter J: Design of Connections." *Steel Construction Manual*. 13th ed. [Chicago, Ill.]: American Institute of Steel Construction, 2005. 16.1-109-6.1-110. Print.
- Cole, Harry A. "Direct Solution for Elastic Prestress Loss in Pretensioned Concrete Girders." *Practice Periodical on Structural Design and Construction* 5.1 (2000): 27-31. Print.
- Gilbertson, Christopher G., and Theresa M. Ahlborn. "A Probabilistic Comparison of Prestress Loss Methods in Prestressed Concrete Beams." *PCI Journal* 49.5 (2004): 52-69. Print.
- "Haunch Girder." <http://www.iowadot.gov/subcommittee/bridgeterms.aspx>. American Association of State Highway and Transportation Officials (AASHTO) Standing Committee on Highways and Subcommittee on Bridges and Structures, 2005. Web. 20 June 2013.
- He, Wenjun, Rouse, Jon M., Sritharan, Sri. (2013). "Creep and Shrinkage of High Performance Concrete, and Prediction of Long-Term Camber of Prestressed Bridge Girders." M.S. Thesis. Iowa State University, Ames, IA.
- Hinkle, Stephen D. (2006). "Investigation of Time-Dependent Deflection in Long Span, High Strength, Prestressed Concrete Bridge Beams." M.S. Thesis, Virginia Polytechnic Institute and State University, Blacksburg, VA.



Hupauf, Tony. Internal Report. University of Washington, 2006.

Iowa DOT. (2011). Iowa LRFD Bridge Design Manual, Retrieved March 2013, from Iowa DOT Design Policies: [www.iowadot.gov/bridge/manuallrfd.htm](http://www.iowadot.gov/bridge/manuallrfd.htm)

Iowa DOT (2011). Index of Beam Standards, Retrieved June 2011 from Iowa DOT: <W:\Highway\Bridge\Standards\Bridges\EnglishBeams.dgn>.

Iowa DOT. (2013). Iowa Department of Transportation Office of Materials IM 570. “Precast Prestressed Concrete Bridge Units.” Retrieved June 2013, from Iowa DOT <http://www.iowadot.gov/erl/current/IM/content/570.pdf>

Iowa DOT. (2013). Iowa Department of Transportation Prestress Manual. “Prestress Inspection.” Retrieved May 2013, from [http://www.iowadot.gov/training/ttcp/training\\_manuals/PrestressManual.pdf](http://www.iowadot.gov/training/ttcp/training_manuals/PrestressManual.pdf)

Jayaseelan, H., Russell, B.W. (2007). Prestress Losses and the Estimation of Long-Term Deflections and Camber for Prestressed Concrete Bridges. Oklahoma State University Final Report.

Jáuregui, David V., Kenneth R. White, Clinton B. Woodward, and Kenneth R. Leitch. "Noncontact Photogrammetric Measurement of Vertical Bridge Deflection." *Journal of Bridge Engineering* 8.4 (2003): 212-22. Print.

Johnson, Brandon Ray. (2012). “Time-Dependent Deformations in Precast, Prestressed Bridge Girders.” M.S. Thesis, Auburn University, Auburn, AL.

Kelly, D.J., Bradberry, T.E., and Breen, J.E. (1987). “Time Dependent Deflections of Pretensioned Beams.” Research Report CTR 381-1, Center for Transportation Research – The University of Texas at Austin.

Lin, T. Y., and N. H. Burns. *Design of Prestressed Concrete Structures*. New York: Wiley, 1981. Print.

Naaman, Antoine E. *Prestressed Concrete Analysis and Design: Fundamentals*. Ann Arbor, Mich: Techno 3000, 2004. Print.

O'Neill, Cullen R., and Catherine E. French. "Validation of Prestressed Concrete I Beams Deflection and Camber Estimates." M.S. Thesis. University of Minnesota, 2012. <http://www.dot.state.mn.us/>. Web. Feb. 2013.

PCI (2010). PCI Design Handbook: Precast and Prestressed Concrete, 7th Edition. Precast/Prestressed Concrete Institute, Chicago, IL.

PCI (1975). “Recommendations for Estimating Prestress Losses,” PCI Committee on Prestress Losses, PCI Journal, Vol. 20(4), 43-75.

- Rosa, M., Stanton, J., and Eberhard, M., 2007. "Improving Predictions for Camber in Precast, Prestressed Concrete Bridge Girders," M.S. Thesis, University of Washington, Seattle, WA.
- Rizkalla, S., Zia, P., and Storm, T. (2011). "Predicting Camber, Deflection, and Prestress Losses in Prestressed Concrete Members," North Carolina State University Final Report.
- Swartz, Brian D., Andrew Scanlon, and Andrea J. Schokker. "AASHTO LRFD Bridge Design Specifications Provisions for Loss of Prestress." *PCI Journal* Fall (2012): 108-32. Print.
- Tadros, M.K., Fawzy, F., Hanna, K.E. (2011). "Precast, Prestressed Girder Camber Variability." *PCI Journal*, (Winter 2011), 135-154.
- Tadros, M.K.; Seguirant, S.J.; and Gallt, J.G. (2003). "Prestress Losses in Pretensioned High-Strength Concrete Bridge Girders." NCHRP Report 496, National Cooperative Highway Research Program (NCHRP).
- Tadros, M. K., Ghali, A., and Meyer, A. W., "Prestress Loss and Deflection of Precast Concrete Members," *PCI Journal*, Vol. 30, No. 1, Chicago, IL (January–February 1985) pp. 114–141.
- Woolf, D., and French, C., "A Camber Study of Mn/DOT Prestressed Concrete I-Girders," M.S. Thesis, University of Minnesota, 1998, pp. 13-14.
- Zia, Paul, H. Kent Preston, and Edwin B. Workman. "Estimating Prestress Losses." *Concrete International* (June 1979): 32-38. Print.

**APPENDIX A: DATA**

The results obtained in this thesis were gathered through field experimentation on 108 PPCBs. The PPCBs were measured from three different precast plants that produce highway bridge girders for the state of Iowa. The data listed below was gathered with a rotary laser level. From these measurements, researchers were able to calculate the camber based on the method found in Chapter 3.

Beams cast after date 11-9-2011 were measured in tenths. Multiplying each measurement by 1.200 will give an appropriate conversion to inches.

Location	Date Cast	Date Released	Time	Beam Type	Left End (inches)	Left Support (inches)	Midspan (inches)	Right Support (inches)	Right End (inches)	Location of Measurement	Notes
Plant C	9/13/2011	9/14/2011	6:00AM	D90	5.8125		5.5625		5.6250	South end of top flange on raked surface (pre-release)	Disregard. Inaccurate data collection.
					6.0000		5.5625		5.6250	Middle of top flange on raked surface (pre-release)	
					6.1250		5.5000		5.6875	North end of top flange on raked surface (pre-release)	
					5.9792		5.5417		5.6458	Average of Top Flange (after release)	
					5.8125		4.7500		5.5625	South end of top flange on raked surface (after release)	
					5.8750		4.6875		5.6250	Middle of top flange on raked surface (after release)	
					6.1250		4.6875		5.7500	North end of top flange on raked surface (after release)	
					5.9375		4.7083		5.6458	Average of Top Flange (after release)	
					59.9375		60.9375		59.7500	Bottom Flange (pre-release)	
					59.8125		59.9375		59.7500	Bottom Flange (after release)	

Plant C	9/13/2011	9/14/2011	6:00AM	D90	5.5000		5.8125	5.8750	South end of top flange on raked surface (pre-release)	Disregard. Inaccurate data collection.
					5.5000		5.7500	5.9375	Middle of top flange on raked surface (pre-release)	
					5.4375		5.7500	5.9375	North end of top flange on raked surface (pre-release)	
					5.4792		5.7708	5.9167	Average of Top Flange (before release)	
					5.5625		5.0000	5.9375	South end of top flange on raked surface (after release)	
					5.5625		4.9375	6.0000	Middle of top flange on raked surface (after release)	
					5.5625		4.8750	5.9375	North end of top flange on raked surface (after release)	
					5.5625		4.9375	5.9583	Average of Top Flange (after release)	
					59.6875		61.0000	60.0000	Bottom Flange (pre-release)	
					59.1250		58.6250	59.5000	Bottom Flange (after release)	
Plant C	9/13/2011	9/14/2011	6:00AM	D90	6.0625		6.0000	6.5625	South end of top flange on raked	Disregard. Inaccurate

[illegible]

						7.6875			7.7500		8.0625	Middle of top flange on raked surface (pre-release)	
						7.5000			7.7500		8.0625	North end of top flange on raked surface (pre-release)	
						7.6458			7.7708		8.0625	Average of Top Flange (before release)	
						7.7500			6.6250		8.0625	South end of top flange on raked surface (after release)	
						7.6250			6.7500		8.1250	Middle of top flange on raked surface (after release)	
						7.6250			6.6250		8.0625	North end of top flange on raked surface (after release)	
						7.6667			6.6667		8.0833	Average of Top Flange (after release)	
						61.8750			62.0625		62.062	Bottom Flange (pre-release)	
						62.0625			60.8125		62.250	Bottom Flange (after release)	
Plant C	9/15/2011	9/16/2011	6:00AM	D90	7.8750				7.6250		7.8750	South end of top flange on raked surface (pre-release)	

[illegible]



									8.1250				7.5625			7.7500	Middle of top flange on raked surface (pre-release)		
									8.1250				7.5000			7.6250	North end of top flange on raked surface (pre-release)		
									8.1667				7.5625			7.7083	Average of Top Flange (before release)		
									8.1875				6.7500				South end of top flange on raked surface (after release)		
									8.1875				6.6250			7.6875	Middle of top flange on raked surface (after release)		
									8.1875				6.6250				North end of top flange on raked surface (after release)		
									8.1875				6.6667			7.7083	Average of Top Flange (after release)		
									62.3125				62.8125			62.063	Bottom Flange (pre-release)		
									62.1250				61.1875			62.125	Bottom Flange (after release)		
Plant A	9/16/2011	9/17/2011	7:30AM	D110	9.3750								9.6250			9.6875	Troweled surface of top flange on raked surface (pre-release)		
					9.3125								9.6875			9.6250	Middle of top flange on raked surface (pre-release)		

[illegible]

								9.4375		9.7500		9.5000	Middle of top flange on raked surface (pre-release)	
								9.1250		9.9375		9.5000	North end of top flange on raked surface (pre-release)	
								9.3542		9.8125		9.5208	Average of Top Flange (before release)	
								9.5625		7.6250		9.6875	Troweled surface of top flange on raked surface (after release)	
								9.6250		7.6250		9.4375	Middle of top flange on raked surface (after release)	
								9.1875		7.7500		9.6250	North end of top flange on raked surface (after release)	
								9.4583		7.6667		9.5833	Average of Top Flange (after release)	
								63.7500		64.1875		63.500	Bottom Flange (pre-release)	
								63.7500		61.6250		63.500	Bottom Flange (after release)	
								63.7500		63.9375		63.500	Bed while beam is still in place (after release)	
Plant A	9/16/2011	9/17/2011	7:30AM	D110				10.2500		9.6875		9.6875	Troweled surface of top flange on raked surface (pre-release)	



[illegible]

Plant C	9/19/2011	9/20/2011	6:00AM	D90	7.8750					7.4375			7.3750					South end of top flange on raked surface (pre-release)	7.3750	
																		Middle of top flange on raked surface (pre-release)	7.3750	
																		North end of top flange on raked surface (pre-release)		
					7.8750					7.3750				7.3125				Average of Top Flange (before release)	7.3542	
																		South end of top flange on raked surface (after release)	7.3750	
					7.8750					6.3125								Middle of top flange on raked surface (after release)	7.3125	
																		North end of top flange on raked surface (after release)	7.3750	
					7.8125					6.2500								Average of Top Flange (after release)	7.3542	
					61.2500					61.0625								Bottom Flange (pre-release)	61.0625	
					61.5000					60.1250								Bottom Flange (after release)	61.1250	
										61.0625								Top of Chamfer on Bed (after release)		

[illegible]







					62.5625			60.1250	60.3125	Bottom Flange (after release with block)	
								61.9375		Top of Chamfer on Bed (after release)	
Plant C	9/21/2011	9/22/2011	6:00AM	D90	8.1875			8.1250	8.1875	South end of top flange on raked surface (pre- release)	
					8.1875			8.1250	8.1875	Middle of top flange on raked surface (pre- release)	
					8.1250			8.0625	8.1250	North end of top flange on raked surface (pre- release)	
					8.1667			8.1042	8.1667	Average of Top Flange (before release)	
					8.2500			7.0000	8.1875	South end of top flange on raked surface (after release)	
					8.2500			6.9375	8.1250	Middle of top flange on raked surface (after release)	
					8.1875			6.8125	8.1875	North end of top flange on raked surface (after release)	
					8.2292			6.9167	8.1667	Average of Top Flange (after release)	
					61.8125			62.1250	61.8125	Bottom Flange (pre-release)	





												surface (after release)	
												South end of top flange on raked surface (after release)	
											6.1250	8.4375	
											6.1042	8.4167	
											62.3750	62.5000	
											60.0625	62.5625	
											62.3125		Bed while beam is still in place (after release)
Plant A	9/23/2011	9/24/2011	7:00AM	D110	8.1875	8.1250					8.1250	8.0625	North Side of top flange on raked surface (pre-release)
											8.0625	8.0000	Middle of top flange on raked surface (pre-release)
											8.5000	8.0625	South end of top flange on raked surface (pre-release)
											8.2292	8.0417	Average of Top Flange (before release)
											5.8750	8.0625	North Side of top flange on raked surface (after release)

										8.2500			5.8750			8.1250	Middle of top flange on raked surface (after release)	
										8.2500			6.1250			8.1250	South end of top flange on raked surface (after release)	
										8.2083			5.9583			8.1042	Average of Top Flange (after release)	
										62.3750			62.6875			62.1875	Bottom Flange (pre-release)	
										62.3750			60.3750			62.1250	Bottom Flange (after release)	
													62.5625				Bed while beam is still in place (after release)	
Plant A	9/23/2011	9/24/2011	7:00AM	D110	8.5625								8.3125			8.0625	North Side of top flange on raked surface (pre-release)	
					8.6250								8.2500			8.0000	Middle of top flange on raked surface (pre-release)	
					8.6875								8.2500			8.0625	South end of top flange on raked surface (pre-release)	
					8.6250								8.2708			8.0417	Average of Top Flange (before release)	
													5.8750			8.0625	North Side of top flange on raked surface (after release)	

										5.8125			8.0625	Middle of top flange on raked surface (after release)	
										5.8750			8.0625	South end of top flange on raked surface (after release)	
										5.8542			8.0625	Average of Top Flange (after release)	
										62.6875			62.3750	Bottom Flange (pre-release)	
										60.1250			62.3125	Bottom Flange (after release)	
										62.3750				Bed while beam is still in place (after release)	
Plant A	9/22/2011	9/24/2011	7:00AM	D110	9.6875					9.2500			8.7500	North Side of top flange on raked surface (pre-release)	
					9.6250					9.3750			8.6250	Middle of top flange on raked surface (pre-release)	
					9.7500					9.3750			8.6250	South end of top flange on raked surface (pre-release)	
					9.6875					9.3333			8.6667	Average of Top Flange (before release)	
					9.7500					6.8125			8.8125	North Side of top flange on raked surface (after release)	

									9.6875			6.8750		8.7500	Middle of top flange on raked surface (after release)	
									9.6875			6.9375		8.6250	South end of top flange on raked surface (after release)	
									9.7083			6.8750		8.7292	Average of Top Flange (after release)	
									63.4375			63.1250		63.0000	Bottom Flange (pre-release)	
									63.1875			60.7500		62.9375	Bottom Flange (after release)	
												63.1250			Bed while beam is still in place (after release)	
Plant A	10/7/2011	10/8/2011	7:00AM						6.1875	BTC4 5		6.4375		6.3125	North Side of top flange on raked surface (pre-release)	
									6.2500			6.2500		6.2500	Middle of top flange on raked surface (pre-release)	
									6.3125			6.4375		6.5000	South end of top flange on raked surface (pre-release)	
									6.2500			6.3750		6.3542	Average of Top Flange (before release)	
									6.1875			6.1875		6.3125	North Side of top flange on raked surface (after release)	



									6.2500		6.2500		6.2500		6.3750	Middle of top flange on raked surface (after release)	
									6.3750		6.3125		6.5000			South end of top flange on raked surface (after release)	
									6.2708		6.25		6.3958			Average of Top Flange (after release)	
									51.3125		51.8750		51.8125			Bed (pre-release)	
																Bottom Flange (after release)	
									51.5625		51.8750		51.7500			Bed while beam is still in place (after release)	
Plant A	10/7/2011	10/8/2011	7:00AM	BTC 45	5.6875	5.9375	6.1250									North Side of top flange on raked surface (pre-release)	
					5.7500	6.0625	6.2500									Middle of top flange on raked surface (pre-release)	
					5.9375	6.3125	6.3750									South end of top flange on raked surface (pre-release)	
					5.7917	6.1042	6.2500									Average of Top Flange (before release)	
					5.6250	5.7500	6.0000									North Side of top flange on raked surface (after release)	

[illegible]



						6.5625												North Side of top flange on raked surface (after release)	7.3125							
						6.5625												Middle of top flange on raked surface (after release)	7.1250							
						6.5625												South end of top flange on raked surface (after release)	6.6875							
						6.5625												Average of Top Flange (after release)	7.0417							
						61.1875												Bottom Flange (pre-release)	60.9375							
						61.0625												Bottom Flange (after release)	61.0625							
						61.0625												Bed while beam is still in place (after release)	61.0625							
Plant A	10/28/2011	10/31/2011	7:45AM	BTC	130	10.5000												North Side of top flange on raked surface (pre-release)	10.3125							
						10.5000												Middle of top flange on raked surface (pre-release)	10.3125							
						10.5000												South end of top flange on raked surface (pre-release)	10.1250							
						10.5000												Average of Top Flange (before release)	10.2500							





[illegible]





					11.7500				11.5625		11.5625	Middle of top flange on raked surface (pre-release)	
					11.6875				11.5625		11.3125	South end of top flange on raked surface (pre-release)	
					11.7083				11.5833		11.4792	Average of Top Flange (before release)	
					11.6875				10.8125		11.5625	North Side of top flange on raked surface (after release)	
					11.8125				10.8125		11.5625	Middle of top flange on raked surface (after release)	
					11.6875				10.8125		11.3125	South end of top flange on raked surface (after release)	
					11.7292				10.8125		11.4792	Average of Top Flange (after release)	
					55.5000				55.3125		55.6250	Bottom Flange from reference point (pre-release)	
					56.2500						56.0000	Bed while beam is still in place (before release)	
					55.4375				54.6875		55.7500	Bottom Flange from reference point (after release)	
					56.3125						56.0625	Bed while beam is still in place (after release)	

[illegible]

					53.6875				52.4375		54.0000	Bottom Flange from reference point (after release)	
					56.0000				55.6875		55.7500	Bed while beam is still in place (after release)	
Plant C	11/3/2011	11/4/2011	6:00AM	C67	11.0000				11.0625		11.0625	North Side of top flange on raked surface (pre- release)	
					11.0625				11.0625		11.0625	Middle of top flange on raked surface (pre- release)	
					11.1250				11.0625		10.6875	South end of top flange on raked surface (pre- release)	
					11.0625				11.0625		10.9375	Average of Top Flange (before release)	
					11.0000				10.3125		11.0625	North Side of top flange on raked surface (after release)	
					11.0625				10.3125		11.0625	Middle of top flange on raked surface (after release)	
					11.0625				10.2500		11.0000	South end of top flange on raked surface (after release)	
					11.0417				10.2917		11.0417	Average of Top Flange (after release)	

						53.8125		53.5625			54.1250	Bottom Flange from reference point (pre-release)	
						55.6250					55.3750	Bed while beam is still in place (before release)	
						53.8125		52.8125			54.0625	Bottom Flange from reference point (after release)	
						56.0000		55.4375			55.3750	Bed while beam is still in place (after release)	
Plant C	11/3/2011	11/4/2011	6:00AM	C67	10.8750	10.8750		11.0625			11.1875	North Side of top flange on raked surface (pre- release)	
						10.8750		11.0000			11.1875	Middle of top flange on raked surface (pre- release)	
					10.8125	10.8750		10.8750			11.0625	South end of top flange on raked surface (pre- release)	
					10.8542			10.9792			11.1458	Average of Top Flange (before release)	
					11.0000			10.3125			11.3750	North Side of top flange on raked surface (after release)	
					11.0000			10.3125			11.4375	Middle of top flange on raked surface (after release)	
					11.0000			10.2500			11.3750	South end of top flange on raked	

														surface (after release)		
														Average of Top Flange (after release)	11.3958	
														Bottom Flange from reference point (pre-release)	53.8750	
														Bed while beam is still in place (before release)	55.8125	
														Bottom Flange from reference point (after release)	54.0000	
														Bed while beam is still in place (after release)	56.0000	
Plant A									BTE 135					North Side of top flange on raked surface (pre-release)	11.3125	
														Middle of top flange on raked surface (pre-release)	11.7500	
														South end of top flange on raked surface (pre-release)	11.5000	
														Average of Top Flange (before release)	11.5208	
														North Side of top flange on raked surface (after release)	12.3750	

										12.6250			9.6875			11.8750	Middle of top flange on raked surface (after release)	
										12.5625			9.5625			11.7500	South end of top flange on raked surface (after release)	
										12.6875			9.6667			12.0000	Average of Top Flange (after release)	
										75.8750			75.6250			75.5000	Bottom Flange (pre-release)	
										76.0000			73.1250			75.5625	Bottom Flange (after release)	
													75.6250				Bed while beam is still in place (after release)	
Plant A	11/9/2011	11/12/2011	7:30AM						BTE 135	12.0625			11.8750			11.7500	North Side of top flange on raked surface (pre-release)	
										11.7500			11.8125			11.6250	Middle of top flange on raked surface (pre-release)	
										11.5000			11.5625			11.6250	South end of top flange on raked surface (pre-release)	
										11.7708			11.7500			11.6667	Average of Top Flange (before release)	
										12.2500			9.3125			11.6875	North Side of top flange on raked surface (after release)	

										11.8125			9.0625			11.5000	Middle of top flange on raked surface (after release)	
										11.5625			8.9375			12.0000	South end of top flange on raked surface (after release)	
										11.8750			9.1042			11.7292	Average of Top Flange (after release)	
										75.3750			75.0625			75.0000	Bottom Flange (pre-release)	
										75.4375			72.5625			75.0625	Bottom Flange (after release)	
													75.1250				Bed while beam is still in place (after release)	
Plant C	11/29/2011	11/30/2011	6:30AM	D105						7.9500			7.9000			8.0000	North Side of top flange on raked surface (pre-release)	
										8.0000			7.8500			8.0500	Middle of top flange on raked surface (pre-release)	
										8.0000			7.8000			8.0500	South end of top flange on raked surface (pre-release)	
										7.9833			7.8500			8.0333	Average of Top Flange (before release)	
										7.9500			5.6500			7.9500	North Side of top flange on raked surface (after release)	

										5.6500			8.0500	Middle of top flange on raked surface (after release)	
										5.6000			8.1500	South end of top flange on raked surface (after release)	
										5.6333			8.0500	Average of Top Flange (after release)	
										51.4500			52.1500	Bottom Flange (pre-release)	
													52.4500	Bed while beam is still in place (before release)	
										49.4500			52.0000	Bottom Flange (after release)	
													52.4500	Bed while beam is still in place (after release)	
Plant C	11/29/2011	11/30/2011	6:30AM	D 105	8.0000					7.8500			7.9000	North Side of top flange on raked surface (pre-release)	
					7.8500					7.8000			7.9500	Middle of top flange on raked surface (pre-release)	
					7.8500					7.7500			7.9500	South end of top flange on raked surface (pre-release)	
					7.9000					7.8000			7.9333	Average of Top Flange (before release)	



[illegible]

						8.0833			7.9333		7.9500	Average of Top Flange (before release)	
						8.2000			5.6000		7.9000	North Side of top flange on raked surface (after release)	
						8.2000			5.6500		7.9000	Middle of top flange on raked surface (after release)	
						8.2500			5.6500		8.0000	South end of top flange on raked surface (after release)	
						8.2167			5.6333		7.9333	Average of Top Flange (after release)	
						50.3000			51.3500		50.7000	Bottom Flange (pre-release)	
						52.3500					52.5000	Bed while beam is still in place (before release)	
						50.1000			48.9500		50.5500	Bottom Flange (after release)	
						52.8000					52.4500	Bed while beam is still in place (after release)	
Plant C	12/6/2011	12/8/2011	6:00AM	D 105	7.0500				6.9500		7.1500	North Side of top flange on raked surface (pre-release)	
					7.0500				7.0000		7.2000	Middle of top flange on raked surface (pre-release)	



[illegible]

Plant C	12/6/2011	12/8/2011	6:00AM	D 105	7.1000			NA	6.8500	North Side of top flange on raked surface (pre-release)	
					7.0500			7.1500	6.8000	Middle of top flange on raked surface (pre-release)	
					7.0500			7.0000	6.8000	South end of top flange on raked surface (pre-release)	
					7.0667			7.0750	6.8167	Average of Top Flange (before release)	
					7.1500			5.1500	6.9000	North Side of top flange on raked surface (after release)	
					7.1500			5.2500	6.9000	Middle of top flange on raked surface (after release)	
					7.1500			5.1500	6.9000	South end of top flange on raked surface (after release)	
					7.1500			5.1833	6.9000	Average of Top Flange (after release)	
					50.6000			50.0500	50.0500	Bottom Flange (pre-release)	
					51.8875				51.6875	Bed while beam is still in place (before release)	
					50.5000			48.2000	49.9000	Bottom Flange (after release)	
					51.8875				51.6375	Bed while beam is still in place (after release)	

[illegible]

																				Bottom Flange (after release)					
																				Bed while beam is still in place (after release)	52.5000				
Plant C	12/20/2011	12/21/2011	6:00AM	D 55																North Side of top flange on raked surface (pre-release)	7.7500				
																				Middle of top flange on raked surface (pre-release)	7.7000				
																				South end of top flange on raked surface (pre-release)	7.7000				
																				Average of Top Flange (before release)	7.7167				
																				North Side of top flange on raked surface (after release)	7.8500				
																				Middle of top flange on raked surface (after release)	7.9000				
																				South end of top flange on raked surface (after release)	7.9500				
																				Average of Top Flange (after release)	7.9000				
																				Bottom Flange (pre-release)					

					52.1500						52.2500	Bed while beam is still in place (before release)	
												Bottom Flange (after release)	
					52.2000						52.4500	Bed while beam is still in place (after release)	
Plant C	12/20/2011	12/21/2011	6:00AM	D 55	7.4000					7.6000	7.7000	North Side of top flange on raked surface (pre-release)	
					7.5500					7.5500	7.7500	Middle of top flange on raked surface (pre-release)	
					7.5500					7.6500	7.7500	South end of top flange on raked surface (pre-release)	
					7.5000					7.6000	7.7333	Average of Top Flange (before release)	
					7.5500					7.4500	7.7000	North Side of top flange on raked surface (after release)	
					7.6000					7.4500	7.7000	Middle of top flange on raked surface (after release)	
					7.6000					7.5500	7.7000	South end of top flange on raked surface (after release)	



						7.5833			7.4833		7.7000	Average of Top Flange (after release)	
						50.3500			50.1500		50.7500	Bottom Flange (pre-release)	
						52.1000					52.0500	Bed while beam is still in place (before release)	
						50.3500			50.0500		50.8000	Bottom Flange (after release)	
						52.2000					52.2000	Bed while beam is still in place (after release)	
Plant C	12/20/2011	12/21/2011	6:00AM	D 55	7.9000				7.5000		7.4500	North Side of top flange on raked surface (pre-release)	
					7.8500				7.5000		7.5500	Middle of top flange on raked surface (pre-release)	
					7.9500				7.5500		7.5000	South end of top flange on raked surface (pre-release)	
					7.9000				7.5167		7.5000	Average of Top Flange (before release)	
					7.8500				7.4000		7.5000	North Side of top flange on raked surface (after release)	
					7.8500				7.4000		7.5500	Middle of top flange on raked surface (after release)	

[illegible]

																			Middle of top flange on raked surface (after release)	7.6500								
																			South end of top flange on raked surface (after release)	7.6500								
																			Average of Top Flange (after release)	7.6167								
																			Bottom Flange (pre-release)	50.0500								
																			Bed while beam is still in place (before release)	52.0000								
																			Bottom Flange (after release)	50.0500								
																			Bed while beam is still in place (after release)	52.0000								
Plant C		12/29/2011	12/30/2011	7:00AM	D 55	7.1000													North Side of top flange on raked surface (pre-release)	7.2000								
																			Middle of top flange on raked surface (pre-release)	7.2000								
						7.0500													South end of top flange on raked surface (pre-release)									
						7.1000													Average of Top Flange (before release)	7.2000								

[illegible]



[illegible]







							44.8500							44.6000	Bed while beam is still in place (after release)		
Plant C	1/18/2012	1/23/2012	6:00AM	C 80			8.1000	8.0500						8.2000	North Side of top flange on raked surface (pre-release)		
							8.0000	8.0000						8.1500	Middle of top flange on raked surface (pre-release)		
															South end of top flange on raked surface (pre-release)		
							7.9500	8.0000						8.1500	Average of Top Flange (before release)		
							8.0167	8.0167						8.1667	North Side of top flange on raked surface (after release)		
							8.1500	6.9000						8.1500	Middle of top flange on raked surface (after release)		
							8.0500	6.8000						8.1000	South end of top flange on raked surface (after release)		
							7.9500	6.8000						8.0500	Average of Top Flange (after release)		
							8.0500	6.8333						8.1000	Bottom Flange (pre-release)		
							43.5500	43.1500						43.3500	Bed while beam is still in place		
							45.0500							44.9500			



							8.0500		6.9167	8.2667	Average of Top Flange (after release)	
							43.5500		43.9000	44.3500	Bottom Flange (pre-release)	
							45.2000			45.1000	Bed while beam is still in place (before release)	
							NA		42.7500	44.3500	Bottom Flange (after release)	
							45.1500			45.0500	Bed while beam is still in place (after release)	
Plant B	1/28/2012	1/30/2012	6:00AM	BTE 155			13.0000		12.8000	12.6500	West Side of top flange on raked surface (pre-release)	Disregard bed deflections due to difficulty with measurement location.
							12.6000		12.7500	12.6000	Middle of top flange on raked surface (pre-release)	
							12.8500		12.6500	12.6000	East end of top flange on raked surface (pre-release)	
							12.8167		12.7333	12.6167	Average of Top Flange (before release)	
									10.7000		West Side of top flange on raked surface (after release)	
									10.8500		Middle of top flange on raked surface	



[illegible]



									18.6000								East end of top flange on raked surface (pre-release)		
									18.5333								Average of Top Flange (before release)		
									16.3500								West Side of top flange on raked surface (after release)		
									16.4500								Middle of top flange on raked surface (after release)		
									16.5000								East end of top flange on raked surface (after release)		
									16.4333								Average of Top Flange (after release)		
									69.0000								Bottom Flange (pre-release)		
										70.8500							Bed while beam is still in place (before release)	70.5500	
									67.9500								Bottom Flange (after release)		
										70.6000							Bed while beam is still in place (after release)	70.8500	
Plant B	2/3/2012	2/6/2012	7:00AM	BTE 155					24.5000								North Side of top flange on raked surface (pre-release)		

[illegible]



Plant B	2/3/2012	2/6/2012	7:00AM	BTE 155						24.5500			North Side of top flange on raked surface (pre- release)	
										24.6000			Middle of top flange on raked surface (pre- release)	
										24.5000			South end of top flange on raked surface (pre- release)	
								0.0000		24.5500		0.0000	Average of Top Flange (before release)	
										23.2000			North Side of top flange on raked surface (after release)	
										23.1500			Middle of top flange on raked surface (after release)	
										23.0000			South end of top flange on raked surface (after release)	
								0.0000		23.1167		0.0000	Average of Top Flange (after release)	
										72.7000			Bottom Flange (pre-release)	
								76.4000				76.9500	Bed while beam is still in place (before release)	
										71.1500			Bottom Flange (after release)	
								76.5000				77.0500	Bed while beam is still in place (after release)	



						41.6500		41.6500		42.6000	Bottom Flange (after release)	
						43.9000				43.9500	Bed while beam is still in place (after release)	
						9.8500		9.2500	6.1500	4.3000	4.3500	North Side of top flange on raked surface (after lift)
						9.7500		9.2500	5.7500	4.0500	4.1500	Middle of top flange on raked surface (after lift)
						9.6000		8.9500	5.6500	3.9000	3.9500	South end of top flange on raked surface (after lift)
						9.7333		9.1500	5.8500	4.0833	4.1500	Average of Top Flange (after lift)
						44.5500			40.9500		39.1000	Bottom Flange (after lift)
Plant C	2/9/2012	2/10/2012	6:00AM	B 55		2.3000			2.1000		2.1500	North Side of top flange on raked surface (pre- release)
						2.2500			2.1000		2.1500	Middle of top flange on raked surface (pre- release)
						2.2500			2.0500		2.1000	South end of top flange on raked surface (pre- release)
						2.2667			2.0833		2.1333	Average of Top Flange (before release)
						2.3000			1.4000		2.1500	North Side of top flange on raked surface (after
												Overhang after lift of 24 in. on each side.

[illegible]

Plant C	2/9/2012	2/10/2012	6:00AM	B 55							North Side of top flange on raked surface (pre-release)	Overhang after lift of 24 in. on each side.
									2.2500	2.2500	2.2500	
										2.2500	2.3000	
									2.1500	2.1500		
									2.2000	2.1500	2.1500	
									2.2000	2.2167	2.2333	
									2.2500	1.5500	2.2500	
									2.1000	1.4500	2.1500	
									2.1000	1.3500	2.0500	
									2.1500	1.4500	2.1500	
									42.2500	42.5000	42.8000	
									44.1500		44.3500	
									42.2000	41.8000	42.7000	
									44.1500		44.3500	



[illegible]





								17.1000			11.9000			8.7500	Middle of top flange on raked surface (after lift)	
								17.0000			11.8500			8.8500	South end of top flange on raked surface (after lift)	
								17.0500			11.9167			8.8167	Average of Top Flange (after lift)	
								49.6500			44.2500			41.7500	Bottom Flange (after lift)	
Plant C	2/13/2012	2/14/2012	6:00AM	B 55	12.6500			12.7500			12.7500			12.7500	North Side of top flange on raked surface (pre-release)	Overhang after lift of 24 in. on each side.
					12.5500			12.7000						12.7500	Middle of top flange on raked surface (pre-release)	
															South end of top flange on raked surface (pre-release)	
					12.5500			12.6000			12.6000			12.7500		
					12.5833			12.6833						12.7500	Average of Top Flange (before release)	
															North Side of top flange on raked surface (after release)	
					12.4500						12.0000			12.8500	Middle of top flange on raked surface (after release)	
					12.3500						11.9000			12.7000	South end of top flange on raked surface (after release)	
					12.2500						11.8500			12.6500		

					12.3500				11.9167	12.7333	Average of Top Flange (after release)	
					43.1000				43.8000	43.5500	Bottom Flange (pre-release)	
					44.7500					44.5500	Bed while beam is still in place (before release)	
					42.9000				43.0000	43.5000	Bottom Flange (after release)	
					44.5500					44.5500	Bed while beam is still in place (after release)	
					15.8500				11.7500	9.0500	North Side of top flange on raked surface (after lift)	
					15.7500				11.6500	9.1000	Middle of top flange on raked surface (after lift)	
					15.7000				11.6000	9.0000	South end of top flange on raked surface (after lift)	
					15.7667				11.6667	9.0500	Average of Top Flange (after lift)	
					48.7500				44.5500	41.7000	Bottom Flange (after lift)	
Plant C	2/13/2012	2/14/2012	6:00AM	B 55	12.7000				12.8000	12.7000	North Side of top flange on raked surface (pre-release)	Overhang after lift of 24 in. on each side.
					12.7000				12.6000	12.7500	Middle of top flange on raked surface (pre-release)	

[illegible]

					15.2500				10.8000	8.4500	South end of top flange on raked surface (after lift)	
					15.2333				10.9667	8.5167	Average of Top Flange (after lift)	
					48.0000				43.7000	41.1500	Bottom Flange (after lift)	
Plant C	2/13/2012	2/14/2012	6:00AM	B 55	12.7500				12.8500	12.8500	North Side of top flange on raked surface (pre-release)	
					12.7000				12.7500	12.8500	Middle of top flange on raked surface (pre-release)	
					12.7000				12.6000	12.7000	South end of top flange on raked surface (pre-release)	
					12.7167				12.7333	12.8000	Average of Top Flange (before release)	
					12.7500				12.1000	12.8000	North Side of top flange on raked surface (after release)	
					12.6500				11.9500	12.7000	Middle of top flange on raked surface (after release)	
					12.5000				11.7000	12.4500	South end of top flange on raked surface (after release)	
					12.6333				11.9167	12.6500	Average of Top Flange (after release)	

					43.0000		42.6500		42.5000	Bottom Flange (pre-release)	
					44.5000				44.5500	Bed while beam is still in place (before release)	
					42.9000		41.8500		42.3000	Bottom Flange (after release)	
					44.4500				44.4500	Bed while beam is still in place (after release)	
					14.6000		10.1500		7.3000	North Side of top flange on raked surface (after lift)	
					14.4000		9.9500		7.1500	Middle of top flange on raked surface (after lift)	
					14.1500		9.8500		6.8500	South end of top flange on raked surface (after lift)	
					14.3833		9.9833		7.1000	Average of Top Flange (after lift)	
					47.1000		42.6500		39.8000	Bottom Flange (after lift)	
Plant A	2/23/2012	2/25/2012	9:00AM	BTC 120	14.6500		13.9000		14.1000	North Side of top flange on raked surface (pre- release)	
					14.7000		14.0000		13.9500	Middle of top flange on raked surface (pre- release)	
					14.7000		14.0000		13.7500	South end of top flange on raked surface (pre- release)	



									13.8000				13.3000	South end of top flange on raked surface (pre-release)	
									13.7000				13.2500	Average of Top Flange (before release)	
									11.3500				13.3500	North Side of top flange on raked surface (after release)	
									11.4500				13.2000	Middle of top flange on raked surface (after release)	
									11.4000				13.2000	South end of top flange on raked surface (after release)	
									11.4000				13.2500	Average of Top Flange (after release)	
									PLATE					Bottom Flange (pre-release)	
									51.4500				51.4500	Bed while beam is still in place (before release)	
									PLATE					Bottom Flange (after release)	
									51.4500				51.5000	Bed while beam is still in place (after release)	
Plant A	2/24/2012	2/25/2012	9:00AM	BTC 120	13.7000				13.2500				13.3500	North Side of top flange on raked surface (pre-release)	





Plant B	2/25/2012	2/27/2012	8:00AM	BTB 95	7.4000		7.4500		7.5500	North Side of top flange on raked surface (pre-release)	Overhang after lift of 24 in. on each side.
					7.1000		7.2500		7.4500	Middle of top flange on raked surface (pre-release)	
					7.0000		7.3500		7.1500	South end of top flange on raked surface (pre-release)	
					7.1667		7.3500		7.3833	Average of Top Flange (before release)	
					7.4000		5.4500		7.6500	North Side of top flange on raked surface (after release)	
					7.2500		5.2500		7.5500	Middle of top flange on raked surface (after release)	
					7.0500		5.3000		7.2000	South end of top flange on raked surface (after release)	
					7.2333		5.3333		7.4667	Average of Top Flange (after release)	
										Bottom Flange (pre-release)	
					42.9500		42.9500		43.0000	Bed while beam is still in place (before release)	
										Bottom Flange (after release)	
					42.9500		42.9500		43.0500	Bed while beam is still in place (after release)	





					24.7000				24.9000		25.2500	South end of top flange on raked surface (pre-release)	
					24.8333				25.0000		25.3000	Average of Top Flange (before release)	
					24.8500				23.8000		25.3500	North Side of top flange on raked surface (after release)	
					25.0500				23.9500		25.2500	Middle of top flange on raked surface (after release)	
					24.2500				23.7000		25.3000	South end of top flange on raked surface (after release)	
					24.7167				23.8167		25.3000	Average of Top Flange (after release)	
												Bottom Flange (pre-release)	
					77.0000						77.4000	Bed while beam is still in place (before release)	
												Bottom Flange (after release)	
					76.9500						77.3500	Bed while beam is still in place (after release)	
					13.6000				12.1000		13.9500	North Side of top flange on raked surface (after lift)	
					13.7000				12.2000		13.9000	Middle of top flange on raked surface (after lift)	

					13.6000			12.1500		14.0000	South end of top flange on raked surface (after lift)	
					13.6333			12.1500		13.9500	Average of Top Flange (after lift)	
Plant B	3/7/2012	3/8/2012	7:45AM	BTE-110	24.9000			24.5000		24.7500	North Side of top flange on troweled surface (pre-release)	Overhang after lift of 12 in. on each side.
					24.9500			24.5500		24.7000	Middle of top flange on raked surface (pre-release)	
					24.7500			24.4500		24.5000	South end of top flange on raked surface (pre-release)	
					24.8667			24.5000		24.6500	Average of Top Flange (before release)	
					24.9500			23.6500		24.7500	North Side of top flange on raked surface (after release)	
					25.1000			23.6500		24.6500	Middle of top flange on raked surface (after release)	
					24.8000			23.7000		24.5000	South end of top flange on raked surface (after release)	
					24.9500			23.6667		24.6333	Average of Top Flange (after release)	
											Bottom Flange (pre-release)	



[illegible]

Plant B	3/13/2012	3/14/2012	7:30AM	BTE 110							North Side of top flange on raked surface (pre- release)-Troweled	Overhang after lift of 24 in. on each side.
					24.4000			24.6000	25.0000		Middle of top flange on raked surface (pre- release)	
					24.2500			24.6000	24.8000		South end of top flange on raked surface (pre- release)	
					24.4000			24.6500	24.8500		Average of Top Flange (before release)	
					24.3500			24.6167	24.8833		North Side of top flange on raked surface (after release)	
					24.4500			23.4500	24.9500		Middle of top flange on raked surface (after release)	
					24.2500			23.4500	24.9000		South end of top flange on raked surface (after release)	
					24.4500			23.4500	25.0000		Average of Top Flange (after release)	
					24.3833			23.4500	24.9500		Bottom Flange (pre-release)	
					76.4000				76.9500		Bed while beam is still in place (before release)	
											Bottom Flange (after release)	
					76.4000				76.8500		Bed while beam is still in place (after	



[illegible]

										24.1000			23.0500			24.2000	South end of top flange on raked surface (after release)	
										24.3167			23.0167			24.3000	Average of Top Flange (after release)	
																	Bottom Flange (pre-release)	
										76.3500						76.4000	Bed while beam is still in place (before release)	
																	Bottom Flange (after release)	
										76.4000						76.4500	Bed while beam is still in place (after release)	
										11.9500			10.4000			12.5500	North Side of top flange on raked surface (after lift)	
										11.8000			10.6500			12.6500	Middle of top flange on raked surface (after lift)	
										11.7500			10.6500			12.7000	South end of top flange on raked surface (after lift)	
										11.8333			10.5667			12.6333	Average of Top Flange (after lift)	
Plant B	3/13/2012	3/14/2012	7:30AM	BTE 110						24.6500			24.3500			24.1500	North Side of top flange on raked surface (pre-release)-Troweled	Overhang after lift of 24 in. on each side.
										24.6500			24.2500			24.1500	Middle of top flange on raked surface (pre-release)	

					24.5000				24.1000		23.9500	South end of top flange on raked surface (pre-release)	
					24.6000				24.2333		24.0833	Average of Top Flange (before release)	
					24.6500				23.3500		24.2000	North Side of top flange on raked surface (after release)	
					24.6500				23.2500		24.1000	Middle of top flange on raked surface (after release)	
					24.5500				23.2000		23.9500	South end of top flange on raked surface (after release)	
					24.6167				23.2667		24.0833	Average of Top Flange (after release)	
												Bottom Flange (pre-release)	
					76.6500						76.3500	Bed while beam is still in place (before release)	
												Bottom Flange (after release)	
					76.7000						76.4000	Bed while beam is still in place (after release)	
									5.3500		6.0000	North Side of top flange on raked surface (after lift)	
					7.6500				5.1500		5.6500	Middle of top flange on raked surface (after lift)	

					7.5000				5.0000		5.3500	South end of top flange on raked surface (after lift)	
					7.5750				5.1667		5.6667	Average of Top Flange (after lift)	
Plant B	3/22/2012	3/23/2012	7:00AM	BTE 110	22.1500				22.3000		22.6000	North Side of top flange on raked surface (pre-release)	Overhang after lift of 12 in. on each side.
					22.1000				22.3000		22.5500	Middle of top flange on raked surface (pre-release)	
					22.2000				22.4000		22.6000	South end of top flange on raked surface (pre-release)	
					22.1500				22.3333		22.5833	Average of Top Flange (before release)	
					22.1500				21.5000		22.5500	North Side of top flange on raked surface (after release)	
					22.1500				21.8500		22.5500	Middle of top flange on raked surface (after release)	
					22.2500				21.6000		22.7000	South end of top flange on raked surface (after release)	
					22.1833				21.6500		22.6000	Average of Top Flange (after release)	
												Bottom Flange (pre-release)	





										surface (pre-release)		each side.
										Middle of top flange on raked surface (pre-release)	22.0000	
										South end of top flange on raked surface (pre-release)	21.9500	
										Average of Top Flange (before release)	22.0000	
										North Side of top flange on raked surface (after release)	22.2000	
										Middle of top flange on raked surface (after release)	22.1500	
										South end of top flange on raked surface (after release)	21.9500	
										Average of Top Flange (after release)	22.1000	
										Bottom Flange (pre-release)		
										Bed while beam is still in place (before release)	74.2500	
										Bottom Flange (after release)		
										Bed while beam is still in place (after release)	74.2500	

							15.5000			13.3000			13.3500	North Side of top flange on raked surface (after lift)	
							15.3500			13.1000			13.3000	Middle of top flange on raked surface (after lift)	
							15.1500			13.0500			13.2500	South end of top flange on raked surface (after lift)	
							15.3333			13.1500			13.3000	Average of Top Flange (after lift)	
Plant A		3/28/2012	4/2/2012	8:00AM	BTB 100		29.4500			29.4500			29.8000	North Side of top flange on raked surface (pre-release)	
							29.5500			29.3500			29.7500	Middle of top flange on raked surface (pre-release)	
										29.3500			29.9500	South end of top flange on raked surface (pre-release)-troweled	
							29.4500			29.3833			29.8333	Average of Top Flange (before release)	
							29.5500			27.4000			29.8500	North Side of top flange on raked surface (after release)	
							29.5500			27.3000			29.7500	Middle of top flange on raked surface (after release)	
							29.4500			27.1500			30.0000	South end of top flange on raked surface (after release)	





										surface (pre-release)-troweled		
										Average of Top Flange (before release)	29.4833	
										North Side of top flange on raked surface (after release)	29.4500	
										Middle of top flange on raked surface (after release)	29.6000	
										South end of top flange on raked surface (after release)	29.4500	
										Average of Top Flange (after release)	29.5000	
										Bottom Flange (pre-release)		
										Bed while beam is still in place (before release)	59.5500	
										Bottom Flange (after release)		
										Bed while beam is still in place (after release)	59.6000	
										North Side of top flange on raked surface (after lift)	29.5000	
										Middle of top flange on raked surface (after lift)	29.5500	
										South end of top flange on raked surface (after lift)	29.5500	

					29.3667		27.2000		29.5333	Average of Top Flange (after lift)	
Plant A	3/30/2012	4/2/2012	8:00AM	BTB 100	29.3500		29.2500		29.1500	North Side of top flange on raked surface (pre-release)	
					29.2500		29.4500		29.3500	Middle of top flange on raked surface (pre-release)	
					29.3500		29.6000		29.4000	South end of top flange on raked surface (pre-release)-troweled	
					29.3167		29.4333		29.3000	Average of Top Flange (before release)	
					29.5000		27.1500		29.2000	North Side of top flange on raked surface (after release)	
					29.3500		27.3000		29.4000	Middle of top flange on raked surface (after release)	
					29.3500		27.5500		29.3500	South end of top flange on raked surface (after release)	
					29.4000		27.3333		29.3167	Average of Top Flange (after release)	
										Bottom Flange (pre-release)	
					59.4500				59.6000	Bed while beam is still in place (before release)	

[illegible]

						29.4000			26.9000		29.2500	Middle of top flange on raked surface (after release)	
						29.5000			26.9500		29.2500	South end of top flange on raked surface (after release)	
						29.4000			26.9333		29.2667	Average of Top Flange (after release)	
												Bottom Flange (pre-release)	
						59.3000					59.5000	Bed while beam is still in place (before release)	
												Bottom Flange (after release)	
						59.4000					59.6500	Bed while beam is still in place (after release)	
						29.3500			26.8500		29.2000	North Side of top flange on raked surface (after lift)	
						29.3500			26.8000		29.2500	Middle of top flange on raked surface (after lift)	
						29.2500			26.8000		29.1000	South end of top flange on raked surface (after lift)	
						29.3167			26.8167		29.1833	Average of Top Flange (after lift)	
Plant C	4/11/2012	4/13/2012	7:00AM	C 80	10.5500				10.4500		10.5000	North Side of top flange on raked surface (pre-release)	Overhang after lift of 34 in. on each side.

					10.4500		10.4500		10.4500		10.5500	Middle of top flange on raked surface (pre-release)	
					10.4000				10.3500		10.5000	South end of top flange on raked surface (pre-release)	
					10.4667				10.4167		10.5167	Average of Top Flange (before release)	
					10.6000				9.5000		10.5500	North Side of top flange on raked surface (after release)	
					10.5000				9.4500		10.5500	Middle of top flange on raked surface (after release)	
					10.4500				9.4000		10.5000	South end of top flange on raked surface (after release)	
					10.5167				9.4500		10.5333	Average of Top Flange (after release)	
												Bottom Flange (pre-release)	
					47.6000						47.8500	Bed while beam is still in place (before release)	
												Bottom Flange (after release)	
					47.6000						47.8500	Bed while beam is still in place (after release)	
					14.4000			14.60	18.4000	24.50	25.0500	North Side of top flange on raked surface (after lift)	

						14.3000	14.60	18.4000	24.45	25.0500	Middle of top flange on raked surface (after lift)	
						14.4000	14.550	18.2500	24.35	24.9500	South end of top flange on raked surface (after lift)	
						14.3667	14.5833	18.3500	24.433	25.0167	Average of Top Flange (after lift)	
Plant C	4/11/2012	4/13/2012	7:00AM	C 80		10.4000		10.3000		10.4500	North Side of top flange on raked surface (pre-release)	Overhang after lift of 36 in. on each side.
						10.3500		10.3000		10.4000	Middle of top flange on raked surface (pre-release)	
						10.3000		10.2500		10.4000	South end of top flange on raked surface (pre-release)	
						10.3500		10.2833		10.4167	Average of Top Flange (before release)	
						10.4500		9.3500		10.4500	North Side of top flange on raked surface (after release)	
						10.4000		9.2500		10.4000	Middle of top flange on raked surface (after release)	
						10.3500		9.1500		10.3500	South end of top flange on raked surface (after release)	
						10.4000		9.2500		10.4000	Average of Top Flange (after release)	





					10.2667					10.2167		10.2833	Average of Top Flange (before release)	
					10.3500					9.2500		10.3500	North Side of top flange on raked surface (after release)	
					10.2000					9.3000		10.2500	Middle of top flange on raked surface (after release)	
					10.2500					9.5000		10.2000	South end of top flange on raked surface (after release)	
					10.2667					9.3500		10.2667	Average of Top Flange (after release)	
													Bottom Flange (pre-release)	
					47.2500							47.4500	Bed while beam is still in place (before release)	
													Bottom Flange (after release)	
					47.2500							47.4500	Bed while beam is still in place (after release)	
					15.6000				15.65	19.2500	25.10	25.7500	North Side of top flange on raked surface (after lift)	
					15.5500				15.60	19.1000	24.95	25.6000	Middle of top flange on raked surface (after lift)	
					15.4000				15.50	18.9500	24.80	25.5000	South end of top flange on raked surface (after lift)	
					15.5167				15.583	19.1000	24.95	25.6167	Average of Top Flange (after lift)	





					20.5500			19.9000	20.2500	Middle of top flange on raked surface (after release)	
					20.7500			20.0000	20.2500	South end of top flange on raked surface (after release)	
					20.6667			19.9667	20.1833	Average of Top Flange (after release)	
										Bottom Flange (pre-release)	
					72.8000				72.6500	Bed while beam is still in place (before release)	
										Bottom Flange (after release)	
					72.8000				72.5500	Bed while beam is still in place (after release)	
					13.2500			12.2000	12.4500	North Side of top flange on raked surface (after lift)	
					13.0500			12.1000	12.4500	Middle of top flange on raked surface (after lift)	
					13.4000			12.1500	12.4000	South end of top flange on raked surface (after lift)	
					13.2333			12.1500	12.4333	Average of Top Flange (after lift)	
Plant B	4/16/2012	4/17/2012	7:30AM	BTE 90	20.3000			20.4500	20.5500	North Side of top flange on raked surface (pre-release) troweled	Overhang after lift of 12 in. on each side.

					20.2500				20.3000		20.1500	Middle of top flange on raked surface (pre-release)	
					20.3500				20.5500		20.3000	South end of top flange on raked surface (pre-release)	
					20.3000				20.4333		20.3333	Average of Top Flange (before release)	
					20.3500				19.9500		20.6500	North Side of top flange on raked surface (after release)	
					20.3500				19.8500		20.2000	Middle of top flange on raked surface (after release)	
					20.4000				19.9500		20.3500	South end of top flange on raked surface (after release)	
					20.3667				19.9167		20.4000	Average of Top Flange (after release)	
												Bottom Flange (pre-release)	
					72.5000						72.6500	Bed while beam is still in place (before release)	
												Bottom Flange (after release)	
					72.5000						72.6500	Bed while beam is still in place (after release)	
					13.2000				12.0500		12.2500	North Side of top flange on raked surface (after lift)	

					13.1500				12.0000		11.8500	Middle of top flange on raked surface (after lift)	
					13.1500				12.0500		12.1000	South end of top flange on raked surface (after lift)	
					13.1667				12.0333		12.0667	Average of Top Flange (after lift)	
Plant B	4/16/2012	4/17/2012	7:30AM	BTE 90	20.4500				20.6000		20.6500	North Side of top flange on raked surface (pre-release) troweled	Overhang after lift of 18 in. on each side.
					20.4500				20.3500		20.6000	Middle of top flange on raked surface (pre-release)	
					20.4000				20.5000		20.6000	South end of top flange on raked surface (pre-release)	
					20.4333				20.4833		20.6167	Average of Top Flange (before release)	
					20.5500				20.2500		20.7000	North Side of top flange on raked surface (after release)	
					20.4500				19.8500		20.5000	Middle of top flange on raked surface (after release)	
					20.4500				19.9000		20.6000	South end of top flange on raked surface (after release)	
					20.4833				20.0000		20.6000	Average of Top Flange (after release)	



					0.0000		23.5167		0.0000	Average of Top Flange (before release)	
					24.1000		22.8000		24.3500	North Side of top flange on raked surface (after release)	
					23.9500		22.7000		24.1500	Middle of top flange on raked surface (after release)	
					23.9500		22.7500		24.1000	South end of top flange on raked surface (after release)	
					24.0000		22.7500		24.2000	Average of Top Flange (after release)	
										Bottom Flange (pre-release)	
					61.4000				61.6000	Bed while beam is still in place (before release)	
										Bottom Flange (after release)	
					61.4000				61.7500	Bed while beam is still in place (after release)	
					12.3000		10.6500		12.1500	North Side of top flange on raked surface (after lift)	
					12.1500		10.6000		11.9500	Middle of top flange on raked surface (after lift)	
					12.1000		10.6500		11.7500	South end of top flange on raked surface (after lift)	
					12.1833		10.6333		11.9500	Average of Top Flange (after lift)	





					61.4500					61.1500	Bed while beam is still in place (after release)	
					12.0000				11.1000	11.8000	North Side of top flange on raked surface (after lift)	
					12.0500				10.9500	11.9000	Middle of top flange on raked surface (after lift)	
					12.2500				10.9000	12.0000	South end of top flange on raked surface (after lift)	
					12.1000				10.9833	11.9000	Average of Top Flange (after lift)	
Plant A	5/9/2012	5/10/2012	9:00AM	C 80					23.6500		North Side of top flange on raked surface (pre-release)	
									23.6000		Middle of top flange on raked surface (pre-release)	
									23.5500		South end of top flange on raked surface (pre-release)	
					0.0000				23.6000	0.0000	Average of Top Flange (before release)	
					23.5500				22.8500	23.7000	North Side of top flange on raked surface (after release)	
					23.5500				22.7500	23.6500	Middle of top flange on raked surface (after release)	

						23.7000	22.7500	23.4500	South end of top flange on raked surface (after release)	
						23.6000	22.7833	23.6000	Average of Top Flange (after release)	
									Bottom Flange (pre-release)	
						61.1500		61.3500	Bed while beam is still in place (before release)	
									Bottom Flange (after release)	
						61.1000		61.4500	Bed while beam is still in place (after release)	
						11.5000	10.7000	11.6000	North Side of top flange on raked surface (after lift)	
						11.6000	10.6500	11.6000	Middle of top flange on raked surface (after lift)	
						11.8500	10.6500	11.6000	South end of top flange on raked surface (after lift)	
						11.6500	10.6667	11.6000	Average of Top Flange (after lift)	
Plant A	5/31/2012	6/4/2012	8:00AM	SBT D 135		14.6000	14.1500	13.9000	North Side of top flange on raked surface (pre-release)	Disregard bed deflections due to difficulty with measurement location.
						14.7500	14.0500	13.7500	Middle of top flange on raked	



					14.8500		11.3500	13.8000	Middle of top flange on raked surface (after lift)	
					14.7500		10.9500	13.8500	South end of top flange on raked surface (after lift)	
					14.7500		11.2333	13.8833	Average of Top Flange (after lift)	
Plant A	6/1/2012	6/4/2012	8:00AM	SBT D 135	13.9500		14.0000	13.5500	North Side of top flange on raked surface (pre-release)	Disregard bed deflections due to difficulty with measurement location.
					14.0500		13.8500	13.8500	Middle of top flange on raked surface (pre-release)	
					13.8500		13.6500	13.6000	South end of top flange on raked surface (pre-release)	
					13.9500		13.8333	13.6667	Average of Top Flange (before release)	
					13.9500		11.3000	13.6000	North Side of top flange on raked surface (after release)	
					14.1500		11.2500	14.0000	Middle of top flange on raked surface (after release)	
					13.8000		11.0500	13.7500	South end of top flange on raked surface (after release)	

					13.9667				11.2000	13.7833	Average of Top Flange (after release)	
											Bottom Flange (pre-release)	
					59.5500					59.5500	Bed while beam is still in place (before release)	
											Bottom Flange (after release)	
					NA					NA	Bed while beam is still in place (after release)	
					14.0000				11.0500	13.5000	North Side of top flange on raked surface (after lift)	
					14.1000				10.9500	13.8000	Middle of top flange on raked surface (after lift)	
					13.9500				10.9000	13.7000	South end of top flange on raked surface (after lift)	
					14.0167				10.9667	13.6667	Average of Top Flange (after lift)	
Plant A	6/1/2012	6/4/2012	8:00AM	SBT D 135	14.1500				13.5000	13.7000	North Side of top flange on raked surface (pre-release)	Disregard bed deflections due to difficulty with measurement location.
					14.3500				13.6500	13.6500	Middle of top flange on raked surface (pre-release)	
					14.2500				13.8000	13.8000	South end of top flange on raked	



					14.2167				11.1167	13.5833	Average of Top Flange (after lift)	
Plant B	6/26/2012	6/27/2012	7:00AM	BTE 145	12.9500				13.4000	13.6500	North Side of top flange on raked surface (pre-release)	Overhang after lift of 24 in. on each side.
					12.9000				13.2000	13.3000	Middle of top flange on raked surface (pre-release)	
					13.1000				13.3000	13.9000	Troweled South end of top flange on raked surface (pre-release)	
					12.9833				13.3000	13.6167	Average of Top Flange (before release)	
					13.0500				11.1000	13.6500	North Side of top flange on raked surface (after release)	
					12.9000				10.9000	13.5000	Middle of top flange on raked surface (after release)	
					13.0500				11.0500	13.9500	South end of top flange on raked surface (after release)	
					13.0000				11.0167	13.7000	Average of Top Flange (after release)	
											Bottom Flange (pre-release)	
					65.0500					65.8000	Bed while beam is still in place	





[illegible]

										surface (pre-release)	each side.
										Middle of top flange on raked surface (pre-release)	
				20.9000				20.3500		20.6500	
										South end of top flange on raked surface (pre-release)	
				21.0500				20.3500		20.6000	
										Average of Top Flange (before release)	
				20.9667				20.3833		20.6667	
										North Side of top flange on raked surface (after release)	
				21.0000				18.3000		20.6000	
										Middle of top flange on raked surface (after release)	
				20.9000				18.1500		20.6000	
										South end of top flange on raked surface (after release)	
				21.0500				18.1500		20.7000	
										Average of Top Flange (after release)	
				20.9833				18.2000		20.6333	
										Bottom Flange (pre-release)	
										Bed while beam is still in place (before release)	
				73.0000						72.8500	
										Bottom Flange (after release)	
										Bed while beam is still in place (after release)	
				73.0000						72.8500	

					32.4500				27.9500	31.1000	North Side of top flange on raked surface (after lift)	
					32.2500				27.6500	30.9500	Middle of top flange on raked surface (after lift)	
					32.3000				27.6500	30.8500	South end of top flange on raked surface (after lift)	
					32.3333				27.7500	30.9667	Average of Top Flange (after lift)	
Plant B	6/28/2012	6/29/2012	7:00AM	BTE 145	21.6000				21.4500	20.9500	North Side of top flange on raked surface (pre-release)	Disregard bed deflections due to difficulty with measurement location.
					21.4000				21.2500	20.9500	Middle of top flange on raked surface (pre-release)	Overhang after lift of 48 in. on each side.
					21.7500				21.1500	21.0000	South end of top flange on raked surface (pre-release)	
					21.5833				21.2833	20.9667	Average of Top Flange (before release)	
					21.6500				19.1500	20.9500	North Side of top flange on raked surface (after release)	
					21.5000				18.9500	20.9500	Middle of top flange on raked surface (after release)	

										21.8500				18.8500				20.9000	South end of top flange on raked surface (after release)	
										21.6667				18.9833				20.9333	Average of Top Flange (after release)	
																			Bottom Flange (pre-release)	
										73.6000								73.0000	Bed while beam is still in place (before release)	
																			Bottom Flange (after release)	
										73.7000									Bed while beam is still in place (after release)	
										30.4000								32.3000	North Side of top flange on raked surface (after lift)	
										30.2500								32.0000	Middle of top flange on raked surface (after lift)	
										30.1000								32.2500	South end of top flange on raked surface (after lift)	
										30.2500								32.1833	Average of Top Flange (after lift)	
Plant C	7/3/2012	7/5/2012	7:00AM	BTD 135						10.3500				10.2000				10.2500	North Side of top flange on raked surface (pre-release)	Overhang after lift of 34 in. and 19.5 in.
										10.3500				10.2000				10.3000	Middle of top flange on raked surface (pre-release)	

					10.3000		10.3000		10.3000	South end of top flange on raked surface (pre-release)	
					10.3333		10.2333		10.2833	Average of Top Flange (before release)	
					10.3500		7.6000		10.3000	North Side of top flange on raked surface (after release)	
					10.4000		7.6000		10.4000	Middle of top flange on raked surface (after release)	
					10.4000		7.6000		10.2500	South end of top flange on raked surface (after release)	
					10.3833		7.6000		10.3167	Average of Top Flange (after release)	
										Bottom Flange (pre-release)	
					55.1000				54.9000	Bed while beam is still in place (before release)	
										Bottom Flange (after release)	
					55.1000				55.0000	Bed while beam is still in place (after release)	
					11.6000		7.1500	9.55	9.8000	North Side of top flange on raked surface (after lift)	
					11.7000		7.3000	9.65	10.0000	Middle of top flange on raked surface (after lift)	

								11.8500	11.55	7.4500	9.85	10.0500	South end of top flange on raked surface (after lift)	
								11.7167	11.3833	7.3000	9.6833	9.9500	Average of Top Flange (after lift)	
Plant C	7/3/2012	7/5/2012	7:00AM	BTD 135				10.3500		10.3500		10.4000	North Side of top flange on raked surface (pre-release)	Overhang after lift of 27 in. and 30.5 in.
								10.4500		10.3500		10.3500	Middle of top flange on raked surface (pre-release)	
								10.3500		10.3000		10.3500	South end of top flange on raked surface (pre-release)	
								10.3833		10.3333		10.3667	Average of Top Flange (before release)	
								10.4500		7.7500		10.4500	North Side of top flange on raked surface (after release)	
								10.5000		7.7500		10.3500	Middle of top flange on raked surface (after release)	
								10.3500		7.7000		10.4500	South end of top flange on raked surface (after release)	
								10.4333		7.7333		10.4167	Average of Top Flange (after release)	
													Bottom Flange (pre-release)	









						11.3500	10.60	14.8000	25.65	26.5500	North Side of top flange on raked surface (after lift)	
						11.1000	11.05	15.0500	25.75	26.8000	Middle of top flange on raked surface (after lift)	
						10.6500	11.35	15.4500	26.15	27.1000	South end of top flange on raked surface (after lift)	
						11.0333	11.00	15.1000	25.85	26.8167	Average of Top Flange (after lift)	
Plant C	7/16/2012	7/18/2012	7:00AM	BTD 135		12.0500		11.8500		11.8000	North Side of top flange on raked surface (pre-release)	Overhang after lift of 0 in. and 13 in.
						12.0000		11.7500		11.8500	Middle of top flange on raked surface (pre-release)	
						11.9500		11.7500		11.8500	South end of top flange on raked surface (pre-release)	
						12.0000		11.7833		11.8333	Average of Top Flange (before release)	
						12.0000		9.0000		11.8500	North Side of top flange on raked surface (after release)	
						12.0000		9.0000		11.9000	Middle of top flange on raked surface (after release)	
						11.9500		9.1000		11.9500	South end of top flange on raked surface (after release)	





						12.3167			6.8333	8.80	8.9667	Average of Top Flange (after lift)	
Plant C	7/18/2012	7/19/2012	7:00AM	BTD 135		10.8500			10.6500		10.8000	North Side of top flange on raked surface (pre-release)	Overhang after lift of 0 in. and 16 in.
						10.8000			10.6000		10.9000	Middle of top flange on raked surface (pre-release)	
												South end of top flange on raked surface (pre-release)	
						10.7500			10.6000		10.9500	Average of Top Flange (before release)	
						10.8000			10.6167		10.8833	North Side of top flange on raked surface (after release)	
						10.8000			7.5500		10.8500	Middle of top flange on raked surface (after release)	
									7.5000		10.9000	South end of top flange on raked surface (after release)	
						10.8000			7.4500		10.9000	Average of Top Flange (after release)	
									7.5000		10.8833	Bottom Flange (pre-release)	
						55.5000					55.3000	Bed while beam is still in place (before release)	







					21.5500			21.8000		21.5000									Middle of top flange on raked surface (pre-release)	21.5000			
					21.6000			21.9000		21.6000									South end of top flange on raked surface (pre-release)	22.2500			
					21.5833			21.8167		21.5833									Average of Top Flange (before release)	21.9333			
					21.6000			20.0000		21.6000									North Side of top flange on raked surface (after release)	22.1000			
					21.5500			20.0500		21.5500									Middle of top flange on raked surface (after release)	21.9500			
					21.6500			20.2000		21.6500									South end of top flange on raked surface (after release)	22.3000			
					21.6000			20.0833		21.6000									Average of Top Flange (after release)	22.1167			
																			Bottom Flange (pre-release)				
					73.6500														Bed while beam is still in place (before release)	74.3000			
																			Bottom Flange (after release)				
					na														Bed while beam is still in place (after release)	74.3000			
					32.0500			30.3000		32.0500									North Side of top flange on raked surface (after lift)	33.8000			

						32.0000			30.1000		33.5500	Middle of top flange on raked surface (after lift)	
						32.0000			30.2500		33.8500	South end of top flange on raked surface (after lift)	
						32.0167			30.2167		33.7333	Average of Top Flange (after lift)	
Plant B	7/24/2012	7/25/2012	6:00AM	BTE 145		21.6500			21.2000		21.3500	North Side of top flange on raked surface (pre-release)	Overhang after lift of 12 in. on each side.
						21.7000			21.1000		21.4000	Middle of top flange on raked surface (pre-release)	
						21.5500			21.1500		21.6500	South end of top flange on raked surface (pre-release)	
						21.6333			21.1500		21.4667	Average of Top Flange (before release)	
						21.7500			19.6000		21.4000	North Side of top flange on raked surface (after release)	
						21.8000			19.5000		21.4500	Middle of top flange on raked surface (after release)	
						21.6500			19.5000		21.7500	South end of top flange on raked surface (after release)	
						21.7333			19.5333		21.5333	Average of Top Flange (after release)	

[illegible]

## APPENDIX B. STRING POTENTIOMETER DATA

String potentiometers were instrumented along the length of the beam and also on the precasting bed. Using these devices to record the Time vs. Displacement allowed researchers to investigate the behavior of PPCBs during the transfer of prestress and verify laser level measurements. Additionally, recording the time when significant events allowed researchers to justify vertical displacement by what was happening at specific times of the release.

Inaccuracies with string potentiometers occurred in some instances due to instrument failure and disruption by workers. In these cases, figures are labeled if data is inaccurate. Listed below are the abbreviations for specific events and the graphs that correspond to the transfer of prestress on multiple PPCBs.

where:   TSRB=top strands, release began  
          TSRC=top strands, release completed  
          VHRB=vertical hold-down, release began  
          VHRC=vertical hold-down, release complete  
          HSRB=harped strands, release began  
          HSRC=harped strands, release completed  
          BSRB=bottom strands, release began  
          BSRC=bottom strands, release completed  
          LB=lifted beam

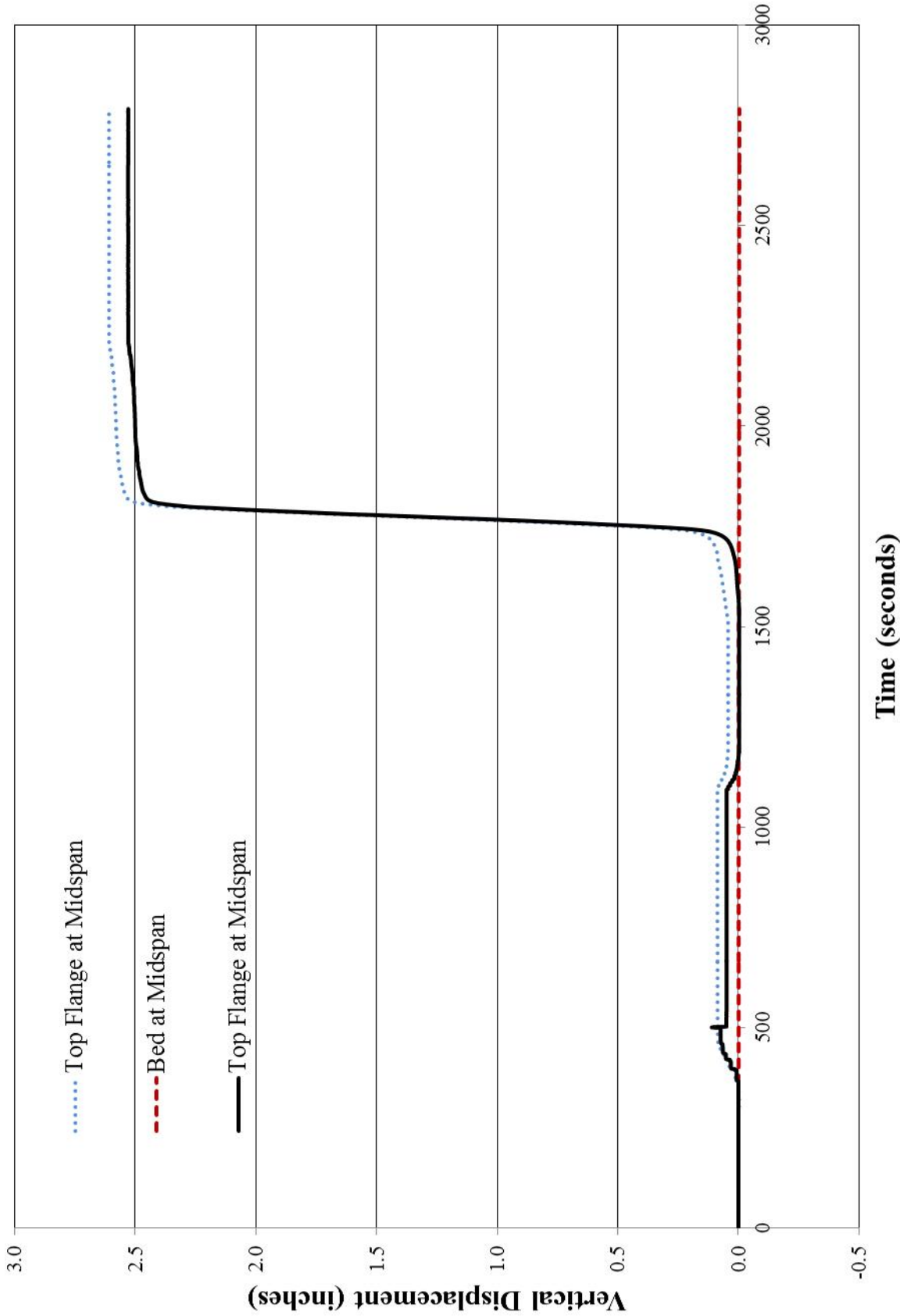


Figure B-1: Time vs. Vertical Displacement for BTE 155

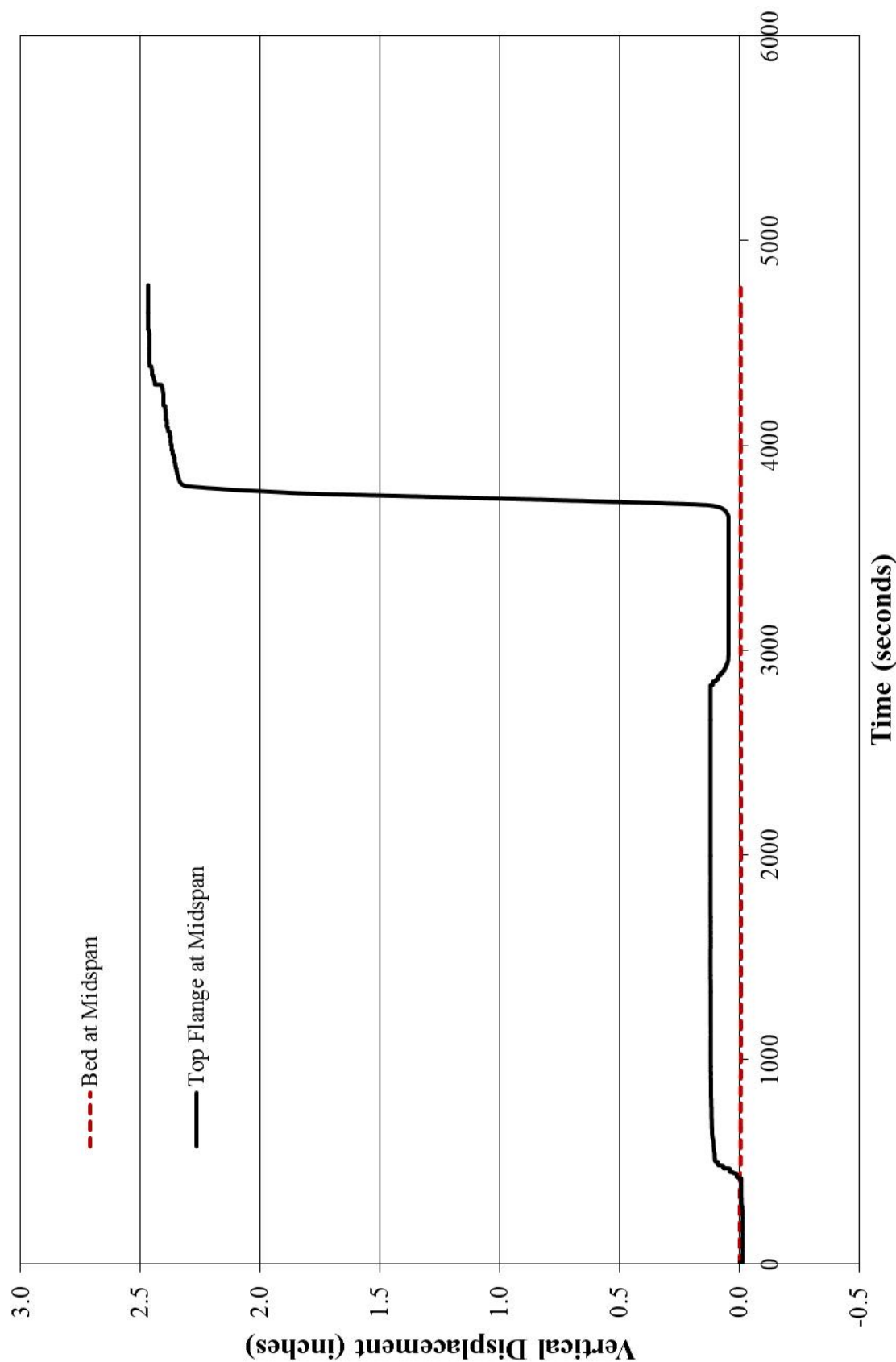


Figure B-2: Time vs. Vertical Displacement of a BTE 155

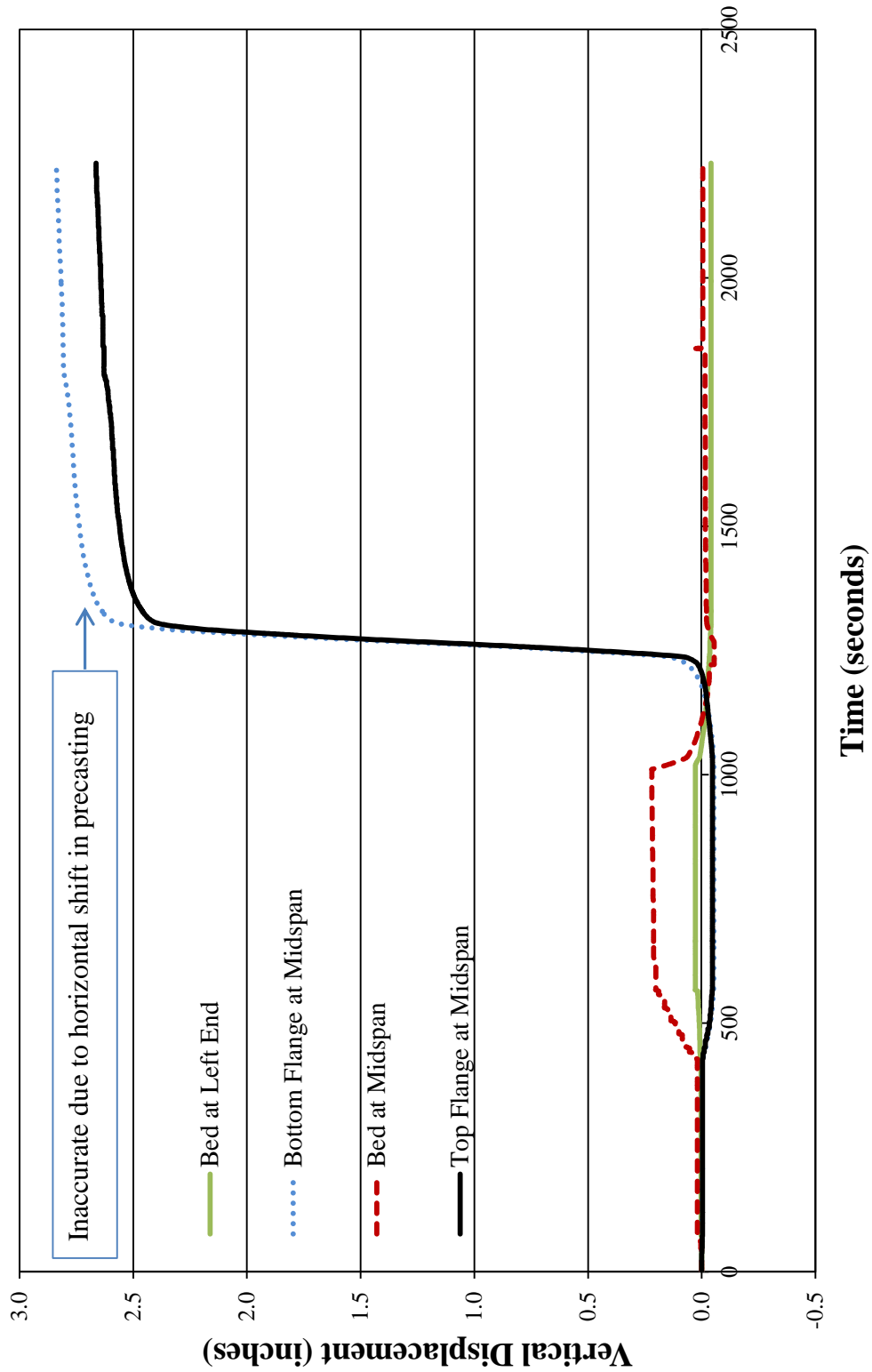


Figure B-3: Time vs. Vertical Displacement for a BTE 155 PPCB

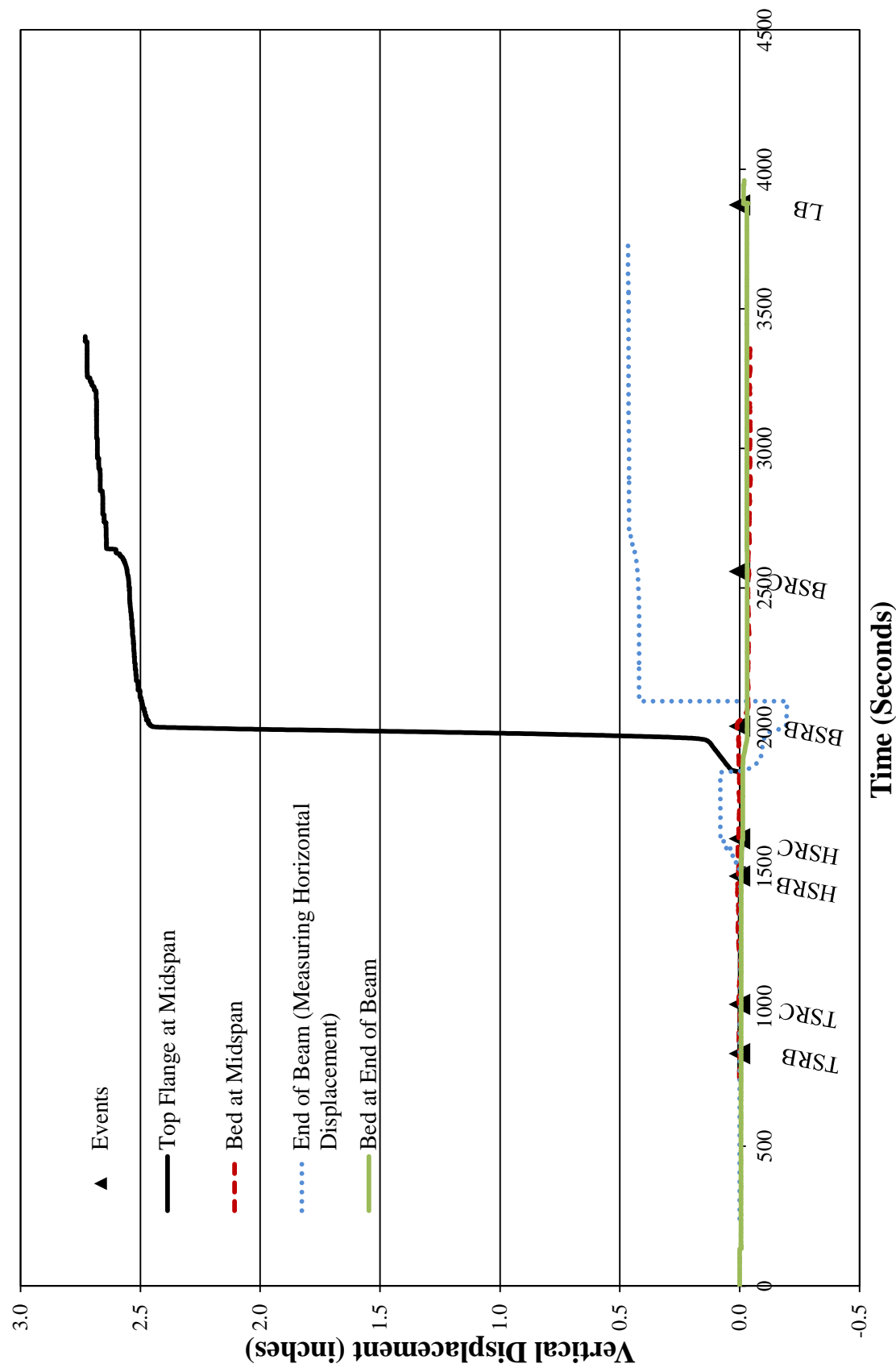


Figure B-4: Time vs. Vertical Displacement for BTE 145



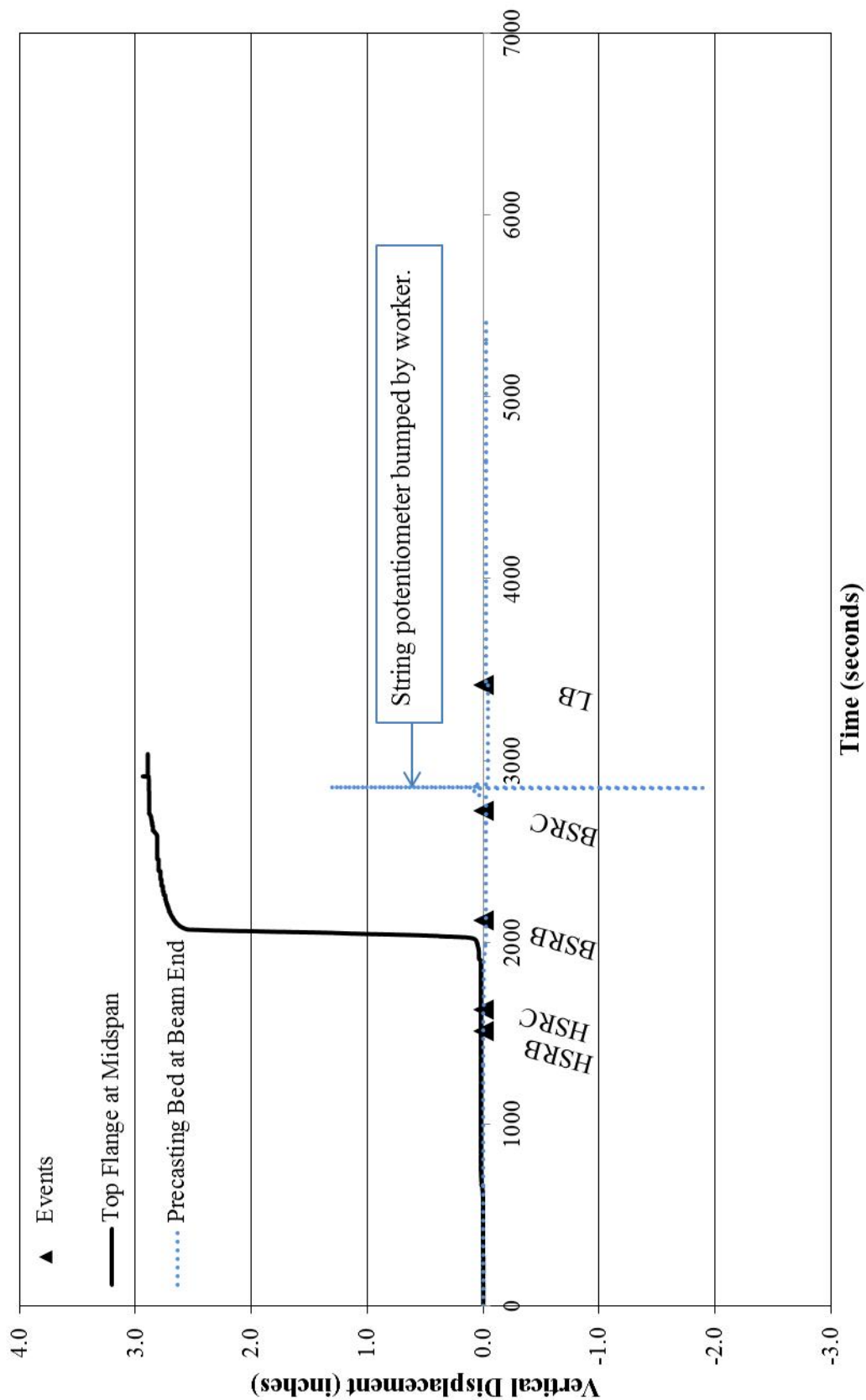


Figure B-5: Time vs. Displacement of a BTE 145 PPCB

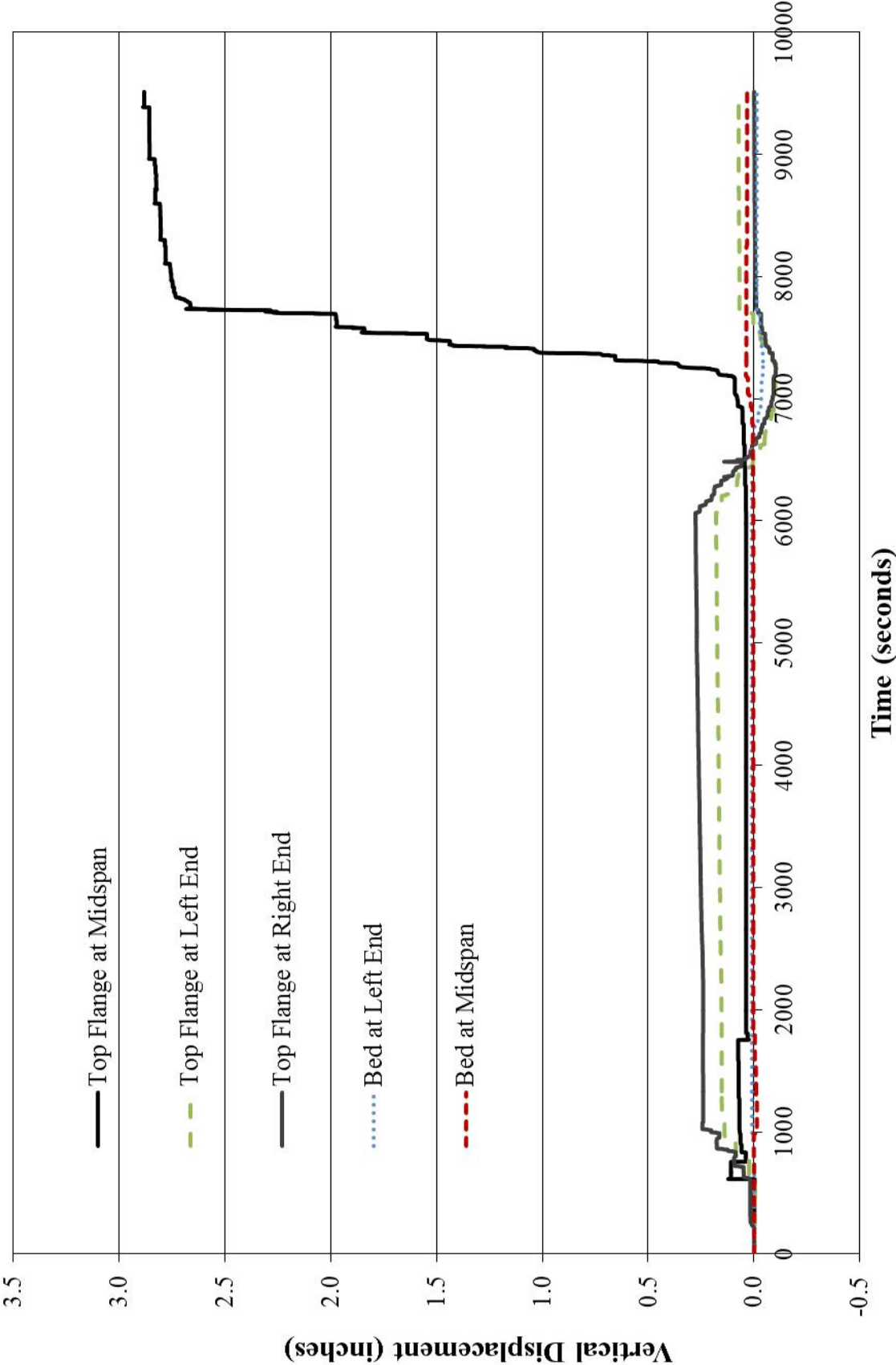


Figure B-6: Time vs. Vertical Displacement for a BTC 130 PPCB

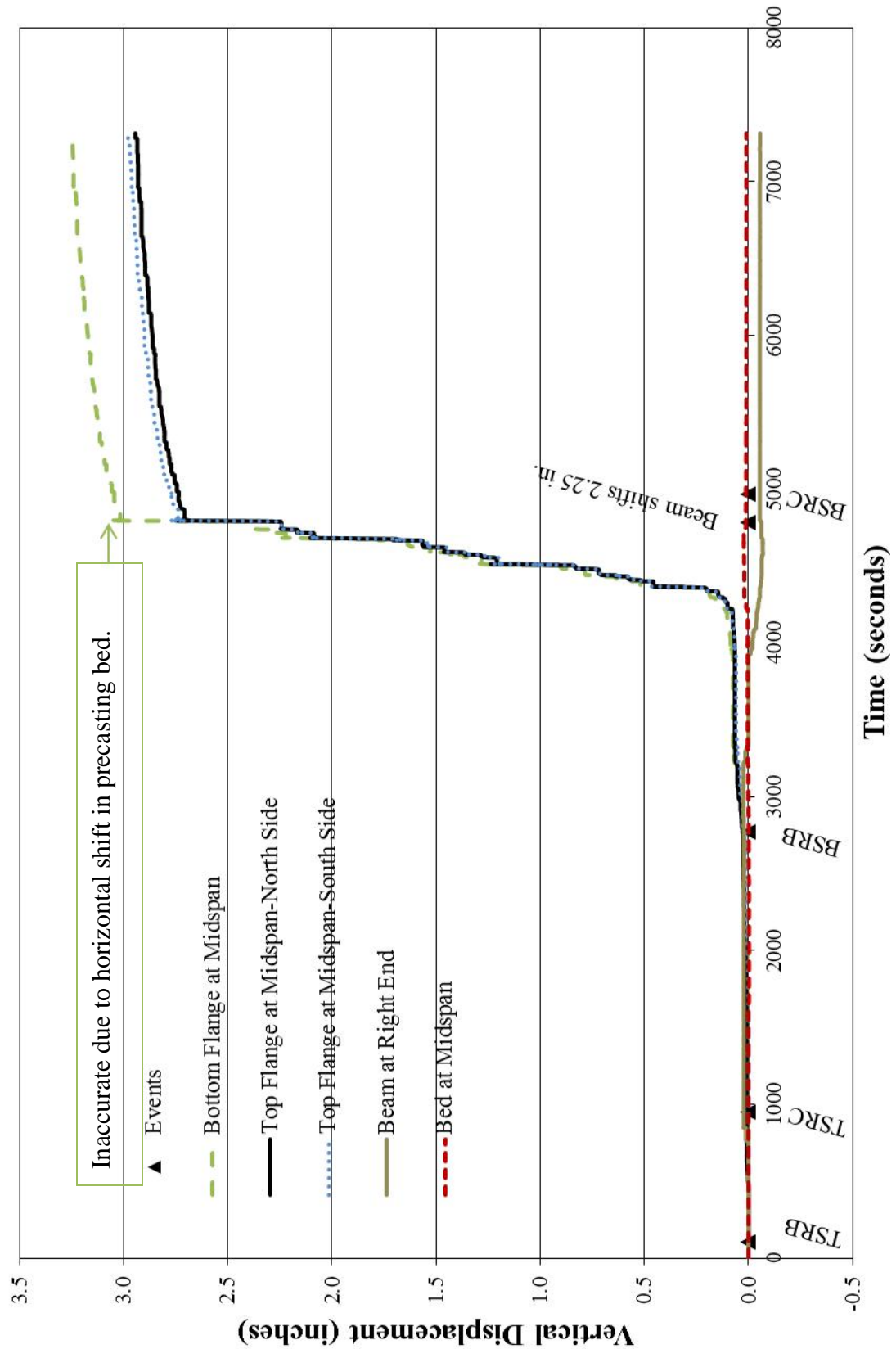


Figure B-7: Time vs. Vertical Displacement for BTC 120

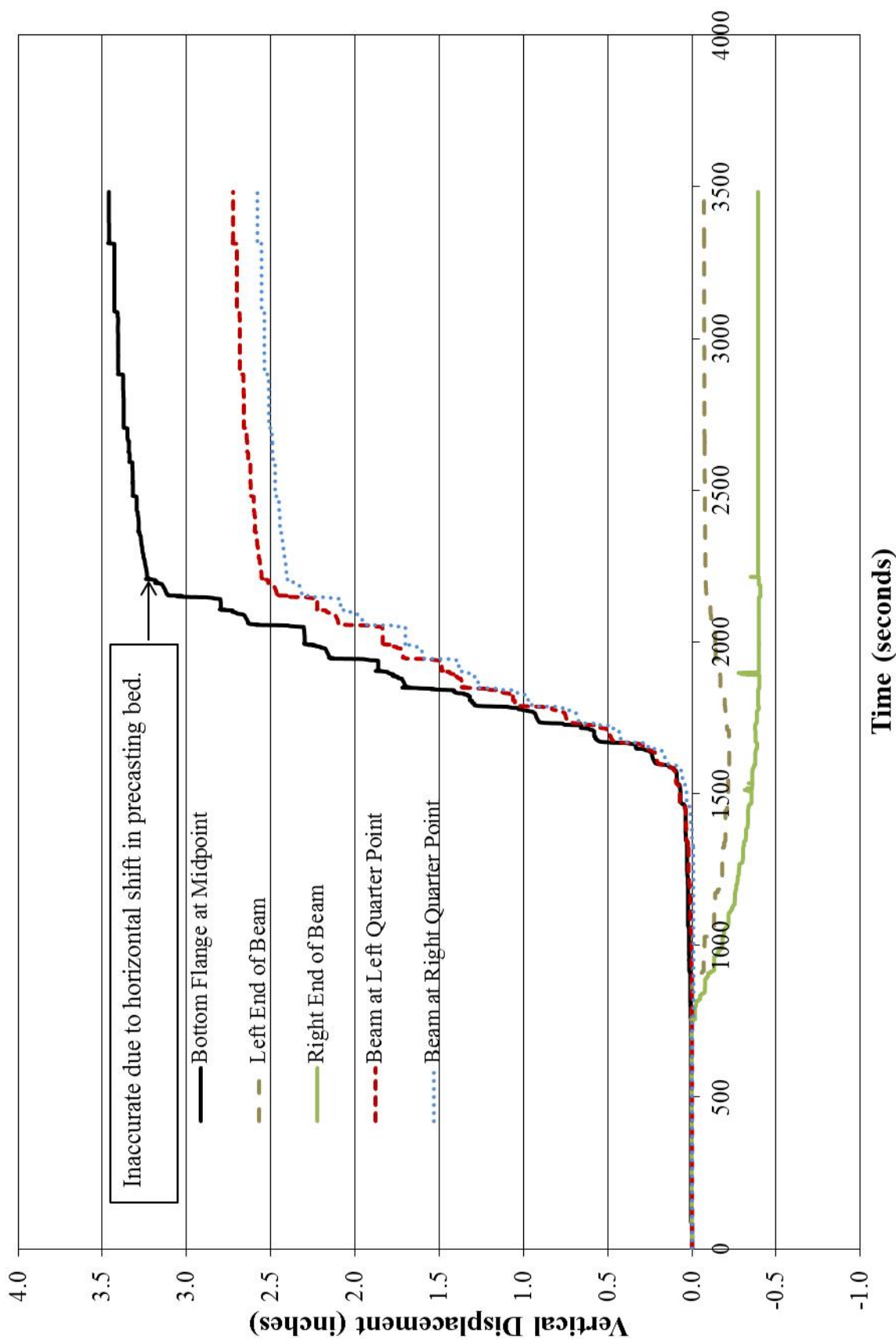


Figure B-8: Time vs. Vertical Displacement of a BTC 120 PPCB

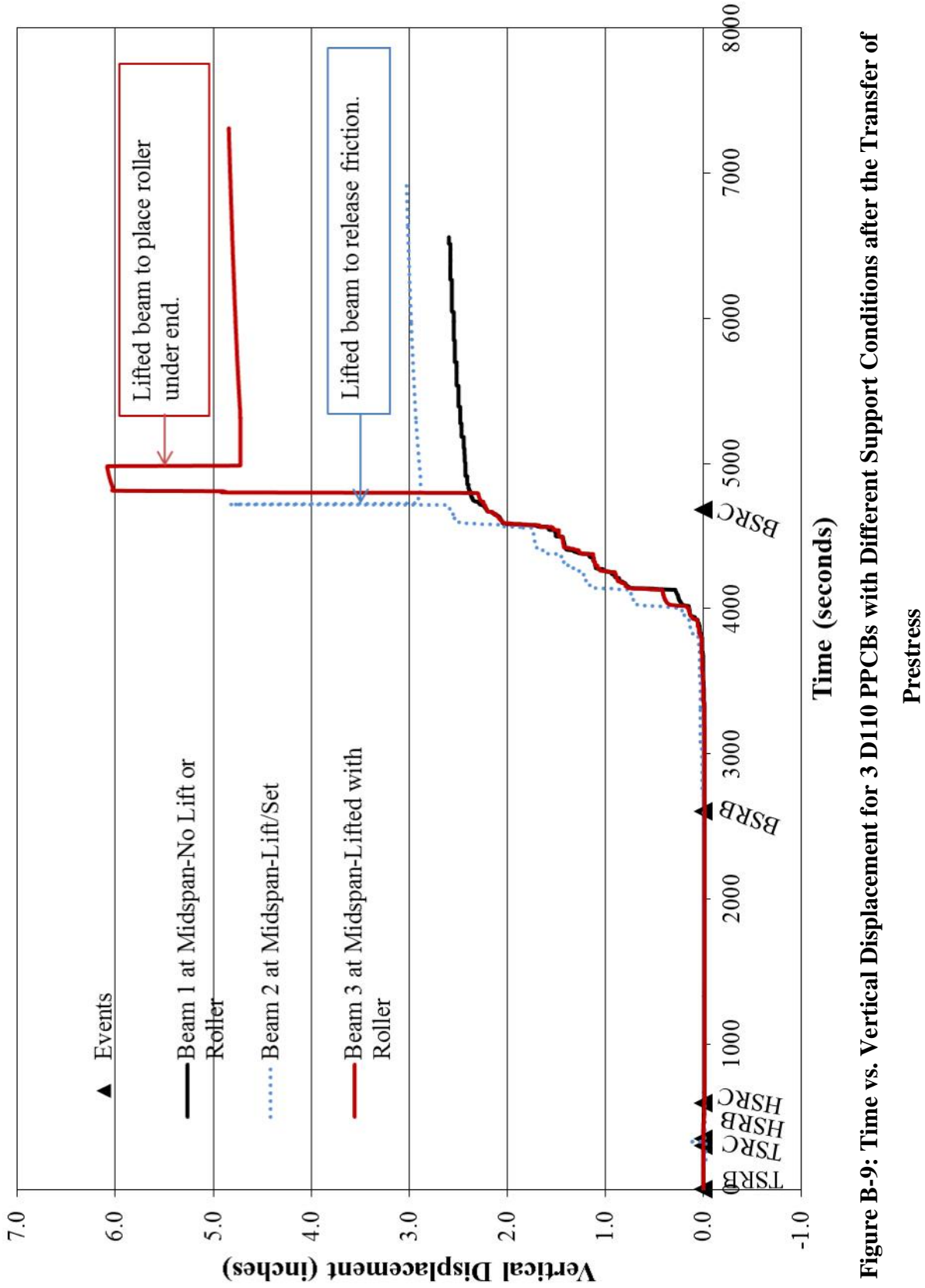


Figure B-9: Time vs. Vertical Displacement for 3 D110 PPCBs with Different Support Conditions after the Transfer of

Prestress

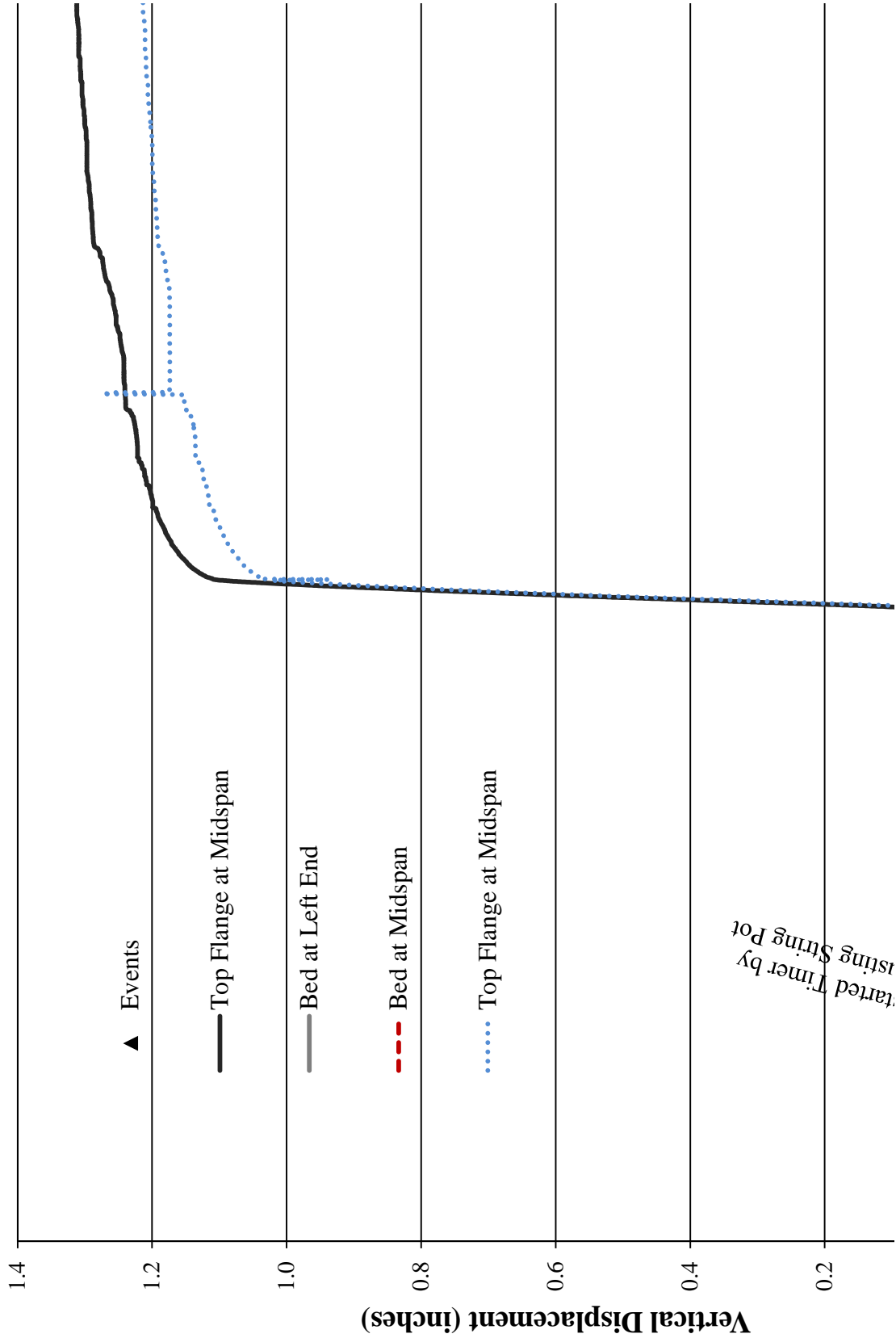


Figure B-10: Time vs. Displacement for a BTE 110

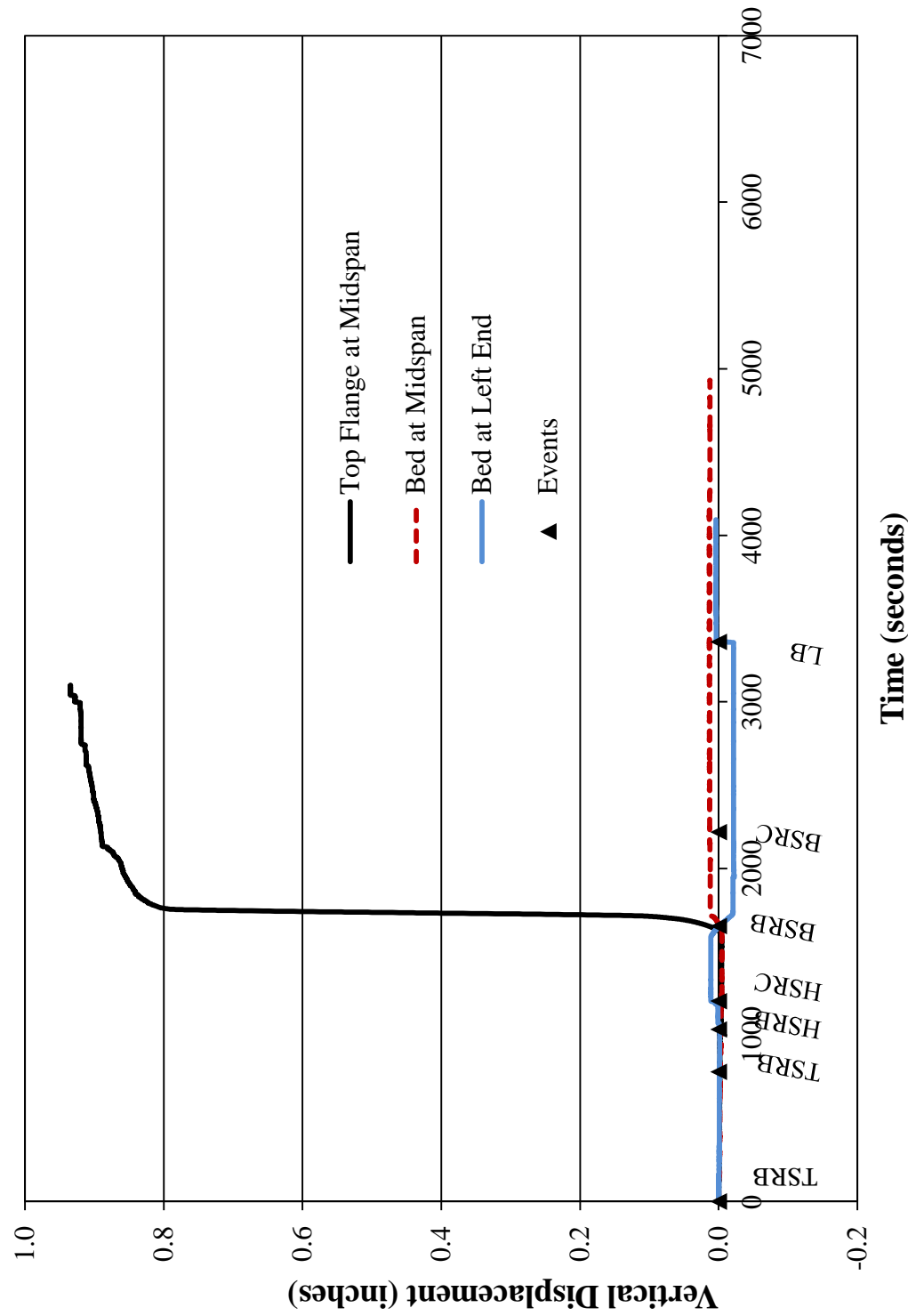


Figure B-11: Time vs. Displacement for a BTE 110

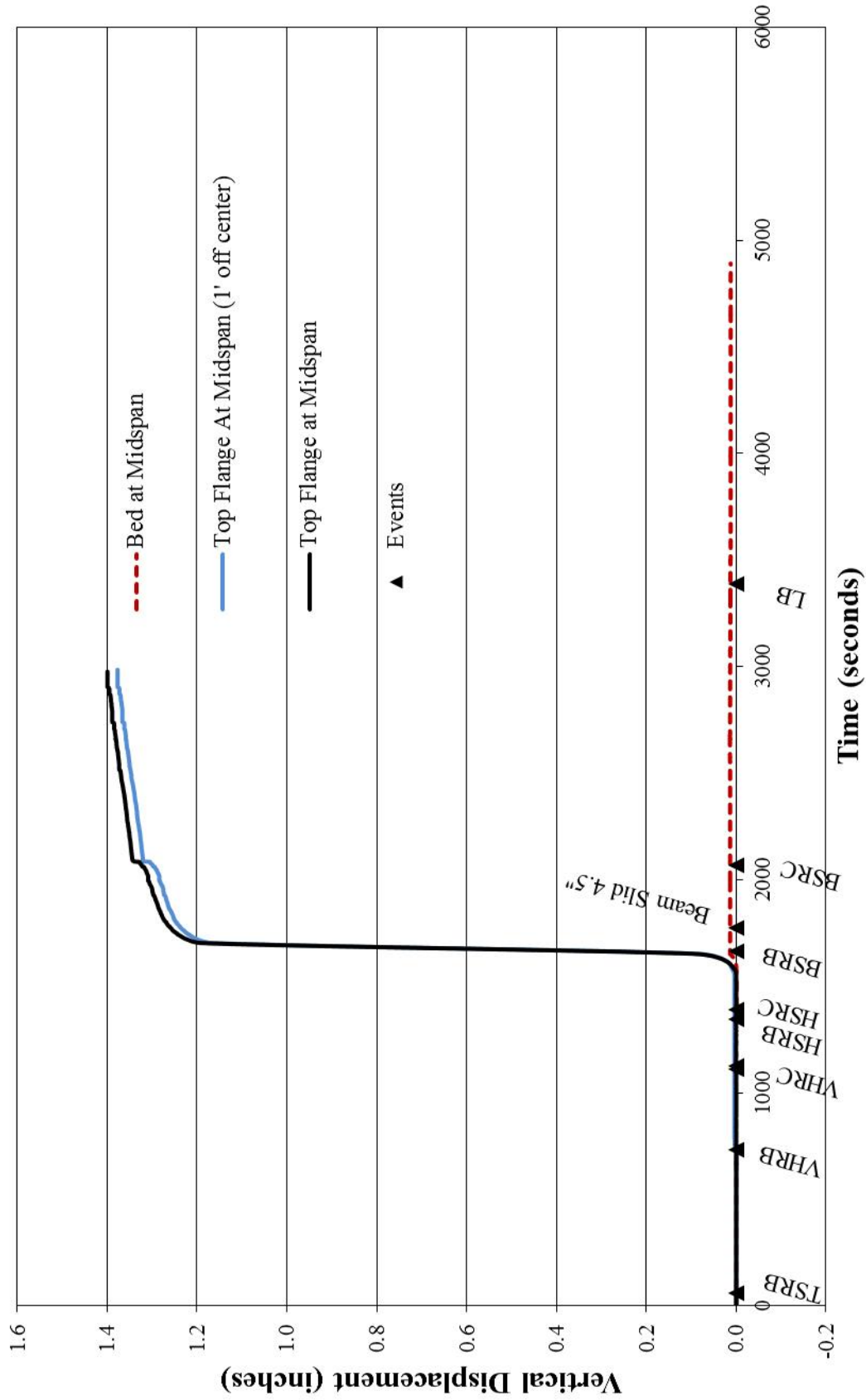


Figure B-12: Time vs Vertical Displacement for a BTE 110 PPCB



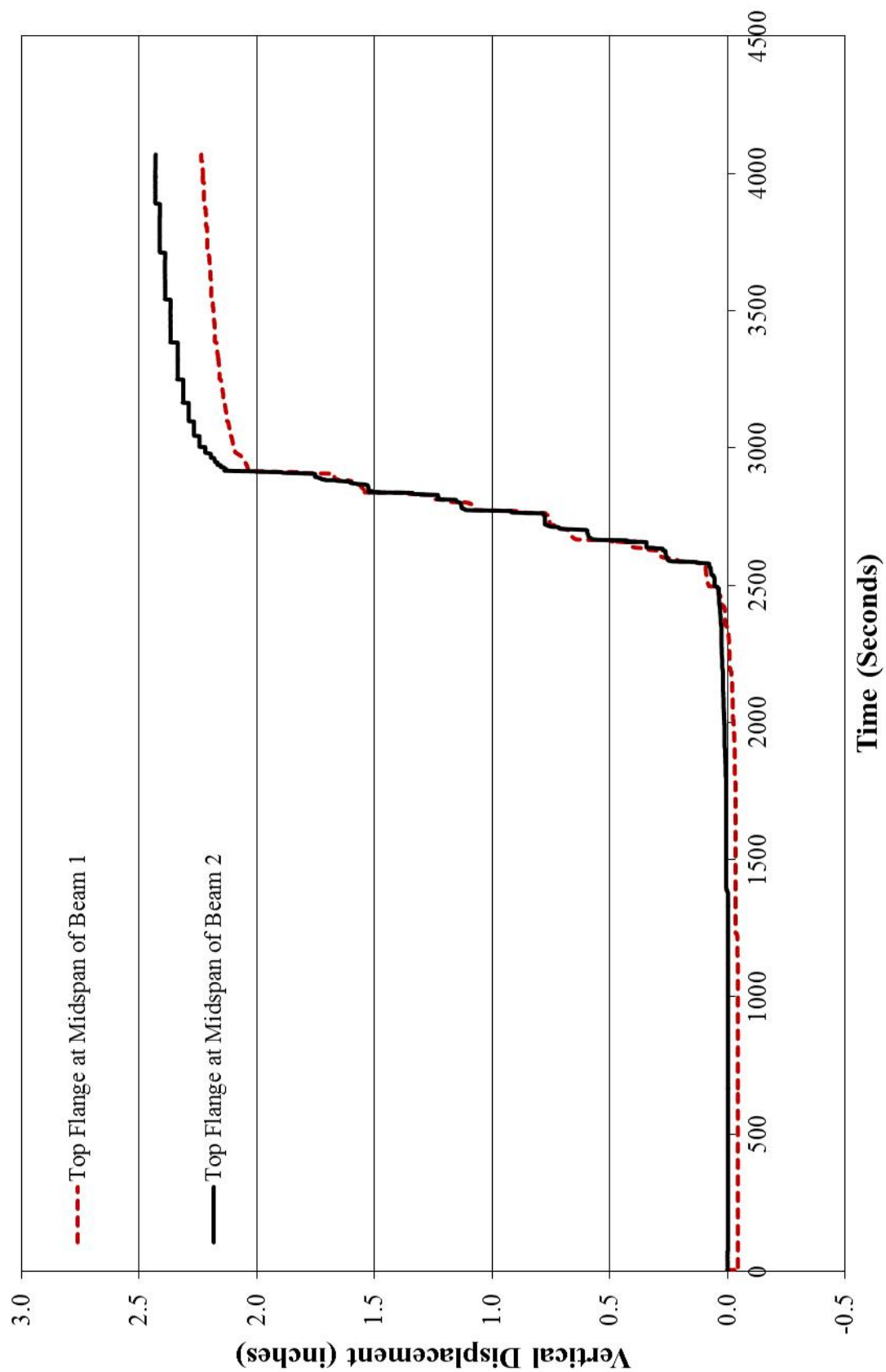


Figure B-13: Time vs. Displacement of a D110 PPCB

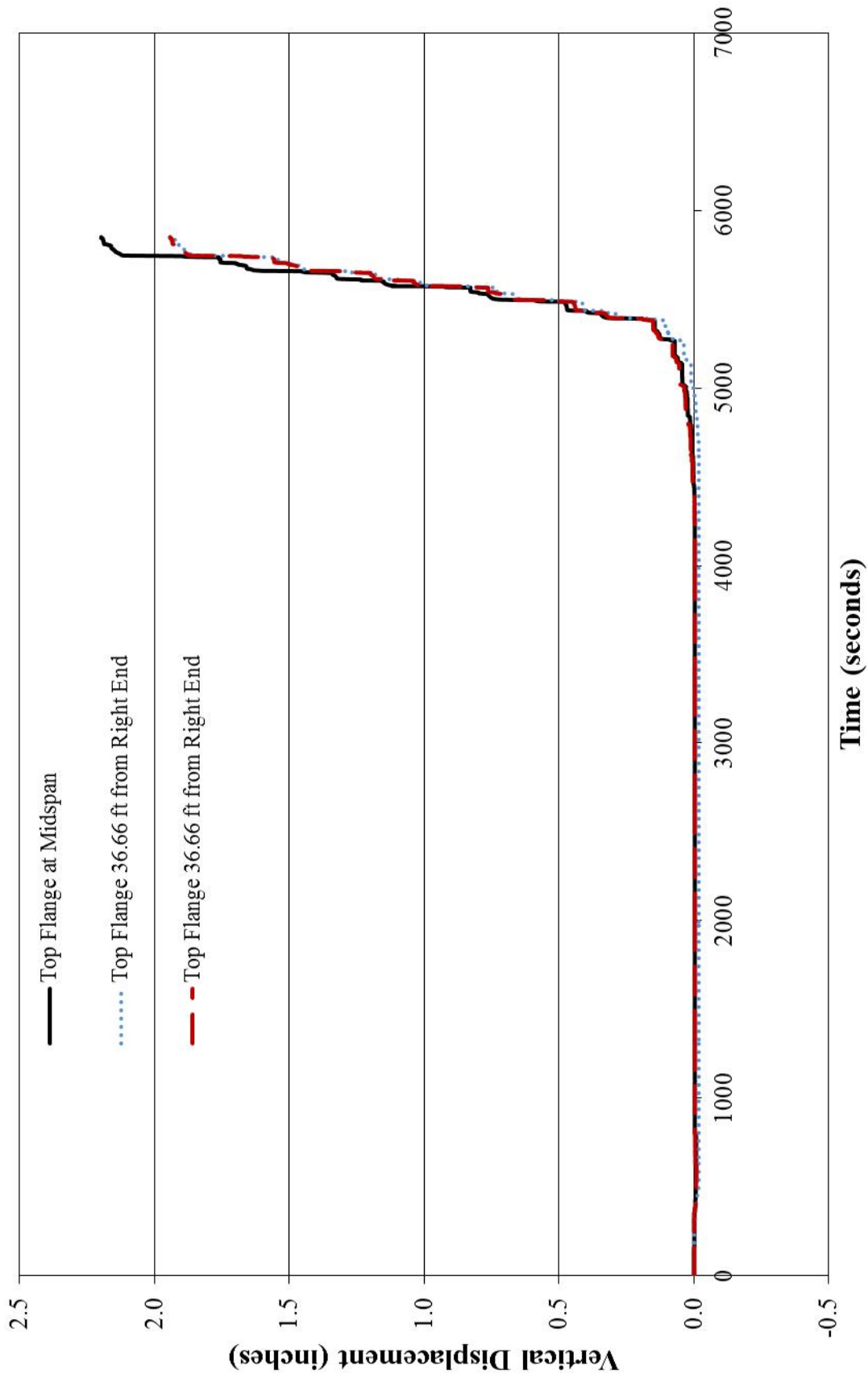
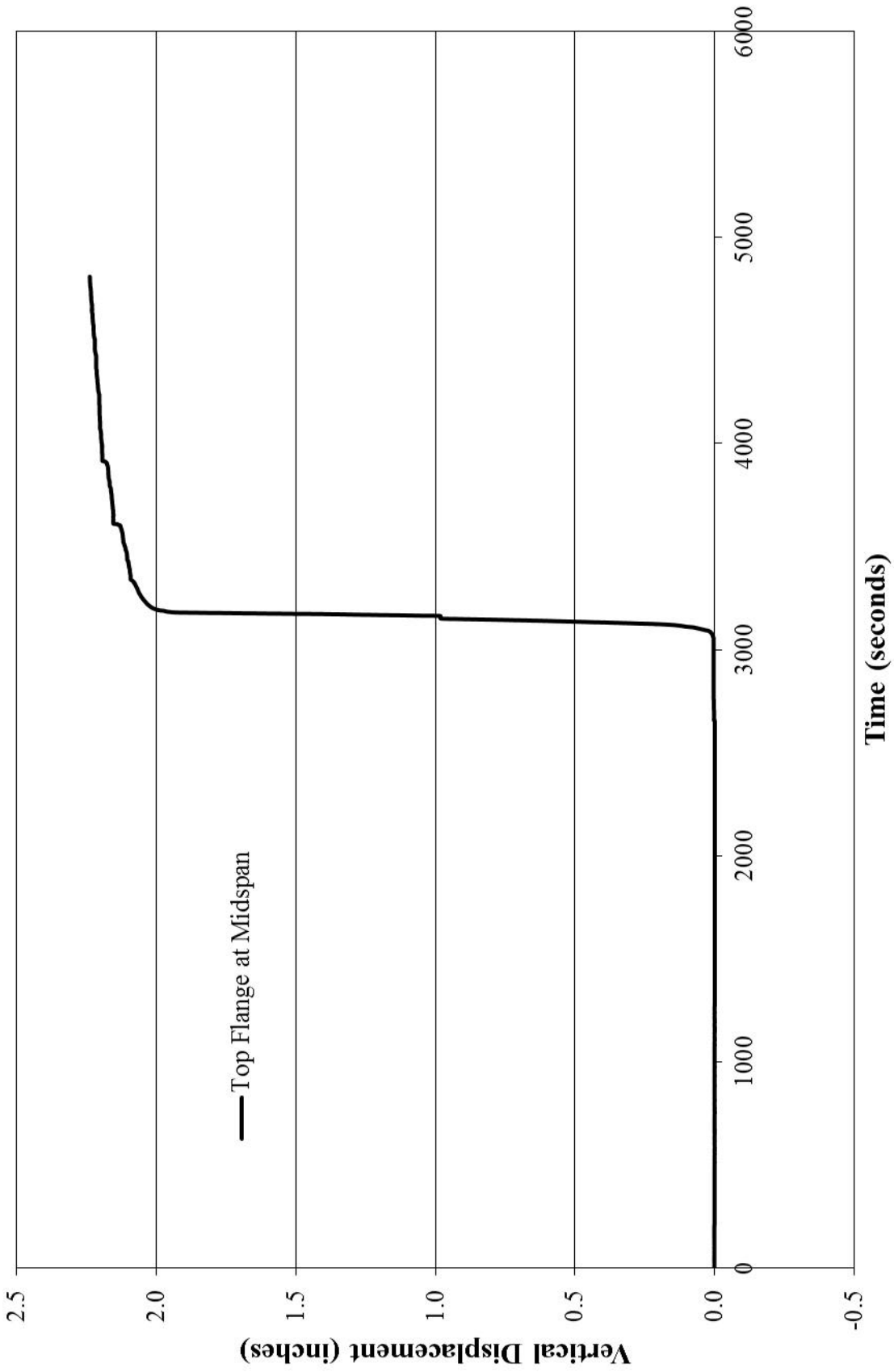


Figure B-14: Time vs. Displacement for a D 110 PPCB



**Figure B-15: Time vs. Displacement of a D 105 PPCB**

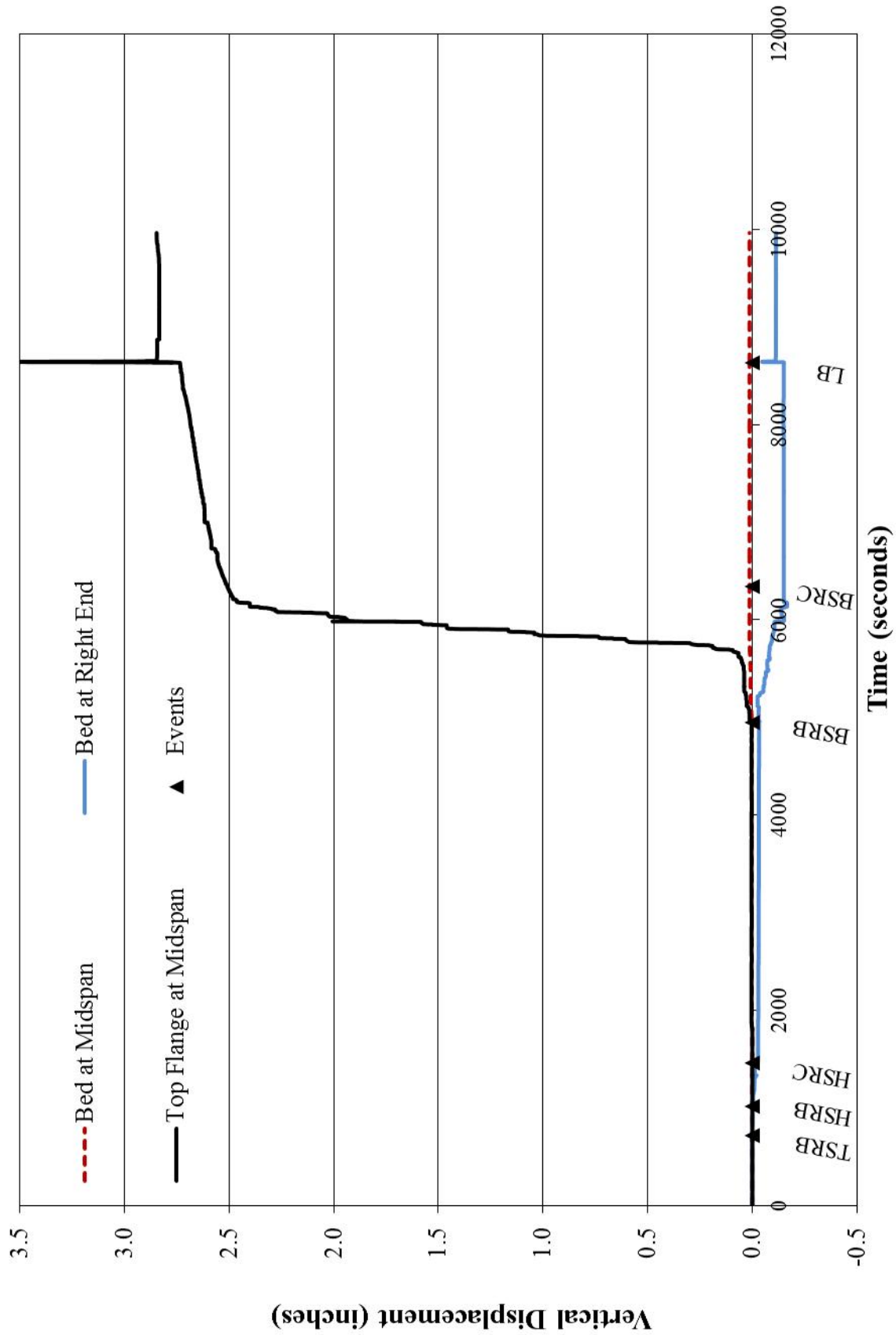


Figure B-16: Time vs. Vertical Displacement for a BTB 100

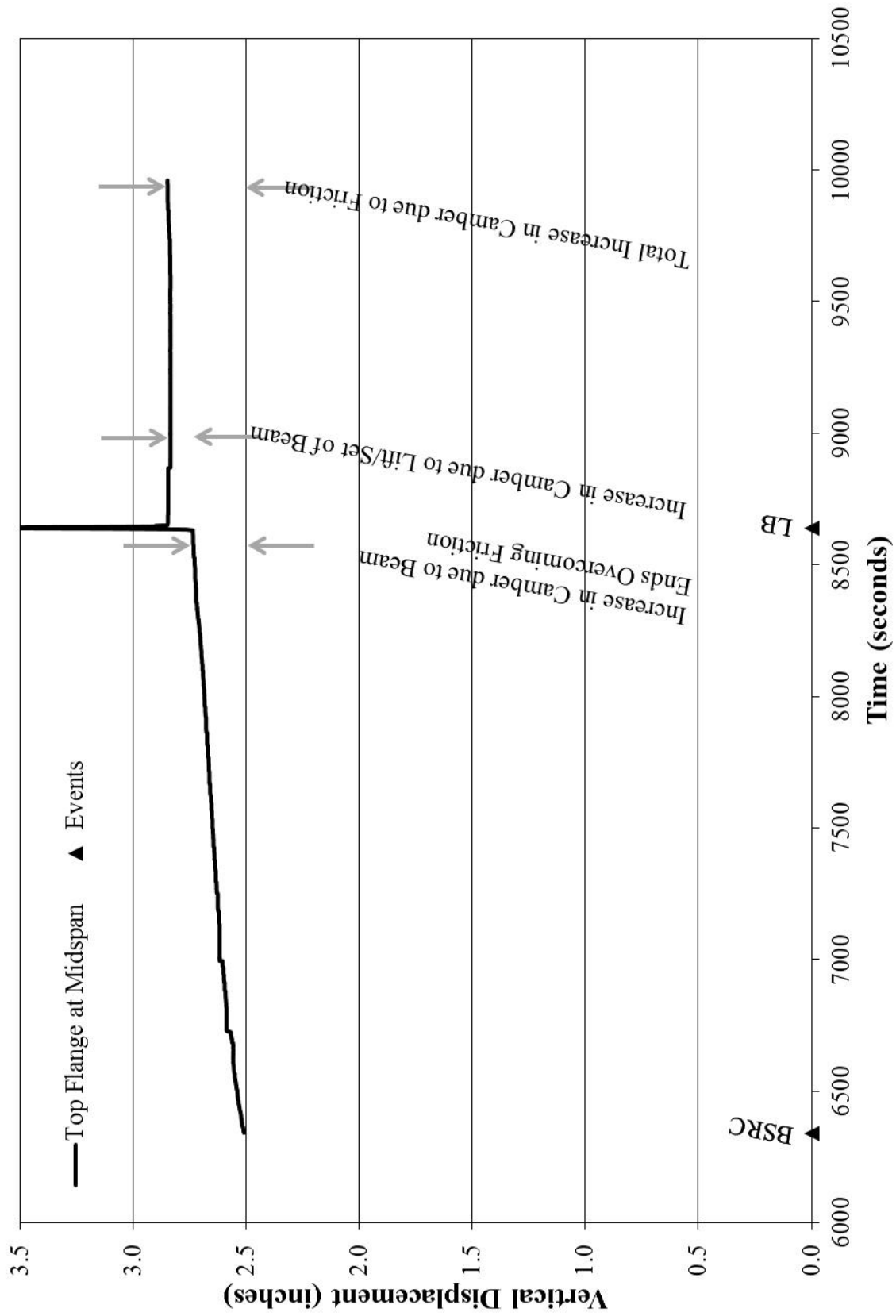


Figure B-17: Time vs. Vertical Displacement for a BTB 100 after release of Prestressing Strands

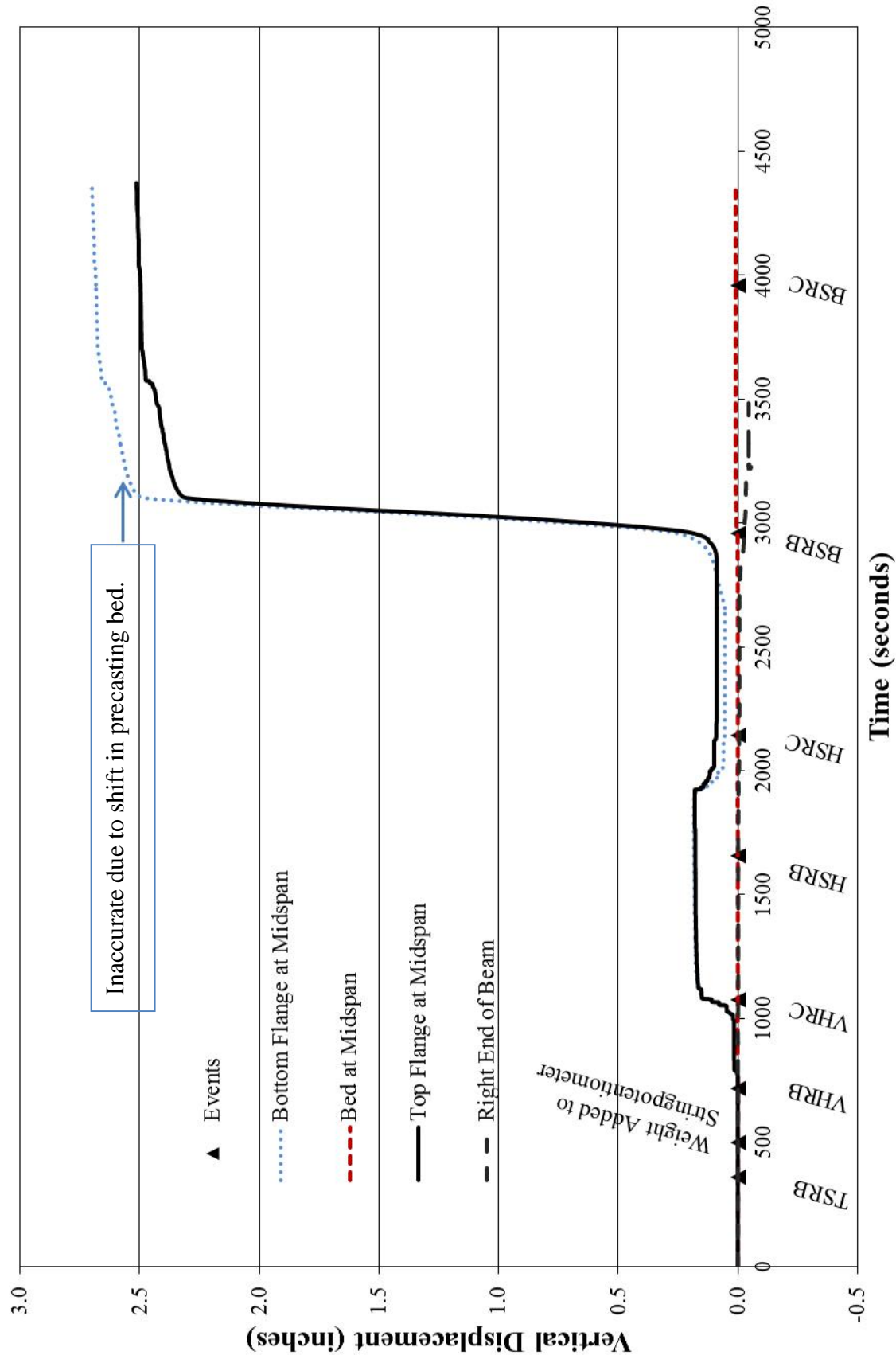


Figure B-18: Time vs. Vertical Displacement for a BTB 95

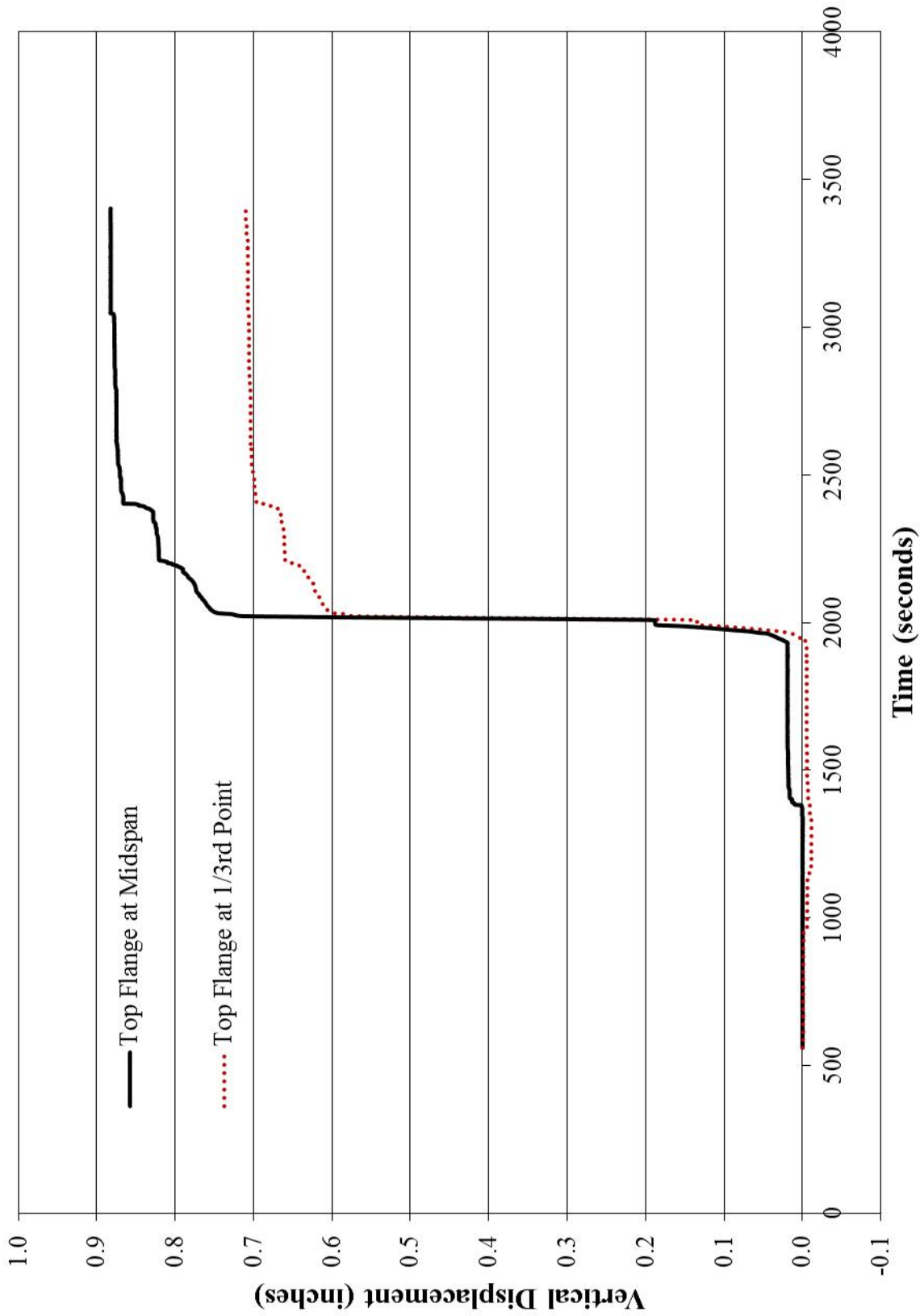


Figure B-19: Time vs Vertical Displacement for D 90

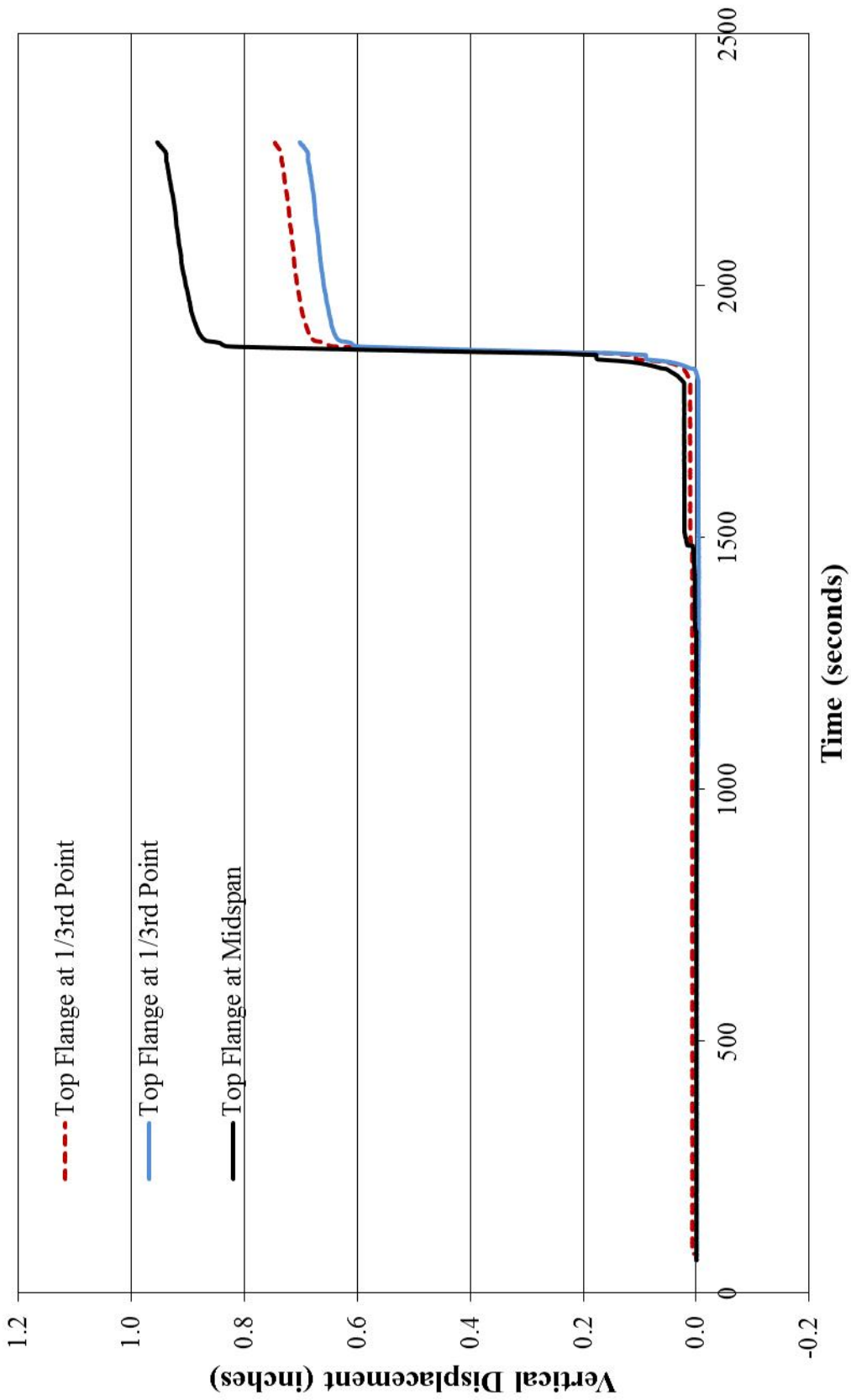
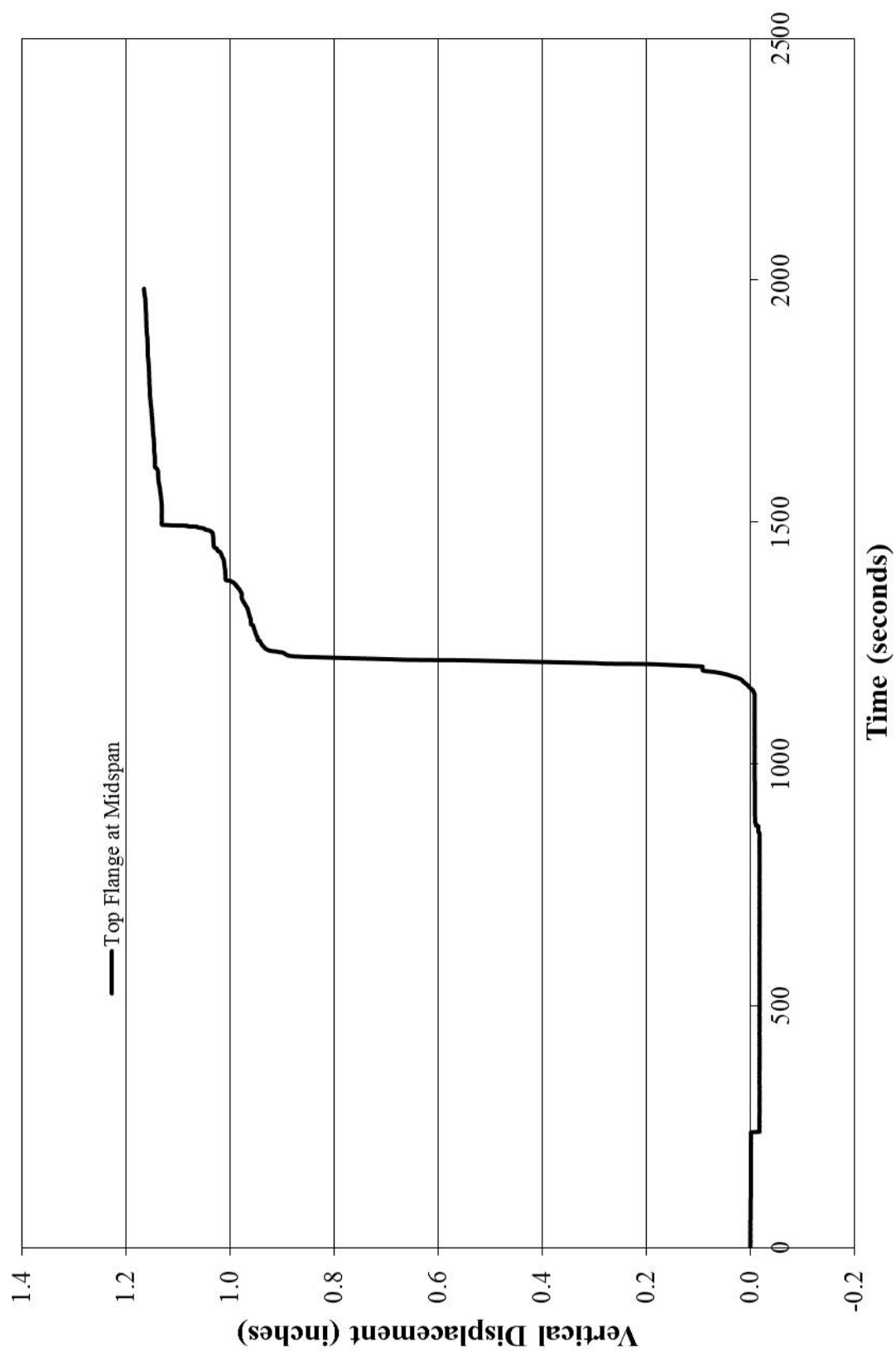


Figure B-20: Time vs. Vertical Displacement of a D 90





**Figure B-21: Time vs. Displacement of a D 90 PPCB**

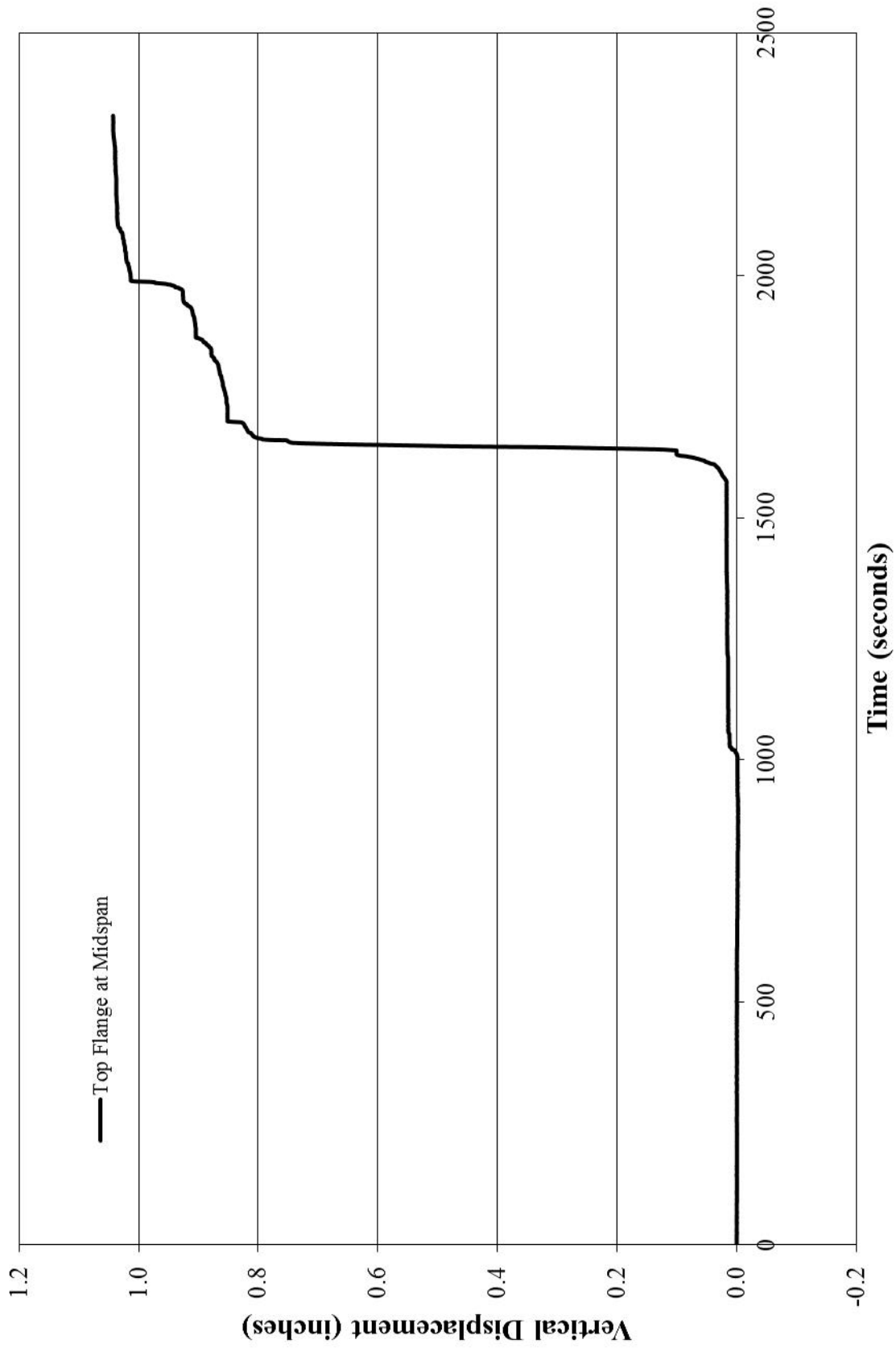


Figure B-22: Time vs. Displacement for a D 90 PPCB

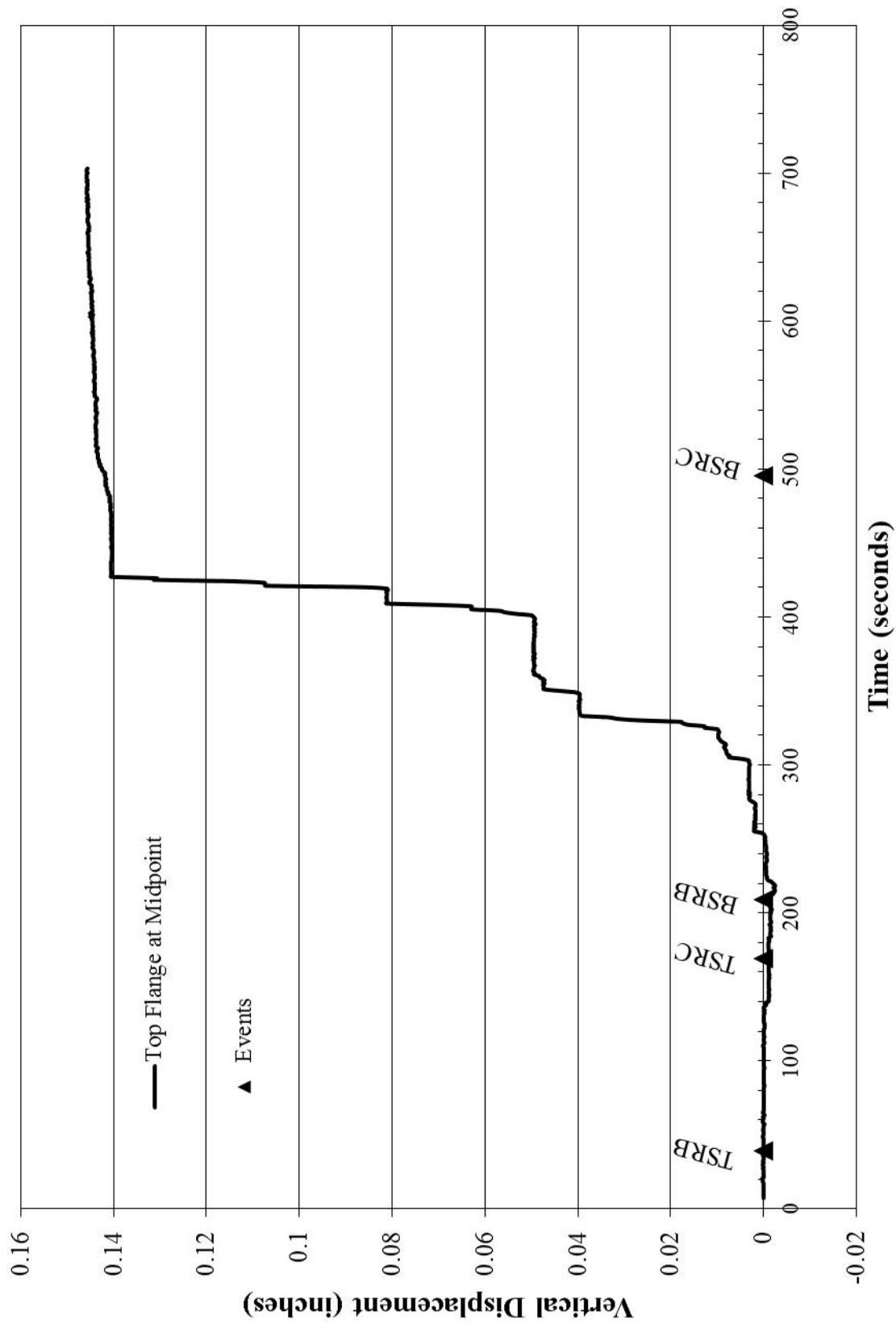


Figure B-23: Time vs. Displacement for a BTC 45 PPCB

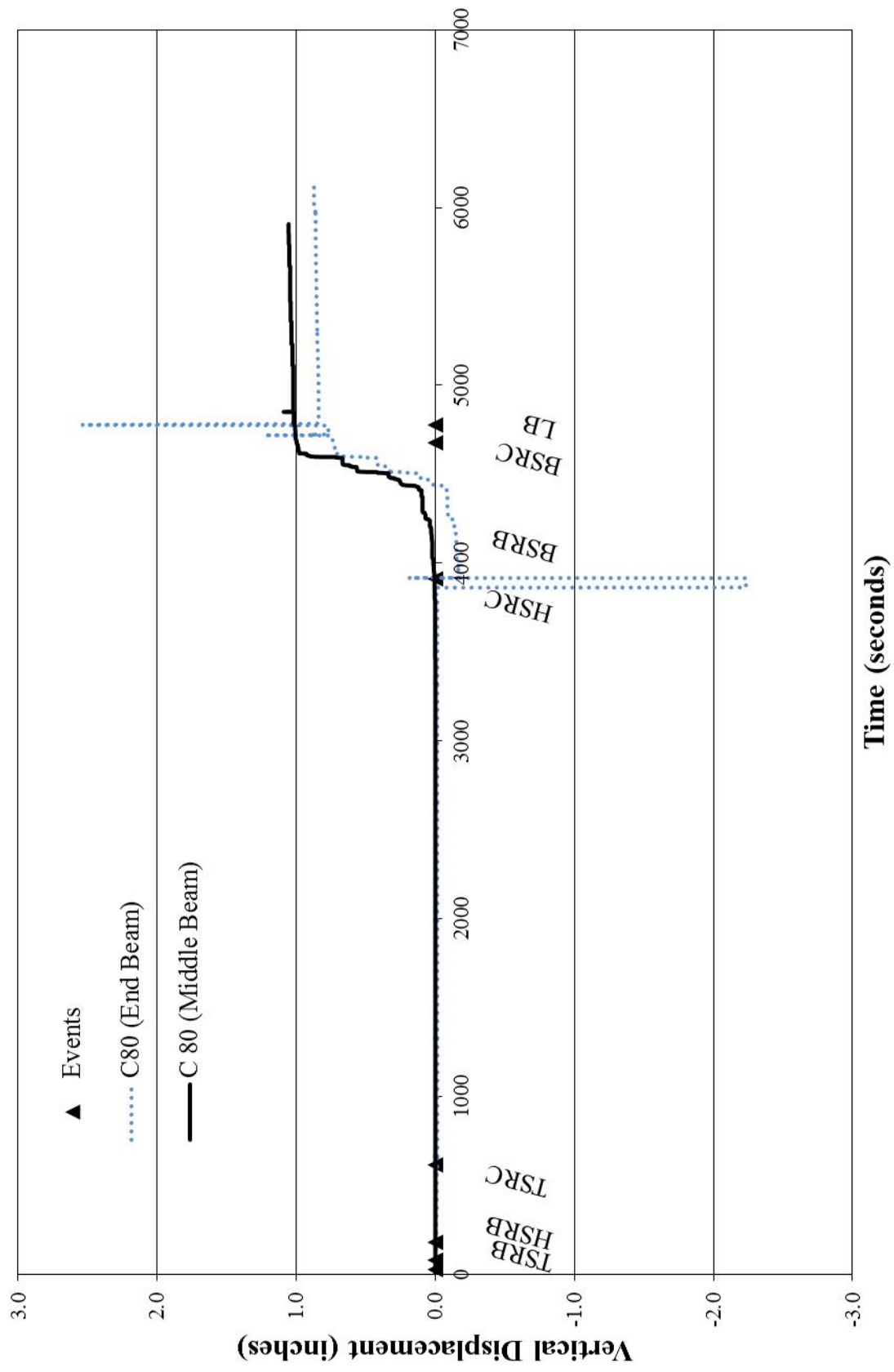


Figure B-24: Time vs. Displacement for C80

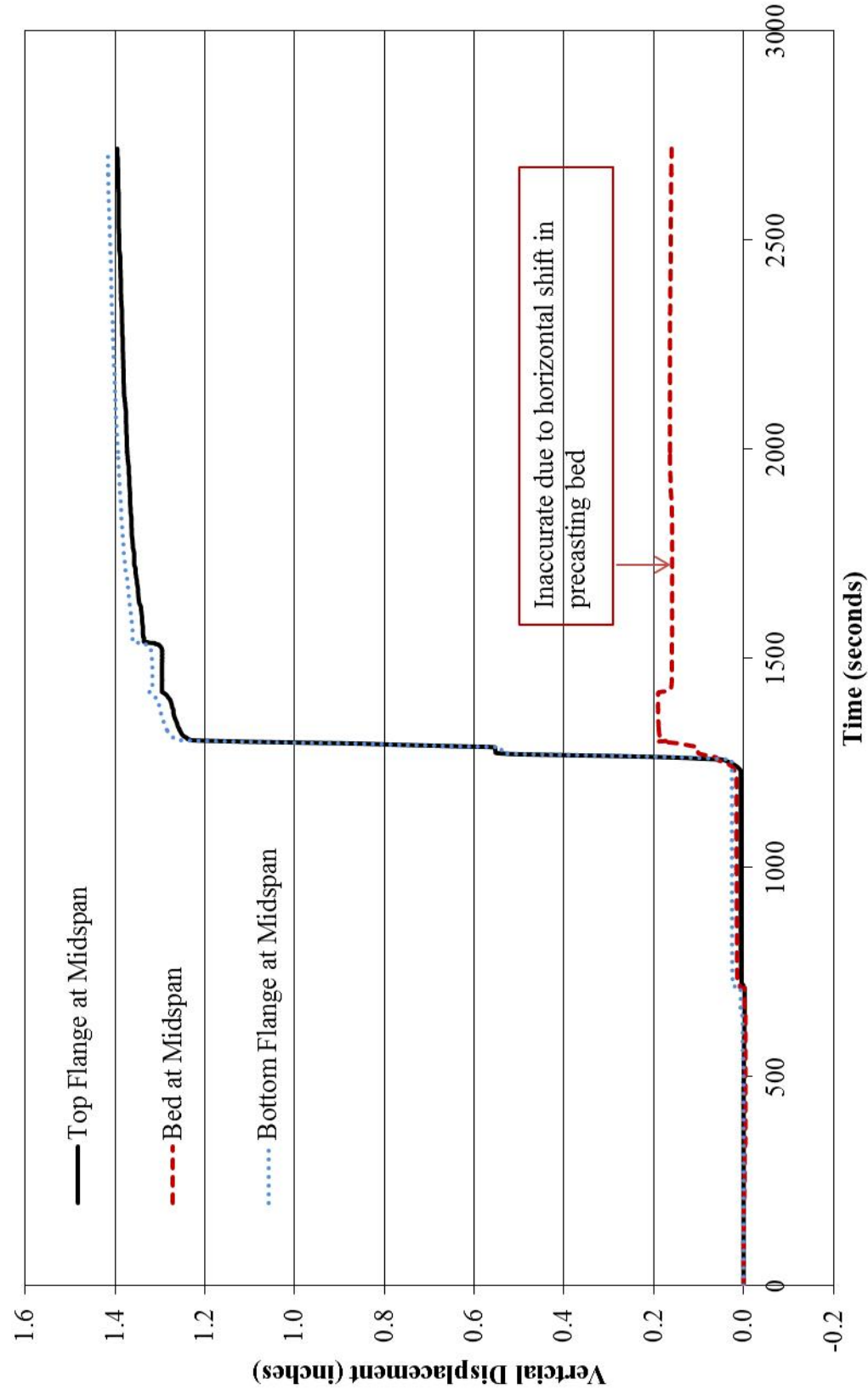


Figure B-25: Time vs. Displacement for a C 80 PPCB

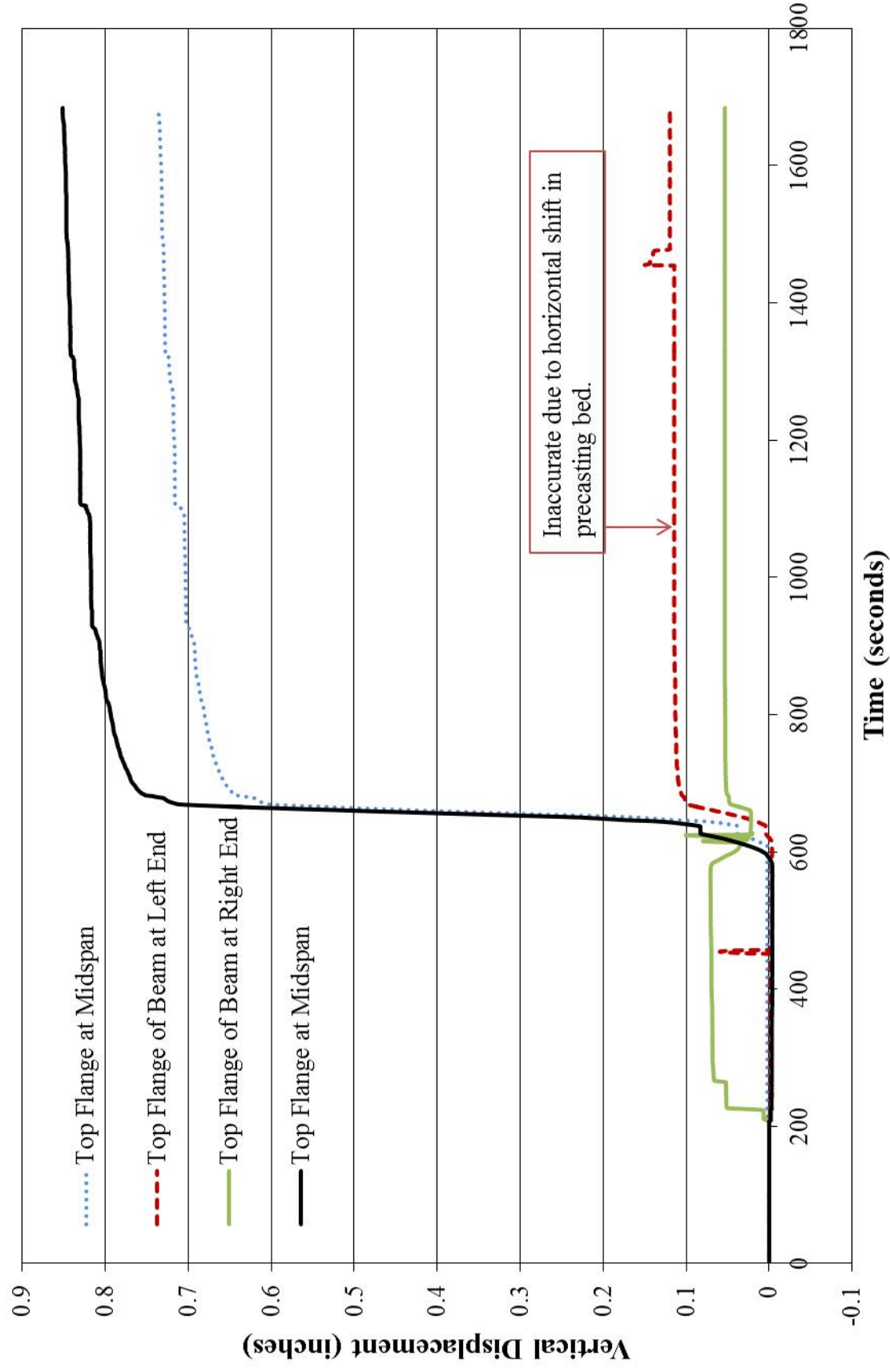


Figure B-26: Time vs. Vertical Displacement of a C67 PPCB

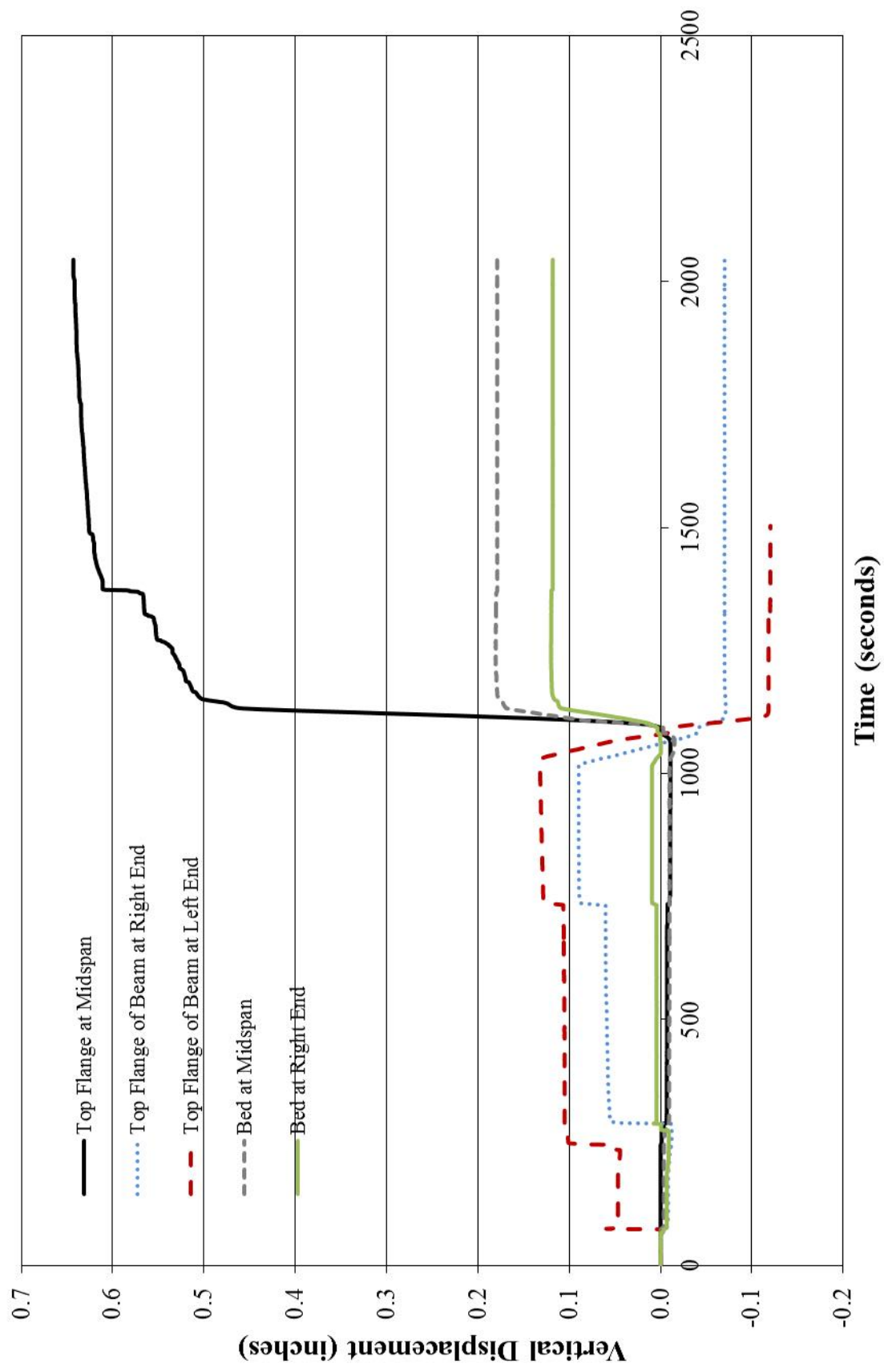


Figure B-27: Time vs. Displacement of a C 67 PPCB

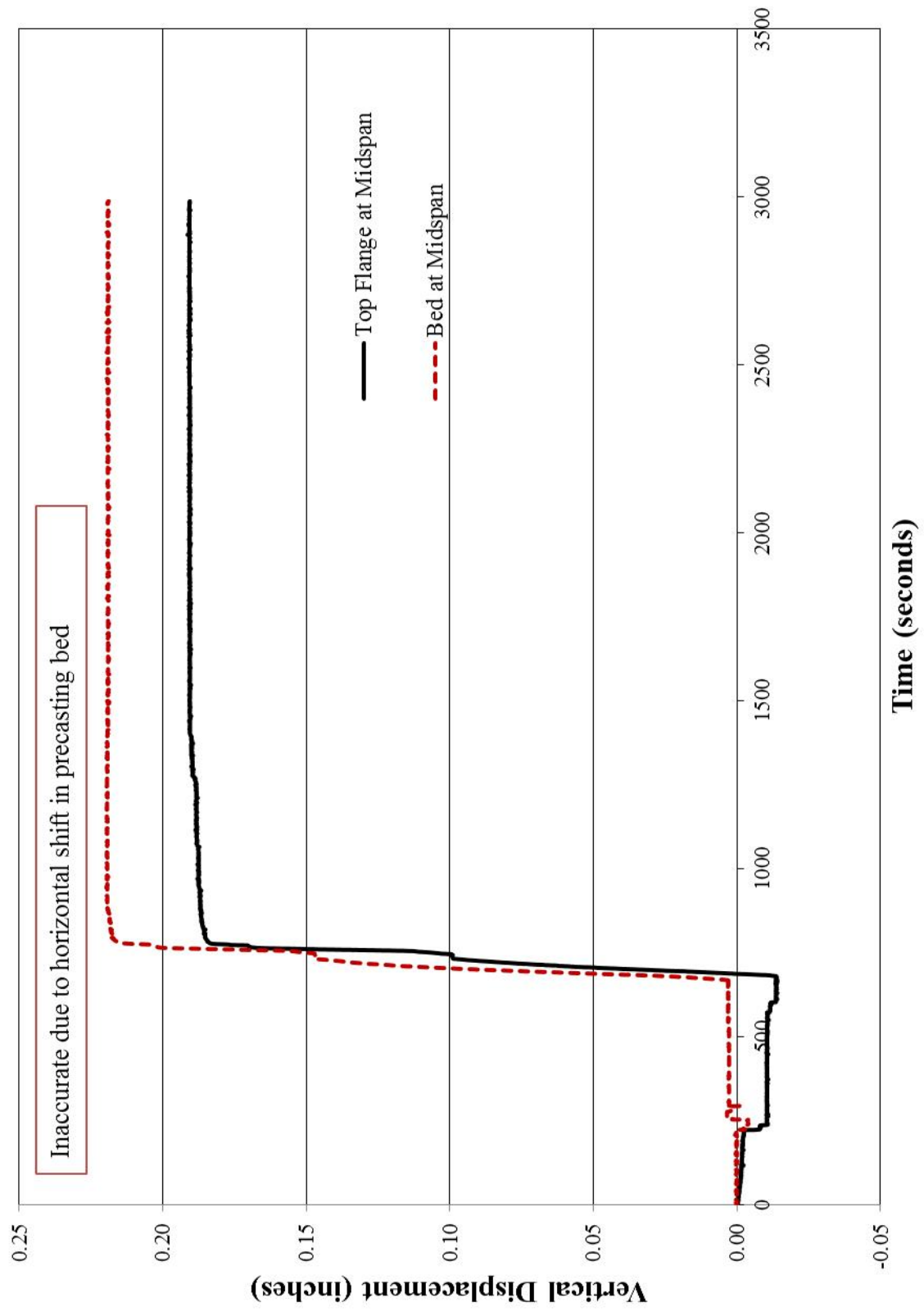


Figure B-28: Time vs. Displacement of a D 55 PPCB



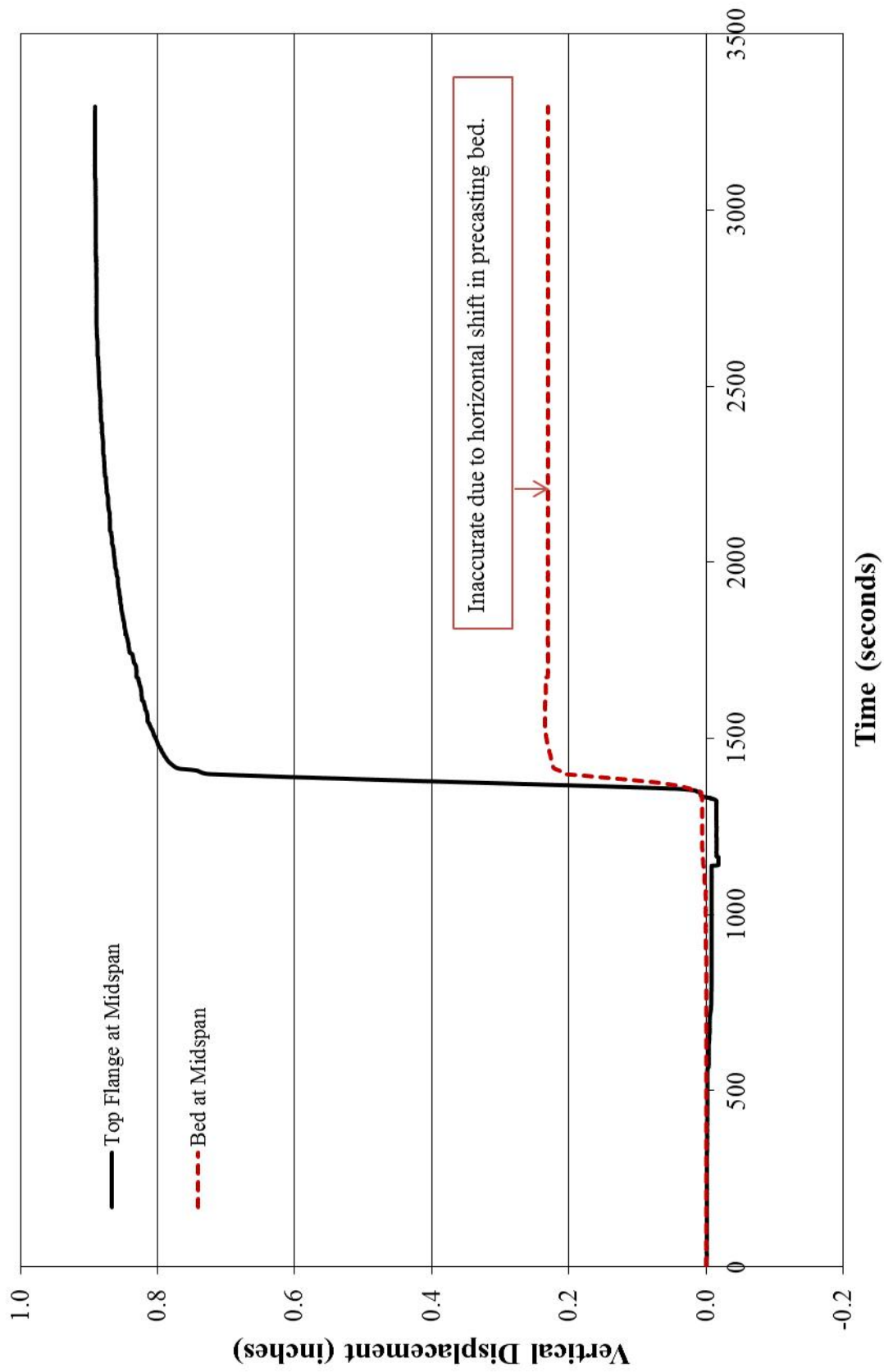


Figure B-29: Time vs. Vertical Displacement for a B55

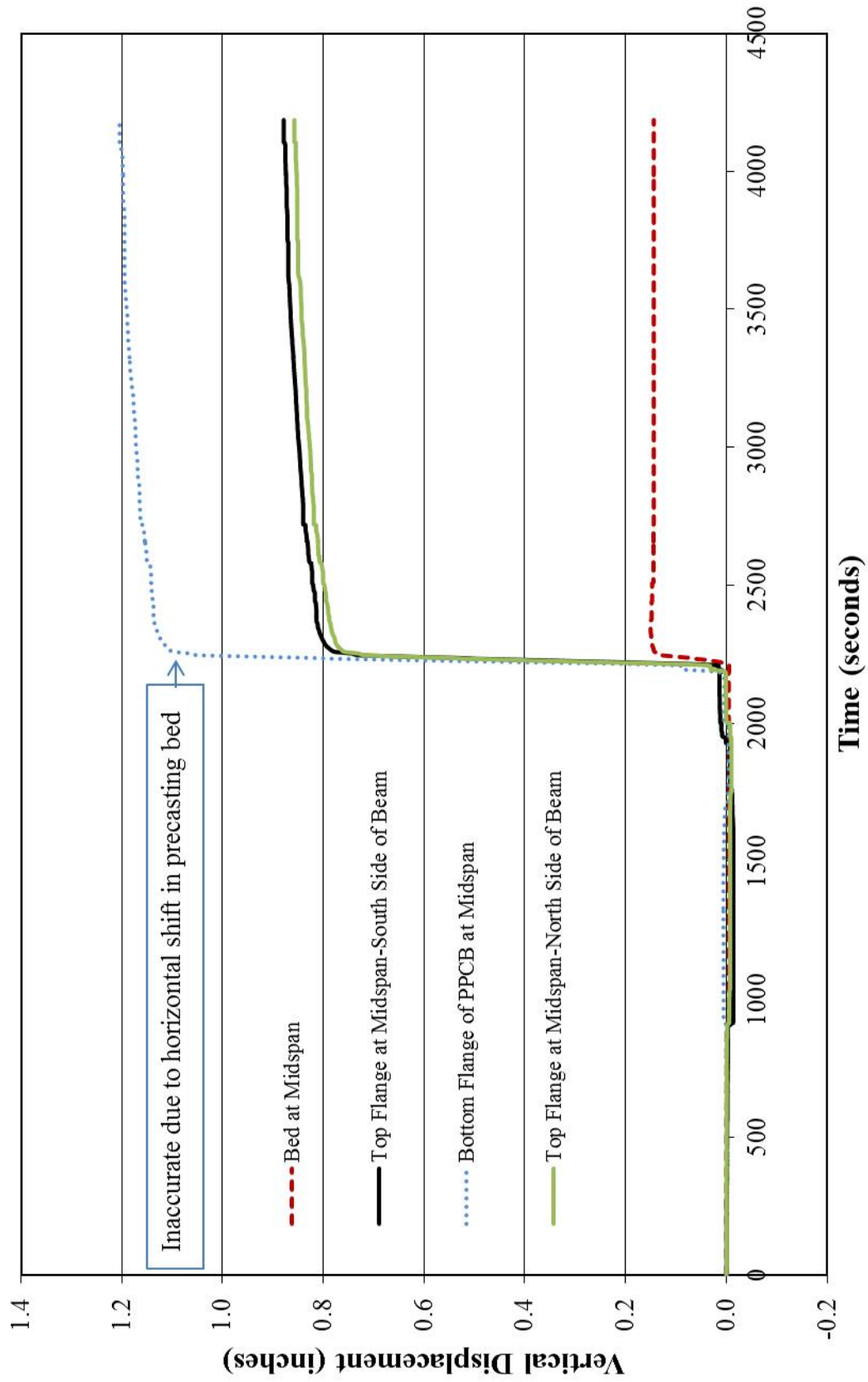


Figure B-30: Time vs. Vertical Displacement for B 55

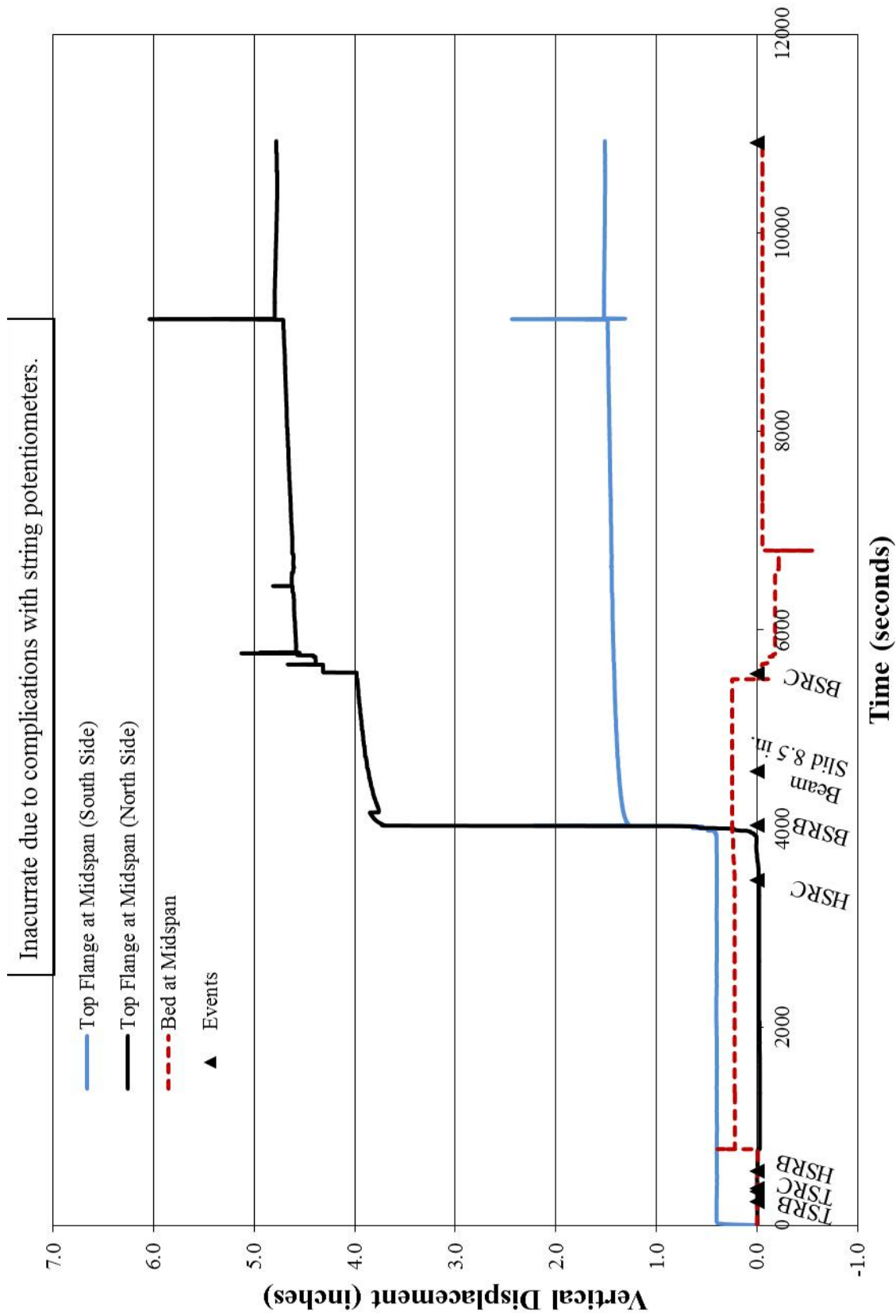


Figure B-31: Time vs. Vertical Displacement for a SBTD 135

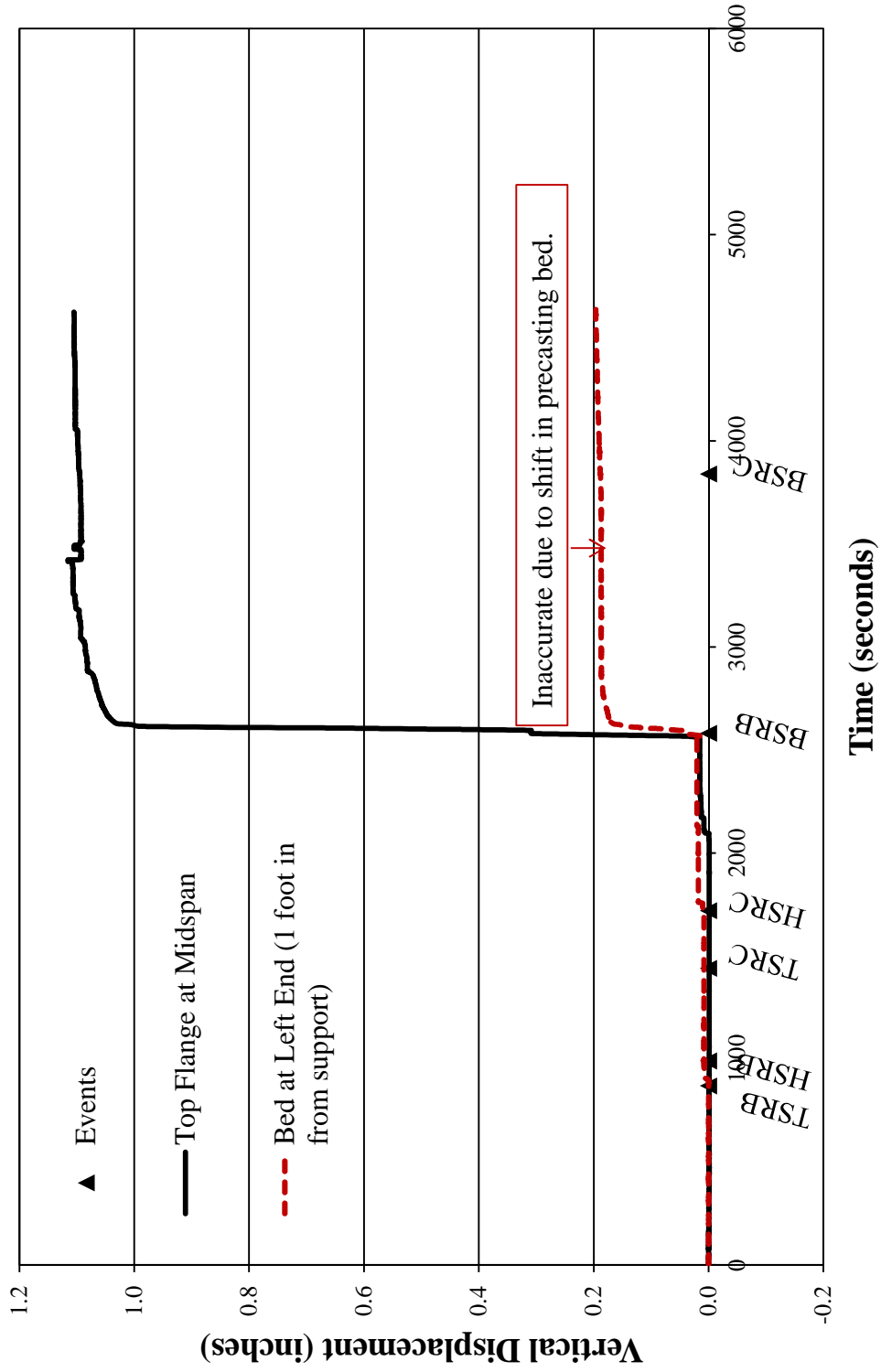
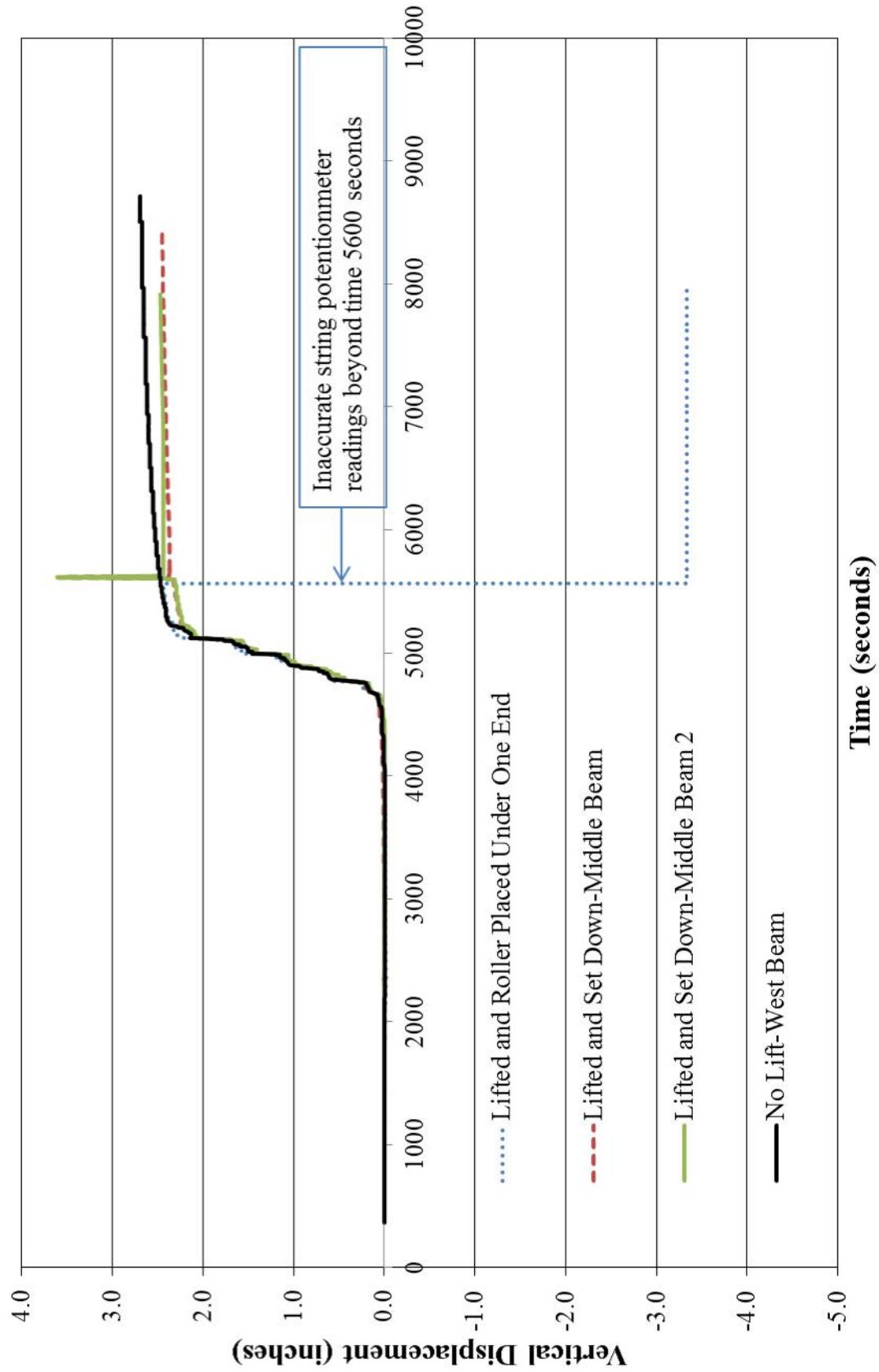


Figure B-32: Time vs. Displacement for a C 80 PPCB



**Figure B-33: Time vs. Vertical Displacement of 3 D 110 PPCBs with Different Support Conditions after Transfer of Prestress**

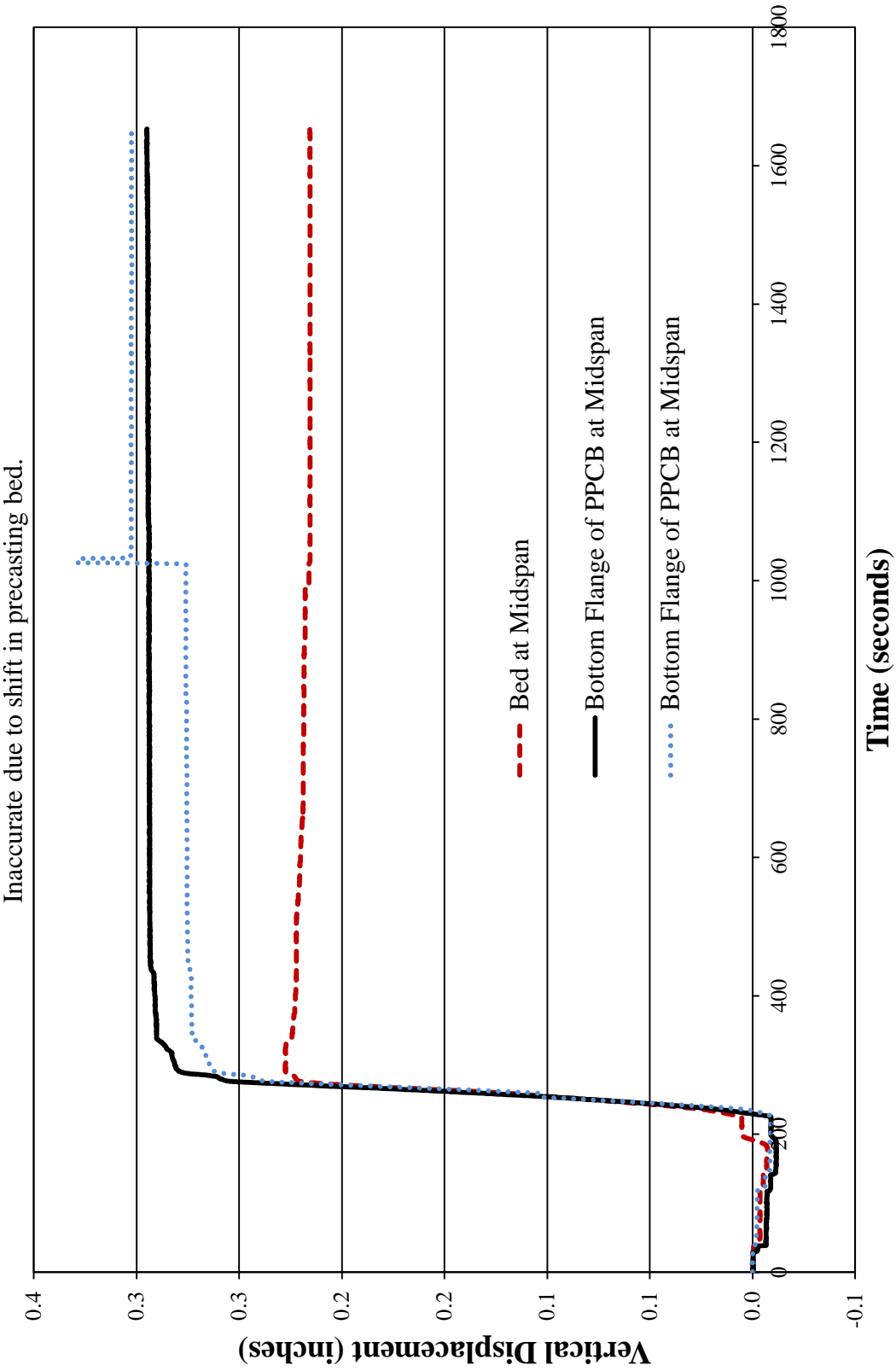


Figure B-34: Time vs. Vertical Displacement for a D60 PPCB

Inaccurate due to complications with string potentiometer readings

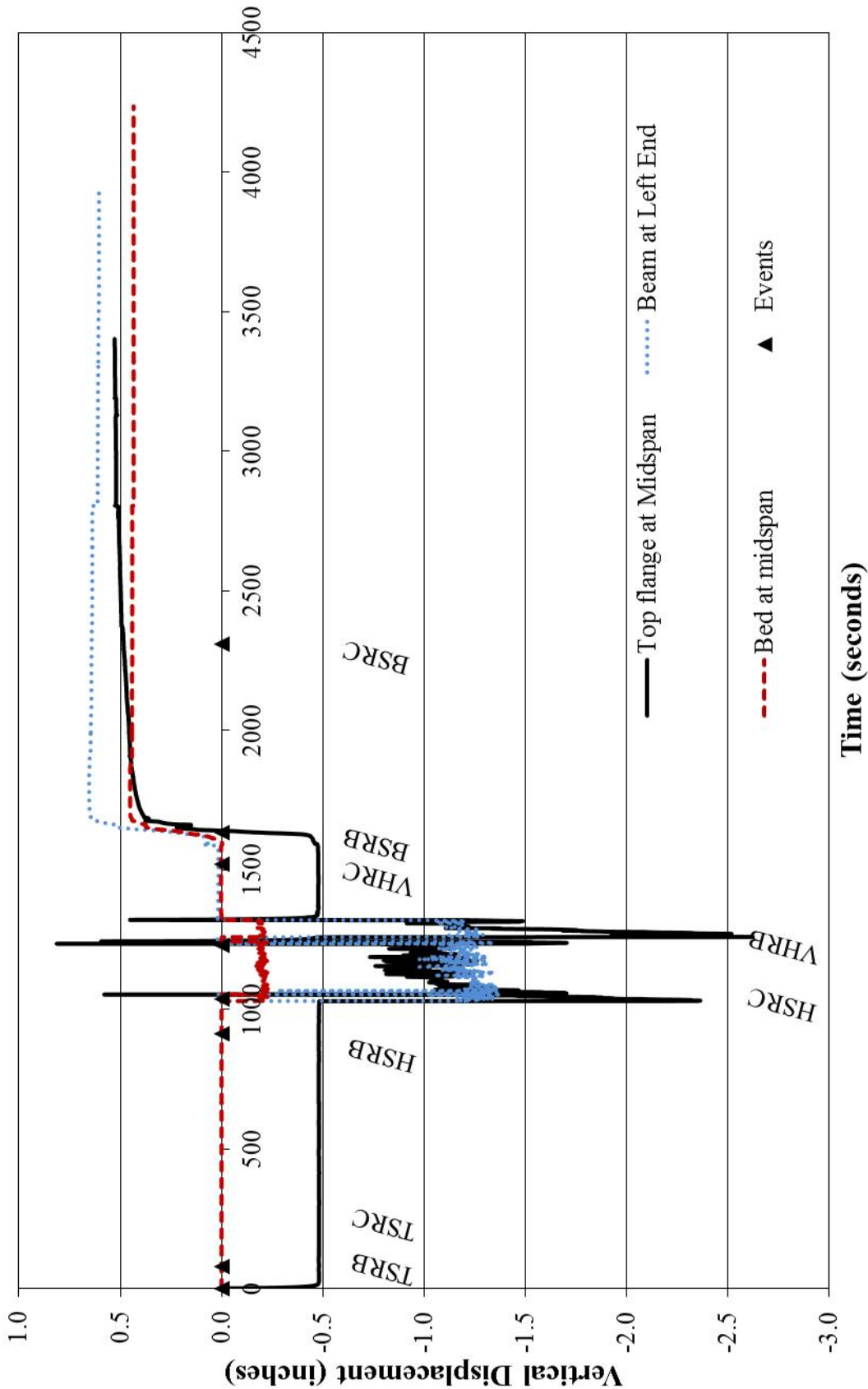


Figure B-35: Time vs. Vertical Displacement of a BTB 135 PPCB

**APPENDIX C: ANALYTICAL DATA**

Results listed in Appendix C are a combination of calculated camber data using the moment area method, comparison of material properties obtained from specifications and as-built values, and additional data that was found as a result of analytically calculating camber data.



### C.1 Transfer Length

The effect of transfer length will decrease the calculated camber. Comparing the effect transfer length has on camber was possible by conducting a parametric study. The calculated camber with and without the AASHTO LRFD (2010) transfer length is listed below. For identical beams listed below, the prestressing force or the modulus of elasticity may be different.

<b>Beams</b>	<b>Calculated Camber with Transfer Length</b>	<b>Calculated Camber without Transfer Length</b>	<b>Camber with Transfer Length /Camber without transfer length)*100</b>	<b>Difference</b>	<b>Percent Difference</b>
BTE 145	3.3346	3.3744	98.82	-0.0398	-1.19
BTE 145	3.4434	3.4837	98.84	-0.0403	-1.16
BTE 145	3.4287	3.4694	98.83	-0.0407	-1.18
BTE 110	1.7705	1.7893	98.95	-0.0188	-1.05
BTE 110	1.6550	1.6724	98.96	-0.0174	-1.04
BTE 110	1.7076	1.7256	98.96	-0.0180	-1.05
BTD 135	3.3593	3.4086	98.55	-0.0493	-1.46
BTD 135	3.6779	3.7324	98.54	-0.0545	-1.47
BTD 135	3.6608	3.7150	98.54	-0.0542	-1.47
BTD 135	3.5591	3.6112	98.56	-0.0521	-1.45
B 55	0.6997	0.7232	96.74	-0.0236	-3.31
B 55	0.7144	0.7383	96.76	-0.0239	-3.30
B 55	0.7561	0.7799	96.95	-0.0238	-3.10
B 55	0.7711	0.7953	96.96	-0.0242	-3.08
C 80	1.1922	1.2212	97.63	-0.0290	-2.40
C 80	1.3178	1.3491	97.68	-0.0312	-2.34
BTE 90	0.9022	0.9121	98.92	-0.0099	-1.09
BTE 155-1 day curing	3.9459	3.9966	98.73	-0.0506	-1.28
BTE 155-2 days curing	3.9072	3.9550	98.79	-0.0478	-1.22
BTE 155-3 days curing	3.6425	3.6877	98.77	-0.0452	-1.23

BTB 95-2 days curing	3.4682	3.5220	98.47	-0.0538	-1.54
BTB 95-3 days curing	3.3588	3.4106	98.48	-0.0518	-1.53
D 55	0.1851	0.1863	99.34	-0.0012	-0.66
D 55	0.1813	0.1825	99.34	-0.0012	-0.66
D 60	0.2977	0.2993	99.45	-0.0016	-0.55
D 90	1.2422	1.2703	97.79	-0.0280	-2.23
D 90	1.2494	1.2779	97.77	-0.0285	-2.25
D 105	2.1988	2.2307	98.57	-0.0319	-1.44
D 105	2.4965	2.5335	98.54	-0.0370	-1.47
C 67	0.7538	0.7570	99.58	-0.0032	-0.42
C 67	0.6803	0.6833	99.56	-0.0030	-0.44
BTC 45	0.2028	0.2043	99.22	-0.0016	-0.78
BTB 130-2 days curing	3.7476	3.7966	98.71	-0.0490	-1.30
BTB 130-3 days curing	3.5611	3.6086	98.68	-0.0476	-1.33
BTB 100-2 days curing	3.0259	3.0763	98.36	-0.0503	-1.65
BTB 100-3 days curing	2.9533	3.0023	98.37	-0.0490	-1.65
BTB 100-4 days curing	2.8621	2.9116	98.30	-0.0494	-1.71
BTB 100-5 days curing	2.8588	2.9082	98.30	-0.0494	-1.71
D110 1 day curing	2.4413	2.4734	98.70	-0.0321	-1.31
D110 2 days curing	2.4248	2.4568	98.69	-0.0321	-1.31
D110 1 day curing	2.3680	2.3994	98.69	-0.0314	-1.32
D110 2 days curing	2.3593	2.3906	98.69	-0.0313	-1.32
BTE 135-3 days curing	2.8588	2.8904	98.91	-0.0316	-1.10
BTE 135-4 days curing	2.8537	2.8853	98.91	-0.0316	-1.10
SBTD 135-3 days curing	3.5504	3.6020	98.57	-0.0516	-1.44
SBTD 135-4 days curing	3.5445	3.5961	98.57	-0.0515	-1.44
BTC 120-1 day curing	3.6055	3.6587	98.55	-0.0531	-1.46

BTC 120-2 days curing	3.5898	3.6428	98.54	-0.0530	-1.47
BTC 120-3 days curing	3.6026	3.6560	98.54	-0.0533	-1.47

<b>Average</b>	2.2369	2.2697	98.52	- 0.0327557	-1.50
<b>Minimum</b>	0.1813	0.1825	96.74	- 0.0545186	-3.31
<b>Maximum</b>	3.9459	3.9966	99.58	- 0.0012029	-0.42
<b>Plant A</b>	2.4571	2.4927	98.59	- 0.0355806	-1.42
<b>Plant B</b>	2.6843	2.7189	98.78	- 0.0345723	-1.23
<b>Plant C</b>	1.7618	1.7911	98.33	- 0.0293429	-1.69

## C.2. Sacrificial Prestressing Strands

Sacrificial prestressing strands, if unaccounted for, will increase the calculated camber.

Comparing the effect sacrificial prestressing strands have on camber was possible by conducting a parametric study. The calculated camber with and without sacrificial prestressing strands is listed below. For identical beams listed below, the prestressing force or the modulus of elasticity may be different.

<b>Beam</b>	<b>Camber with Sacrificial Strands (inches)</b>	<b>Camber without Sacrificial Strands (inches)</b>	<b>Difference in Camber Between No Sacrificial Strands and Sacrificial Strands (inches)</b>	<b>Percent Difference</b>	<b>(Camber without Sacrificial Prestressing Strands/Camber with Sacrificial Strands)*100</b>
BTE 145	3.3346	3.4882	0.1536	4.50	104.61
BTE 145	3.4434	3.4693	0.0259	0.75	100.75
BTE 145	3.4287	3.5393	0.1107	3.18	103.23
BTE 110	1.7705	1.8437	0.0732	4.05	104.13
BTB 135	3.6779	3.7316	0.0537	1.45	101.46
B 55	0.7561	0.7848	0.0287	3.72	103.79
C 80	1.1922	1.2448	0.0525	4.31	104.40
C 80	1.3178	1.3480	0.0301	2.26	102.29
BTE 90	0.9022	0.9624	0.0602	6.46	106.67
BTE 155-1 Day Curing	3.9459	4.0243	0.0783	1.97	101.99
BTE 155-2 Days Curing	3.9072	3.9870	0.0798	2.02	102.04
BTE 155-3 Days Curing	3.6425	3.7226	0.0801	2.17	102.20
BTB 95	3.4682	3.5630	0.0948	2.70	102.73
D 90	1.2422	1.2689	0.0266	2.12	102.14

D 105	2.1988	2.2279	0.0292	1.32	101.33
BTB 100	3.0259	3.0890	0.0631	2.06	102.08
D110	2.3680	2.3994	0.0314	1.32	101.33
BTE 135	2.8588	2.9119	0.0531	1.84	101.86
SBTD 135	3.5445	3.6065	0.0620	1.73	101.75
BTC 120	3.6055	3.6670	0.0614	1.69	101.70
Average				2.58	102.62
Maximum				6.46	106.67
Minimum				0.75	100.75
Plant A				1.82	101.83
Plant B				3.09	103.15
Plant C				2.58	102.63

### C.3 Prestress Force

The applied prestress force was recorded by precasters and obtained from tensioning sheets. The Iowa Department of Transportation also specifies what the design stresses to be applied to the beams immediately before the transfer of prestress. Comparing the designed and as-built prestress force values allowed researchers to compare the accuracy of applied prestress. For identical beams listed below, the as-built prestressing force or the measured release strengths that affect the modulus of elasticity may be different.

<b>Designed and Applied Prestress</b>				
<b>Beams</b>	<b>Iowa Department of Transportation Designed Prestress (kips)</b>	<b>Applied Prestress (kips)</b>	<b>Difference (kips)</b>	<b>Ratio (Applied Prestress / Designed Prestress)</b>
BTE 145	2213	2190.408	22.592	0.989791234
BTE 145	2213	2201.726	11.274	0.994905558
BTE 145	2213	2179.5501	33.4499	0.984884817
BTE 110	1276	1273.051	2.949	0.997688871
BTD 135	2297	2256.63	40.37	0.982424902
BTD 135	2297	2280.63	16.37	0.992873313
BTD 135	2297	2280.63	16.37	0.992873313
BTD 135	2297	2293.95	3.05	0.998672181
B 55	468	505.15	-37.15	1.079380342
B 55	468	509.87	-41.87	1.089465812
C 80	936	926.91	9.09	0.990288462
C 80	936	936.181	-0.181	1.000193376
BTE 90	851	856.58	-5.58	1.006556992
BTE 155-1 Day Curing	2468	2467.42	0.58	0.999764992
BTE 155-2 Days Curing	2468	2532.17	-64.17	1.02600081
BTE 155-3 Days	2468	2482.111	-14.111	1.005717585

Curing				
BTB 95-2 Days Curing	1786	1833.769	-47.769	1.026746361
BTB 95-3 Days Curing	1786	1831.409	-45.409	1.025424972
D 55	510	516.338	-6.338	1.012427451
D 60	596	609.924	-13.924	1.023362416
D 90	936	909.121	26.879	0.97128312
D 90	936	900.54	35.46	0.962115385
D 105	1362	1381.83	-19.83	1.014559471
D 105	1362	1378.92	-16.92	1.012422907
C 67	766	781.94	-15.94	1.020809399
BTC 45	425	424.915	0.085	0.9998
BTB 130-2 Days Curing	2212	2299.845	-87.845	1.039712929
BTB 130-3 Days Curing	2212	2297.1312	-85.1312	1.038486076
BTB 100-2 Days Curing	1871	1847.68	23.32	0.987536077
BTB 100-3 Days Curing	1871	1846.845	24.155	0.987089792
BTB 100-4 Days Curing	1871	1845.87	25.13	0.98656868
BTB 100-5 Days Curing	1871	1845.36	25.64	0.986296098
D110-1 Day Curing	1446	1454.6646	-8.6646	1.005992116
D110-2 Days Curing	1446	1451.6896	-5.6896	1.003934716
D110-1 Day Curing	1446	1443.485	2.515	0.998260719
D110-2 Days Curing	1446	1440.51	5.49	0.99620332
BTE 135-3 Days Curing	1958	1995.0991	-37.0991	1.018947446
BTE 135-4 Days Curing	1958	1993.44715	-35.44715	1.018103754
BTC 120-1 Day Curing	2127	2193.9151	-66.9151	1.03145985
BTC 120-2 Days Curing	2127	2189.0555	-62.0555	1.029175129
BTC 120-3 Days Curing	2127	2186.21256	-59.21256	1.027838533

<b>Average</b>	-11.0362	1.0087
<b>Standard Deviaton</b>	33.9093	0.0250
<b>Maximum</b>	40.3700	1.0895
<b>Minimum</b>	-87.8450	0.9621
<b>Plant A</b>	-19.5668	1.0086
<b>Plant B</b>	-10.6194	1.0057
<b>Plant C</b>	-0.9753	1.0109



#### C.4 Prestress Losses

The prestress losses will reduce the applied prestress force and affect the calculated camber. Comparing the effect prestress losses have on camber was possible by conducting a parametric study. The calculated camber with and without a prestress losses is listed below. For identical beams listed below, the as-built prestressing force or the measured release strengths that affect the modulus of elasticity may be different.

Beams	Prestress Force Before Losses (kips)	Prestress Force After Losses (kips)	Difference in Prestress without and with losses (kips)	((Prestress with Losses/Prestress without Losses)-1)*100	Camber with Losses (inches)	Camber without Losses (inches)	Difference in Camber without and with losses (inches)	Percent Difference	((Camber with Losses/Camber without Losses)-1)*100
BTE 145	2223.22	2042.99	180.23	8.82	3.3346	3.8819	0.5473	15.17	-14.10
BTE 145	2233.746	2062.17	171.58	8.32	3.4434	4.0037	0.5603	15.05	-13.99
BTE 145	2211.57	2040.32	171.25	8.39	3.4287	3.9967	0.5680	15.30	-14.21
BTE 110	1292.82	1199.71	93.11	7.76	1.7705	1.9949	0.2243	11.92	-11.25
BTD 135	2295.18	2125.88	169.30	7.96	3.3593	3.9142	0.5549	15.26	-14.18
BTD 135	2319.18	2141.45	177.73	8.30	3.6779	4.3110	0.6332	15.85	-14.69
BTD 135	2319.18	2142.14	177.04	8.26	3.6608	4.2879	0.6271	15.78	-14.63
BTD 135	2332.5	2154.74	177.76	8.25	3.5591	4.1624	0.6034	15.63	-14.50
B 55	514.4	486.23	28.17	5.79	0.7561	0.8143	0.0582	7.41	-7.15
B 55	519.46	490.73	28.73	5.85	0.7711	0.8310	0.0599	7.47	-7.20
C 80	942.76	894.37	48.39	5.41	1.1922	1.2904	0.0982	7.91	-7.61
C 80	950.578	902.42	48.16	5.34	1.3178	1.4397	0.1218	8.83	-8.46

BTE 90	870.06	816.78	53.28	6.52	0.9022	0.9903	0.0881	9.31	-8.90
BTE 155-1 Day Curing	2505.84	2311.48	194.36	8.41	3.9459	4.6409	0.6950	16.19	-14.97
BTE 155-2 Days Curing	2578.97	2382.58	196.39	8.24	3.9072	4.5661	0.6589	15.55	-14.43
BTE 155-3 Days Curing	2529.618	2340.94	188.68	8.06	3.6425	4.2523	0.6099	15.45	-14.34
BTB 95-2 Days Curing	1867.659	1720.46	147.20	8.56	3.4682	3.9587	0.4904	13.21	-12.39
BTB 95-3 Days Curing	1867.659	1721.75	145.91	8.47	3.3588	3.8291	0.4703	13.09	-12.28
D 55	523.908	499.21	24.70	4.95	0.1851	0.2009	0.0158	8.20	-7.88
D 60	620.62	585.95	34.67	5.92	0.2977	0.3276	0.0299	9.55	-9.12
D 90	924.086	876.09	48.00	5.48	1.2422	1.3645	0.1223	9.38	-8.96
D 90	915.19	867.26	47.93	5.53	1.2494	1.3745	0.1250	9.53	-9.10
D 105	1405.79	1307.76	98.03	7.50	2.1988	2.4832	0.2844	12.15	-11.45
D 105	1405.79	1300.82	104.97	8.07	2.4965	2.8474	0.3510	13.13	-12.33
C 67	795.6	740.325	55.28	7.47	0.7538	0.8471	0.0934	11.66	-11.02
BTC 45	431.43	412.65	18.78	4.55	0.1976	0.2028	0.0051	2.56	-2.53
BTD 130-2 Days Curing	2337.81	2161.67	176.14	8.15	3.7476	4.3326	0.5850	14.48	-13.50
BTD 130-3 Days Curing	2337.81	2162.15	175.66	8.12	3.5611	4.1289	0.5678	14.77	-13.75
BTB 100-2 Days Curing	1881.35	1800.11	81.24	4.51	3.0259	3.4258	0.3998	12.40	-11.67
BTB 100-3 Days Curing	1881.35	1771.48	109.87	6.20	2.9533	3.3509	0.3976	12.61	-11.86
BTB 100-4 Days Curing	1881.35	1751.16	130.19	7.43	2.8621	3.2498	0.3877	12.69	-11.93
BTB 100-5 Days Curing	1881.35	1750.1	131.25	7.50	2.8588	3.2498	0.3910	12.80	-12.03
D110-1 Day Curing	1477.2196	1371.79	105.43	7.69	2.4413	2.7811	0.3398	13.01	-12.22
D110-2	1477.2196	1367.86	109.36	7.99	2.4248	2.7772	0.3524	13.55	-12.69

[illegible]

### C.5 Release Strength

The release strengths that were measured from various beams at three different precast plants are listed below. Additionally, the designed and measured release strengths are compared to each other.

Plant	Girder Type	Date of Casting	Date of Release	Target $f'_{ci}$	Average of Measured $f'_{ci}$	Target $f'_{ci}$ / Measured $f'_{ci}$	Percent Difference of Target and Measured $f'_{ci}$
Plant C	D90	9/13/2011	9/14/2011	4500	8000	0.5625	77.7778
Plant C	D90	9/13/2011	9/14/2011	4500	8000	0.5625	77.7778
Plant C	D90	9/13/2011	9/14/2011	4500	8000	0.5625	77.7778
Plant C	D90	9/15/2011	9/16/2011	4500	6823.33	0.6595	51.6296
Plant C	D90	9/15/2011	9/16/2011	4500	6823.33	0.6595	51.6296
Plant C	D90	9/15/2011	9/16/2011	4500	6823.33	0.6595	51.6296
Plant A	D110	9/16/2011	9/17/2011	6500	7170.67	0.90647	10.3179
Plant A	D110	9/16/2011	9/17/2011	6500	7170.67	0.90647	10.3179
Plant A	D110	9/16/2011	9/17/2011	6500	7170.67	0.90647	10.3179
Plant A	D110	9/15/2011	9/17/2011	6500	7170.67	0.90647	10.3179
Plant C	D90	9/19/2011	9/20/2011	4500	5926.67	0.75928	31.7037
Plant C	D90	9/19/2011	9/20/2011	4500	5926.67	0.75928	31.7037
Plant C	D90	9/19/2011	9/20/2011	4500	5926.67	0.75928	31.7037
Plant C	D90	9/20/2011	9/21/2011	4500	5630	0.79929	25.1111
Plant C	D90	9/20/2011	9/21/2011	4500	5630	0.79929	25.1111

Plant C	D90	9/20/2011	9/21/2011	4500	5630	0.79929	25.1111
Plant A	D110	9/23/2011	9/24/2011	6500	7413.67	0.87676	14.0564
Plant A	D110	9/23/2011	9/24/2011	6500	7413.67	0.87676	14.0564
Plant A	D110	9/23/2011	9/24/2011	6500	7413.67	0.87676	14.0564
Plant A	D110	9/22/2011	9/24/2011	6500	7413.67	0.87676	14.0564
Plant A	BTC45	10/7/2011	10/8/2011	4500	6936.67	0.64873	54.1481
Plant A	BTC45	10/7/2011	10/8/2011	4500	6936.67	0.64873	54.1481
Plant A	BTC120	10/21/2011	10/24/2011	8000	8505	0.94062	6.3125
Plant A	BTC120	10/21/2011	10/24/2011	8000	8505	0.94062	6.3125
Plant A	BTD130	10/28/2011	10/31/2011	8000	8220	0.97324	2.75
Plant A	BTD130	10/29/2011	10/31/2011	8000	7755	1.03159	-3.0625
Plant C	C67	10/31/2011	11/1/2011	4500	6151.67	0.73151	36.7037
Plant C	C67	10/31/2011	11/1/2011	4500	6151.67	0.73151	36.7037
Plant C	C67	10/31/2011	11/1/2011	4500	6151.67	0.73151	36.7037
Plant C	C67	11/3/2011	11/4/2011	4500	4893.33	0.91962	8.74074
Plant C	C67	11/3/2011	11/4/2011	4500	4893.33	0.91962	8.74074
Plant C	C67	11/3/2011	11/4/2011	4500	4893.33	0.91962	8.74074
Plant A	BTE135	11/8/2011	11/12/2011	7000	7450	0.9396	6.42857
Plant A	BTE135	11/9/2011	11/12/2011	7000	7450	0.9396	6.42857
Plant C	D105	11/29/2011	11/30/2011	6000	6421.67	0.93434	7.02778
Plant C	D105	11/29/2011	11/30/2011	6000	6421.67	0.93434	7.02778
Plant C	D105	11/29/2011	11/30/2011	6000	6421.67	0.93434	7.02778
Plant C	D105	12/6/2011	12/8/2011	6000	8643.33	0.69418	44.0556

Plant C	D105	12/6/2011	12/8/2011	6000	8643.33	0.69418	44.0556
Plant C	D105	12/6/2011	12/8/2011	6000	8643.33	0.69418	44.0556
Plant C	D55	12/20/2011	12/21/2011	4500	6528.33	0.6893	45.0741
Plant C	D55	12/20/2011	12/21/2011	4500	6528.33	0.6893	45.0741
Plant C	D55	12/20/2011	12/21/2011	4500	6528.33	0.6893	45.0741
Plant C	D55	12/20/2011	12/21/2011	4500	6528.33	0.6893	45.0741
Plant C	D55	12/20/2011	12/21/2011	4500	6528.33	0.6893	45.0741
Plant C	D55	12/29/2011	12/30/2011	4500	6831.67	0.6587	51.8148
Plant C	D55	12/29/2011	12/30/2011	4500	6831.67	0.6587	51.8148
Plant C	D60	1/3/2011	1/4/2011	4500	5348.33	0.84138	18.8519
Plant C	D60	1/3/2011	1/4/2011	4500	5348.33	0.84138	18.8519
Plant C	D105	-	-	6000	6240	0.96154	4
Plant C	D105	-	-	6000	6240	0.96154	4
Plant C	D105	-	-	6000	6240	0.96154	4
Plant C	D105	-	-	6000	9623.33	0.62348	60.3889
Plant C	D105	-	-	6000	9623.33	0.62348	60.3889
Plant C	D105	-	-	6000	9623.33	0.62348	60.3889
Plant C	D60	-	-	4500	7683.33	0.58568	70.7407
Plant C	D60	-	-	4500	7683.33	0.58568	70.7407
Plant C	D60	-	-	4500	7683.33	0.58568	70.7407
Plant C	D60	-	12/13/2011	4500	7683.33	0.58568	70.7407
Plant C	D60	-	12/13/2011	4500	7683.33	0.58568	70.7407
Plant C	D60	-	-	4500	9056.67	0.49687	101.259
Plant C	D60	-	-	4500	9056.67	0.49687	101.259

Plant C	D60	-	-	4500	9056.67	0.49687	101.259
Plant C	D60	-	-	4500	9056.67	0.49687	101.259
Plant C	D60	-	-	4500	9056.67	0.49687	101.259
Plant C	D55	-	-	4500	6158.33	0.73072	36.8519
Plant C	D55	-	-	4500	6158.33	0.73072	36.8519
Plant C	D55	-	-	4500	6158.33	0.73072	36.8519
Plant C	D55	-	-	4500	6158.33	0.73072	36.8519
Plant C	D55	-	-	4500	6158.33	0.73072	36.8519
Plant C	C80	1/18/2012	1/23/2012	5000			
Plant C	C80	1/18/2012	1/23/2012	5000			
Plant C	C80	1/18/2012	1/23/2012	5000			
Plant B	BTE155	1/28/2012	1/30/2012	8000	9633.33	0.83045	20.4167
Plant B	BTE155	1/28/2012	1/30/2012	8000	9633.33	0.83045	20.4167
Plant B	BTE155	2/1/2012	2/2/2012	8000	8121	0.9851	1.5125
Plant B	BTE155	2/1/2012	2/2/2012	8000	8121	0.9851	1.5125
Plant B	BTE155	2/3/2012	2/6/2012	8000	10357.7	0.77237	29.4708
Plant B	BTE155	2/3/2012	2/6/2012	8000	10357.7	0.77237	29.4708
Plant C	B55	2/9/2012	2/10/2012	6000	6480	0.92593	8
Plant C	B55	2/9/2012	2/10/2012	6000	6480	0.92593	8
Plant C	B55	2/9/2012	2/10/2012	6000	6480	0.92593	8
Plant C	B55	2/9/2012	2/10/2012	6000	6480	0.92593	8
Plant C	B55	2/13/2012	2/14/2012	6000	6391.67	0.93872	6.52778
Plant C	B55	2/13/2012	2/14/2012	6000	6391.67	0.93872	6.52778
Plant C	B55	2/13/2012	2/14/2012	6000	6391.67	0.93872	6.52778

Plant C	B55	2/13/2012	2/14/2012	6000	6391.67	0.93872	6.52778
Plant A	BTC120	2/23/2012	2/25/2012	8000	8610	0.92915	7.625
Plant A	BTC120	2/23/2012	2/25/2012	8000	8610	0.92915	7.625
Plant A	BTC120	2/24/2012	2/25/2012	8000	8610	0.92915	7.625
Plant B	BTB95	2/25/2012	2/27/2012	8000	9081.67	0.8809	13.5208
Plant B	BTB95	2/24/2012	2/27/2012	8000	9081.67	0.8809	13.5208
Plant B	BTE 110	3/7/2012	3/8/2012	5000	6089.67	0.82106	21.7933
Plant B	BTE 110	3/7/2012	3/8/2012	5000	6089.67	0.82106	21.7933
Plant B	BTE 110	3/7/2012	3/8/2012	5000	6089.67	0.82106	21.7933
Plant B	BTE 110	3/13/2012	3/14/2012	5000	5598.33	0.89312	11.9667
Plant B	BTE 110	3/13/2012	3/14/2012	5000	5598.33	0.89312	11.9667
Plant B	BTE 110	3/13/2012	3/14/2012	5000	5598.33	0.89312	11.9667
Plant B	BTE 110	3/22/2012	3/23/2012	5000	6550	0.76336	31
Plant B	BTE 110	3/22/2012	3/23/2012	5000	6550	0.76336	31
Plant B	BTE 110	3/22/2012	3/23/2012	5000	6550	0.76336	31
Plant A	BTB 100	3/28/2012	4/2/2012	8000	10324.3	0.77487	29.0542
Plant A	BTB 100	3/29/2012	4/2/2012	8000	10324.3	0.77487	29.0542
Plant A	BTB 100	3/30/2012	4/2/2012	8000	10324.3	0.77487	29.0542
Plant A	BTB 100	3/31/2012	4/2/2012	8000	10324.3	0.77487	29.0542
Plant C	C 80	4/11/2012	4/13/2012	5000	9885	0.50582	97.7
Plant C	C 80	4/11/2012	4/13/2012	5000	9885	0.50582	97.7
Plant C	C 80	4/11/2012	4/13/2012	5000	9885	0.50582	97.7
Plant C	C 80	4/11/2012	4/13/2012	5000	9885	0.50582	97.7
Plant B	BTE 90	4/16/2012	4/17/2012	5000	5013.33	0.99734	0.26667



Plant B	BTE 90	4/16/2012	4/17/2012	5000	5013.33	0.99734	0.26667
Plant B	BTE 90	4/16/2012	4/17/2012	5000	5013.33	0.99734	0.26667
Plant A	C 80	5/9/2012	5/10/2012	5000	7373.33	0.67812	47.4667
Plant A	C 80	5/9/2012	5/10/2012	5000	7373.33	0.67812	47.4667
Plant A	C 80	5/9/2012	5/10/2012	5000	7373.33	0.67812	47.4667
Plant A	SBTD13 5	5/31/2012	6/4/2012	8000	8236.67	0.97127	2.95833
Plant A	SBTD13 5	6/1/2012	6/4/2012	8000	8236.67	0.97127	2.95833
Plant A	SBTD13 5	6/1/2012	6/4/2012	8000	8236.67	0.97127	2.95833
Plant B	BTE 145	6/26/2012	6/27/2012	7500	8065.67	0.92987	7.54222
Plant B	BTE 145	6/26/2012	6/27/2012	7500	8065.67	0.92987	7.54222
Plant B	BTE 145	6/28/2012	6/29/2012	7500	7749.67	0.96778	3.32889
Plant B	BTE 145	6/28/2012	6/29/2012	7500	7749.67	0.96778	3.32889
Plant C	BTD 135	7/3/2012	7/5/2012	8000	9674.33	0.82693	20.9292
Plant C	BTD 135	7/3/2012	7/5/2012	8000	9674.33	0.82693	20.9292
Plant C	BTD 135	7/10/2012	7/11/2012	8000	8218.33	0.97343	2.72917
Plant C	BTD 135	7/10/2012	7/11/2012	8000	8218.33	0.97343	2.72917
Plant C	BTD 135	7/16/2012	7/18/2012	8000	8991.67	0.88971	12.3958
Plant C	BTD 135	7/16/2012	7/18/2012	8000	8991.67	0.88971	12.3958
Plant C	BTD 135	7/18/2012	7/19/2012	8000	8118.33	0.98542	1.47917
Plant C	BTD 135	7/18/2012	7/19/2012	8000	8118.33	0.98542	1.47917
Plant B	BTE 145	7/24/2012	7/25/2012	7500	8120.67	0.92357	8.27556
Plant B	BTE 145	7/24/2012	7/25/2012	7500	8120.67	0.92357	8.27556

C.6 Compressive Strengths

A summary of the designed and measured release strengths is listed below.

Design Release Strength										
	4500	5000	5500	6000	6500	7000	7500	8000	8500	
Plant A										
Average	6936.66	7373.33			7292.17	7450		8915.88		
Standard Dev.	-	-			129.89	-		951.48		
Plant B										
Average		5812.83					7978.67	9298.42		
Standard Dev.		596.64					179.08	873.00		
Plant C										
Average	6269.51	9885		6905.83				8750.67		
Standard Dev.	874.22	-		942.29				674.95		
Total										
Average	6315.52	6916.53		6905.83	7292.17	7450	7978.67	8874.99		
Standard Dev.	859.81	1738.56		942.29	129.89	-	179.08	804.57		

### C.7 Moment of Inertia

Calculating camber using different moment of inertia values were conducted for five different beams. The calculated camber, percent difference, and the error associated with moment of inertia was evaluated using a parametric study.

<b>Camber (inches)</b>				
<b>Beam</b>	<b><math>I_{tr}</math> along the Length of the beam</b>	<b><math>I_{tr}</math> at the Midspan of the PPCB</b>	<b><math>I_{tr}</math> at the End of the PPCB</b>	<b><math>I_g</math></b>
<b>B55</b>	0.7433	0.7327	0.7319	0.7599
<b>C80</b>	1.4328	1.4090	1.3989	1.4694
<b>BTE 110</b>	1.5519	1.5151	1.5033	1.6014
<b>BTD 135</b>	4.0420	3.9395	3.8786	4.1941
<b>BTE 145</b>	3.4930	3.4044	3.3335	3.5963

<b>Percent Difference with <math>I_{tr}</math> Along the Length of the Beam</b>			
<b>Beam</b>	<b><math>I_{tr}</math> at the Midspan of the PPCB</b>	<b><math>I_{tr}</math> at the End of the PPCB</b>	<b><math>I_g</math></b>
<b>55</b>	-1.44	-1.54	2.21
<b>C80</b>	-1.68	-2.39	2.52
<b>BTE 110</b>	-2.40	-3.18	3.14
<b>BTD 135</b>	-2.57	-4.13	3.69
<b>BTE 145</b>	-2.57	-4.67	2.91

<b>Error with <math>I_{tr}</math> at Midspan</b>	<b>Error with <math>I_{tr}</math> at end</b>	<b>Error with <math>I_g</math></b>
98.58	98.47	102.24
98.34	97.63	102.55
97.63	96.87	103.19
97.46	98.45	108.13
97.46	95.43	102.96

### C.8. Analytical, Measured, and Designed Camber

The analytical camber was calculated for various beams based on material properties and prestress force. Using 3 different modulus of elasticity's allowed researchers to determine which method gave the best agreement with the measured values. The design camber that was specified by the Iowa Department of Transportation was calculated using the moment area method from CONSPAN and is listed below. The measured camber value was taken by a rotary laser level. Certain beams measured friction and while others estimated the friction values. Additionally, the analytical camber was calculated by using the as-built tensioning values and also adjusting the modulus of elasticity by  $\pm 20\%$  to determine the upper and lower bound.

Plant	Girder Type	Date of Release	Analytical Camber (inches)		Design Camber (inches)		Measured Camber (inches)		Analytical Camber (inches)	
			(Eci found from creep frames using plant cylinders)	(Eci found from AASHTO using plant $f_{ci}$ values)	(Eci found from AASHTO using ISU's lab $f_{ci}$ values)	Iowa DOT (Adjusted)	Instantaneous Camber (support accounts for)	Camber based on Estimated friction value from Non-linear analysis	Upper Bound Camber based on +20% increase in Modulus	Upper Bound Camber based on -20% increase in Modulus
Plant C	D90	9/14/2011	1.14842	1.24224	1.1761	1.4		0.98732	1.541356	1.07964
Plant C	D90	9/14/2011	1.14842	1.24224	1.1761	1.4		1.11232	1.541356	1.07964
Plant C	D90	9/14/2011	1.14842	1.24224	1.1761	1.4		1.23732	1.541356	1.07964

Plant C	D90	9/16/2011	1.14842	1.24224	1.1761	1.4	1.4		1.50832	1.541356	1.07964
Plant C	D90	9/16/2011	1.14842	1.24224	1.1761	1.4	1.4		1.41432	1.541356	1.07964
Plant C	D90	9/16/2011	1.14842	1.24224	1.1761	1.4	1.4		1.04932	1.541356	1.07964
Plant A	D110	9/17/2011	3.01285	2.44128	2.48511	2.83	2.83		2.42157	3.181072	2.201423
Plant A	D110	9/17/2011	3.01285	2.44128	2.48511	2.83	2.83		2.34857	3.181072	2.201423
Plant A	D110	9/17/2011	3.01285	2.44128	2.48511	2.83	2.83		2.72357	3.181072	2.201423
Plant A	D110	9/17/2011	3.0014	2.42476	2.47583	2.83	2.83		2.44257	3.181072	2.201423
Plant C	D90	9/20/2011	1.14842	1.24224	1.1761	1.4	1.4		1.45632	1.541356	1.07964
Plant C	D90	9/20/2011	1.14842	1.24224	1.1761	1.4	1.4		1.19532	1.541356	1.07964
Plant C	D90	9/20/2011	1.14842	1.24224	1.1761	1.4	1.4		1.37232	1.541356	1.07964
Plant C	D90	9/21/2011	1.12934	1.24941	1.15654	1.4	1.4		1.51832	1.541356	1.07964
Plant C	D90	9/21/2011	1.12934	1.24941	1.15654	1.4	1.4		1.37232	1.541356	1.07964
Plant C	D90	9/21/2011	1.12934	1.24941	1.15654	1.4	1.4		1.32032	1.541356	1.07964
Plant A	D110	9/24/2011	2.97063	2.36796	2.4509	2.83	2.83		2.56757	3.181072	2.201423
Plant A	D110	9/24/2011	2.97063	2.36796	2.4509	2.83	2.83		2.44257	3.181072	2.201423
Plant A	D110	9/24/2011	2.97063	2.36796	2.4509	2.83	2.83		2.55657	3.181072	2.201423
Plant A	D110	9/24/2011	2.95952	2.35929	2.4419	2.83	2.83		2.50457	3.181072	2.201423
Plant A	BTC45	10/8/2011	0.25747	0.20276	0.20448	0.26	0.23		0.30737	0.23589	0.159993
Plant A	BTC45	10/8/2011	0.25747	0.20276	0.20448	0.26	0.23		0.2342	0.23589	0.159993
Plant A	BTC120	10/24/2011	4.69817	3.60264	3.92619	3.82	3.45		3.54294	4.506432	3.11249
Plant A	BTC120	10/24/2011	4.69817	3.60264	3.92619	3.82	3.45		3.38694	4.506432	3.11249
Plant A	BTD130	10/31/2011	4.61053	3.74759	3.84208	3.91	3.33		3.14833	4.4497	3.073178
Plant A	BTD130	10/31/2011	4.59852	3.56107	3.83228	3.91	3.33		2.73133	4.4497	3.073178
Plant C	C67	11/1/2011	0.71004	0.75378	0.72651	0.92	0.92		0.87216	0.908362	0.653078
Plant C	C67	11/1/2011	0.71004	0.75378	0.72651	0.92	0.92		0.89316	0.908362	0.653078
Plant C	C67	11/1/2011	0.71004	0.75378	0.72651	0.92	0.92		1.02816	0.908362	0.653078
Plant C	C67	11/4/2011	0.71004	0.75378	0.72651	0.92	0.92		1.07016	0.908362	0.653078
Plant C	C67	11/4/2011	0.71004	0.75378	0.72651	0.92	0.92		1.15316	0.908362	0.653078

Plant C	C67	11/4/2011	0.71004	0.75378	0.72651	0.92	0.92		0.97616	0.908362	0.653078
Plant A	BTE135	11/12/2011	3.5631	2.85885	2.95679	3.2	2.83		2.86985	3.581174	2.47861
Plant A	BTE135	11/12/2011	3.56971	2.85368	2.96216	3.2	2.83		3.02585	3.581174	2.47861
Plant C	D105	11/30/2011	2.39855	2.49646	2.45131	2.42	2.42		2.94665	2.68271	1.904305
Plant C	D105	11/30/2011	2.39855	2.49646	2.45131	2.42	2.42		2.69665	2.68271	1.904305
Plant C	D105	11/30/2011	2.39855	2.49646	2.45131	2.42	2.42		3.08665	2.68271	1.904305
Plant C	D105	12/8/2011	2.38997	2.19876	2.44339	2.42	2.42		2.36665	2.68271	1.904305
Plant C	D105	12/8/2011	2.38997	2.19876	2.44339	2.42	2.42		2.36665	2.68271	1.904305
Plant C	D105	12/8/2011	2.38997	2.19876	2.44339	2.42	2.42		2.62665	2.68271	1.904305
Plant C	D55	12/21/2011	0.17841	0.18506	0.18283	0.24	0.24		0.38424	0.22087	0.154893
Plant C	D55	12/21/2011	0.17841	0.18506	0.18283	0.24	0.24		0.36424	0.22087	0.154893
Plant C	D55	12/21/2011	0.17841	0.18506	0.18283	0.24	0.24		0.48424	0.22087	0.154893
Plant C	D55	12/21/2011	0.17841	0.18506	0.18283	0.24	0.24		0.34424	0.22087	0.154893
Plant C	D55	12/21/2011	0.17841	0.18506	0.18283	0.24	0.24		0.32424	0.22087	0.154893
Plant C	D55	12/30/2011	0.17841	0.18128	0.18283	0.24	0.24		0.37424	0.22087	0.154893
Plant C	D55	12/30/2011	0.17841	0.18128	0.18283	0.24	0.24		0.43424	0.22087	0.154893
Plant C	D60	1/4/2011	0.26269	0.29772	0.2691	0.35	0.35		0.66524	0.358612	0.254216
Plant C	D60	1/4/2011	0.26269	0.29772	0.2691	0.35	0.35		0.68524	0.358612	0.254216
Plant C	D105	-	2.39855	2.49646	2.45131	2.42	2.42			2.68271	1.904305
Plant C	D105	-	2.39855	2.49646	2.45131	2.42	2.42			2.68271	1.904305
Plant C	D105	-	2.39855	2.49646	2.45131	2.42	2.42			2.68271	1.904305
Plant C	D105	-	2.38997	2.19876	2.44339	2.42	2.42			2.68271	1.904305
Plant C	D105	-	2.38997	2.19876	2.44339	2.42	2.42			2.68271	1.904305
Plant C	D105	-	2.38997	2.19876	2.44339	2.42	2.42			2.68271	1.904305
Plant C	D60	-	0.26269	0.29772	0.2691	0.35	0.35			0.358612	0.254216
Plant C	D60	-	0.26269	0.29772	0.2691	0.35	0.35			0.358612	0.254216
Plant C	D60	-	0.26269	0.29772	0.2691	0.35	0.35			0.358612	0.254216
Plant C	D60	12/13/2011	0.26269	0.29772	0.2691	0.35	0.35			0.358612	0.254216

Plant C	D60	12/13/2011	0.26269	0.29772	0.2691	0.35	0.35			0.358612	0.254216
Plant C	D60	-	0.26269	0.29772	0.2691	0.35	0.35			0.358612	0.254216
Plant C	D60	-	0.26269	0.29772	0.2691	0.35	0.35			0.358612	0.254216
Plant C	D60	-	0.26269	0.29772	0.2691	0.35	0.35			0.358612	0.254216
Plant C	D60	-	0.26269	0.29772	0.2691	0.35	0.35			0.358612	0.254216
Plant C	D60	-	0.26269	0.29772	0.2691	0.35	0.35			0.358612	0.254216
Plant C	D55	-	0.17841	0.18506	0.18283	0.24	0.24			0.22087	0.154893
Plant C	D55	-	0.17841	0.18128	0.18283	0.24	0.24			0.22087	0.154893
Plant C	D55	-	0.17841	0.18506	0.18283	0.24	0.24			0.22087	0.154893
Plant C	D55	-	0.17841	0.18128	0.18283	0.24	0.24			0.22087	0.154893
Plant C	D55	-	0.17841	0.18128	0.18283	0.24	0.24			0.22087	0.154893
Plant C	C80	1/23/2012				1.64	1.64		1.43783		
Plant C	C80	1/23/2012				1.64	1.64		1.52783		
Plant C	C80	1/23/2012				1.64	1.64		1.63783		
Plant B	BTE155	1/30/2012	5.03377	3.90717	4.28159	4.16	3.72		3.80277	4.797646	3.489251
Plant B	BTE155	1/30/2012	5.03377	3.90717	4.28159	4.16	3.72		3.98277	4.797646	3.489251
Plant B	BTE155	2/2/2012	4.75375	3.94592	4.049	4.16	3.72		3.96277	4.800951	3.527707
Plant B	BTE155	2/2/2012	4.75375	3.94592	4.049	4.16	3.72		4.07277	4.800951	3.527707
Plant B	BTE155	2/6/2012	4.81943	3.64248	4.1036	4.16	3.72		3.36277	4.451865	3.233647
Plant B	BTE155	2/6/2012	4.81943	3.64248	4.1036	4.16	3.72		4.06277	4.451865	3.233647
Plant C	B55	2/10/2012	0.72579	0.75611	0.74405	0.85	0.85	1.10037		0.860439	0.593336
Plant C	B55	2/10/2012	0.72579	0.75611	0.74405	0.85	0.85	1.30037		0.860439	0.593336
Plant C	B55	2/10/2012	0.72579	0.75611	0.74405	0.85	0.85	1.12037		0.860439	0.593336
Plant C	B55	2/10/2012	0.72579	0.75611	0.74405	0.85	0.85	1.05037		0.860439	0.593336
Plant C	B55	2/14/2012	0.73559	0.77114	0.7541	0.85	0.85	0.93		0.860439	0.593336
Plant C	B55	2/14/2012	0.73559	0.77114	0.7541	0.85	0.85	0.88037		0.860439	0.593336
Plant C	B55	2/14/2012	0.73559	0.77114	0.7541	0.85	0.85	0.89037		0.860439	0.593336
Plant C	B55	2/14/2012	0.73559	0.77114	0.7541	0.85	0.85	0.92997		0.860439	0.593336



Plant A	BTC120	2/25/2012	4.71061	3.5898	3.93635	3.82	3.45		2.99094	4.506433	3.112494
Plant A	BTC120	2/25/2012	4.71061	3.5898	3.93635	3.82	3.45		3.09094	4.506433	3.112494
Plant A	BTC120	2/25/2012	4.73188	3.60551	3.95372	3.82	3.45		3.16094	4.506433	3.112494
Plant B	BTB95	2/27/2012	4.33	3.46822	3.62515	3.61	3.07	2.7584		4.28322	3.052014
Plant B	BTB95	2/27/2012	4.32069	3.3588	3.61727	3.61	3.07	2.2884		4.150845	2.951146
Plant B	BTE										
Plant B	110	3/8/2012	1.52633	1.65498	1.54445	1.9	1.61	1.7838		2.09694	1.48248
Plant B	BTE										
Plant B	110	3/8/2012	1.52633	1.65498	1.54445	1.9	1.61	1.33188		2.09694	1.48248
Plant B	BTE										
Plant B	110	3/8/2012	1.52633	1.65498	1.54445	1.9	1.61	1.4938		2.09694	1.48248
Plant B	BTE										
Plant B	110	3/14/2012	1.52633	1.77053	1.54445	1.9	1.61	1.5338		2.09694	1.48248
Plant B	BTE										
Plant B	110	3/14/2012	1.52633	1.77053	1.54445	1.9	1.61	1.5938		2.09694	1.48248
Plant B	BTE										
Plant B	110	3/14/2012	1.52633	1.77053	1.54445	1.9	1.61	1.5488		2.09694	1.48248
Plant B	BTE										
Plant B	110	3/23/2012	1.52633	1.70758	1.54445	1.9	1.61	1.33188		2.09694	1.48248
Plant B	BTE										
Plant B	110	3/23/2012	1.52633	1.70758	1.54445	1.9	1.61	1.31188		2.09694	1.48248
Plant B	BTE										
Plant B	110	3/23/2012	1.52633	1.70758	1.54445	1.9	1.61	1.13188		2.09694	1.48248
Plant A	BTB										
Plant A	100	4/2/2012	4.06328	2.85877	3.37745	3.19	3.19	2.88		3.72583	2.55496
Plant A	BTB										
Plant A	100	4/2/2012	4.0682	2.86212	3.38146	3.19	3.19	2.74		3.72583	2.55496
Plant A	BTB										
Plant A	100	4/2/2012	4.20203	2.95328	3.49054	3.19	3.19	2.7		3.72583	2.55496
Plant A	BTB										
Plant A	100	4/2/2012	4.30824	3.02593	3.57735	3.19	3.19	2.83		3.72583	2.55496
Plant C	C 80	4/13/2012	1.38666	1.20226	1.42038	1.64	1.64	1.3161		1.500423	1.037038
Plant C	C 80	4/13/2012	1.38666	1.20226	1.42038	1.64	1.64	1.3365		1.500423	1.037038
Plant C	C 80	4/13/2012	1.38666	1.20226	1.42038	1.64	1.64	1.5121		1.500423	1.037038

Plant C	C 80	4/13/2012	1.38666	1.20226	1.42038	1.64	1.64	1.1325		1.500423	1.037038
Plant B	BTE 90	4/17/2012	0.73407	0.90219	0.74324	0.92	0.78	0.821		1.123412	0.782302
Plant B	BTE 90	4/17/2012	0.73407	0.90219	0.74324	0.92	0.78	0.727		1.123412	0.782302
Plant B	BTE 90	4/17/2012	0.73407	0.90219	0.74324	0.92	0.78	0.841		1.123412	0.782302
Plant A	C 80	5/10/2012	1.72962	1.31785	1.39819	1.64	1.64	1.11			
Plant A	C 80	5/10/2012	1.72962	1.31785	1.39819	1.64	1.64	1.12			
Plant A	C 80	5/10/2012	1.72962	1.31785	1.39819	1.64	1.64	1.18			
Plant A	SBTD1 35	6/4/2012	4.55105	3.54452	3.81178	4.2	3.57	3.43		4.70383	3.25464
Plant A	SBTD1 35	6/4/2012	4.55887	3.5504	3.81178	4.2	3.57	3.48		4.70383	3.25464
Plant A	SBTD1 35	6/4/2012	4.55887	3.5504	3.81178	4.2	3.57	2.94		4.70383	3.25464
Plant B	BTE 145	6/27/2012	4.173	3.443	3.57	3.7	3.29	3.8006		4.154767	3.01734
Plant B	BTE 145	6/27/2012	4.173	3.443	3.57	3.7	3.29	3.5806		4.154767	3.01734
Plant B	BTE 145	6/29/2012	4.089	3.429	3.5	3.7	3.29	3.5318		4.2168	3.067566
Plant B	BTE 145	6/29/2012	4.089	3.429	3.5	3.7	3.29	3.6818		4.2168	3.067566
Plant C	BTD 135	7/5/2012	3.78322	3.35927	3.85896	4.2	3.57	3.8236		4.088425	2.991263
Plant C	BTD 135	7/5/2012	3.78322	3.35927	3.85896	4.2	3.57	3.8284		4.088425	2.991263
Plant C	BTD 135	7/11/2012	3.87284	3.66078	3.95061	4.2	3.57	4.01087		4.088425	2.991263
Plant C	BTD 135	7/11/2012	3.87284	3.66078	3.95061	4.2	3.57	4.0168		4.088425	2.991263
Plant C	BTD 135	7/18/2012	3.8976	3.55908	3.97592	4.2	3.57	4.01934		4.088425	2.991263
Plant C	BTD 135	7/18/2012	3.8976	3.55908	3.97592	4.2	3.57	3.9425		4.088425	2.991263
Plant C	BTD 135	7/19/2012	3.87284	3.67786	3.95061	4.2	3.57	4.39082		4.088425	2.991263



### C.9 Effect of Camber by $f'_{ci}$

Camber is affected by the modulus of elasticity. When calculating camber using the AASHTO LRFD method, the release strength affects the modulus of elasticity. Determining the effect of increasing the release strength has on camber was conducted with the following graphs.

	$I_{tr}$	Design $f'_{ci}$	Design $E_{ci}$	Deflection Due to Prestress	Deflection Due to the Beam Self- Weight	Camber Value
BTE 145	439193	7500	5034.93	7.4670	3.8159	3.6511
BTE 145	439193	sample of ACI 363 for modulus	4464	8.4221	4.3040	4.1181
BTE 110	430402	5000	3960.6	3.5692	1.6179	1.9513
BTB 95-2days	102330	8000	5200.05	6.0584	2.3302	3.7282
BTE 90	426254	5000	3960.6	1.7022	0.7399	0.9623
BTE 155-1 day	439864	8000	5200.05	8.9982	4.8057	4.1925
BTD 135	295328	8000	5265.96	7.6171	3.8228	3.7943
B 55	62696.5	6000	4560.46	1.0299	0.3024	0.7275
D 55	217262	4500	3949.47	0.3838	0.1683	0.2156
D 60	218225	4500	3949.47	0.5560	0.2359	0.3202
D 90	218999	4500	3949.47	2.5962	1.1640	1.4322
D 105	222751	6000	4560.46	4.4196	1.8246	2.5951
C 67	119744	4500	3949.47	1.4661	0.6040	0.8620
C 80-Polk County	117952	5000	4163.11	2.8132	1.1374	1.6758
BTC 45	179599	4500	4166.88	0.3359	0.1015	0.2344
BTD 130	294584	8000	5555.84	6.9235	3.2425	3.6810
BTB 100-2 days	102227	8000	5555.84	6.1685	2.7935	3.3750
D 110	222411	6500	5007.97	4.6668	2.0737	2.5931
BTE 135-3 days	433871	7000	5197.02	5.9472	2.9467	3.0006
SBTD 135-3 days	294841	8000	5555.84	7.5069	3.6081	3.8988
BTC 120-1 day	184299	8000	5555.84	7.2957	3.4879	3.8078
C80-Plant A	119027	5000	4392.28	2.6624	1.1072	1.5552
sample of ACI 363 for modulus	439193	sample of ACI 363 for modulus	4464	8.4221	4.3040	4.1181

<b>5% Increase in <math>f'_{ci}</math></b>	<b>5% Increase in <math>E_{ci}</math></b>	<b>Deflection Due to Prestress</b>	<b>Deflection Due to the Beam Self- Weight</b>	<b>Camber Value</b>	<b>Percent of Design Release Camber</b>
7875	5159.27	7.2953	3.7240	3.5714	97.82
	4549	8.2740	4.2235	4.0505	98.36
5250	4058.4	3.4871	1.5789	1.9082	97.79
8400	5328.47	5.9189	2.2740	3.6449	97.77
5250	4058.4	1.6626	0.7221	0.9405	97.74
8400	5328.47	8.7913	4.6899	4.1015	97.83
8400	5396.01	7.4421	3.7307	3.7115	97.82
6300	4673.08	1.0060	0.2951	0.7109	97.72
4725	4047.01	0.3751	0.1642	0.2109	97.82
4725	4047.01	0.5434	0.2302	0.3133	97.84
4725	4047.01	2.5360	1.1359	1.4000	97.75
6300	4673.08	4.3187	1.7806	2.5381	97.81
4725	4047.01	1.4335	0.5895	0.8440	97.91
5250	4265.92	2.7479	1.1100	1.6379	97.74
4725	4269.78	0.3280	0.0990	0.2290	97.71
8400	5693.05	6.7641	3.1644	3.5997	97.79
8400	5693.05	6.0262	2.7262	3.3000	97.78
6825	5131.64	4.5601	2.0238	2.5363	97.81
7350	5325.36	5.8102	2.8756	2.9346	97.80
8400	5693.05	7.3343	3.5212	3.8132	97.80
8400	5693.05	7.1278	3.4039	3.7239	97.80
5250	4500.75	2.6008	1.0805	1.5203	97.76
	4549	8.2740	4.2235	4.0505	98.36
				<b>Average</b>	<b>97.82</b>

<b>10% Increase in <math>f'_{ci}</math></b>	<b>10% Increase in <math>E_{ci}</math></b>	<b>Deflection Due to Prestress</b>	<b>Deflection Due to the Beam Self-Weight</b>	<b>Camber Value</b>	<b>Percent of Design Release Camber</b>
8250	5280.68	7.1351	3.6383	3.4968	95.77
	4633	8.1326	4.1470	3.9857	96.78
5500	4153.91	3.4104	1.5426	1.8678	95.72
8800	5453.86	5.7888	2.2217	3.5671	95.68
5500	4153.91	1.6257	0.7055	0.9202	95.63
8800	5453.86	8.5983	4.5820	4.0163	95.80
8800	5522.99	7.2789	3.6449	3.6340	95.78
6600	4783.05	0.9837	0.2883	0.6954	95.58
4950	4142.24	0.3669	0.1604	0.2064	95.77
4950	4142.24	0.5317	0.2249	0.3068	95.81
4950	4142.24	2.4798	1.1098	1.3699	95.65
6600	4783.05	4.2246	1.7397	2.4849	95.76
4950	4142.24	1.4030	0.5759	0.8271	95.95
5500	4366.31	2.6869	1.0845	1.6025	95.62
4950	4370.26	0.3208	0.0968	0.2240	95.57
8800	5827.02	6.6154	3.0916	3.5238	95.73
8800	5827.02	5.8935	2.6635	3.2300	95.70
7150	5252.4	4.4605	1.9772	2.4833	95.77
7700	5450.68	5.6824	2.8095	2.8729	95.74
8800	5827.02	7.1733	3.4402	3.7331	95.75
8800	5827.02	6.9711	3.3256	3.6455	95.74
5500	4606.66	2.5434	1.0556	1.4877	95.66
	4633	8.1326	4.1470	3.9857	96.78
				<b>Average</b>	<b>95.77</b>

<b>15% Increase in <math>f'_{ci}</math></b>	<b>15% Increase in <math>E'_{ci}</math></b>	<b>Deflection Due to Prestress</b>	<b>Deflection Due to the Beam Self-Weight</b>	<b>Camber Value</b>	<b>Percent of Design Release Camber</b>
8625	5399.36	6.9852	3.5584	3.4269	93.86
	4715.1	7.9989	4.0748	3.9242	95.29
5750	4247.27	3.3387	1.5087	1.8300	93.78
9200	5576.44	5.6671	2.1729	3.4942	93.72
5750	4247.27	1.5912	0.6900	0.9012	93.65
9200	5576.44	8.4177	4.4813	3.9364	93.89
9200	5647.12	7.1261	3.5648	3.5613	93.86
6900	4890.55	0.9629	0.2820	0.6809	93.59
5175	4235.34	0.3592	0.1569	0.2023	93.86
5175	4235.34	0.5206	0.2199	0.3007	93.91
5175	4235.34	2.4272	1.0854	1.3418	93.68
6900	4890.55	4.1365	1.7014	2.4350	93.83
5175	4235.34	1.3745	0.5633	0.8112	94.10
5750	4464.44	2.6299	1.0606	1.5693	93.64
5175	4468.48	0.3139	0.0946	0.2193	93.57
9200	5957.98	6.4762	3.0236	3.4526	93.80
9200	5957.98	5.7692	2.6049	3.1643	93.76
7475	5370.45	4.3673	1.9338	2.4336	93.85
8050	5573.18	5.5628	2.7478	2.8150	93.82
9200	5957.98	7.0226	3.3646	3.6580	93.82
9200	5957.98	6.8245	3.2525	3.5720	93.81
5750	4710.2	2.4897	1.0324	1.4572	93.70
	4715.1	7.9989	4.0748	3.9242	95.29
				<b>Average</b>	<b>93.85</b>

<b>20% Increase in <math>f'_{ci}</math></b>	<b>20% Increase in <math>E_{ci}</math></b>	<b>Deflection Due to Prestress</b>	<b>Deflection Due to the Beam Self-Weight</b>	<b>Camber Value</b>	<b>Percent of Design Release Camber</b>
9000	5515.49	6.8445	3.4834	3.3611	92.06
	4795	7.8730	4.0069	3.8661	93.88
6000	4338.62	3.2714	1.4769	1.7944	91.96
9600	5696.37	5.5528	2.1271	3.4256	91.88
6000	4338.62	1.5588	0.6754	0.8833	91.80
9600	5696.37	8.2482	4.3870	3.8612	92.10
9600	5768.58	6.9827	3.4897	3.4930	92.06
7200	4995.73	0.9433	0.2760	0.6672	91.71
5400	4326.43	0.3520	0.1536	0.1984	92.05
5400	4326.43	0.5103	0.2153	0.2950	92.13
5400	4326.43	2.3779	1.0626	1.3153	91.83
7200	4995.73	4.0537	1.6656	2.3881	92.03
5400	4326.43	1.3476	0.5514	0.7962	92.37
6000	4560.46	2.5764	1.0383	1.5381	91.79
5400	4564.59	0.3075	0.0926	0.2149	91.69
9600	6086.12	6.3456	2.9600	3.3856	91.98
9600	6086.12	5.6526	2.5501	3.1025	91.93
7800	5485.96	4.2798	1.8930	2.3868	92.04
8400	5693.05	5.4505	2.6899	2.7606	92.00
9600	6086.12	6.8812	3.2937	3.5874	92.01
9600	6086.12	6.6869	3.1840	3.5029	91.99
6000	4811.5	2.4392	1.0107	1.4285	91.85
	4795	7.8730	4.0069	3.8661	93.88
				Average	92.05



<b>30% Increase in <math>f'_{ci}</math></b>	<b>30% Increase in <math>E_{ci}</math></b>	<b>Deflection Due to Prestress</b>	<b>Deflection Due to the Beam Self-Weight</b>	<b>Camber Value</b>	<b>Percent of Design Release Camber</b>
9750	5740.7	6.5872	3.3468	3.2404	88.75
	4949.96	7.6395	3.8814	3.7581	91.26
6500	4515.77	3.1483	1.4190	1.7293	88.62
10400	5928.97	5.3438	2.0437	3.3001	88.52
6500	4515.77	1.4996	0.6489	0.8506	88.40
10400	5928.97	7.9382	4.2149	3.7234	88.81
10400	6004.12	6.7205	3.3528	3.3677	88.76
7800	5199.72	0.9075	0.2652	0.6423	88.29
5850	4503.09	0.3389	0.1476	0.1913	88.75
5850	4503.09	0.4913	0.2069	0.2845	88.85
5850	4503.09	2.2877	1.0209	1.2668	88.45
7800	5199.72	3.9023	1.6003	2.3021	88.71
5850	4503.09	1.2985	0.5298	0.7687	89.18
6500	4746.68	2.4787	0.9976	1.4811	88.38
5850	4750.98	0.2959	0.0890	0.2069	88.26
10400	6334.64	6.1068	2.8439	3.2630	88.64
10400	6334.64	5.4395	2.4501	2.9894	88.57
8450	5709.96	4.1198	1.8188	2.3010	88.74
9100	5925.51	5.2453	2.5844	2.6609	88.68
10400	6334.64	6.6225	3.1645	3.4580	88.69
10400	6334.64	6.4353	3.0591	3.3762	88.66
6500	5007.97	2.3471	0.9711	1.3760	88.48
	4949.96	7.6395	3.8814	3.7581	91.26
				<b>Average</b>	<b>88.75</b>

<b>40% Increase in <math>f'_{ci}</math></b>	<b>40% Increase in <math>E_{ci}</math></b>	<b>Deflectio n Due to Prestress</b>	<b>Deflection Due to the Beam Self- Weight</b>	<b>Camber Value</b>	<b>Percent of Design Release Camber</b>
10500	5957.41	6.3573	3.2250	3.1322	85.79
	5099.07	7.4274	3.7679	3.6595	88.86
7000	4686.24	3.0383	1.3674	1.6709	85.63
11200	6152.79	5.1571	1.9693	3.1877	85.50
7000	4686.24	1.4467	0.6253	0.8214	85.36
11200	6152.79	7.6612	4.0615	3.5997	85.86
11200	6230.77	6.4861	3.2309	3.2553	85.79
8400	5396.01	0.8756	0.2556	0.6200	85.22
6300	4673.08		0.1422		
6300	4673.08	0.4744	0.1993	0.2750	85.90
6300	4673.08	2.2072	0.9837	1.2234	85.42
8400	5396.01	3.7670	1.5420	2.2249	85.74
6300	4673.08	1.2545	0.5105	0.7440	86.31
7000	4925.86	2.3914	0.9613	1.4302	85.34
6300	4930.32	0.2854	0.0858	0.1997	85.19
11200	6573.76	5.8934	2.7404	3.1530	85.66
11200	6573.76	5.2490	2.3609	2.8881	85.57
9100	5925.51	3.9767	1.7526	2.2241	85.77
9800	6149.19	5.0619	2.4904	2.5715	85.70
11200	6573.76	6.3914	3.0494	3.3419	85.72
11200	6573.76	6.2104	2.9479	3.2626	85.68
7000	5197.02	2.2647	0.9357	1.3290	85.45
	5099.07	7.4274	3.7679	3.6595	88.86
				<b>Average</b>	<b>85.78</b>